Human Embryonic Stem Cell-Derived Retinal Pigment Epithelium Transplantation in Advanced Neovascular Age-Related Macular Degeneration

Odysseas Georgiadis

Institute of Ophthalmology, University College of London and
Moorfields Eye Hospital, NHS Foundation Trust

Supervisors: Professor Lyndon Da Cruz and Professor Peter J. Coffey

Thesis submitted for the degree of Doctor of Medicine (Research) – MD(Res)
University College of London

June 2020

I, Odysseas Georgiadis, confirm that the work presented in this thesis is my own. Where information has been obtained with the help of others, I confirm that this has been indicated in this thesis and summarized at the end of Chapter 2 (Methods).

Abstract

Age-related macular degeneration (AMD) remains one of the leading causes of permanent vision impairment worldwide. It is a disorder of the central retina that manifests with irreversible cell loss, primarily affecting the retinal pigment epithelium (RPE) and subsequently the retina and choroid, leading to blindness through atrophy or neovascularization and exudation. Current treatments are only able to suppress the progression of the early and moderate neovascular AMD, mainly by controlling leakage and haemorrhage, while there is no established therapy for the atrophic type or the advanced neovascular type. RPE transplantation strategies have been attempted with promising outcomes; however, their operational complexity combined with the large patients' volume has underlined the need for more accessible cell sources and a more feasible surgical paradigm.

This thesis aims to examine the feasibility, safety and efficacy of transplantation of a human Embryonic Stem Cell (hESC)-derived RPE sheet in patients with severe neovascular (n) AMD. A fully differentiated hESC-RPE monolayer on a coated synthetic basement membrane (BM) has been bioengineered ex vivo and, using a purpose-designed surgical tool, has been implanted in the subretinal space of two patients with nAMD and acute vision decline. Systemic immunosuppression was administered during the peri-operative periods, while only local, intra-ocular steroids were given for the longer term. The patients were followed-up in a prospective study to assess the safety, and the structural and functional outcomes of this strategy for two years post-operatively.

Both subjects demonstrated good safety outcome with no signs of local or distal tumorigenicity or uncontrolled proliferation from the implanted cells. Both showed reconstruction of the RPE-BM complex sufficient to support the retinal structure and the rescue and preservation of the photoreceptors, during the study period. Furthermore, both patients showed significant gain in their visual function, in terms of fixation, retinal light sensitivity, visual acuity and reading speed, maintained for two years. Most importantly, in both cases

there was a clear co-localisation of the structural support, provided by the transplant, with the areas of functional improvement.

The work in this thesis provides proof that the reconstruction of the RPE using hESC on synthetic BM can rescue and preserve the retinal structure and function over the long term, in severe neovascular AMD.

Impact Statement

The work presented in this thesis provides evidence of feasibility, safety and efficacy of the submacular transplantation of a hESC-derived RPE on a synthetic basement membrane, as a potential regenerative strategy for advanced neovascular AMD, a form of the disease that is currently untreatable and causes permanent blindness. It shows that it is possible to overcome challenges, such as the cellular differentiation and tissue bioengineering, but also the complexity of the surgical delivery of the transplant in the most critical location for the visual function, the macula.

The capacity of stem cells for indefinite self-renewal and their pluripotency to differentiate towards any specialized cell line make them an incomparable source for transplants production. The proposed surgical paradigm, using a purpose-designed delivery tool, pre-loaded with the transplant, constitutes a more straightforward and efficient approach, suggesting a significant reduction of the complications. Furthermore, this paradigm of cell delivery can have a broader application on variable ocular conditions.

The continuation of this study, with the involvement of more patients, is expected to lead to the standardization of the technique and finally to its approval from administrative authorities as a competent and safe therapeutic strategy. Thus, a future implementation in the routine ophthalmic surgical practice may lead to the management of millions of patients who suffer from this disease. An extension of the indications to include other degenerative and dystrophic conditions that target the RPE is also plausible.

The absence of serious adverse events and the preservation of the structure and function with only local immunosuppression for the long term encourages the continuation and widening of the research in cell therapies in further human trials. The safety outcomes of this work can also oppose recent concerns about the potential side effects of cell therapies that were lately raised after the publication of some very negative outcomes from poorly regulated and profit-driven “Stem Cell Clinics”. Thus, the study in this thesis highlights the necessity of a solid scientific design and unambiguous ethical methodology, always focused in the patients’ safety and care, as well as the scientific progress in the field.

Further from its potential applications in ophthalmology, this work also advocates for the use of stem cells in other medical specialties. The range of diseases that result in cell loss is immense and the promising results of such early human studies can constitute a springboard for more rapid advancements in cell replacement strategies.

Finally, the work in this thesis represents a complete example of translational medicine. The described approach, starting from the bioengineering of the hESC-RPE transplant and ending to the long-term therapeutic effect in the patients’ vision, covers the whole “bench-to-bedside” spectrum, involving a multi-disciplinary, high collaborative team of researchers, technicians and clinicians, whose common aim is to renovate the way healthcare is delivered.

Publications related to this thesis

- Georgiadis, O., da Cruz, L., & Coffey, P. (2017). Stem Cell-Derived RPE Transplantation: The Feasibility and Advantages of Delivery as Monolayers. In *Cellular Therapies for Retinal Disease* (Vol. 85, pp. 19–31). Cham: Springer, Cham. http://doi.org/10.1007/978-3-319-49479-1_2
- Da Cruz, L., Fynes, K., Georgiadis, O., Kerby, J., Luo, Y. H., Ahmado, A., et al. (2018). Phase 1 clinical study of an embryonic stem cell–derived retinal pigment epithelium patch in age-related macular degeneration. *Nature Biotechnology*, *15*, 283. http://doi.org/10.1038/nbt.4114
- Georgiadis, O., Coffey, P., and Da Cruz, L. (2019). Cell Delivery: Surgical Approaches. In *Cell-Based Therapy for Degenerative Retinal Disease,* Stem Cell Biology and Regenerative Medicine. Springer, pp.167-192 http://DOI: 10.1007/978-3-030-05222-5_10

Conference oral presentations presenting data from this thesis

- Georgiadis, O., Fynes, K., Luo, Y., Nommiste, B., Zhong, J., Ramsden, C., Coffey, P.J., DaCruz, L. Human Embryonic Stem Cell-derived Retinal Pigment Epithelium sheet transplantation in severe neovascular Age-Related Macular Degeneration: 18-month survival and structural outcomes, **The 2018 Annual Meeting of the Association for Research in Vision and Ophthalmology (ARVO), Honolulu, HI, USA.**
- DaCruz, L., Fynes, K., Georgiadis, O., Nommiste, B., Carr, A.F., Ramsden, C., Vugler, A., Whiting, P., Loudon, P., Coffey, P.J. Improvement and stabilization of vision for 18 months after Human Embryonic Stem Cell-derived, RPE sheet transplantation on a synthetic basement membrane for treatment of severe, wet Age-Related Macular Degeneration, **The 2018 Annual Meeting of the Association for**

Research in Vision and Ophthalmology (ARVO), Honolulu, HI, USA.

- Georgiadis, O., DaCruz, L. Outcome After Transplantation of A Human Embryonic Stem Cell-Derived RPE in Patients With Advanced Neovascular AMD, **The 18th EURETINA Congress, Vienna, Austria (2018).**
- Georgiadis, O. Stem Cells in AMD. In "The Future of Medical Retina", **The 14th Greek Vitreo-Retinal Society Congress, Athens, Greece (2019).**
- Georgiadis, O., DaCruz, L., Stem Cell-Derived Retinal Pigment Epithelium Transplantation for Age-Related Macular Degeneration, **The 52nd Panhellenic Ophthalmology Congress, Athens, Greece (2019).**

Acknowledgements

Throughout the completion of this work, I have received a great deal of support and assistance. Fist of all, I would like to thank my supervisor, Professor Lyndon Da Cruz, for his inspiration, constant encouragement and invaluable guidance during the development of my clinical and research work. I feel truly privileged to have had Lyndon as my mentor over these years. I am also grateful to Professor Pete Coffey for his supervision, his enthusiasm and his constructive guidance. Without him and his laboratory, this project would not have been possible.

I am indebted to the Moorfields Eye Charity and the Michael Uren Foundation for funding my research. I am also most grateful to the Moorfields Eye Hospital and the NIHR Biomedical Research Centre for Ophthalmology for providing the infrastructure and the facilities for its completion.
I would like to thank the London Project to Cure Blindness and the Moorfields Eye Charity for providing support to travel for conferences to communicate my research.

I wish to thank my previous clinical supervisor, Ms Tina Xirou, who encouraged me to come to the UK and work in research. I would like to acknowledge my colleagues, Yvonne Luo and Conor Ramsden (previous Ph.D. students of Pr. Da Cruz), who shared their experience when I first started this work. I would like to thank the staff in the Clinical Research Facilities of Moorfields for all their hard work during the patients' visits. I am particularly grateful to our ophthalmic photographers, Monica Clemo and Vincent Rocco, who did an amazing work in the clinical imaging. I also want to thank Joe Zhong for passing on his expertise in Adaptive Optics and helping me with the image processing.

I owe a big thank you to the two patients, Mrs. P.M. and Mr. D.W. that participated in my project. Without their selfless offer and their inexhaustible patience throughout this intense study, we would not have made it that far.

To conclude, I cannot forget to thank my partner, Sofia, for her unconditional support and patience during these indeed very intense years, and my friends and family for offering valuable relaxation during my study breaks.

Abbreviations

ACT	Advanced Cell Technology
AE	Adverse Event
AO	Adaptive Optics
AF	Autofluorescence
AMD	Age-related Macular Degeneration
ASC	Adipose-derived Stem Cell
BCVA	Best Corrected Visual Acuity
BM	Basement Membrane
BSS	Balanced Salt Solution
CF	Counting Fingers
CFF	Colour Fundus Photography
CNTF	Ciliary Neurotrophic Factor
CNV	Choroidal Neovascularization
CS	Contrast Sensitivity
ECT	Encapsulated Cell Technology
EDI	Enhanced Depth Imaging
ELM	External Limiting Membrane
EOG	Electrooculogram
ERG	Electroretinography
ERM	Epiretinal Membrane
ESC	Embryonic Stem Cell
ETDRS	Early Treatment Diabetic Retinopathy Study
FAF	Fundus Autofluorescence
GA	Geographic Atrophy
hESC	Human Embryonic Stem Cell
HLA	Human Leukocyte Antigen
HM	Hand Motion
hRPC	Human Retinal Progenitor Cell
hUTC	Human Umbilical Tissue-derived Cell
ICGA	Indocyanine Green Angiography

IPCV	Idiopathic Polypoidal Choroidal Vasculopathy
iPSC	Induced Pluripotent Stem Cell
IR	Infrared
IS	Inner Segment
LE	Left Eye
LogCS	Logarithm of Contrast Sensitivity
LogMAR	Logarithm of Minimal Angle of Resolution
LPCB	London Project to Cure Blindness
MHC	Major Histocompatibility Complex
MNREAD	Minnesota low-vision Reading test
MNRSmax	Minnesota Reading Speed maximum
MMD	Myopic Macular Degeneration
MP	Microperimetry
MP1	Microperimeter 1
MSC	Mesenchymal Stem Cell
NSR	Neurosensory Retina
OCT	Optical coherence tomography
ONL	Outer Nuclear Layer
OPL	Outer Plexiform Layer
OS	Outer Segment
PED	Pigment Epithelial Detachment
PDGF	Platelet-Derived Growth Factor
PEDF	Pigment Epithelial Derived Factor
PDT	Photodynamic Therapy
POS	Photoreceptor’s Outer Segment
PPV	Pars Plana Vitrectomy
PR	Photoreceptor
PVR	Proliferative Vitreo-Retinopathy
RAP	Retinal Angiomatous Proliferation
RCS	Royal College of Surgeons
RD	Retinal Detachment
RE	Right Eye

ROSO	Removal Of Silicon Oil
RPE	Retinal Pigment Epithelium
SAE	Serious Adverse Event
SD	Standard Deviation
SD-OCT	Spectral Domain Optical Coherence Tomography
SLO	Scanning Laser Ophthalmoscope
SMH	Submacular haemorrhage
SRF	Subretinal Fluid
TIA	Transient Ischaemic Attack
TPA	Tissue Plasminogen Activator
UCL	University College London
U/S	Ultrasound
VA	Visual Acuity
VEGF	Vascular Endothelial Growth Factor

Table of contents

List of Figures

List of Tables

Chapter 1

Introduction and Background

1.1. The Retinal Pigment Epithelium

1.1.1. The normal retinal pigment epithelium and its role in visual function. The retinal pigment epithelium (RPE) is a monolayer of hexagonal, pigmented cells, derived from neuro-ectoderm. The RPE lies on a specialized basement membrane – Bruch's membrane and is located between the light-sensitive photoreceptors' outer segments and the Bruch's membrane - choriocapillaris complex (**Fig. 1-1**). The RPE together with the photoreceptors, constitute a structural and functional unit that provides the transducing interface for visual perception (Strauss, 2005).

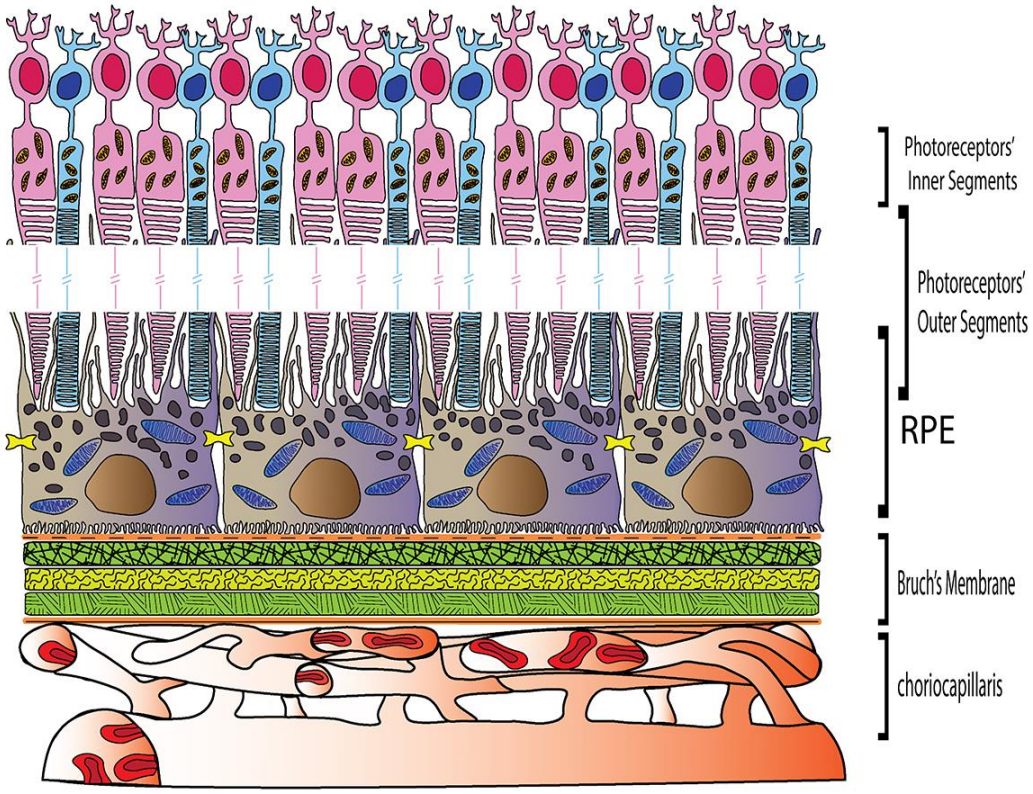

Figure 1-1: Graphic representation of the RPE demonstrating cell polarization and monolayer organization with intracellular tight junctions, interdigitation with the photoreceptors' outer segments and interface with Bruch's membrane and the choriocapillaris.

The numerous functions of the RPE, by which it contributes to normal retinal function, can be summarized under two broad, conceptual headings – *Barrier* and *Support*. Firstly, the RPE constitutes a barrier (in conjunction with Bruch's membrane) between the neural retina and the choroid. In terms of the

barrier function there are two components – one physiological and the other, physical. The physiological barrier is formed by intercellular tight junctions (zonulae occludentes) between RPE cells that prevent the passage of large molecules from the choriocapillaris to the subretinal space. This tight junction barrier constitutes the outer 'blood-retinal barrier'. The physical barrier is constructed by the extracellular matrix found in Bruch's and surrounding the RPE, many components of which are produced by the RPE cells (Campochiaro, Jerdon, & Glaser, 1986).

The second broad function of the RPE is the provision of cellular *support* to the neuro-retina. In terms of this physiological support, the most critical specific metabolic function of the RPE is the regeneration of bleached opsins, taking place in the cytosol of the RPE cells. The recycling of the visual pigments together with phagocytosis of the photoreceptors' outer segments, which are shed in a circadian manner, represent critical parts of the physiological visual cycle and photoreceptor maintenance. Additionally, RPE participates in retinal polyunsaturated fatty acid metabolism and cellular and extracellular homeostasis; it secretes growth factors including PEDF and VEGF; it maintains the subretinal space and the extraphotoreceptor matrix and it absorbs light and protects against photo-oxidative stress. The many critical functions of the RPE explain the catastrophic effect on vision when this layer is lost or dysfunctional. It also underlies the rationale and attraction of research into RPE transplantation for the treatment of many retinal diseases.

Central to its function as a *barrier* and as a *support* for photoreceptors, the RPE must maintain two important features. Firstly, its existence as a monolayer and secondly, its orientation (polarization). RPE cells need to be uniformly polarized in order for the microvilli of their apical cellular membranes to interdigitate with the photoreceptors thereby facilitating outer-segment phagocytosis (**Fig. 1-1**). Polarization is also important for the regulation of ion and water transport from the apical side to the basolateral surface. This active transport is the way that the RPE implements the removal of water that is generated by the metabolic activity of the photoreceptors and constantly flowing from the vitreous through the retina, from the subretinal space to the

choroidal vasculature. Additionally, by removing water, the RPE establishes an adhesive force that contributes to the attachment of the neural retina (Strauss, 2005).

Both of the critical features of the RPE – physical barrier and physiological support - depend on the active interface with its specialized basement membrane, which is the innermost layer of Bruch's membrane. The consistent adherence between RPE and Bruch's constitutes a physical barrier, which prevents cellular migration, but also allows the regulation of diffusion between retina and choroid.

1.1.2. The RPE in age-related macular degeneration

Diseases or conditions that affect the RPE have an impact on normal retinal function and thus on sight. Aging of the RPE, as well as a variety of pathological factors, such as genetic defects, medications, dietary (vitamin A) insufficiency, can impair its homeostatic functions and affect the photoreceptor renewal process. Subsequently, deterioration or loss of the RPE cells results in corresponding atrophy of the overlying photoreceptors and underlying choriocapillaris.

Age-related macular degeneration is the leading cause of permanent visual impairment in the over 55 age group worldwide (de Jong, 2006). It is a complex degenerative disease caused by a chronic, low-grade inflammation in the central outer retina, which leads to degeneration of the RPE and Bruch's membrane. The RPE and Bruch's membrane complex is thought by many to be the primary target of AMD. It starts with accumulation of cellular metabolic by-products around this complex ("*drusen"*), and in later stages leads to atrophy, when its *support* role is compromised – termed dry AMD (Figure 1-2a). Alternatively, when its *barrier* function is defective as a result of progressive cell loss, or by participating in the inflammatory process, the endpoint is choroidal neovascularization – termed wet degeneration (nAMD) (**Fig. 1-2b**). The common endpoint for both pathways is cell-loss, especially within the photoreceptor/RPE/choroid complex (de Jong, 2006; Jager, Mieler, & Miller, 2008). Geographic Atrophy (GA, advanced dry AMD) is expected to affect 3.8 million adults by the year 2050 (Rein, 2009). Even patients with the

neovascular type of the disease (nAMD) that is currently controlable using anti-vascular endothelial growth factor (anti-VEGF) injection treatments, eventually manifest atrophy, combined with fibrovascular scar formation in the macular area. Furthermore, although the treatment may halt the progression of disease there are significant drawbacks both for the patients, regarding the duration of therapy and the risk of complications, and for the health systems, regarding the financial burden of treating constantly increasing numbers of patients.

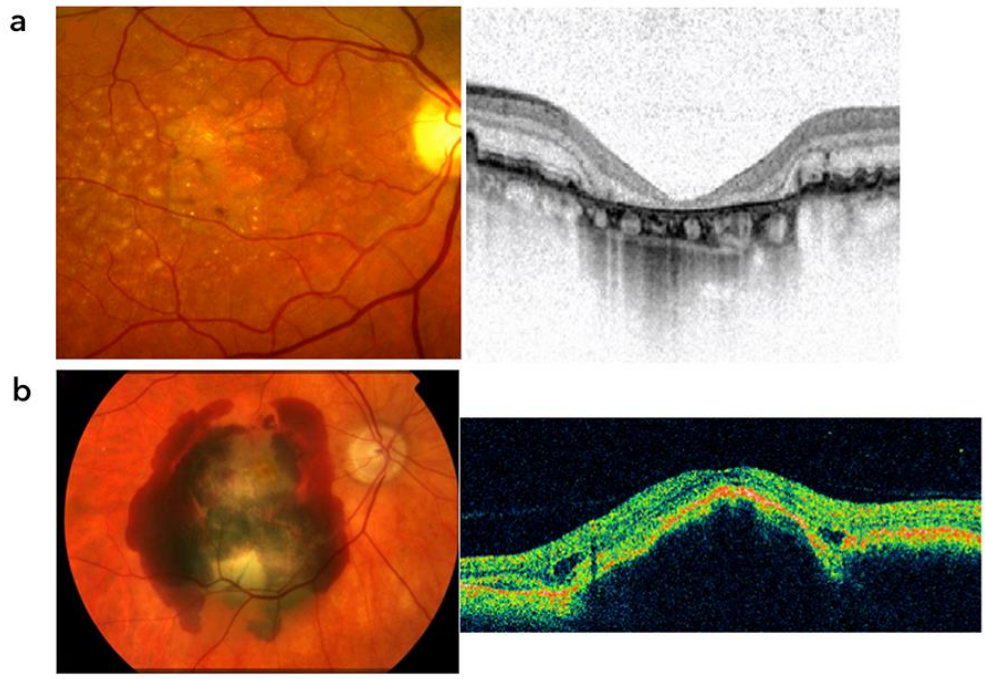

Figure 1-2: Clinical manifestation of the two forms of AMD
a. Colour fundus photo and macular optical coherence tomography (OCT) scan showing geographic atrophy and central loss of retina layers in dry AMD. **b**. Colour fundus photo in wet AMD showing severe submacular haemorrhage and macular OCT scan showing that, despite the severity of the haemorrhage, the layers of central retina are preserved.

1.1.3. RPE replacement in AMD

1.1.3.1. Scientific background

Given that RPE loss and dysfunction plays an important part in retinal degenerative conditions, it is not surprising that RPE replacement has been proposed as a potential treatment in these settings. The aim of RPE

transplantation is to retard or halt the loss of photoreceptors associated with the defective RPE-Bruch's membrane-choriocapillaris complex and support their regeneration. Numerous research projects have shown that RPE replacement not only can prevent the progression of AMD, but also may reverse the disease process.

The Royal College of Surgeons (RCS) paradigm has been one of the main animal models for proof-of-principle RPE transplantation studies. Extensive in vivo experiments on the RCS rat model have demonstrated the plausibility of photoreceptor rescue after RPE transplantation. This dystrophic strain of rat has a recessive mutation in the MERTK gene, resulting in failure of the RPE to phagocytose shed rod outer segments (D'Cruz et al., 2000). This defect leads to accumulation of subretinal debris, photoreceptor death and eventually, retinal vascular changes and retinal degeneration. The preliminary studies of RPE transplantation in the RCS rat showed retardation and/or restoration of these changes (Li & Turner, 1988), (R. Lopez et al., 1989; Lund et al., 2001; Seaton & Turner, 1992) (A.-J. Carr, Vugler, Hikita, et al., 2009a; Vugler et al., 2008; S. Wang, Lu, & Lund, 2005). Furthermore, the transplanted RPE seemed to halt the reduction of central retinal thickness, demonstrating preservation of the outer nuclear layer, outer plexiform layer, and photoreceptors inner and outer segment (Li & Turner, 1988), (da Cruz, Chen, Ahmado, Greenwood, & Coffey, 2007).

1.1.3.2. Proof of principle for human RPE transplantation

Various techniques have been proposed to replace the diseased RPE, with a view to reconstructing the RPE-neural retina interface. These include retinal translocation and autologous RPE-choroidal free grafting. The former aims to move the macular neuro-retina away from the diseased area, to overlay a healthy, extra-macular RPE. The latter aims to achieve intra-operative harvesting of healthy RPE and choroid from a distal area and grafting it under the macula.

Macular translocation surgery for AMD is a well described operation that aims in repositioning of the macula onto a healthier RPE and choroid, usually in the paramacular region (Machemer & Steinhorst, 1993). Although it

is not strictly a RPE transplantation procedure, it can be considered as such, since it results in a “new” healthy RPE area lying under the relocated fovea (Figure 1-3a, b) (da Cruz et al., 2007). The long-term post-operative outcomes of this approach demonstrate improvement in both the visual acuity and the quality of life of a significant proportion of patients (Chen et al., 2010) (Cahill, Stinnett, Banks, Freedman, & Toth, 2005; Chen et al., 2009). However, the complexity of the technique, the necessity for further surgery for ocular muscle repositioning to avoid torsional diplopia, and the significant rate of complications, including retinal detachment, proliferative vitreo-retinopathy, epiretinal membranes and macular hole, have resulted in considering this approach unviable for the disease group it aims to treat (Chen et al., 2010).

Autologous RPE-choroidal transplantation for AMD is a surgical approach that has evolved through many stages from submacular RPE/choroid pedicle flap rotation (Peyman et al., 1991) to submacular donor RPE/choroid free graft transposition (Stanga et al., 2001a) submacular injection of suspension of RPE cells from the peripheral fundus (Binder et al., 2002), and submacular insertion of RPE/choroid patch graft from the peripheral fundus (Figure 1-3c, d) (van Meurs & Van Den Biesen, 2003). The latter group have published long-term outcomes for 133 patients who underwent autologous RPE-Choroid grafting after vitrectomy and CNV excision (van Zeeburg, Maaijwee, Missotten, Heimann, & van Meurs, 2012). They demonstrated modest overall outcomes, in terms of visual acuity, nevertheless 5% of patients were showed to have best corrected visual acuity better than 20/40, after four years of follow-up. More recently, the reported a 13.5-year survival for one of their grafts, with the receiver maintaining a 20/32 visual acuity (van Zeeburg, Maaijwee, & van Meurs, 2018).

Both macular translocation and autologous RPE transplantation have supported the rationale for RPE replacement and showed it to be beneficial. However, these procedures are extremely demanding in terms of surgical skills and operation times and in addition they are associated with a significant risk of potentially serious complications. Furthermore, the quality of the RPE replacement is limited due to the age of the patient and the damage that may occur to the tissue during the transplantation procedure. Due to these

limitations a treatment using an allogenic cell-derived RPE delivered with a simpler surgical technique may offer a safer and more effective treatment.

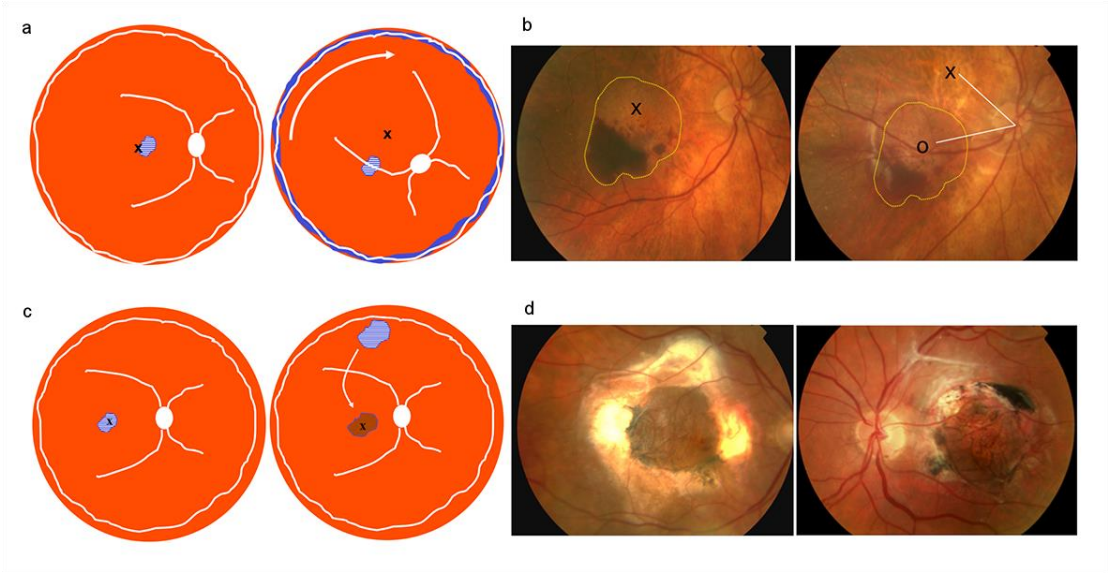

Figure 1-3: Macular translocation and RPE transplantation techniques
a and b. Graphic representation and colour fundus photos of macular translocation surgery: rotation of retina after 360° retinotomy and reposition of the macula (x) over a paramacular area of healthy RPE (o).
c. Graphic representation of RPE transplantation surgery: harvesting autologous RPE/choroid graft from the peripheral (superior) fundus and trasplantation underneath central macula (x).
d. Post-operative colour fundus photos of two cases of RPE autologous transplantation.

1.2. Introduction to cell-based therapies.

1.2.1. The eye, an appropriate target.

The eye has been identified as one of the most amenable organs to be targeted by the first generation of cellular regenerative medicine techniques. It is easily accessible surgically, the transplanted cells are directly visible and there are multiple imaging examinations that, in general, use only light sources and provide the ability to document structural and functional outcomes with minimal risk. Additionally, the eye and especially the vitreous and subretinal spaces are immune-privileged sites, theoretically able to tolerate foreign antigens or non-histocompatible cells without eliciting an

immune response. Hence, the risk of tissue rejection after cell transplantation theoretically, may be reduced. Furthermore, it is a small organ and the majority of retinal degenerative diseases initially target one single type of cells (e.g. RPE cells), in a way that cell therapies can be focused on replacing one specific cell group, by transplanting a small number of cells. These advantages together with the invaluable combination of established surgical experience and current development in experimental retinal surgery have put retinal-degenerative diseases at the forefront of cell-based clinical research.

In addition to the imaging and access advantages of the eye, progress in laboratory methods of differentiation and cultivation has increased the availability of various types of potentially therapeutic cells (table 1-1). As a result, numerous clinical trials involving retinal and RPE transplantation have commenced worldwide, some of which show encouraging primary results, in terms of safety and efficacy (tables 1-2, 1-3, 1-4).

1.2.2. Forms of cells for therapeutic delivery

1.2.2.1. Cell Suspension

A cell suspension consists of a liquid medium – usually a balance salt solution, in which single cells or small aggregates of cells are floating. The cells have previously undergone differentiation, outgrowth, isolation, trypsinisation and purification, as well as characterization assessments, so that, ideally only the desired cell type is included in the suspension.

Cell delivery in the form of a suspension holds the major advantage that it requires a relatively simpler surgical intervention than implanting a sheet. Cells can be injected into the intravitreal or subretinal space via small gauge cannulas, causing only minimal injury to the retina.

Currently the most common approach for implanting a cell suspension is subretinal delivery via the pars plana, trans-vitreal route (Figure 1-4c). This requires a standard pars plana vitrectomy and transretinal access to the subretinal space. Less common, but also less invasive is the intravitreal injection, which does not necessitate an actual surgery, but only a simple transcleral injection of the suspension into the vitreous cavity (Figure 1-4b).

Although this is plausible for gene therapy it is less likely to be a route used for cellular delivery, due to uncertainty on the behaviour and orientation of the cells towards the target tissues. Finally, a completely different method uses an "external" suprachoroidal access to deliver the cell suspension, using a purpose-designed micro-catheter, which is advanced through the sclera and through the choroid into the subretinal space (**Fig. 1-4a**).

1.2.2.2. The limitations of the cell suspension method.

The initial approaches of SC-derived RPE delivery using cell suspensions have demonstrated feasibility, but also limitations in cell survival and integration. The critical importance of the two previously mentioned basic characteristics of the RPE (monolayer formation and cellular polarization) could account for the lack of success seen in some attempts to replace the RPE by injecting freshly harvested or cultured cells into the subretinal space in the form of a cell suspension. Although transplantation of an RPE cell suspension may lead to the formation of a monolayer, occasionally it may also lead to uneven distribution of the injected cells and formation of multiple layers of RPE which alternate with bare areas of basal lamina (Crafoord, Algvere, Seregard, & Kopp, 1999), (Binder, 2011). Crafoord et al. have examined the long-term outcomes of RPE allografts in rabbits and showed that this sectional irregular distribution may result in an increased risk of graft failure, as well as damage of the adjacent photoreceptors (Crafoord et al., 1999).

Other problems that have been identified in delivering suspensions are the shearing forces that are applied on the suspension during the injection, leading to cell death, the need to isolate the cells and therefore deliver them in a less differentiated form and the possibility of cell loss due to the potential reflux of the cells from the injection site. For the cells that survive the delivery, a defective or diseased basement membrane may constitute a hostile environment for the new cells and affect their survival and ability to form a functional polarised monolayer.

Transplantation trials using cell suspensions have highlighted the critical role of a healthy Bruch's membrane for the survival and function of the transplanted RPE cells. Several groups have demonstrated that RPE cell

suspensions applied on an aged or damaged Bruch's membrane, are prone to unsuccessful integration with the host tissue and may fail to survive and remain functional for prolonged periods. (Gullapalli, Sugino, Van Patten, Shah, & Zarbin, 2005; Tezel, Kaplan, & Del Priore, 1999; Tsukahara et al., 2002) This inability of the RPE cells to grow well on defective Bruch's membranes is considered the major cause of failure for such approaches to support retina in the long term and restore photoreceptor function and vision in human eyes.(Binder et al., 2004) (Gullapalli et al., 2005)

Although the importance of Bruch's membrane for the success of the RPE transplantation had initially been overlooked, most recent developments in this field have invested efforts to support RPE grafts with BM-mimicking artificial membranes. Based on these findings transplantation of a polarized RPE monolayer as a sheet on an artificial Bruch's membrane has been proposed as a potentially promising approach.(Binder, 2011) (Diniz et al., 2013)

1.2.2.3. Cell Sheets/Patches

A cell sheet/patch transplant system consists of a biocompatible substrate or scaffold, seeded with the therapeutic cells in a way that they form a cellular monolayer (e.g. a RPE monolayer patch) on a biocompatible membrane. The scaffold provides the supportive surface necessary for the cells to attach, proliferate, differentiate and meet their structural and functional role after transplantation. Additionally, the artificial membrane provides the required structural rigidity for the manipulations during the delivery process.

In contrast to cell suspension delivery, transplantation of a cell-sheet or patch requires a more complex surgical procedure. It usually requires a novel, purpose-designed device capable of holding, protecting and delivering the graft in a way that maintains proper apical-base orientation throughout its transplantation into the subretinal space. Furthermore, an adequately sized retinal incision is necessary for the sheet to be implanted. However, the complexity of the delivery procedure is considered acceptable as the benefits of a sheet transplant are great, in terms of cell polarization, integration to the host tissues and larger and continuous size of treated area.

1.2.2.4. The potential superiority of a cell/sheet method.

The most prevalent stem cell based RPE patch transplant system consists of a biocompatible substrate or scaffold, seeded with stem cell derived RPE cells. The aim of the scaffold is to provide a supportive surface for cells to attach, proliferate, differentiate, and perform their normal functions after transplantation while providing structural rigidity that aids delivery (Hynes & Lavik, 2010). Preclinical studies designed to compare suspension method against sheet transplantation in rats showed superiority of the later, in terms of longer survival and integration with host (Diniz et al., 2013). Another recent study by Thomas et al. has demonstrated 75% survivability of RPE cells derived from human embryonic stem cells, when cultured as a monolayer on a parylene membrane and transplanted as a patch into the subretinal space of Royal College of Surgeons rats (RCS). This study also showed a significant rescue of outer nuclear layer cells as well as higher response to light stimulus in the patch-transplantation RCS group, when compared to control groups (B. B. Thomas et al., 2016).

In contrast to single-cell suspensions, cellular sheets supported by biomedical scaffolds, can form a more structurally rigid, transplantable graft, which allows the delivery of an already mature, polarised monolayer of cells to a specific destination. Therapeutic Stem Cell-derived RPE cells demonstrate the ability to adhere and grow on various candidate substrates and retain the critical characteristics of in-situ RPE, such as apical polarization, tight junctions, pigmentation and structural and metabolic integration with overlying photoreceptors and underlying choriocapillaris (Pennington & Clegg, 2016). These retained characteristics make the RPE sheets on the transplanted patch more likely to meet the dual role of host RPE namely to provide photoreceptor support and act as a barrier.

1.2.2.5. Cell Devices - Encapsulated Cell Technology (ECT)

ECT consists of a semipermeable polymer membrane capsule loaded with mammalian cells that have been genetically engineered to constantly secrete therapeutic proteins.

Patented by Neurotech Pharmaceuticals, this novel drug delivery platform has offered an approach of overcoming the blood-retinal barrier,

which - like the blood-brain - barrier restricts access of large molecules from the blood stream to neuro-retinal tissue. The circumvention of this barrier is one of the major challenges for long-term sustained delivery of proteins to the retina, for the treatment of a broad spectrum of eye diseases.

The semipermeable membrane of ECT device allows the secreted protein to diffuse out and nutrients to diffuse in, but prevents access by the host immune system, thereby providing a sustainable supply of the therapeutic factor over an extended period of time, possibly years. In addition, the encapsulated cell implants can be retrieved from the eye at any time, providing an additional level of safety (**Fig. 1-4d**).

The most common therapeutic agents delivered by ECT are neurotrophic factors. These proteins can influence survival, proliferation, differentiation and function of neurons and other cells in the nervous system and seem to hold a promising ability to retard progression of neurodegenerative disease. For the purpose of retinal neuroprotection the most studied protein is ciliary neurotrophic factor (CNTF).

It is anticipated that with further development of the ECT, future implants will become smaller and able to inserted in different locations, either anchored or free-floating in the vitreous cavity or implanted subretinally. They would be able to release specific proteins that are otherwise dysfunctional in retinal and RPE and choroidal cells, as a result of hereditary dystrophies

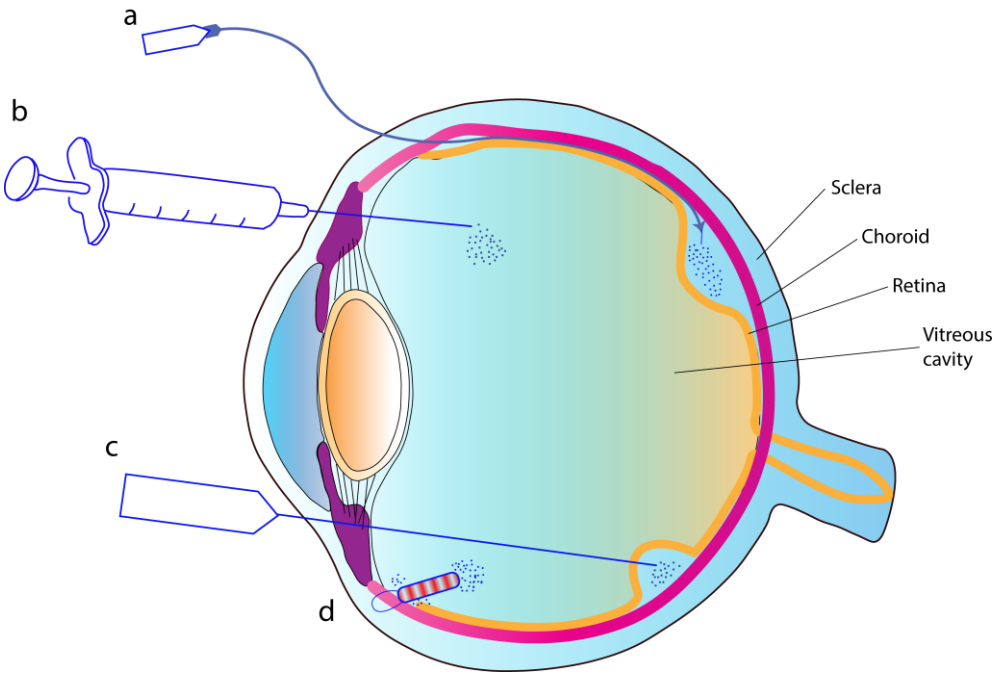

Figure 1-4: Cell delivery approaches. Eye drawing illustrating the different access points and surgical approaches for therapeutic cells delivery.
a. Suprachoroidal approach: purpose designed microcatheter progressing through the potential space between retina and choroid, to inject the therapeutic cells into induced subretinal bleb.
b. Intravitreal approach: injection of the therapeutic cells directly into the vitreous cavity.
c. Transvitreal approach: injection of the therapeutic cells into the subretinal space via the vitreous cavity, after inducing a subretinal bleb with a small gauge cannula.
d. Cell device approach: intravitreal implantation and scleral fixation of therapeutic cell-loaded micro-device, which releases therapeutic factors into the vitreous cavity

1.3. Introduction to Human Embryonic Stem Cells

1.3.1. General aspects and derivation

Stem cells are characterised by i) unlimited self-renewal (immortality) and ii) the potential to differentiate into any cell type (pluripotency). Human embryonic stem cells (hESC) are pluripotent cells derived from the inner cell mass of the 5 day-old human blastocyst (**Fig. 1-5**). The process involves culturing the conceptus to the morula or blastocyst stage of human embryos that in most cases have been donated for research purposes and would be otherwise discarded as excess or unsuitable for implantation in the IVF

program. hESC were initially harvested, isolated and characterized from human blastocysts in 1998 by Thomson et al. who demonstrated their ability to differentiate into all three germ layers when transplanted into mice (Thomson et al., 1998). They are also able to proliferate extensively *in vitro*, to maintain a normal euploid karyotype over extended culture and to express high levels of Oct4 and show telomerase activity (Hoffman & Carpenter, 2005). These characteristics render hESC a potentially unlimited source of cells for cell replacement therapies with enormous potential for regenerative medicine.

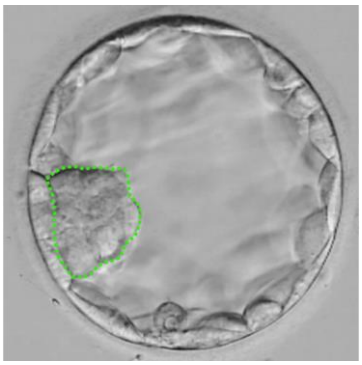

Figure 1-5: The 5-days human blastocyst. The inner cell mass is highlighted by the green dotted line.

1.3.2. hESC-derived RPE

The first report of differentiating RPE-like cells from ESCs was by Kawasaki et al. in 2002 (Kawasaki et al., 2002). This group used monkey ESCs cultured in a differentiating medium in the presence of stromal cells derived from mouse bone marrow. They reported that their ES-derived RPE-like cells expressed typical RPE markers, they had extensive and functional apical microvilli and were able to show phagocytosis of latex beads. The next important step was made in 2004 by Klimanskaya et al., when they developed an original protocol for human ESC-derived RPE cells without co-culture with animal cells or factors, demonstrating reproducible generation of RPE from hESC (Klimanskaya et al., 2004).

During the last decade, numerous researchers have explored various differentiation strategies to derive RPE cells from stem cells. In order to confirm the differentiation into RPE cells, several methods have been

developed that can verify the structural and functional characteristics of RPE. These methods include:

- Histology: microscopic examination of the histological aspects of the generated RPE cells, e.g. hexagonal shape, pigmentation, organization in a monolayer, polarization and the presence of tight junctions (Sonoda et al., 2009).
- Physiology: assessment of RPE cells functioning as a barrier: measurement of water and ion transport resistance through the epithelial monolayer (Sonoda et al., 2009) and as support: phagocytosis potency demonstrated with intracellular tracing of polystyrene beads (Kevany & Palczewski, 2010) or labelled photoreceptor outer segments, either bovine or human (A.-J. Carr, Vugler, Lawrence, et al., 2009b).
- Molecular biology: differential distribution of surface molecules among basal and apical cell membrane. Analysis of the sectional concentration of proteins, such as receptors, growth factors, channels and transporters (Zhu et al., 2011).
- Genetics: demonstration of RPE “signature genes” involved in melanogenesis, intercellular tight junctions, visual cycle, phagocytosis, sensory perception, water and ion transport, oxidoreductase metabolism (Strunnikova et al., 2010). Exclusion of gene and protein expression associated with early development and absence of pluripotency or non-epithelial differentiation (A.-J. Carr, Vugler, Lawrence, et al., 2009b).
- Immunology: investigation of polarized secretion of RPE specific cytokines, such as VEGF, TGF-β2, PEDF, PDGF (Zhu et al., 2011).

1.4. Therapeutic approaches of advanced neovascular AMD before the stem cell technology.

Currently the most common therapeutic approach for neovascular AMD is a course of repeated intravitreal injections of anti-VEGF agents, such as *ranibizumab* and *aflibercept* (Solomon, Lindsley, Vedula, Krzystolik, & Hawkins, 2019). New agents are being developed, such as the recently FDA approved *brolucizumab* (Yannuzzi & Freund, 2019), but the mainstay of the

treatment remains the same: the blocking of the VEGF to prevent the abnormal blood vessel growth. This approach can slow down the disease progression, improve the vision and often offer a long-term control, especially in cases of mild and moderate severity. However, in more advanced cases, complicated with submacular haemorrhage (SMH) and scarring, or established atrophy, anti-VEGF treatment alone offers limited, if any, help. For these cases, various alternative methods have been proposed, ranging from relatively minimal interventions, such as intravitreal injection of gas to displace the submacular blood, to complex surgical procedures to remove the blood and the CNV and reconstruct the submacular space.

1.4.1. Minimal interventions (Table 3-5):

1.4.1.1. Intravitreal anti-VEGF monotherapy

Although there is no randomized controlled trial evaluating its efficacy in AMD-related SMH, anti-VEGF monotherapy appears to offer some visual improvement in several studies (Chang et al., 2010),(Iacono et al., 2014),(Sacu et al., 2008),(Shienbaum et al., 2013). Stanescu-Segall et al. have reviewed 122 relevant cases from the literature and have calculated an increase in median VA from 20/153 pre-treatment to 20/117 post-treatment, which equals less than 10 ETDRS letters (Stanescu-Segall, Balta, & Jackson, 2016).

1.4.1.2. Intravitreal gas monotherapy

Pneumatic displacement of the SMH by an expansile gas bubble has been tried since 1996. 0.3 mL of undiluted C_3F_8 or 0.5 mL of undiluted SF_6 are injected intravitreally, followed by an anterior chamber paracentesis to control the intraocular pressure. Prone posturing of the patient is required post-operatively. Several cases have reported a more favorable visual outcome, comparing to the natural history of the SMH (Cakir, Cekiç, & Yilmaz, 2010), (Fujikawa et al., 2013), (GOPALAKRISHAN et al., 2007). However, that might also reflect the fact the cases selected for gas monotherapy are usually of lower severity. In a major review of such cases, the mean VA improved from

20/726 to 20/324 an equivalent to approximately 15 ETDRS (Stanescu-Segall et al., 2016)

1.4.1.3. Intravitreal anti-VEGF and gas

This combined procedure is simple and can be performed in an office setting and thus obviates the need of operating room. An anti-VEGF agent is injected intravitreally, followed by a bubble of expansile gas (as in 1.4.1.2), under topical anaesthetic. A small number of case series has been published with up to 12 months of follow-up (Chawla, Misra, & Khemchandani, 2009),(Kitahashi et al., 2014) (Nourinia, Bonyadi, & Ahmadieh, 2010) and the mean post-treatment VA has been calculated in a review to be 20/144 (Stanescu-Segall et al., 2016), which is approximately 30 ETDRS letters.

1.4.1.4. Intravitreal TPA and gas

Tissue plasminogen activator has played a pivotal role in the efforts to treat SMH (Handwerger, Blodi, Chandra, Olsen, & Stevens, 2001),(Fujikawa et al., 2013) (Hassan et al., 1999),(HESSE, SCHROEDER, HELLER, & KROLL, 2000). This serine protease forms a complex with fibrin to activate plasminogen to plasmin, which subsequently can dissolve the clot. Combined with expansile gas, it can increase the efficacy of the latter by liquefying the blood, which is subsequently more easily displaced by the bubble. Several cases have been published and have been reviewed to demonstrate an increase in the mean VA from 20/576 to 20/200, approximately equivalent of 23 letters as a mean difference (Stanescu-Segall et al., 2016).

1.4.1.5. Intravitreal anti-VEGF and gas and TPA

This approach combines the above methods of dissolving/displacement of the SMH with treatment of the underlying CNV (R. Guthoff, Guthoff, Meigen, & Goebel, 2011),(Meyer, Scholl, Eter, Helb, & Holz, 2008),(Papavasileiou, Steel, Liazos, McHugh, & Jackson, 2013),(Sacu et al., 2008). It can be delivered in an outpatient setting under topical anaesthetic, as soon as possible after the SMH occurred, preferably within 72h (although the “therapeutic window” varies in different reports). In five studies reviewed by Stanescu-Segall et al.,

the mean change of the VA was found from 20/200 to 20/100 equivalent to 15 ETDRS letters (Stanescu-Segall et al., 2016).

1.4.2. Surgical approaches (table 3-6)

Surgical approaches, based on pars-plana vitrectomy, have the main advantage of a more complete and certain SMH removal. Additionally they may decrease the VEGF levels by increasing the oxygenation of vitreous and also relieve any vitreomacular traction.

Very few level 1, high quality, randomised clinical trials have been accomplished to examine the results of submacular surgery and all were conducted before the prevalence of the anti-VEGFs. These studies included CNV excision with or without removal of subretinal haemorrhage and with or without tissue plasminogen activator injection (tPA) (Bressler et al., 2004; 2000; Lewis & s, 1997).

1.4.2.1. PPV and SMH removal

The largest of the level 1 trials, the Submacular Surgery Trials (SST) Pilot Study, included a cohort of patients with subretinal haemorrhage for which, after 36 months of follow-up, they reported improvement of visual acuity for 20% of recruited patients, while 51% experienced VA deterioration. At their last follow-up, only 14% of subjects demonstrated a VA of at least 20/160(Bressler et al., 2004). However, a meta-analysis by Falkner et al., which examined 16 studies conducted between 1992 and 2004 and included 264 cases of surgical removal of subretinal blood, revealed markedly better results than the SST group. Their model-based estimates were of 62% for improvement of vision post-operatively - with 43% showing a VA of at least 20/200 - and only 13% for vision loss. The mean VA was estimated to have increased by an equivalent of 22 ETDRS letters. However, from these 16 studies only 10 concerned patients with CNV and only 2 were relatively large case series with more than 30 subjects (Falkner, Leitich, Frommlet, Bauer, & Binder, 2006).

1.4.2.2. PPV and TPA and gas

Standard PPV followed by a micro gauge injection of TPA into the subretinal space and gas or air tamponade to displace the liquefied clot. Only few case series are available in the literature (Haupert et al., 2001),(OLIVIER, 2004),(Sandhu, Manvikar, & Steel, 2010), which when reviewed showed no improvement in the mean VA post-operatively, (Stanescu-Segall et al., 2016).

1.4.2.3. PPV and TPA and gas, and anti-VEGF

TPA is injected either subretinally or intravitreally after vitrectomy followed by gas injection to displace the clot. Subsequent intravitreal administration of anti-VEGF aims to suppress the CNV complex. This approach seem to have the most favorable results in several published series (Arias L & J, 2010),(Sandhu et al., 2010),(Treumer, Klatt, Roider, & Hillenkamp, 2009),(Treumer, Roider, & Hillenkamp, 2012; van Zeeburg & van Meurs, 2013). The mean improvement of visual acuity has been calculated to an equivalent to 40 letters and a mean post-treatment VA at 20/171(Stanescu-Segall et al., 2016).

1.4.2.4. PPV and subretinal TPA+anti-VEGF and gas

Combined subretinal injection of TPA and anti-VEGF following vitrectomy and followed by gas injection to displace the clot. Treumer et al. reported a series of 41 eyes with 17 months follow-up (mean) demonstrating a mean VA improvement of an equivalent to 14 ETDRS letters and mean post-operative VA at 20/151, (Treumer et al., 2009; 2012).

1.4.2.5. Macular translocation

The rationale of this approach has already been mentioned in section 1 of this chapter. It is a highly demanding surgery that consists of a PPV, an induced retinal detachment, a 360° retinotomy and rotation and relocation of the retina, with or without subsequent rotation of the globe. In a systematic meta-analysis of 792 cases, the mean baseline and mean final visual acuities were 0.15 and 0.18 respectively, which reflects an improvement of less than 5 ETDRS letters in average, while the percentage of patients with at least 20/200 VA was reduced post-operatively(Falkner et al., 2006). In the only

level 1 self-controlled clinical trial of macular translocation, which included 32 cases, 37% of subjects appeared worse vision post-operatively and 10% showed some VA improvement (Lüke, 2001).

1.4.2.6. RPE autologous/homologous transplantation

This has also been described in section 1. It is another highly demanding surgical procedure, which includes preparation of a large retinal flap around the macular area, excision of the CNV and SMH and subretinal transplantation of either an autologous RPE graft or a homologous RPE-choroid-Bruch's membrane patch. Chen et al. compared the results of this approach with the macular translocation reviewing 12 cases of each and they found RPE transplantation inferior to macular translocation (Chen et al., 2009). Falkner et al. reviewed 94 relevant cases and found equal rates for improving and worsening of visual acuity post-operatively (26% for both), while the change in mean VA was 0.01 in decimal scale, which is less than 5 ETDRS letters (Falkner et al., 2006).

Numerous reports and small cases series have recorded positive outcomes from these surgical interventions. However, the lack of large, level 1 studies, the technical complexity of such procedures and the high risk of complications such as retinal detachment, proliferative vitreoretinopathy (PVR), macular hole, RPE rip, vitreous haemorrhage and recurrent SMH, are still limiting their application in a larger scale.

1.5. hESC-derived RPE in treatment of AMD

1.5.1. Scientific background

The first preclinical demonstration of possible efficacy of murine ESC-derived neural precursor cells transplantation for AMD was reported by Schraermeyer et al. in 2001 (Schraermeyer et al., 2001). This group used the RCS rat to show that subretinal injection of mouse ESC can prevent photoreceptor degeneration and loss. However, the safety of this preliminary approach was subsequently found inadequate, since the mouse ESC seemed able to

generate tumor formation after implantation in various adult tissue sites (Arnhold, Klein, Semkova, Addicks, & Schraermeyer, 2004).

Klimanskaya et al. also demonstrated that transplantation of hESC-derived RPE into the sub-retinal space of the RCS rat at 6 weeks of age, when the photoreceptors are still alive, was associated with extensive photoreceptor rescue.(Klimanskaya et al., 2004), (Lund et al., 2006). They showed preservation of the outer plexiform layer (ONL) in the treated rats, while this layer was found severely diminished in the control animal group, which had received sham-injections. Further histological examinations of the transplanted donor cells showed positive staining with RPE-specific markers, such as RPE65 and bestrophin. On the contrary, testing for human-specific proliferating cell nuclear antigen (PCNA) was found negative, indicating the absence of continuous cell division. There was also no tumorigenic effect among the hESC-RPE cell populations. Additionally, the transplanted cells were found distributed subretinally and adjacent to the host RPE layer and remained viable for more than 100 days post-implantation.

Lu et al. studied the transplantation of hESC-derived RPE in the RCS rat and Elov14 mouse (B. Lu et al., 2009). The latter constitutes an animal model for Stargardt degeneration. They demonstrated long-term survival of the transplanted cells, as well as preservation of the photoreceptor integrity in a dose-depended fashion. The donor cells survived for more than 220 days in the RCS rats and the PR rescue effect was found after doses as little as 20,000 cells, while similar preservation was also found in the Elov14 mouse series. Long-term safety data showed no gross or microscopic evidence of uncontrolled proliferation or tumour formation, suggesting that hESC could serve as a potentially safe and inexhaustible source for regenerative cell therapies (B. Lu et al., 2009).

1.5.2. Clinical trials of RPE transplantation – Human data

1.5.2.1. The Advanced Cell Technology trial - cell suspension / dry AMD. The first phase I/II study to examine the safety and tolerability of subretinal transplantation of hESC-RPE in humans has been sponsored by *Ocata*

Therapeutics, Inc. (named *Advanced Cell Technology,* Incorporated (ACT) until November 2014). In this open label, multicentre prospective study patients with advanced dry AMD and Stargardt's disease received subretinal cell suspensions of hESC-RPE (specifically line MA09-hRPE). The trial has been conducted in four centres in the USA and Schwartz *et al* have published the study methods and the 18 months outcomes for 18 patients, 9 with advanced dry AMD (age > 55 years) and 9 with advanced STGD (age > 18 years) (Schwartz et al., 2012; 2015; Schwartz, Tan, Hosseini, & Nagiel, 2016). Both groups were divided in three dose cohorts each (50000, 100000 and 150000 cells) and transplanted patients were followed up for a median of 22 months, by use of systemic, ophthalmic and imaging examinations. Tacrolimus and mycophenolate mofetil were used for immunosuppression for about 12 weeks. Authors have reported no serious ocular or systemic safety issues, including evidence of adverse proliferation or rejection. Any adverse events were associated with either immunosuppression or the vitreoretinal surgery itself. 72% of patients (13 of 18) showed areas with increasing subretinal pigmentation, consistent with transplanted RPE. In terms of functional outcomes, visual acuity and vision-related quality-of-life demonstrated improvement in the majority of subjects. Among 7 of the 9 AMD subjects who were followed-up for 12 months, 3 eyes showed a VA increase of at least 15 ETDRS letters, 1 eye improved by 13 letters and 3 eyes were found stable (change of less than or equal to 10 letters). Similarly, 7 STGD patients had a 12 months follow-up VA assessment with 3 of them showing an improvement of at least 15 ETDRS letters, 3 remaining stable and one losing more than 10 letters of VA. Although they did not demonstrate a clear structure-function correlation between post-operative fundus pigmentation, autofluorescence and corresponding visual acuitues, these results offer the first evidence of medium- to long-term safety, transplant survival and possible function of pluripotent stem cell-derived therapeutic cells in degenerative retinal disease. Consequently, they suggest hESCs as a potentially safe source cells for therapy of medical conditions that require tissue replacement.

1.5.2.2. The CHA Biotech trial – cell suspension / dry AMD

A similar method was used by Song et al., who injected a hESC-RPE cell suspension in the subretinal space of four patients, 2 with dry AMD and 2 with STGD. They used a dose of 50,000 cells, which they delivered after PPV and induced retinal detachment. After one year of follow-up, the two AMD subjects showed less than 10 ETDRS letters VA improvement (1 and 9 letters respectively), while the two STGD subjects showed more than 10 letters improvement (12 and 19 letters respectively).(Song et al., 2015)

1.5.2.3. The AMY Medical University trial – cell suspension / wet AMD

The hESC-RPE cell suspension approach was also recently adopted by Yong Liu et al., in a phase I human clinical study for treatment of neovascular AMD (Liu et al., 2018). They transplanted their therapeutic suspension (Q-CTS-hESC-2-RPE) in the subretinal space of 3 patients, after a surgical operation to remove the neovascular membrane. The patients were followed up for 12 months, during which no transplant-related adverse events were observed. They report anatomical signs of new RPE-like formations in areas previously void of RPE. The early functional results were promising for all 3 subjects; however, after 12 months only one of them had maintained a significant gain in visual acuity. The range of VA increase at year 1 was from 11 to 26 ETDRS letters.

1.5.2.4. The RIKEN project – cell sheet / wet AMD

Mandai et al. examined the feasibility of transplanting a cell sheet comprised of induced pluripotent stem cell (iPSC)-derived RPE cells in one patient with neovascular AMD (Mandai et al., 2017). This RPE sheet was derived from the patient's skin fibroblasts using iPSC methods, so technically constituted an autograft, which was implanted in the subretinal space of the patient's eye, after PPV and removal of the fibrotic CNV. They did not use any substrate as a basement membrane for the iPSC-RPE seeding. They reported good anatomical outcome post-surgery. However, in terms of the graft's function there was no change in visual acuity post-operatively, which remained at 20/200. Similarly, they did not demonstrate any improvement in light sensitivity, which remained 0 dB in the microperimetry examination. The

subject's fixation also remained unstable, however it showed some improvement in terms of location, by shifting closer to the fovea.

1.5.2.5. The California Project - cell sheet / dry AMD

Regenerative Patch Technologies (RPT) in collaboration with the California Institute for Regenerative Medicine (CIRM) and the University of Southern California Eye Institute, have commenced a phase I/IIa clinical trial to explore the safety and tolerability of subretinal hESC-RPE sheet implants in patients with dry AMD and geographic atrophy involving the central fovea (Kashani et al., 2018). The graft consisted of an H9 line hESC-derived RPE monolayer on an ultrathin Parylene membrane. 4 patients have been operated and the reported follow-up period was up to one year. Improvement of vision (up to 17 ETDRS letters) was achieved in one of the subjects and maintained for up to 4 months. The other 3 subjects showed no significant gain in visual acuity. Improvement of fixation stability was also reported, as well as identification of RPE clusters and fragments of ELM in the optical coherence tomography scans of the treated area.

1.5.2.6. The London Project to Cure Blindness – cell sheet / wet AMD

The London Project to Cure Blindness (LPCB) and University College London, supported by Pfizer, have commenced a trial to reconstruct the anatomy of the RPE in a Phase I study, which constitutes the subject of this MD(Res) degree.

We have developed a lozenge shaped patch that consists of a thin vitronectin coated medical-grade polyester membrane on which we have immobilised cultured hESC-RPE cells derived from a hESC line known as SHEF-1.3 (A.-J. F. Carr et al., 2013). The lozenge shaped membrane had approximate dimensions 6 mm x 3 mm, and was seeded with a approximately 100,000 RPE cells forming a confluent monolayer cell sheet, at a nominal dose of 5800 cells/mm^2. The patch was transplanted to replace RPE in the eyes of subjects with acute, declining untreatable or treatment failing wet AMD.

The aim of this Phase I trial was to evaluate the safety and feasibility/efficacy of treating subjects with wet AMD in whom there was rapidly progressing vision loss associated with RPE tears, sub-macular haemorrhage or failing anti-VEGF treatment. The recent history of vision loss indicated that the neural retina is functioning and therefore had the potential to improve vision. Improvement of vision has been easier to document and has manifested over a shorter period of time than the outcome in atrophic disease, where the endpoint would have been a reduction in the rate of future vision loss.

We have utilized subretinal microsurgery techniques and a purpose designed injector to transplant the patch into the submacular space. The first 2 patients have been transplanted and they are the subjects of this MD(Res) project. A further 8 are planned to be recruited in the future. Patients were selected with sudden severe vision loss from subretinal and sub-RPE haemorrhage or RPE tears. Transient perioperative systemic and intraocular depot corticosteroids are being used for immunosuppression. Subjects were followed up for at least 2 years, during which they were examined with systemic and ophthalmic, clinical, laboratory and functional tests. The overall goal of this trial is to demonstrate whether a hESC-derived RPE immobilized on a membrane and implanted as a patch can offer a safe and effective treatment approach for degenerative maculopathies.

1.6. Safety concerns – poorly regulated human trials

Despite the early data showing safety and efficacy in hESC-based transplantation for AMD, there have also been widespread and justified concerns about the potential risk of these strategies. The publicity achieved by the primary human trials has led to opportunistic efforts to commercialize such therapeutic approaches. Combined with the unmet therapeutic need of this potentially blinding disease and the desperation of thousands of patients who suffer from it, it has triggered the development of numerous so-called “Stem-cell Clinics”, where unregulated or poorly scrutinized stem cell “treatments” are offered, often without having the elaborate clinical research background to support their claims (Taylor-Weiner & Graff Zivin, 2015), (L. G.

Turner, 2015), (Kuriyan, Albini, & Flynn, 2017a), (Daley, 2017), (Nirwan, Albini, Sridhar, Flynn, & Kuriyan, 2019). Cases of serious adverse reactions to such “treatments”, causing even complete blindness, have already occurred and publicly disseminated (Kuriyan et al., 2017b), threatening to undermine the scientific progress in the field and also the public trust in stem cell-related approaches. Although promising, these approaches remain experimental and in very early stages, which makes the need for good quality data on their long-term stability and safety more critical for the progress in this field.

1.7. Aims of this Thesis

The aims of this thesis are:

1. To examine and describe the feasibility and safety of transplantation of a hESC-derived RPE on a synthetic basement membrane, in 2 patients with acute vision loss due to severe neovascular AMD.
2. To describe the short and long-term survival, behaviour and structural and functional outcomes of the hESC-RPE cells, transplanted in the submacular space of these two patients and compare it with other therapeutic approaches.
3. To examine the role of immunosuppression in the survival of the hESC-RPE allograft.

Table 1-1: Types of therapeutic cells: Definitions and classification

Category	Definition
Stem Cells (SC)	Cells in undifferentiated state, capable of infinite proliferation and able to differentiate into various cell types.
Totipotent SC (a.k.a. omnipotent)	Cells capable of differentiation into both embryonic and extra-embryonic cell types. Able to generate a complete, viable organism.
Pluripotent SC	Cells capable of differentiation and tissue generation of any of the three embryonic germ layers, i.e. ectoderm, mesoderm and endoderm.
Multipotent SC	Cells capable of differentiation into limited cell types, able to generate tissue of a single germ layer.
Oligopotent SC	Cells capable of differentiation into only a few cell types e.g. myeloid, lymphoid SC.
Unipotent SC	Cells capable of differentiation only into their own cell type, but retain ability to self-renew.
Human embryonic SC (hESC)	Pluripotent SC obtained from a 5-day old blastocyst.
Induced pluripotent SC (iPSC)	Pluripotent SC obtained by adult somatic cells by de-differentiation through genetic reprogramming.
Mesenchymal SC (MSC)	Multipotent stromal cells capable of differentiation into variable cell types, i.e. chondrocytes, myocytes, adipocytes and osteoblasts.
Adipose derived SC (ASC)	Series of MSC derived from adipose tissue, capable of differentiation into endodermal, mesodermal and ectodermal tissues
Human umbilical tissue-derived cells (hUTC)	Series of MSC derived from human umbilical cord tissue
Hunan retinal progenitor cells (hRPC)	Partially differentiated cells obtained from fetal neural retina, capable of differentiation into retinal cell, but not for infinite replication

Table 1-2: Recent and current cell transplantation studies - Cell suspension approach.

Study ID	Study title	Phase	Sponsor/Collaborators	Location	Target disease	Cell source	Delivery approach	Registration date
NCT02467634	Study of HUCNS-SC Subretinal Transplantation in Subjects With GA of AMD (RADIANT)	II	SemCells, Inc.	Various retina and vitreous associates, Arizona, California, Illinois, Michigan, New York, Texas, Utah, US	Dry AMD	HuCNS-SC	Cell suspension – subretinal injection	Jun-2015
NCT02464436	Safety and Tolerability of hRPC in Retinitis Pigmentosa	I/II	ReNeuron Limited	Massachusetts Eye and Ear Infirmary, Masschusetts, US	RP	hRPC	Cell suspension - subretinal injection	May-2015
ChiCTR-ONB-15007477	Clinical study of subretianl transplantation of human bone marrow mesenchymal stromal cells with or without embryonic retinal progenitor cells in treatment of retinal pigmentosa	New Treatment Measure Clinical Study	Southwest Hospital, Shapingba District, Chongqing, China. National Basic Research Program (973 Program)	Southwest Hospital, Third Military Medical University, Shapingba District, Chongqing, China.	RP	hBMMSC (Human bone marrow mesenchymal SC) with or without RPC	Cell suspension – subretinal injection	Oct-2015
ChiCTR-OCB-15007054	Clinical study of subretinal transplantation of clinical human embryonic stem cells derived retinal pigment epitheliums in treatment of dry age-related macular degeneration diseases	New Treatment Measure Clinical Study	Institute of zoology, chinese academy of sciences.	Beijing Tongren Hospitol,Capital Medical University, China	Dry AMD	hESC-RPE	Not Provided	Sep-2015
ChiCTR-OPC-15006757	Treatment of Dry Age-related Macular Degeneration using fetal retinal pigment epithelium	I	The First Affiliated Hospital of Nanjing Medical	The First Affiliated Hospital of Nanjing Medical University, China	Dry AMD	Fetal RPE	Not Provided	Jul-2015

			University					
ChiCTR-OCB-15006423	Clinical study of subretinal transplantation of human embryo stem cell derived retinal pigment epitheliums in treatment of macular degeneration diseases	New Treatment Measure Clinical Study	Southwest Hospital, Shapingba District, Chongqing, China	Southwest Hospital, Shapingba District, Chongqing, China	Macular Degeneration Diseases	hESC-RPE	Not Provided	May-2015
NCT02320812	Safety of a Single, Intravitreal Injection of Human Retinal Progenitor Cells (jCell) in Retinitis Pigmentosa	I/II	jCyte, Inc.	The Garvin Herbert Eye Institute, Univ California Irvine Retina-Vitreous Associates Medical Group, LA, California, US	RP	hRPC	Cell suspension - intravitreal injection	Dec-2014
NCT02286089	Safety and Efficacy Study of OpRegen for Treatment of Advanced Dry-Form Age-Related Macular Degeneration	I/II	Cell Cure Neurosciences Ltd.	Hadassah Ein Kerem University Hospital, Israel	Dry AMD	hESC-RPE	Cell suspension – subretinal injection	Nov-2014
NCT02280135	Clinical Trial of Intravitreal Injection of Autologous Bone Marrow Stem Cells in Patients With Retinitis Pigmentosa	I	Red de Terapia Cellular, Spanish NHS, Hospital Universitario Virgen de la Arrixaca, Fundacion para la Formacion e Investigacion Sanitarias de la Region de Murcia Public Health Service, Murcia, Instituto Murciano de	Clinical Universitary Hospital Virgen de la Arrixaca, Murcia, Spain	RP	Autologous BMSC	Cell suspension - intravitreal injection	Oct-2014

			Investigación Biosanitaria Virgen de la Arrixaca					
NCT02122159	Research With Retinal Cells Derived From Stem Cells for Myopic Macular Degeneration	I/II	Ocata Therapeutics, University of California	University of California, LA, US	Myopic Macular Degeneration	hESC-RPE	Cell suspension – subretinal injection	Apr-2014
NCT01920867	Bone Marrow Derived Stem Cell Ophthalmology Treatment Study (SCOTS)	Not Provided	Retina Associates of South Florida/MD Stem Cells	Retina Associates of South Florida, Florida, US; Al Zahra Private Hospital, United Arab Emirates	Retinal Disease, Macular degeneration, Hereditary retinal dystrophy, Optic nerve disease, glaucoma	Autologous BMSC	Cell suspension - retrobulbar, subtenon, intravitreal, intraocular, subretinal and intravenous injection	Aug-2013
NCT01914913	Clinical Study to Evaluate Safety and Efficacy of BMMNC in Retinitis Pigmentosa	I/II	Chaitanya Hospital, Pune	Chaitanya Hospital, Pune, India	RP	Autologous BMMNSC (mononuclear cells)	Cell suspension - Intravitreal injection	Jul-2013
NCT02016508	Intravitreal Injection of Human Bone Marrow Derived Mesenchymal Stem Cell in Patients With Dry Age-related Macular Degeneration (AMD)	I/II	Al-Azhar University	Al-Azhar University, Egypt	Dry AMD	BMSC	Cell suspension - intravitreal injection	May-2013
NCT01674829	A Phase I/IIa, Open-Label, Single-Center, Prospective Study to Determine the Safety and	I/IIa	CHABiotech CO., Ltd	CHA Bundang Medical Center, Korea	Dry AMD	hESC-RPE	Cell-suspension – subretinal injection	Aug-2012

	Tolerability of Sub-retinal Transplantation of Human Embryonic Stem Cell Derived Retinal Pigmented Epithelial (MA09-hRPE) Cells in Patients With Advanced Dry Age-related Macular Degeneration (AMD)							
NCT01736059	Clinical Trial of Autologous Intravitreal Bone-marrow CD34+ Stem Cells for Retinopathy	I	University of California, Davis	University of California, Davis, California, US	Dry AMD, DR, RVO, RP, Hereditary Macular Degeneration	BMSC	Cell suspension - intravitreal injection	Jul-2012
NCT01632527	Study of Human Central Nervous System Stem Cells (HuCNS-SC) in Age-Related Macular Degeneration (AMD)	I/II	StemCells, Inc.	Retina-Vitreaous Associates Medical Group and Byers Eye Institute at Stanford, California; New York Eye and Ear Infirmary, New York; Retina research Institute of Texas and Retina Foundation of the Southwest, Texas, US	Dry AMD	HuCNS-SC (Human neural stem cells)	Cell suspension – subretinal injection	Jun-2012
NCT01625559	Safety and Tolerability of MA09-hRPE Cells in Patients With Stargardt's Macular Dystrophy	I	CHABiotech CO., Ltd	Republic of Korea	Stargardt's Macular Dystrophy	hESC-RPE	Cell suspension – subretinal injection	Jun-2012
NCT01531348	Feasibility and Safety of Adult Human Bone Marrow-derived Mesenchymal Stem Cells by Intravitreal Injection in Patients With Retinitis Pigmentosa	I	Mahidol University, Ministry of Health, Thailand	Siriraj Hospital Mahidol University, Bangkok, Thailand	RP	BMSC	Cell suspension - intravitreal injection	Feb-2012

NCT01344993, NCT02463744 (Dry AMD) and NCT01345006 NCT02445612 NCT01469832 (Stargadt's)	Safety and tolerability of sub-retinal transplantation of hESC derived RPE (MA09-hRPE) cells in patients with advanced dry age related macular degeneration (Dry AMD) and Stargadt's Macular Dystropthy	I/II	Ocata Therapeutics Inc. (Formerly: Advanced Cell Technology Inc. ACT), Astellas Institute for Regenerative Medicine	Jules Stein Eye Institute, California; Bascom Palmer Eye Institute, Florida; Mass Eye and Ear, Massachusetts; Wills Eye Institute, Pennsylvania, US	Dry AMD, Stargardt's Macular Dystrophy	hESC-RPE	Cell suspension – subretinal injection	Apr-2011
NCT01226628	A safety study of CNTO 2476 in patients with age-related macular degeneration	I	Janssen Research & Development, LLC	Arcadia, California, Philadelphia, Pensylvania, US	Dry AMD	hUTC	Cell suspension – subretinal injection	Oct-2010
CTRI/2010/091/00639	A Clinical Trial to Evaluate the Effect of Bone Marrow Derived Stem Cell in Diseases Like Dry Age Related Macular Degeneration and Retinitis Pigmentosa	I	Indian Council of Medical Research, India	All India Institute of Medical Sciences, Ansari Naga, India	Dry AMD, RP	BMSC (mononuclear cells)	Cell suspension - intravitreal injection	May-2010
NCT01560715 NCT01068561 NCT01518127 and NCT01518842	Intravitreal Bone Marrow-Derived Stem Cells in Patients With RP Macular Degeneration and Ischemic Retinopathy	I	University of Sao Paolo	Rubens Siqueira Research Center, Brazil	RP, Dry AMD, Iscemic Retinopathy	Autologous BMSC	Cell suspension - intravitreal injection	Feb-2010 Sep-2011 Jan-2012 Mar-2012

Table 1-3: Recent and current cell transplantation studies - Cell sheet approach.

Study ID	Study title	Phase	Sponsor/Collaborators	Location	Target disease	Cell source	Delivery approach	Registration date
NCT02590692	Study of Subretinal Implantation of Human Embryonic Stem Cell-Derived RPE Cells in Advanced Dry AMD	I/IIa	Regenerative Patch Technologies (RPT)	University of California, US	Dry AMD	hESC-RPE	Cell sheet – subretinal implantation	Oct-2015
JPRN-UMIN000011929	A Study of transplantation of autologous induced pluripotent stem cell (iPSC) derived retinal pigment epithelium cell sheet in subjects with exudative age related macular degeneration	Not Provided (Safety/Exploratory)	RIKEN Institute	RIKEN, IBRI-Kobe Hospital, Japan	Wet AMD	iPSC-RPE	Cell sheet – subretinal implantation	Oct-2013
NCT01691261	A Study Of Implantation Of Human Embryonic Stem Cell Derived Retinal Pigment Epithelium In Subjects With Acute Wet Age Related Macular Degeneration And Recent Rapid Vision Decline	I	Pfizer, London Project to Cure Blindness, University College London	Moorfields Eye Hospital, University College London, UK	Wet AMD	hESC-RPE	Cell sheet – subretinal implantation	Sep-2012

Table 1-4: Recent and current transplantation studies - Device delivery approach.

Study ID	Study title	Phase	Sponsor/Collaborators	Location	Target disease	Cell source	Delivery approach	Registration date
NCT01949324	A Phase 2 Multicenter Randomized Clinical Trial of CNTF for MacTel	II	Neurotech Pharmaceuticals	Jules Stein Eye Institute, California, Bascom Palmer, Florida, Emory University, Georgia, National Eye Institute, Maryland, Massachusetts Eye and Ear Infirmary, University of Michigan, Retina Associates of Cleveland, Ohio, University of Wisconsin, US. Centre for Eye Research, East Melbourne, Lions Eye Institute, Nedlands, Australia.	MacTel (Type 2)	Human Cells releasing CNTF	ECT Intraocular Implant (NT-501)	Sep-2013
NCT01648452	CNTF Implants for CNGB3 Achromatopsia	I/II	National Eye Institute	National Institutes of Health Clinical Center, Maryland, US	Achromatopsia (CNGB3)	Intraocular Implant Releasing CNTF	Intraocular implantation	Jul-2012
NCT01530659	Retinal Imaging of Subjects Implanted With Ciliary Neurotrophic Factor (CNTF)-Releasing Encapsulated Cell Implant for Early-stage Retinitis Pigmentosa	II	Neurotech Pharmaceuticals, University of California	University of California, San Francisco, US	RP, Usher syndrome type 1, 2.	Human Cells releasing CNTF	ECT intraocular implant (NT-501)	Jan-2012
NCT01327911	Ciliary Neurotrophic Factor (CNTF) Safety Trial in Patients With Macular Telangiectasia (Mactel)	I	Neurotech Pharmaceuticals, The Lowy Medical Research	Jules Stein Eye Institute, LA, California, Retina Associates of Cleveland, Ohio US	MacTel (Type 2)	Human Cells releasing CNTF	ECT Intraocular Implant (NT-501)	Jsn-2011

			Institute Limited					
NTC00447954 NTC00447980 NTC00447993	A Study of Encapsulated Cell Technology (ECT) Implant for Participants With - Atrophic Macular Degeneration, - Late Stage Retinitis Pigmentosa, and - Early stage Retinitis Pigmentosa	II/III	Neurotech Pharmaceuticals	Retina-Vitreous Associates Medical Group, Beverly Hills California, Retina Group of Florida, Baschom Palmer Institute, Florida, Ophthalmic Consultants of Boston, Massachusetts, Beaumont Eye Institute, Michigan, Univeristy of Utah, US	Dry AMD Early RP Late RP	Human NTC-201 Cells Releasing Ciliary Neurotrophic Factor (CNTF)	Encapsulated Cell Technology (ECT) intraocular implant (NT-501)	Mar-2007

Chapter 2

Methods

2.1. Laboratory methods – Manufacturing of the hESC-RPE patch

The human embryonic stem cell-derived retinal pigment epithelium patch implant described in this thesis, has been prepared and cut to final form at Cells For Sight (Institute of Ophthalmology – University College London) under the umbrella of the London Project to Cure Blindness, and sponsored by Pfizer Inc. All preparations were performed according to Good Medical Practice (GMP) conditions and in GMP licenced facilities.

The RPE cells were differentiated from a hESC line known as Shef-1.3, expanded under GMP conditions at the Stem Cell Derivation Facility, Centre for Stem Cell Biology (CSCB), University of Sheffield. The cells for transplantation were prepared to the state of confluent RPE at Roslin Cells Ltd. (Edinburgh, UK). Differentiation was achieved by using a spontaneous method, which was first described for Shef 1.3 by Vugler et al. (Vugler et al., 2008) (**Fig. 2-1**). hESC passage and expansion was carried out in recombinant human Vitronectin (VTN-N) (Life technologies) coated culture vessels. Medium was removed from cultures and hESC were washed with PBS-/-, incubated with EDTA (Sigma) until the cell colonies begin to detach. Cells were re-suspended in Essential 8 (E8) medium (Life Technologies) and seeded onto VTN-N-coated culture vessels. HESC were replenished with E8 medium daily and passaged every 3-4 days depending on visual observations of colony morphology and size.

HESC differentiation was carried out in flasks coated with plasma-derived vitronectin (Amsbio). Sets underwent regular media replenishment with E8 medium for up to 14 days until hESC colonies were approximately 80 to 100% confluent and then transitioned to TLP medium containing KO-DMEM; 2-Mercaptoethanol; NEAA; KOSR and L-glutamine (Life Technologies). Cells were maintained on a twice-weekly media replenishment regimen. RPE cells appear in culture as distinct pigmented foci, visible to the naked eye, which continue to expand in diameter and can be maintained in this culture system for up to 22 weeks.

RPE foci were manually isolated using sterile microblades (Interfocus) and collected in TLP medium (Vugler et al., 2008). Pooled foci were washed with PBS-/- and incubated at 37+/-2ºC with Accutase (Sigma) until a cell suspension is observed. The suspension was then passed through a 70µm cell strainer (Corning), washed in TLP medium and counted. The cells were plated on CELLstart^{TM}- coated (Life Technologies) 48-well plates at 4.8x10^4 cells/well. Cells were maintained on a twice-weekly media replenishment regime of TLP medium until they formed a confluent, pigmented cell sheet with cobblestone morphology, generally for a minimum of 5 weeks.

To ensure safety and purity of the RPE, it was essential to exclude the possibility of undifferentiated hESCs being administered to a patient. In situ hybridization was used to assess hESC impurity. Samples of differentiated cells were prepared as a monolayer on microscope slides. Specific oligonucleotide probes against LIN28A mRNA were used to evaluate the presence of hESC in the RPE population. LIN28A stained cells were identified using a nuclear stain (the International Stem Cell Initiative (International Stem Cell Initiative et al., 2007)). If any LIN28A positive cells were detected, the RPE batch would be rejected. Differentiated RPE were further assessed using immunocytochemistry against the melanosome-specific protein PMEL17, an RPE cellular marker. PMEL17 positively stained cells were counted and expressed as a percentage of total cells. Upon testing of cells on representative cell patches, the RPE purity ranged from 99.8 to 100% on positive staining of PMEL17.

RPE cells were assessed using a light microscope for pigmentation, cobblestone morphology, health and signs of contamination and processed further only if they passed this visual check (**Fig. 2-2**). Media was removed, cells were washed with PBS-/- and incubated at 37+/-2ºC with Accutase for 1-2 hrs until a cell suspension was observed. The suspension was passed through a 70µm cell strainer then washed in TLP medium and counted. Cells were then seeded (1.16x10^5 cells/well) onto the polyester membrane of transwells coated in plasma-derived vitronectin. TLP medium was added to the outer well containing the insert, and the plate then incubated at 37±2°C. The RPE cells were maintained with twice-weekly TLP media replenishment until required for drug product manufacture.

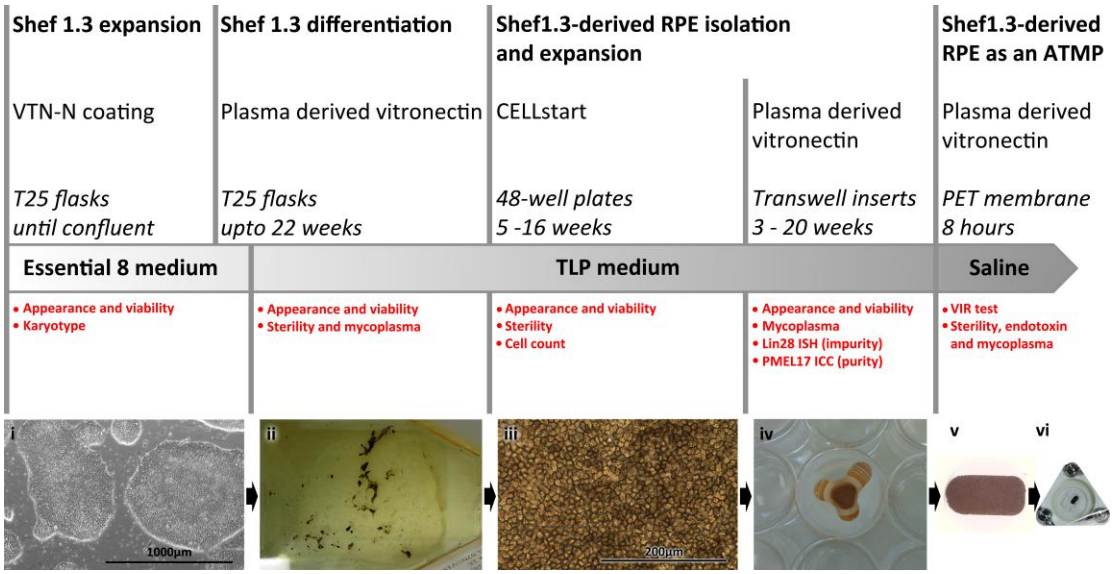

Figure 2-1: The manufacturing timeline for the hESC-RPE-BM patch. This figure depicts a schematic representation of the manufacturing process deriving RPE from Shef 1.3 hESC, their immobilisation onto a vitronectin-coated membrane and subsequent cut into a therapeutic 'patch'. In bold at the top are named the various stages of differentiation. In normal text in the next row is the coating on the plastic-ware for each step. In bold in the grey area the media used at each step is indicated. In red the various tests and checks carried out on the cultures are listed. Finally, the bottom row contains brightfield images illustrating the chronological stages of manufacture. These are (i) Shef1.3 hESC colonies expanded on recombinant human vitronectin (VTN-N) in E8 media (ii). Spontaneously differentiated RPE cells appearing as distinct pigmented foci (iii). Following manual dissection, dissociated, and filtration to achieve a pure single-cell RPE population, these RPE are seeded onto CellStart-coated tissue-culture plastic where expanding RPE cells establish their classic pigmented, cobblestone morphology (iv). Fully differentiated RPE seeded at confluence onto a vitronectin-coated PET membrane transwell insert. (v) A therapeutic 'patch' consisting of the RPE monolayer immobilised on the vitronectin-coated PET membrane that has been cut from the transwell. (v). Following release tests the patch is supplied to the surgical team in a custom-manufactured single-use sterile container in saline where it is viable for up to 8 hrs. PEDF – pigment epithelium derived factor; PMEL17 – premelanosome marker 17; ICC – immunocytochemistry; ISH – in situ hybridisation; IMPD – Investigational Medicinal Product Dossier; PET - polyethylene terephthalate; VIR test – Visual Inspection release test; ELISA - enzyme-linked immunosorbent assay (Figure from article published by the author (da Cruz et al., 2018)).

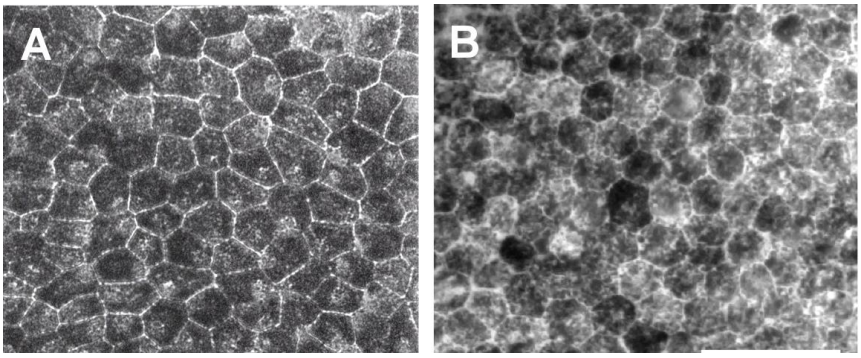

Figure 2-2: Microscopic correspondence between natural and derived human RPE: hESC-derived "0-year-old" RPE (A) showing analogous cell shape, size and pigmentation with the RPE of a 17-year-old human (B).

Characterization of the hESC Shef 1.3-derived RPE cells was conducted using immunocytochemistry, electron micrography and a phagocytosis functional assessment (**Fig. 2-3**).

Immunocytochemistry: Immunostaining was performed as described previously (Skottman, Dilber, & Hovatta, 2006). Briefly, cells were fixed in cold 4% paraformaldehyde (PFA) in 0.1M phosphate buffer and then blocked and incubated with an appropriate combination of the following primary antibodies: TRA-1-60 (Life Technologies); Ki67 (VectorLabs); CRALBP (Thermo Scientific); PMEL17 (Dako); MERTK (Abcam) and ZO-1 (Life Technologies). They were then incubated in the appropriate secondary antibodies including AlexaFluor 647 conjugated donkey anti-mouse Ig-G (Life Technologies), 594 conjugated donkey anti-rabbit Ig-G (Life Technologies) and Dylight 488 conjugated donkey anti-mouse Ig-M (Startech). Nuclei were stained using Hoechst 33342 (Life Technologies).

Transmission electron microscopy (TEM)**:** RPE cells immobilized on a membrane were fixed in Karnovsky's fixative and prepared for TEM as described previously (Skottman et al., 2006).

PEDF assay on spent media was completed using a developmental ELISA (Meso Scale Discovery Platform S600, Mesoscale, USA) according to manufacturers' instructions**.**

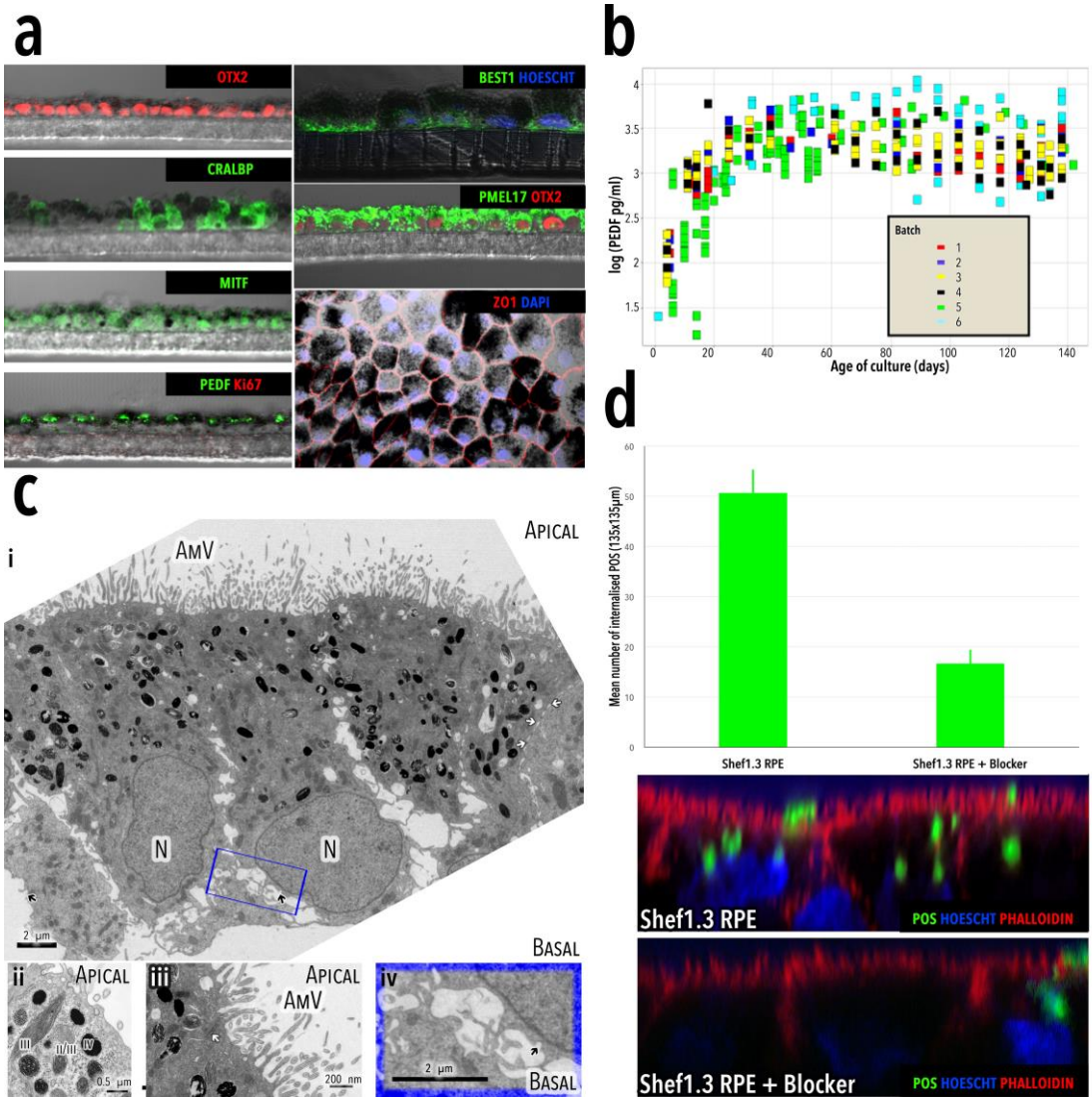

Figure 2-3: Cell characterization of the Shef 1.3 hESC-derived RPE:
(a) Confocal brightfield immunofluorescent micrographs depicting staining for typical regional RPE markers as part of the characterization of the monolayer as RPE. Predominantly apical PEDF and basal BEST1 expression confirms polarity of these cells. PMEL17 expression confirms presence of premelanosomes and correct ZO1 expression allows easy identification of tight junctions. Absence of Ki67 confirms that cells are not proliferating. Other characteristic RPE markers (CRALBP, MITF, OTX2) are also present crucial for melanogenesis and visual cycle. BEST1 – bestrophin 1; CRALBP – cellular retinyladehyde-binding protein; DAPI – diamidino-2-phenylidole; MITF – microthalmia transcription factor; OTX2 – orthodenticle homeobox 2; PEDF – pigment epithelium-derived factor; PMEL17 – premelanosome protein 17 and ZO1 – zonula occludens 1.
(b) Quantification of pigmented epithelium derived growth factor (PEDF) secretion in spent culture medium during late expansion phase, analysed using an ELISA assay. The classical RPE PEDF secretion asymptote is visible from around 3 weeks onwards. Each different coloured box represents a separate batch of tested cells.
(c) Electron micrographs of RPE cells, illustrating the classical ultrastructure associated with normal RPE function including tight junctions (white arrows; I

and iii), basal infoldings (black arrows; i and iv), apical microvilli (i-iii) and melanin granules (i-iii) revealing various stages of melanogenesis (ii; stage II/III, III melanosomes and stage IV mature melanosomes). N – nucleus, AmV – apical microvilli.
(d) Demonstration of *Shef 1.3 derived RPE* phagocytosis by the ability of Shef 1.3 derived RPE cells to internalise photoreceptor outer segments (POS). The level of phagocytosis was also examined after treatment of the Shef 1.3 RPE with MERTK antibody (Shef1.3 RPE + blocker). Data shown are mean internalised POS ± SEM (n=9). Pre-incubation with MERTK antibody had significant effect on the number of POS ingested by Shef1.3 RPE ($p<0.00001$, Student t-test, (n=9)). Below the graph, confocal micrographs show the internalised POS with a green fluorescent marker (POS) in Shef 1.3 derived RPE and relative absence in Shef 1.3 RPE with MERTK antibody (Shef1.3 RPE + blocker)(Figure from article published by the author (da Cruz et al., 2018)).

On the day of surgery, the transwell was removed from the culture plate and the hESC-RPE was seeded on a basement membrane-like artificial substrate. The membrane was 10µm thick polyethylene terephthalate (PET), with a 0.4µm pore size at a density of $1x10^8$ pores/cm^2 (Sterlitech, Kent, Washington, USA). The hESC-RPE-BM sheet was placed directly onto the purpose designed punch-cutting device. The transplant was cut with a single, sharp move, thus minimising the tissue trauma and the cell loss. The final product or 'patch', consisted of a monolayer of RPE on the human vitronectin coated polyester substrate (BM), approximately 30 µm thick in total, which was placed into the storage solution (0.9% sodium chloride) within the storage container that was then sealed (**Fig. 2-4**). The patch was assessed visually through the clear lid of the storage container for integrity, pigmented cell coverage and viability. The patch was transported out of the GMP facility and transferred to the operating theatre.

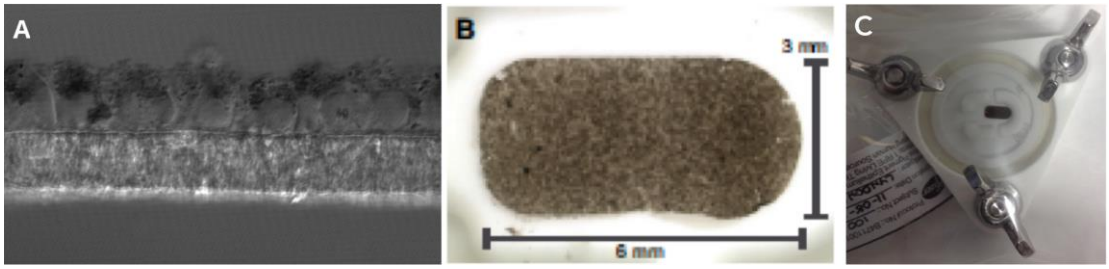

Figure 2-4: The hESC-RPE on a synthetic BM patch. A: Cross-section of the patch showing a monolayer of polarised RPE cells on top of a polyester membrane. B: En face photo of the patch showing lozenge shape, size and pigmentation. C: Patch within the storage container.

2.2. Clinical methods - Subjects

Approval was granted from the U.K. Medicines and Health Products Regulatory Authority (MHRA), the Gene Therapy Advisory Committee (GTAC), the Moorfields Research Governance Committee and the London - West London & GTAC Research Ethics Committee. The study complied with Good Clinical Practice guidelines according to the European Clinical Trials Directive (Directive 2001 EU/20/EC), the Declaration of Helsinki and has an independent External Data Monitoring Committee (E-DMC). Informed consent was obtained from each subject.

Two subjects with acute visual deterioration due to severe neovascular AMD received the trial hESC-RPE implant and both were followed-up for at least two years.

2.2.1. Baseline characteristics - Subject 1 (Figure 2-5a)

The first subject was a 60-year-old Caucasian female who had been suffering from bilateral Polypoidal Choroidal Vasculopathy (PCV), an idiopathic exudative maculopathy, which is broadly considered as a subtype of neovascular age-related macular degeneration (wet AMD), commonly presenting with pigment epithelial detachment (PED), neurosensory retinal detachment and subretinal haemorrhage. She had initially appeared with a large subretinal haemorrhage in her left eye, for which she was treated with a series of three, monthly, intravitreal anti-VEGF injections and subsequently a vitrectomy for persistent vitreous haemorrhage. The course of her disease left her with a compromised visual acuity in her left eye (LE), which was stabilised to approximately 2/60 (Snellen VA). One and a half years later, she presented with a large PED in her right eye (RE), which was attempted to be treated with an intravitreal anti-VEGF injection, but failed and lead to a large subretinal haemorrhage, occupying almost the whole macular area and causing acute RE vision deterioration to the level of counting fingers (CF). According to the course of her disease, she met the inclusion criteria for our trial and she was recruited for the investigational SC-derived RPE graft implantation in her RE.

2.2.2. Baseline characteristics - Subject 2 (Figure 2-5b)

The second subject was an 84-year-old Caucasian male who had been suffering from bilateral wet AMD, which for the RE was initially attempted to be treated with a course of two, monthly, intravitreal anti-VEGF injections. The treatment did not succeed to suppress the activity of the disease, resulting in worsening of macular oedema, a RPE tear and a large submacular haemorrhage with subsequent break-through into the vitreous. His RE vision dropped acutely to the level of hand motion perception (HM) and as he met the inclusion criteria, he was recruited to participate in the study.

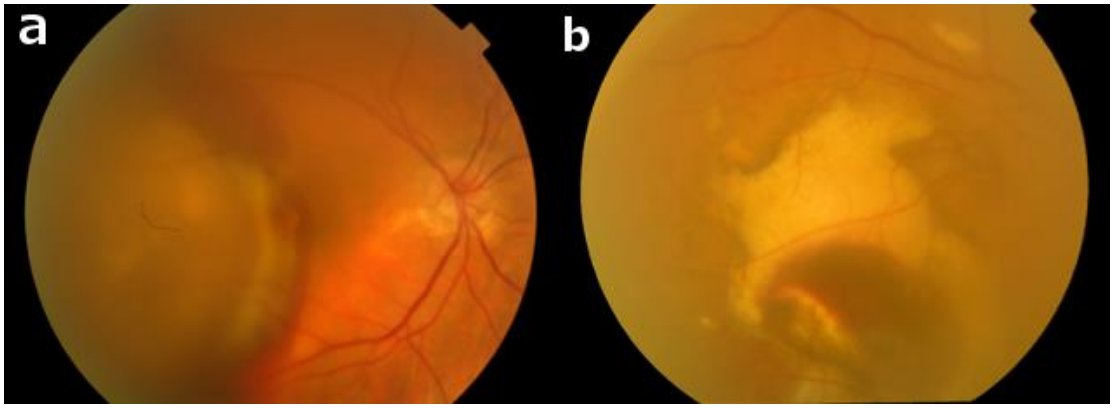

Figure 2-5: Baseline condition of the macula of the two subjects.
a. Colour fundus photo of Subject 1 at screening, showing a large subretinal haemorrhage and neuro-retina detachment involving the temporal part of the macula up to the fovea.
b. Colour fundus photo of Subject 2 at screening, showing a combination of an old (appearing white, due to decomposed haemoglobin) and new (appearing red, as more recent) subretinal haemorrhage, occupying almost the whole macular area. The compromised clarity of the photo indicates the presence of a “spil-over” vitreous haemorrhage too.

2.3. Clinical methods - Surgical procedures

2.3.1. hESC-Derived RPE patch implantation procedure

The main study intervention was a surgical operation to insert a single hESC-RPE patch (PF-05206388) into the subretinal space of one eye (study eye) with follow-up of at least 2 years. The nominal dose strength was 100000 cells on 17 mm^2 (5800 cells/mm^2).

The first surgical procedure involved the following steps: The subject underwent standard general anaesthesia prior to surgery. Surgery

commences with routine preparation and sterilisation of the eye with povidone iodine 5%. Following drying of the skin, the face and eye was draped with standard vitrectomy disposable sterile drapes and the eyelids separated with a disposable Barraquer speculum. A conjunctival peritomy with standard 23 gauge infusion and 2 scleral ports were prepared before completion of a pars plana vitrectomy (PPV) with induction of posterior vitreous detachment (PVD) if not present. 360 degrees Argon Laser retinopexy was performed in the retinal periphery. A detachment of the neurosensory retina was induced at the macula using a 41 Gauge (41G) *de Juan* cannula. The retinotomy was enlarged with a 20G MVR blade and the sub-retinal space was irrigated to remove all blood and fibrin. The temporal scleral port was widened and a purpose-designed delivery device was used for insertion of the investigational product into the subretinal space, so as to minimise to protect the cells from mechanical damage (**Fig. 2-6**). The patch was loaded using forceps, straight from the container into the tip of the injector, where it was partially folded in a semi-cylindrical (“taco-like”) shape (**Fig. 2-6B**). Subsequently, the injector was advanced in the vitreous cavity to reach the posterior pole, where the retinotomy had been prepared, broad enough to enclose the tip of the tool. The patch was then gently pushed out through the tip by the mechanically driven rod of the device, and released into the submacular space (**Fig. 2-6D**). Compression of the macular detachment with heavy liquid was performed until the macula was re-attached and the retinotomy was lasered. A routine search in the retinal periphery was completed with cryotherapy to any breaks. Air/fluid exchange was carried out followed by air/silicone oil exchange. The ports were closed and the infusion removed. 40 mg of triamcinolone acetonide and 250 mg of cefuroxime were injected in the sub-tenon space, together with a local anaesthetic (0.5% bupivacaine).

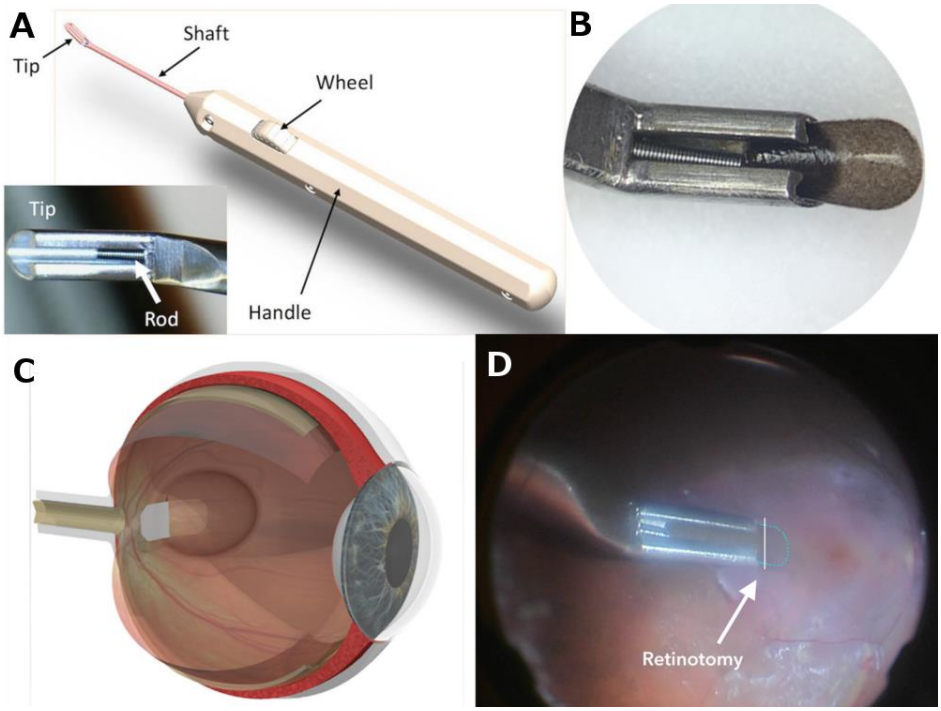

Figure 2-6: The purpose-designed tool and the surgical implantation. A: the insertion tool comprised of handle, shaft and tip, which is also shown magnified (bottom left). B: A simulated patch loading in the tip of the introducer. C: Schematic representation of the submacular insertion of the implant. D: Photograph taken from the operating microscope showing the subretinal implantation of the graft through the retinotomy.

Subject 1 had significant cataract noted at screening, which was removed at the same time of this surgical procedure via standard of care carried out at Moorfields Eye Hospital – Phacoemulsification and intraocular lens insertion.

2.3.2. Removal of Silicone Oil (ROSO) procedure

The second surgical procedure was planned for the 10th post-transplantation week, to remove from the eye the oil inserted at the initial transplantation surgery.

General or local anaesthesia – according to subject's preference – was delivered. Standard PPV preparation and draping of the eye was carried out. A 23 G infusion was placed and a second port was created to aspirate the oil using either active or passive modalities. Following the ROSO the retina was examined with a third port added to receive a light pipe. Air/fluid exchanges were performed until the complete ROSO from the vitreous cavity. All ports

were closed and a standard fluocinolone acetonide implant was either sown to the temporal sclera with a prolene suture or injected intra-vitreally. Subconjunctival cefuroxime 250 mg was injected as a prophylaxis.

2.4. Clinical methods - Structural assessments

2.4.1. Biomicroscopic Evaluation

The biomicroscope is and instrument that consists of a special beam of light in the form of a slit and a pair of magnifiers mounted on a frame in order to examine the eye. Using it allows the specialist to see a magnified and illuminated image of the eye. In order to see inside the eye, special lenses need to be held between the light and the eye. These lenses do not touch the eye but allow a wide field illuminated view of the retina. The subject keeps the chin on a special frame that keeps the head and eye still. The biomicroscope examination is a standard way of examining the eye in the clinic. Subjects were imposed to full ophthalmological examination using a Haag-Streit 900 slit-lamp (Koeniz, Switzerland), including both anterior and posterior segments of the eye, during screening and during study visits on days 0, 2, on weeks 1, 2, 4, 8, 10, 12, 16, 24, 36, 52 and on months 18 and 24.

2.4.2. Fundus photography

Colour and red-free fundus photographs were acquired using the Topcon TRC Retinal Camera (Oakland, NJ, USA). After full dilatation of pupils, colour and red-free photos of the fundus from each eye are acquired.
The following provides information as to the method used; variations that would provide sufficient information for an accurate assessment of structure were also permitted.
For digital capture of fundus images, the following fields were required:

- Field 1 – Disc: Centre the optic disc at the intersection of the cross hairs in the ocular.
- Field 2 – Macula: Centre the macula at the intersection of the cross hairs in the ocular.

- Field 3 – Temporal to Macula: Macula at the nasal edge of the field.

A stereoscopic fundus reflex photograph was also taken to document media opacities. Fundus photographs were obtained during screening and on study weeks 2, 4, 8, 10, 12, 16, 24, 36, 52, and months 18 and 24.

Series of CF photos and image editing software (Adobe Photoshop, Adobe Inc., CA, US) were used for the study of the patch's location, post-implantation. Specific landmarks were set on the CF photos, namely the centre of the optic disc (**od**) and two bifurcations of retinal vessels, one superior (**bf1**) and one inferior (**bf2**) to the patch (**Fig. 2-7**). The two diagonals (**d1** and **d2**) and geometric centre of the patch (**gc**) were also detected and marked.

To examine a possible linear movement along the retinal plane, the distance of the geometric centre of the patch from the predefined retinal landmarks was measured, in CF photographs from weeks 2, 4, 12, 24 and 52. Specifically, the disc-to-patch distance (**od-gc**) was used for the nasal-temporal (horizontal) direction, while the distances between the two bifurcations and the patch's centre (**bf1-gc** and **bf2-gc**) were used for the superior-inferior (vertical) direction. To examine a rotational movement, the angle (**^**) between the diagonal (**d1**) of the patch and the "optic disc – to – centre of the patch" direction (**od-gc**) was also measured in the corresponding photographs. The width of the patch, known to be 3 mm, was used as a constant for the distance calculation in the CF photos.

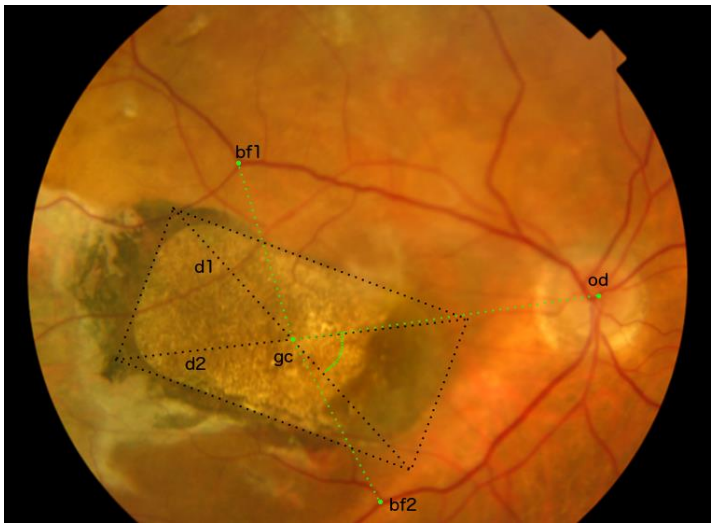

Figure 2-7: Landmarks for the patch's location: CF photo (post-implantation) showing the retinal landmarks used to examine the stability of the patch's location during the follow-up.

2.4.3. Fundus Fluorescein angiography (FFA)

A fluorescein angiogram is a test that provides information about the blood perfusion of the retina. The examination is performed by injecting a sodium-based dye (20% Fluorescein NaCl) into an arm vein. On average the dye appears in the retinal blood vessels10-15 seconds after injection. As the dye travels through the retinal blood vessels, an ophthalmic photographer takes pictures of the retina with a special camera. The Topcon fundus camera was used for this study.

Any abnormalities on the retina or retinal vasculature, such as microaneurysms and neovascularisation would be highlighted by the dye. Transit of fluorescein may also show: leaking, staining or by its inability to get through blocked blood vessels. In addition, the dye may be visible through window defects of the retinal pigment epithelium following laser or scarring. FFA was obtained during screening and on weeks 4, 8, 12, 24 and 52, using the Topcon TRC Retinal Camera (Oakland, NJ, USA). Indocyanine Green angiograms were obtained during subjects' screening, to confirm eligibility.

2.4.4. Optical Coherence Tomography

Spectral domain optical coherence tomography (SD-OCT) allows visual assessment of the retinal segmentation due to the differential optical density and reflective properties of its layers. A superluminescent diode provides wide bandwidth low-coherent light for the interferometer within SD-OCT. A spectrometer then performs Fourier analysis of the spectral fringe to determine the reflectivity as a function of depth of tissue. This is the equivalent of an A-scan on an ultrasound. With fast scanning speed (20,000-40,000 A scans per second), the SD-OCT is able to produce 2 and 3 dimensional images of the macula.

The following provides guidance as to the method used; variations that provide sufficient information for an accurate assessment of structure were also permitted.

The target eye is dilated with one drop each of tropicamide 1% and phenylephrine 2.5%. The Spectralis OCT device was used (Heidelberg Engineering GmbH, Heidelberg, Germany). We used high speed volume scan and high speed Enhanced Depth Imaging (EDI) volume scan to cover the

central 20° x 20° with 49 sections, ART 12 protocol, centred on the fovea. This was done concurrently with infrared (IR) and autofluorescence (AF) imaging. Two optimal scan sets (with IR or AF) were acquired using the follow-up option. OCT scans were captured during screening and on weeks 4, 8, 12, 16, 24, 36, 52, and months 18 and 24.

2.4.5. B-mode Orbital Ultrasound

B-mode ultrasound (U/S) testing involves measuring the return echoes from ultrasound delivered through a closed eyelid. The probe is applied to the lid skin and coupled with a conducting gel. It measures the length of the eye (axial length) and images the echogenic interfaces inside the eye to give an indication of the retinal contour, even in the presence of opacity of the ocular media. U/S scans were captured using the ACUSON Sequoia512 system (Siemens Healthcare, USA), during screening and on weeks 4, 8, 16, 24, 36 and 52.

2.4.6. Adaptive Optics Imaging

An adaptive optics (AO) camera uses a deformable mirror to reduce optical aberration of light reflected from the human eye. This improves the lateral resolution of the camera to enable visualisation of the cone photoreceptor outer segment tips that act as closely packed wave-guiding optical fibres.

The used system was the ImagineEyes RTx1 Camera (Orsey, France). The following provides guidance as to the method used; variations that provide sufficient information for an accurate assessment of structure were also permitted.

Pupils were dilated with 1 drop each of tropicamide 1% and phenylephrine 2.5%. The subject rested their head on a chin rest to align with the system. The AOC system was switched on for data collection to start. Alignment and data collection was repeated for several retinal locations. AO images were obtained during screening and on weeks 16, 24, 36, 52 and months 18 and 24.

2.4.7. Fundus Autofluorescence

The RPE contains melanin and lipofuscin pigments. Autofluorescence (AF) produced by both of these pigments can be visualised by various modalities of the Heidelberg Spectralis confocal scanning laser ophthalmoscope (SLO). The patterns seen in these images provide information on the health and physiology of the RPE cells as well as their disease progression.

Short-wavelength (blue or green) excitation to the fundus produces AF. This has been shown to derive from the RPE lipofuscin. Similarly, near-infrared (red) excitation to the fundus also produces AF. This was first reported by Piccolino et al. using a video-imaging system while investigating pseudofluorescence in ICG angiography (Piccolino, Borgia, Zinicola, Iester, & Torrielli, 1996). However, Keilhauer and Delori showed that the source of near-infrared AF was melanin within the RPE and choroid (Keilhauer & Delori, 2006).

The Heidelberg Spectralis SLO device was used (Heidelberg Engineering GmbH, Heidelberg, Germany). Images were acquired with 30° x 30° field to cover the macula and centred on the fovea. This field size is large enough to collect light simultaneously from the retina and choroid, while rejecting light originating from the lens and from a large part of the vitreous. The SLO was switched to short-wavelength at 488 nm for autofluorescence A[488] imaging (FA mode). And a series of images were acquired until the acceptable image quality was achieved. AF photographs were captured during screening and on weeks 4, 8, 12, 24, 36, 52, and months 18 and 24.

2.5. Clinical Methods – Functional assessments

2.5.1. Fixation and Microperimetry

The examination of a subject's fixation assesses their ability to maintain their gaze position on a single given location. For this, a specific pre-selected target (most commonly a cross) is projected by the examining device onto the subject's retina, for at least 30 seconds, and the subject is instructed to keep looking at the target, as steadily as possible. During the exam, the device is tracking and recording the span of the eye movements. The results are then

reflected as percentage of the subject's fixation points, falling within a specific radius from the centre of the given target.

Microperimetry (MP) measures light sensitivity (the minimum luminance of a white spot stimulus, which superimposed on a white background of uniform luminance is necessary for the stimulus perception) and uses an eye tracking system to maintain the location of the stimuli regardless of any changes in fixation. This allows the stimulus to be projected consistently in a pre-selected retinal area.

In our study, fundus-controlled fixation and Microperimetry (MP) were performed using purpose-designed stimuli grids and testing protocols set in the Nidek MP-1 microperimeter (NAVIS software version 1.7.2; Nidek Technologies, Padova, Italy). Special effort was applied to adjust the examining grid in order to be projected onto the treated area. The Nidek MP-1 allows the examiner to view the fundus on the computer monitor while it is imaged in real time by an infrared fundus camera (768 x 576 pixels resolution; 45° field of view). Fixation target and stimuli are projected on to the liquid crystal display (LCD) within the MP1 for the subject to view. The examiner can also view the overlaid graphic of the threshold values and fixation loci as part of the video image on the computer monitor. Background luminance is set at 1.27 cd/m^2 (white, within the high-mesopic range). Stimulus intensity can be varied in 1 dB (0.1 log) steps from 0 to 20, where 0 dB represents the brightest luminance of 127 cd/m^2. Therefore, the total range is 2 log units. The MP1 also incorporates an automated tracking system to compensate for eye movement during examination. An infrared image of the fundus is captured immediately prior to the examination to allow areas with high contrast (e.g., large vessels, disc margin or pigmented lesions) to be chosen for tracking. This reference landmark is tracked every 40 ms (25 Hz) to allow correction of the stimulus position on the internal LCD in order to maintain the same test locations on the fundus.

Pupils were dilated with one drop each of tropicamide 1% and phenylephrine 2.5%, at least 15 minutes prior to microperimetry, in a darkened room. Both eyes were tested individually with the contralateral covered. For fixation tests, a 2°- 3° single red-cross target was used and subjects were asked to fixate steadily for a 30 seconds recording of fixation

stability. After the fixation assessment, subjects had a brief training session to allow familiarisation with the microperimetry test and to practise the correct operation of the response trigger relative to the stimulus target. This was then followed immediately by the microperimetry test. For the test stimulus, the colour was white, the duration was set to 200 ms and the size was initially Goldmann III (26 min of arc or 0.4 degrees), increased to Goldmann V (104 min of arc or 1.7 degrees) if the subject would not respond to Goldmann III stimuli. We used a customised grid covering the retinal area corresponding to the transplanted patch. The same fixation and microperimetry tests were performed up to 3 times for the study eye with a short break in between each. For the non-study eye one assessment of each microperimetry and fixation was done.

Automated or manual alignment and registration of the infrared images was performed for follow-up microperimetry by selecting 2 high contrast landmarks within 2 separate 2 x 2 square regions (e.g. the vascular arcades, disc or pigmented lesion). The software could then automatically detect the same landmarks in the follow-up infrared image. Fixation and Microperimetry were examined during screening and on weeks 4, 16, 24, 36, 52, and months 18 and 24.

2.5.2. Best Corrected Visual Acuity

Visual acuity is a measure of the spatial resolution of the visual processing system and is assessed by requiring the subject to identify so-called optotypes, which are represented as black symbols against a white background (hence at maximum contrast), from a defined distance.

For the purposes of this study, the Best Corrected Visual Acuity (BCVA) was tested using the Early Treatment of Diabetic Retinopathy Study (ETDRS) chart. Each line of this chart has 5 letters the size of which increases from line to line in steps of 0.1 logarithm of minimum angle of resolution (logMAR). Each correctly read letter is assigned to 0.02 logMAR, which results in a 35 letter score being equivalent to 1.0 logMAR or 6/60 and an 85 letter score being equivalent to 0.0 logMAR or 6/6. The subject is firstly examined at 4 m distance. When 20 or more letters are read correctly at 4 m, the VA score is equal to the total number of letters read correctly plus 30. If

fewer than 20 letters are read correctly at 4 m, the visual acuity letter score is equal to the total number of letters read correctly at 4 m (number recorded on line 1.0) plus the total number of letters read correctly at 1 m in the first six lines.

Each assessment started with a subjective refraction test, using trial lenses, in order to obtain the best possible refractive correction for each eye. The test was conducted in each eye separately, by blocking the fellow eye with a patch. The subjects were asked to look directly at the chart and eccentric viewing was excluded by observation of the subject during the test.

BCVA was examined during screening, on days 0 and 2, weeks 1, 2, 4, 8, 12, 16, 24, 36, 52, and months 18 and 24.

2.5.3. Contrast Sensitivity

Contrast sensitivity (CS) is a measure of the ability to discern between luminance of different levels in a static image. Diminished CS may cause decreased visual function in spite of normal or near-normal visual acuity (Hashemi et al., 2012).

For the purposes of this study, CS was examined using the Pelli-Robson contrast sensitivity chart. This chart comprises of letters with a descending contrast relative to a white background. The letter sequences are organised into triplets within each, all letters have the same contrast. Each line has two triplets and the contrast decreases from one triplet to the next, even within one line. The chart follows the luminance, font, and letter spacing recommendations of the Committee on Vision of the National Academy of Sciences and National Research Council. The test was conducted in each eye separately. The subjects were asked to read progressively lower contrast letters from a distance of 1 m. Room illumination was kept at 85 cd/m^2. The score calculated in log units could range from 0 to 2.25. The achieved CS score was the log unit of the last triplet where at least 2 of the 3 letters where read correctly.

2.5.4. Reading Ability

The subject's reading ability was assessed using the Minnesota Reading Test (MNREAD). The MNREAD charts were used to assess the visual processing

capabilities and eye-movement control required for normal text reading. In these charts each sentence contains 60 characters (including a space between each word and at the end of each line) printed as three lines with even left and right margins. The vocabulary used in the sentences is selected from high-frequency words that appear in second- and third-grade reading material. The charts contain sentences with 19 different print sizes. From the recommended viewing distance of 40 cm the print size ranges from +1.3 to -0.5 logMAR (Snellen equivalents: 20/400-20/6). The reading ability is considered to be reflected at the maximum reading speed (RSmax) value, as explained bellow.

The test was conducted in each eye separately. The subjects were asked to read each sentence separately and the examiner was recording the time (in seconds) required, as well as the number of errors made by the subject for each sentence. For each of the read sentences, a reading speed (RS) value in words per minute was calculated using the formula:
RS (words/minute) = 60 x (number of words read – number of errors) / (time in seconds). The RSmax was then derived as the mean of the three fastest sentences read at each visit.

The MNREAD test was performed during screening and on weeks 4, 8, 16, 24, 36, 52, and months 18 and 24.

2.6. Clinical methods – Immunosuppression

Both subjects received an immunosuppressive regimen in association with the two surgical procedures (the hESC-RPE transplantation operation and the removal of oil operation). For the first surgery, both subjects received oral prednisolone in a course starting from 2-4 days pre-operatively with 1 mg/kg/day dose (up to 60 mg/day maximum) and continued for at least 2 weeks after the surgery. Subsequently, the dose was tailed off over at least 2 further weeks. For the second procedure, both subjects received 1 mg/kg/day prednisolone starting 1 week pre-operatively and continued for 2 weeks post-operatively and tailed off within 1 further week. Additionally, at the end of the transplantation procedure, each subject received a single dose of sub-tenon

triamcinolone (40mg), reflecting the standard of care for this type of ocular surgery. Finally, each subject received an intravitreal implant of fluocinolone acetonide, as a long-lasting local immunosuppressive, at the end of the oil removal operation.

2.7. Clinical methods – Safety assessments

2.7.1. Ocular oncologist review

Both subjects underwent ophthalmic examination by a specialized ocular oncologist on post-op. weeks 2, 4, 8, 12, 16, 24, 36 and 52. This also included review of B-mode orbital ultrasound (2.4.5) for the exclusion of any ocular or orbital tumor formation.

2.7.2. Physical examination

Both subjects underwent physical examination at baseline, at screening/day 0, weeks 10 and 52 and months 18 and 24. This would include assessment of the general appearance, cardiovascular (including Electrocardiography), respiratory, central and peripheral nervous systems, musculoskeletal, gastrointestinal system and lymph nodes. Examination would be further focused, according to any symptoms and general health issues reported by the subjects.

2.7.3. Laboratory tests

Full blood count (FBC), basic blood biochemistry - including renal and liver function - and basic urinalysis were regularly examined during the 1st year's follow-up visits (screening, day 0, weeks 1, 2, 4, 8,12,16, 24, 36 and 52).

2.7.4. Radiology

A chest X-Ray image was captured at screening and at year 1. A liver ultrasound was performed and reviewed by a specialist hepatologist, at screening and weeks 24 and 52.

2.7.5. Electroretinogram (ERG) and Electrooculogram (EOG)

The full-field ERG is a mass electrical response of the retina to photic stimulation. It is a test to assess the overall functional status of the retina, by recording the electrical responses of the eye after stimulation with a light source (flash). There are two main components of the recording: the a-wave, which is the first negative component that reflects the general physiological health of the photoreceptors in the outer retina, and the b-wave, which follows the former and reflects the health of the inner retinal layers, including the bipolar and Muller cells. The amplitudes and timings of both components will be measured and documented.

The EOG measures the changes of the electric potential between the cornea and the Bruch's membrane (thus between the anterior and posterior pole of the globe), during from-side-to-side eye movements in alternated bright light and dark adaptation conditions. The potential is expected to be low in the dark ("dark trough") and rise significantly when the light is turned on ("light peak"). The "light peak" to "dark trough" ratio is then calculated and normally should be approximately 2:1 or greater. Ratios less than 1.7 are considered abnormal.

Both ERG and EOG were performed according to the International Society for Clinical Electrophysiology of Vision (ISCEV) standards, using the Espion Visual Electrophysiology System (Diagnosys LLC, MA, US) in screening and weeks 12 and 52, and were reviewed by a specialist electrophysiologist, in order to exclude potential toxicity of the investigational implant, to the retina and the RPE.

2.8. Contributions to the study methods

- The primary protocol and ethics forms for the phase I study of the implantation of the hESC-RPE, as well as the long-term follow-up study were written by Professor Lyndon Da Cruz and Professor Peter J. Coffey in collaboration with Pfizer clinical and regulatory teams (Appendix 2 and 3). The author contributed to the amendments of the original study protocols.

- The hESC-derived RPE patch graft was grown by the Roslin Cells Ltd. (Edinburgh, UK). The final preparation of the patch was done at Cells for Sight, Institute of Ophthalmology laboratory, directed by Professor Peter J. Coffey.
- All surgical procedures described in this thesis were performed by Professor Lyndon Da Cruz
- The biomicrospopy examination and the physical examination were performed by the author.
- The BCVA, CS and MNREAD tests were performed by independent research optometrists. All data were collected and analysed by the author.
- The fundus photography, angiograms, OCTs and AF images were obtained by specialised research photographers. The author directed and provided instructions to customise imaging procedures. All imaging data were collected and analysed by the author.
- The AO retinal images were obtained by the author and a specialised psychophysicist. The images were analysed by the author.
- The fixation and MP examinations were performed by the author. The customized stimuli grid was designed and programmed in the Nidek MP-1 software by the author. All relevant data were obtained and analysed by the author.
- The physical examination was carried out by the author.
- The chest Rx and U/S were obtained by specialised radiologists. The images were analysed by the author.
- The blood test results were assessed by the author.
- The electrophysiological tests of the two subjects were performed by the Electrodiagnostic Department,of Moorfields Eye Hospital and interpreted by Professor Graham Holder and Dr. Anthony Robson, of the named department.

Chapter 3

First year outcomes - Structure

Introduction

The baseline condition of the two subjects has been described in the methods chapter, as well as the surgical procedure that included standard vitrectomy and submacular implantation of the investigational hESC-RPE patch. Subject 1 also had the crystalline lens of her study eye removed by standard phacoemulsification and replaced with an artificial intraocular lens at the same operation. This was in order to facilitate the introduction of the patch inserting device and to exclude any effect of an advancing cataract onto the study outcomes. Subject 2 was already pseudophakic when recruited.
In this chapter I will present the structural outcomes for the first post-operative year, starting from the safety of our treatment and continuing with the anatomical results, as these were assessed by multimodal imaging techniques.

Results

3.1. Outcome of surgical operation

By the end of their operations, both subjects had the hESC-RPE patch implanted, intact and secured in the subretinal space of their macula, properly orientated - with the artificial basement membrane adjacent to the choriocapillaris and the polarised RPE cells immediately under the neuro-retina. Silicone oil was used to fill the vitreous cavity and stabilise the retina for the early post-operative period.

At this point it would be useful to mention two specific intra-operative incidences that we came across, one for each subject: In subject one we experienced some tissue resistance while positioning the patch under the fovea, which we believe resulted in placing the nasal ¼ (approximately) of the patch under the host RPE, thus in the sub-RPE space instead of the subretinal space (**Fig. 3-3 & 3-8**). In the second subject we experienced some difficulty while manipulating the patch with the micro-surgical forceps, which

we believe it resulted in traumatising the inferior temporal edge of the implant causing either a small detachment of the hESC-RPE from its artificial BM, or an inadvertent removal of a small fragment of the hESC-RPE (**Fig. 3-4**).

The second operation, for the removal of the silicone oil (ROSO) had been planned for the post-transplantation week 10. For the first subject it was performed as per protocol and the whole procedure was straightforward and was combined with the insertion of a long-acting fluocinolone acetonide steroid implant (*RETISERT*, Bausch & Lomb) into the vitreous cavity. However, the second subject had a post-operative complication after the initial (implantation) surgery consisting of an inferior tractional retinal detachment (RD) due to proliferative vitreo-retinopathy (PVR), which was detected on his week 8 visit. This RD was surgically repaired 3 weeks later with a further vitrectomy, epiretinal membrane peeling and inferior retinectomy under silicone oil. The oil was retained and its removal was deferred for a future date and finally took place during follow-up month 5. The fluocinolone acetonide steroid implant for this subject (*ILUVIEN*, Alimera Sciences) was inserted during the RD repair operation (week 11) and subsequently it was identified and retained in the vitreous cavity during the ROSO operation.

3.2. Safety outcomes

All of the assessments for safety have been documented in the methods section (Chapter 2). It is out of the scope of this chapter to report in detail all of the results of the general health examinations and I will focus on the abnormal ones, which have been recorded as adverse events (AEs) within the study.

Generally, the hESC-derived RPE transplant was well tolerated by both subjects without significant safety concerns that were attributable to the implanted cells. No signs of severe rejection or uncontrolled proliferation were detected, during the first follow-up year. We reported a total of 16 AEs, 10 for the first subject and 6 for the second. From those, 10 were ocular - 7 for subject 1, 3 for subject 2 - and 6 were general health-related. 3 were

considered as serious adverse events (SAEs), since their management required admission to the hospital and/or further surgery. None of the AEs or SAEs was assessed as being caused by the investigational hESC-RPE patch. The ocular AEs were all related to the surgical operations. The non-ocular ones were either related to the concomitant medications or were unrelated to the study procedures and medications.

3.2.1. Subject 1 SAEs:

- Conjunctival dehiscence over the scleral Retisert implantation site in the study eye, 1 week after the second procedure (study week 12): considered as a SAE, since the subject had to be admitted in the hospital and undergo an additional operation (“conjunctival flap”) to repair the dehiscence. It was resolved without sequelae.

3.2.2. Subject 1 AEs:

- Hyphaema in the study eye, at post-op week 1: related to the initial surgery and spontaneously resolved without sequelae within one week.
- Corneal oedema in the study eye, at post-op week 1: related to the initial surgery and spontaneously resolved without sequelae within one week.
- Metamorphopsia (distorted vision) in the study eye, from week 6 onwards: considered as related to the procedure or background disease, as this has also been reported by patients who have had macula off retinal detachments (Lina, Xuemin, Qinmei, & Lijun, 2015) or AMD (Wiecek, Lashkari, Dakin, &Bex, 2015).
- Oral inflammation at post-op week 6: related to a gum inflammation, unrelated to the study procedures.
- Hypotony with choroidal effusion in the study eye, one week after the second study procedure for ROSO and fluocinolone implant (study week 12): related to the surgery and spontaneously resolved without sequelae within 4 weeks.
- Exposure of scleral suture loop through conjunctiva of the study eye, at month 6: related with the fluocinolone implant procedure. A loop of the

scleral nylon suture used to suspend the steroid implant into the vitreous cavity eroded the overlying conjunctiva and was intermittently protruding. The loop was cut and removed, however, the protrusion recurred later from another loop, due to conjunctival thinning. No further action was taken, since the thinning of conjunctiva decreased the chances for a permanent repair and also the AE was intermittent and did not persist in consecutive visits.

- Reduction of rod ERG in study eye at month 6: possibly related to the study procedures. No action was taken, since the ERG is a general index of the retinal function and not specific for the host macula.
- Worsening of arterial hypertension at month 9: Not related to the study. Management with amendment of antihypertensive treatment.
- Emesis during the FFA imaging at month 10: related to the study procedure (injection of Fluorescein NaCl solution). Single episode – no treatment required.

3.2.3. Subject 2 SAEs:

- Retinal detachment (RD) at week 8: related to the initial study procedure and constituted a SAE since it required admission and additional surgical treatment. The RD was associated with proliferative vitreo-retinopathy (PVR) with the RD localized to the inferior, peripheral retina. It was asymptomatic since it did not affect the subject's macula or the study patch. It was surgically repaired three weeks later and resolved without sequelae.
- Hyperglycemia secondary to oral prednisolone at post-op week 2: related to the concomitant perioperative medication (oral prednisolone). The subject was a type II diabetic and his blood sugar control was compromised by the steroid agent. This was a SAE, since it required hospitalization and addition of insulin in his regular anti-glycemic regiment.

3.2.4. Subject 2 AEs:

- Anaemia at week 8: unrelated to the study patch, possible relation with concomitant prednisolone. Resolved spontaneously without sequelae after 1 month.
- Epiretinal fibrosis and ERM in the study eye: related to the study procedures and to the aforementioned PVR RD. No treatment decided, since it might put the hESC-RPE patch at risk and the ERM did not seem to induce severe traction, as seen in OCT scans (**Fig. 3-11**).
- Reduction of cone ERG in the study eye: related to the study procedures and most probably to the longer retaining of the silicone oil due to the PVR RD. Resolved by year 1, when potentials returned to the baseline levels.
- Skin rash (Grover's disease) at year 1: idiopathic – unrelated to the study patch or the study procedures.

B-Mode orbital ultrasound, as well as regular review by a specialist ocular oncologist did not reveal any signs of tumorigenicity in either of the two subjects. The rest of the safety assessments, such as blood tests, chest radiography and liver ultrasound were also maintained within normal limits or showing clinically insignificant abnormalities.

3.3. Structural outcomes: Survival of the investigational patch, observation and description during year 1.

During the first year of follow-up, the hESC-RPE patch was examined by stereo-biomicroscopy, colour fundus (CF) photography, fundus fluorescein angiography and spectral domain optical coherence tomography, in terms of location, pigmentation, survival and structural relation with the host RPE.

3.3.1. Colour Fundus Photography – visual assessment.

In both subjects a uniformly pigmented patch was visually identified in the immediate post-implantation period. Both the slit-lamp fundoscopy and the observation of a series of CF photos showed that the graft retained its shape

and size, its subretinal position and its location in the macular area, without any obvious migration in the eye of the observer. The pigmentation of the implant remained over the bulk of its surface but showed changes over time. Its overall hue in the CF photos remained fairly consistent in the eye of the examiner, throughout the 12-month follow-up period (**Fig. 3-2**).

In order to accurately examine the patch's location for imperceptible changes over time, specific landmarks were set on the subjects' fundus photographs. The method is described in chapter 2 (section 2.4.2).

Since the patch retained its rectangular shape, without any noticeable malformation, and remained in the subretinal space without anteroposterior migration, as shown in the OCT scans during the follow up (section 3.3.2), the only possible movement would be along the plane of the retina, either linear or rotational. The distances between the centre of the patch and the centre of the disc and the two bifurcations were measured, as well as the angle between the patch's diagonal and the disc-to-patch line. The results are demonstrated in **table 3-1**.

The orientation of the patch, in terms of rotation, remained stable in both subjects throughout year 1. The measured angle (**od-gc^d1**) showed very minimal changes, which for subject 1 were from a minimum of 0.4° to a maximum of 1.3° and for subject 2 from 0.3° to 0.6°. The small range of these changes, combined with the fact that they were noticed in both directions (clockwise and counter-clockwise) in different time points, shows that the differences are most probably attributed to the margin of error of the calculation method, rather than an actual rotation of the patch.

In subject 1, the range of the **od-gc** changes was from 0.03 to 0.33 mm. The fact that these were noticed in both directions (temporally and nasally), and that the difference between the first (week 2) and last (year 1) measurement was only 0.06 mm, show that there was no significant migration in the horizontal axis. The range of the **bf1-gc** and **bf2-gc** changes was between 0.05 and 0.45 mm. Interestingly, the largest change was noticed around week 12, and was a decrease in both superior and inferior distances. This shows that the difference was most probably caused by changes in the retinal structure (the two bifurcations "approaching" each other and the

corresponding edges of the patch) and not from an actual movement in the vertical axis. The fact that this happened after the ROSO operation, where some retinal transformation is expected, and that the horizontal position was found stable, both support this assumption.

In subject 2, the **od-gc** changes ranged from 0.03 to 0.12 in both directions, which again shows good stability in the horizontal axis. The distance from the bifurcations showed larger variance, from 0.05 to 0.45 mm. On week 4, there is a small reduction in the **bf1-gc** and a larger increase in the **bf2-gc**. This could mean a superior migration of the patch. However, the fact that it is not symmetrical (0.06 against 0.21 mm) and that it was followed by an opposite change for **bf2-gc** in week 24 probably means that it was caused by the retinal changes due to the aforementioned inferior retinal detachment, which by week 24 had been repaired to a fully flat retina. This is also supported by the fact that the year 1 measurements are very close to the initial ones on week 2. Similarly to the first subject, based on these study, a systematic migration of the patch is very unlikely.

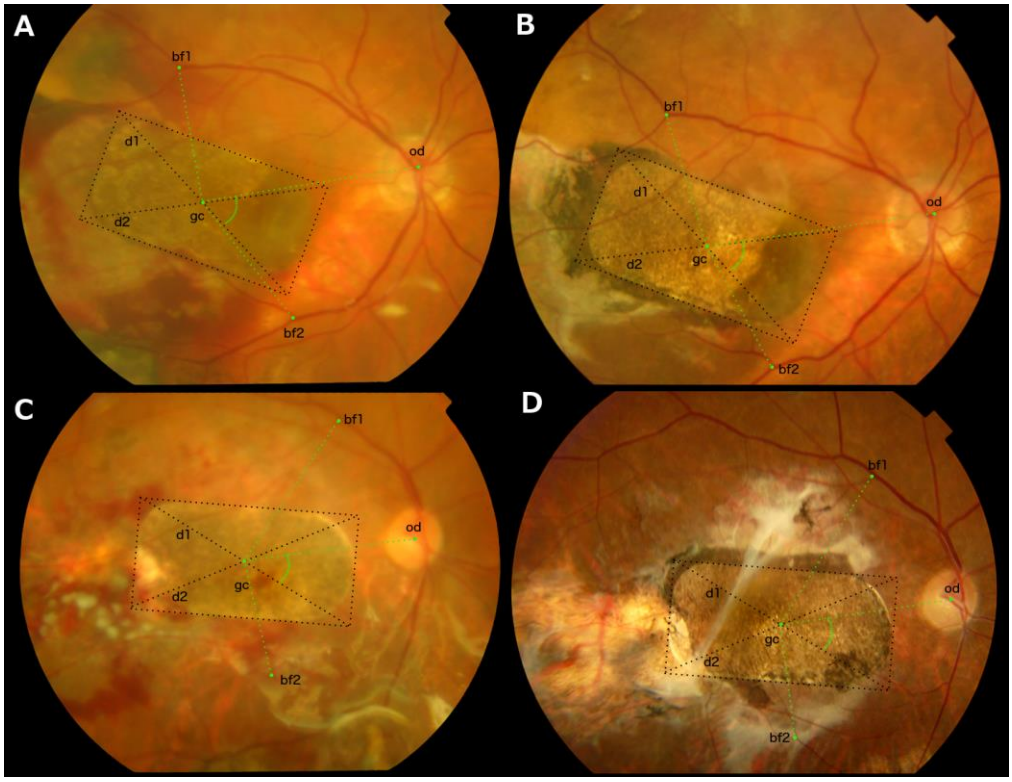

Figure 3-1: Assessment of the patch's location during year 1. Week 2 and year 1 CF photos from subject 1 (A&B) and 2 (C&D), respectively. Measured distances and angles are shown with green dotted lines, as described in main text. The method is described in chapter 2.

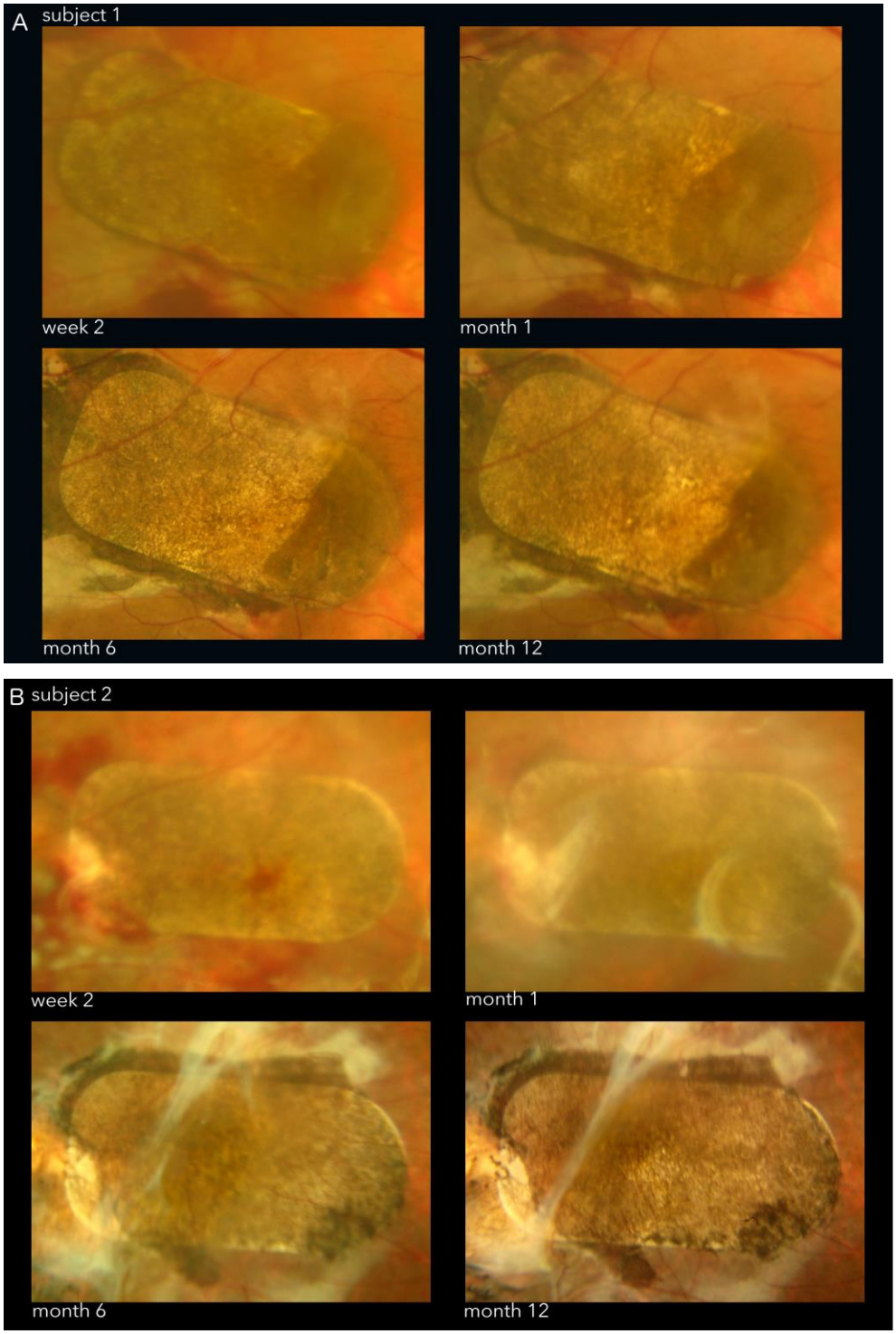

Figure 3-2: Pigmentation of the hESC-RPE patch during year 1. Series of CF photos showing the course of the graft's pigmentation from the early post-operative period up to the end of year 1 (A for the first subject and B for the second). The clarity in the early photos is slightly compromised due to the presence of the silicon oil. (Detailed description of the course of pigmentation for both subjects is included in the main text).

Table 3-1: Measurements of the patch's position and orientation during year 1, for both subjects.

Subject 1				
	od-gc (mm)	**bf1–gc** (mm)	**bf2–gc** (mm)	**od-gc^d1** (degrees)
W2	5.85	3.66	3.93	56.4°
W4	5.79 (-0.06)	3.51 (-0.05)	3.75 (-0.18)	55.5° (-0.9)
W12	5.46 (-0.33)	3.39 (-0.22)	3.30 (-0.45)	54.2° (-1.3)
W24	5.76 (+0.30)	3.39 (0.00)	3.54 (+0.24)	54.8° (+0.6)
W52	5.79 (+0.03)	3.45 (+0.06)	3.45 (-0.09)	55.2° (+0.4)
Subject 2				
W2	4.68	4.62	3.18	38.8°
W4	4.71 (+0.03)	4.56 (-0.06)	3.39 (+0.21)	39.4° (+0.6)
W12	4.56 (-0.03)	4.53 (+0.09)	2.88 (-0.12)	39.1° (+0.3)
W24	4.56 (-0.03)	4.53 (+0.09)	2.88 (-0.12)	39.1° (+0.3)
W52	4.62 (+0.06)	4.65 (+0.12)	3.03 (+0.15)	39.5° (+0.4)

In terms of the uniformity of the implant's pigmentation, we have made some particular observations for each subject: In the first subject's CF photos we can detect a segment of the patch that shows denser pigmentation. This segment initially involved approximately the nasal 1/3 of its surface (right end in the CF pictures) and with time it seemed to constrict and by the end of the first post-operative year it covered approximately the nasal 1/4 of the patch (**Fig. 3-3 and 3-5A**). Taking into consideration the manipulation of the patch and the host tissues during the surgery (section 3.1 of this chapter), we assume that the nasal end of the it was inserted underneath the host RPE (instead of subretinally), resulting in a "double" layer of RPE and thus a darker hue of pigmentation. The pigmentation of the rest of the patch's surface did not show significant changes, during the follow-up period. However, looking more thoroughly at the 12 month CF photo we can detect 3 distinctive intensities of pigmentation (**Fig. 3-3**):

(i) the aforementioned darker hue of the nasal segment,

(ii) a wedge-shaped area in the middle of the patch which lost some of its pigmentation and became less saturated by the end of the follow-up period, and

(iii) the more evenly saturated temporal ½ of the patch which also remained more stable with time.

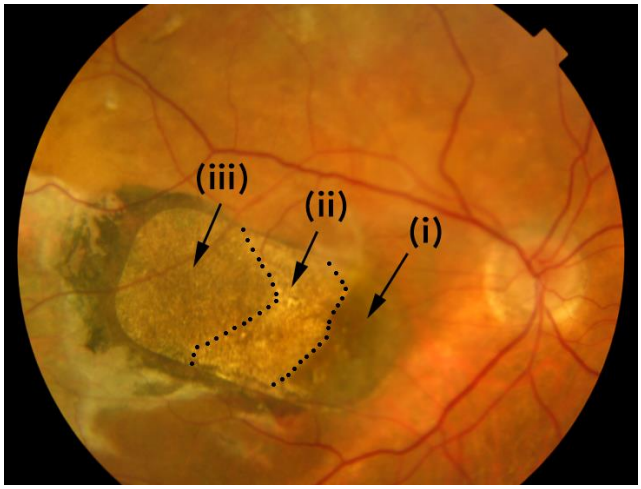

Figure 3-3: Course of the pigmentation of the patch in subject 1. CF photo of subject 1 on post-op month 12, showing the 3 areas (i-iii) of distinct pigmentation

Similarly, in the second subject's CF photos we can also detect some distinctive areas of pigmentation (**Fig. 3-4**):

(i) a significantly darker part, covering the bottom right corner of the patch. Its pigmentation initially appeared homogenous with the rest of the patch, but it increased with time, to obtain its darkest hue at 12 months of follow-up.

(ii) a slightly de-pigmented hue on the middle nasal part, which lost a portion of its pigmentation with time.

(iii) a dark hue on the middle temporal part, which remained stable throughout the first year, and

(iv) a small evidently de-pigmented area located at the inferior-temporal end of the patch (bottom left corner in the CF pictures). This area appears consistently decolorized from the immediate post-implantation period and its shape, size and intensity do not seem to change throughout the first year. As mentioned in the 3.1 section, this area represents the effect of surgical trauma caused by the intra-operative manipulation of the patch, which resulted in either "peeling" of a small fragment of the hESC-RPE off the substrate membrane, or detaching the fragment from the artificial BM in a "PED-like" defect. A probable removal of the vitronectin coating of the artificial BM could also explain the lack of hESC-RPE growth to cover this area post-operatively.

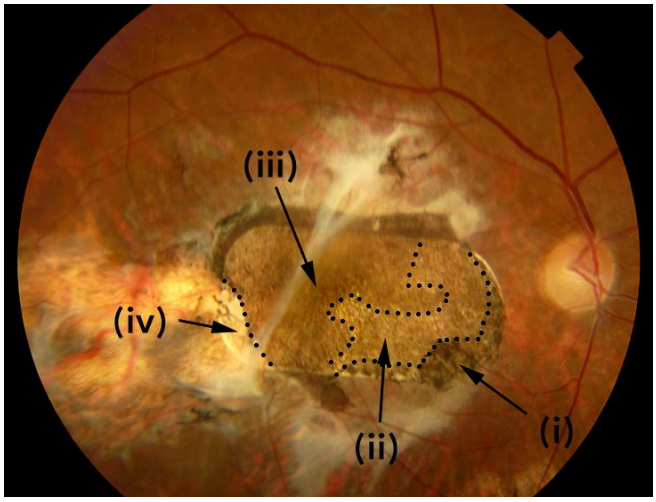

Figure 3-4: Course of the pigmentation of the patch in subject 2. CF photo of subject 2 on post-op month 12, showing the 4 areas of different pigmentation

Both cases had an expansion of the patch's pigmentation outside its margins. This was first noticed from the early post-implantation follow-ups and was located on the temporal and inferior edges for subject 1, and on the superior and inferior edges for subject 2. This expansion was advancing until approximately 12 weeks post-transplantation for both cases and then slowed down until month 6 and thereafter showed no further significant growth until the end of the first year (**Fig. 3-5B**). A more detailed assessment of this finding will be presented in chapter 5.

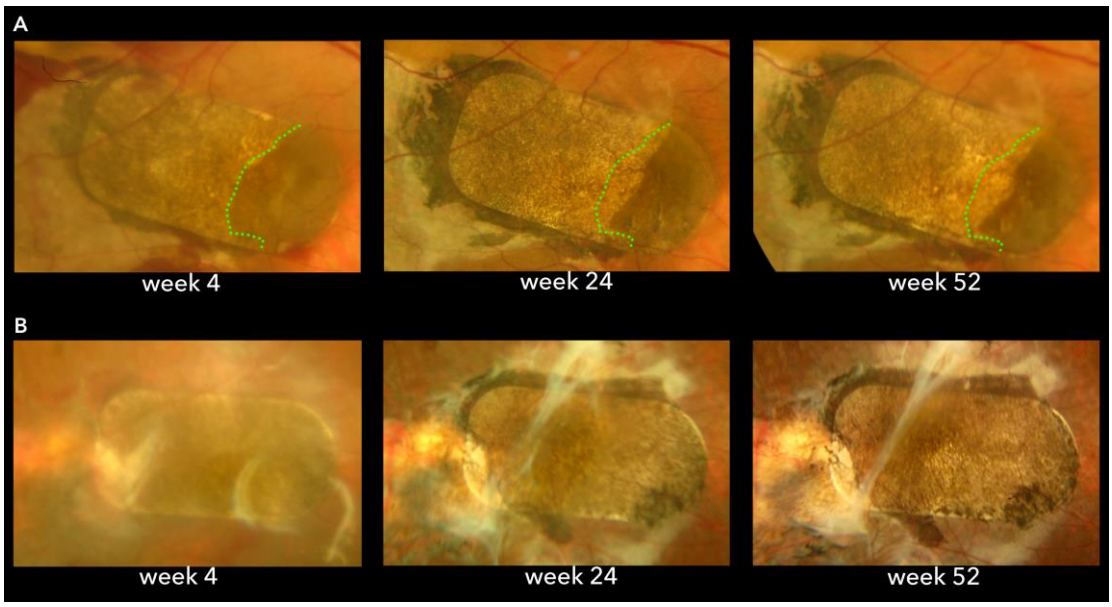

Figure 3-5: Extension of the pigmentation during year 1. CF photographs of the grafted area - (A) for subject 1 and (B) for subject 2 - showing the extension of the pigmentation outside the borders of the patch. The dotted green line on subject one's patch (A) highlights the contraction with time of the presumed "double-RPE" area of the patch (area "i" in Figure 3-3).

3.3.2. Optical Coherence Tomography

In this part, I will mainly focus on the structural appearance of the hESC-RPE-BM complex, as captured by SD-OCT scans during the 1st post-implantation year. The OCT characteristics of the related neurosensory retina (NSR) will be described in the next chapter, where scans from both years of the study period will be analysed and the ultrastructure and remodelling of the NSR will be discussed.

The first subject's early post-operative SD-OCT scans showed the hESC-RPE layer as a continuous, outer retinal, hyper-reflective band. This band demonstrated equivalent reflectivity with the host RPE and was optically distinguished from both the inner, narrow and less dense optically ellipsoid zone and the outer, optically denser and more reflective layer, which represented the synthetic BM (polyester substrate). Thus, the complex of hESC-RPE and artificial BM appears as a dual hyper-reflective band with its inner component corresponding to the hESC-RPE cells and its outer "brighter" component corresponding to the artificial membrane (**Fig. 3-6**).

Further observation of the SD-OCT scans revealed the following features of the hESC-RPE-BM complex:

- Homogenous thickness of RPE-BM band throughout the patch's surface. This ranged from 30 to 35 μm various cross sections around the foveal centre (**Fig. 3-8**, temporal side).
- No obvious structural disruption of the complex, no major defects or interruption of the RPE line.
- No distinct detection of the artificial BM as an isolated layer "bare" of hESC-RPE. This would be expected in case of RPE atrophy/rejection/death/absence as the BM is expected to "survive" independently and consistently appear as a thin hyper-reflective OCT layer, just anterior to the choroidal vessels. (Bloom & Singal, 2011)
- No increased signal back scattering from the choroid (as seen for example in RPE tears (Spaide & Curcio, 2011)).
- No increased signal penetration past the RPE band (as seen for example in cases of RPE absence due to atrophy (Spaide & Curcio,

2011)). On the contrary, the implant was found to block the “normal” OCT signal penetration, in a way that the underlying choroid was ill-defined (in subject 2), or even undetectable (in subject 1) in the SD-OCT b-scans. This hyper-reflectance of the patch produced a characteristic square angle cut-off pattern at the margins of the patch, due to the steep transition from blocked to normal choroidal reflectance, immediately outer to the graft’s edges (**Fig. 3-7**).

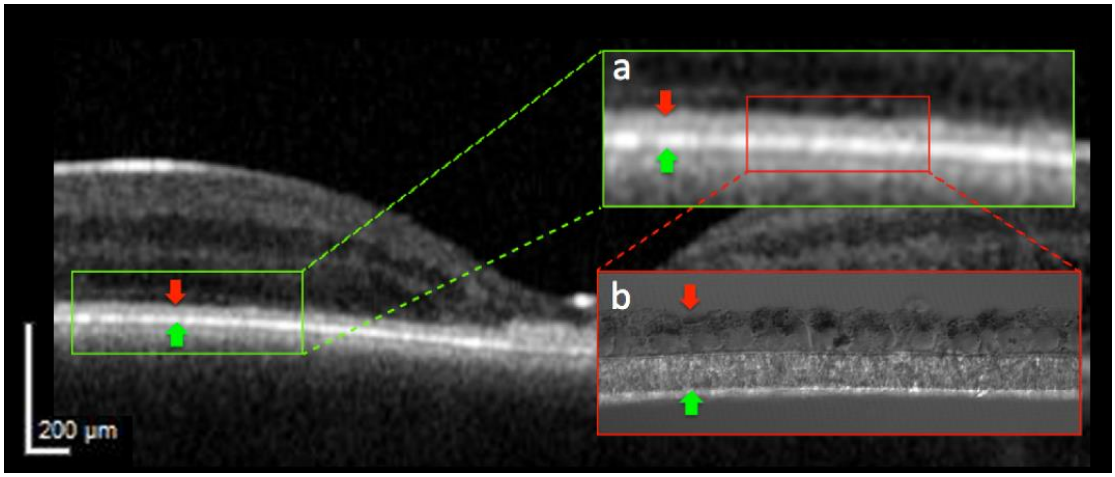

Figure 3-6: First post-operative SD-OCT b-scan of the study. Obtained at week 2 from subject 1, it shows the restoration of the foveal structure and preservation of retinal segmentation. (a): Magnification of the outer layers demonstrates the dual layer of hESC-RPE (red arrows) on synthetic BM (green arrows), resembling consistently the cross section of the graft as seen in the pre-implantation light microscope photograph in (b).

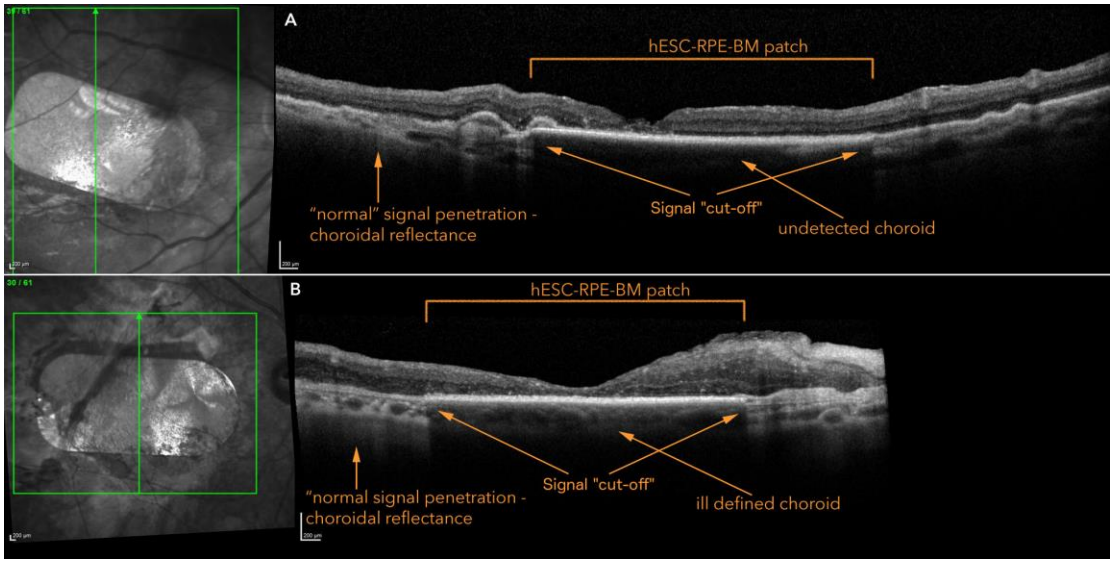

Figure 3-7: Year 1 SD-OCT scans of both subjects showing increased choroidal reflectance outside the borders of the graft and complete (A) or partial (B) decrease of the choroidal signal below the graft, for subject 1 and 2 respectively (signal "cut-off").

- In subject 1 the nasal 1/3 of the patch was inadvertently implanted underneath the host RPE (sub-RPE instead of the planned subretinal position - as mentioned in section 3.3.1). This part can be detected post-operatively as a thicker hyper-reflective layer, outer to the neurosensory retina, which we believe that represents a "double" RPE layer constituted by the outer hESC-RPE (transplant) and inner host-RPE on top. The thickness of this "double" RPE layer was found close to the sum of the thickness of the hESC-RPE-BM complex (known to be approximately 30 μm) plus the thickness of the host RPE, which has been reported to range between 17.5 μm to 28.2 μm, 17.7 μm to 25.4 μm and 18 μm to 24.6 μm, when measured within a radius of 0.5 mm, 1.5 mm and 3 mm from the centre of the fovea respectively (Karampelas et al., 2013) (**Fig. 3-8**).

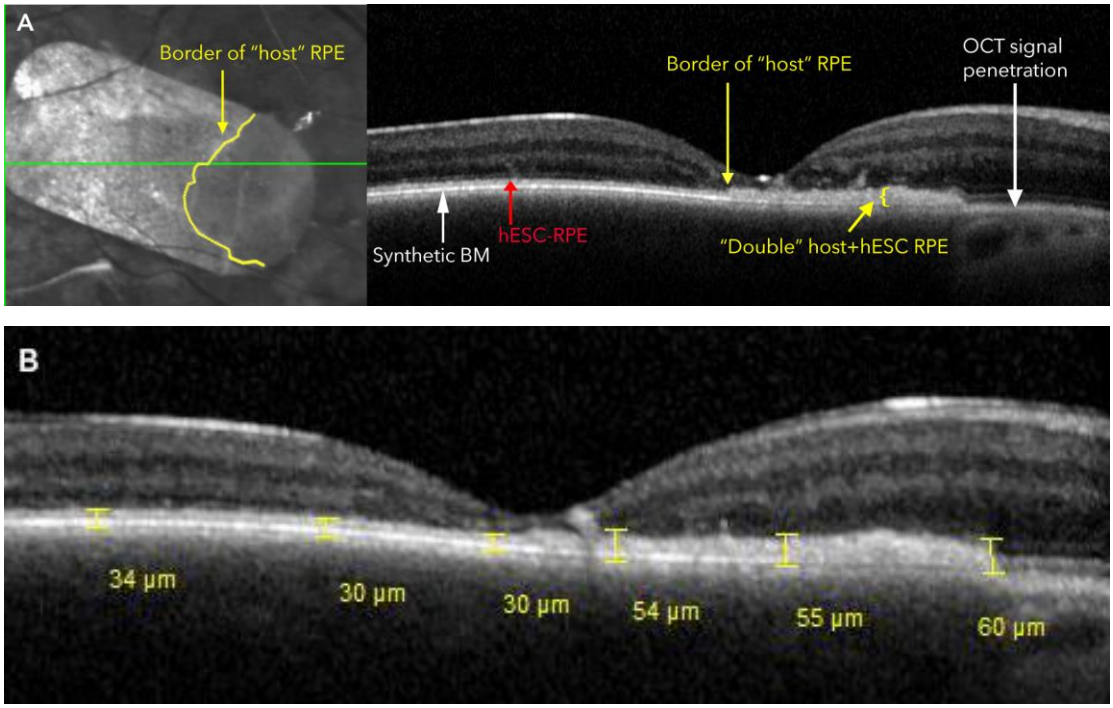

Figure 3-8: Week 4 SD-OCT of subject 1 through the hyper-pigmented area of the patch (area 'i'). A: en face and b-scan images showing the borders of the area underneath the fovea and its nasal edge being distinct from the host retina. B: thickness measurements of the RPE-BM complex within 3 mm radius from the foveal centre.

- In subject 2 there is a small, de-pigmented area located in the inferior temporal corner of the patch (as seen in section 3.3.1). OCT scans through this area showed a disturbance of the hESC-RPE band showing thickening and a "PED-like" formation where the hESC-RPE layer seems detached from the underlying polyester membrane (**Fig. 3-9**). This "defect" of the patch probably represented scarred and/or detached hESC-RPE caused by the damage from its surgical manipulation. It remained stable during the study period.
- Presence of small retinal pigment epithelial detachments (PED) on the patch. These were found in both subjects and detected close to the margins of the patch, as elevations of the hESC-RPE band and separation from the synthetic BM (**Fig. 3-10**).

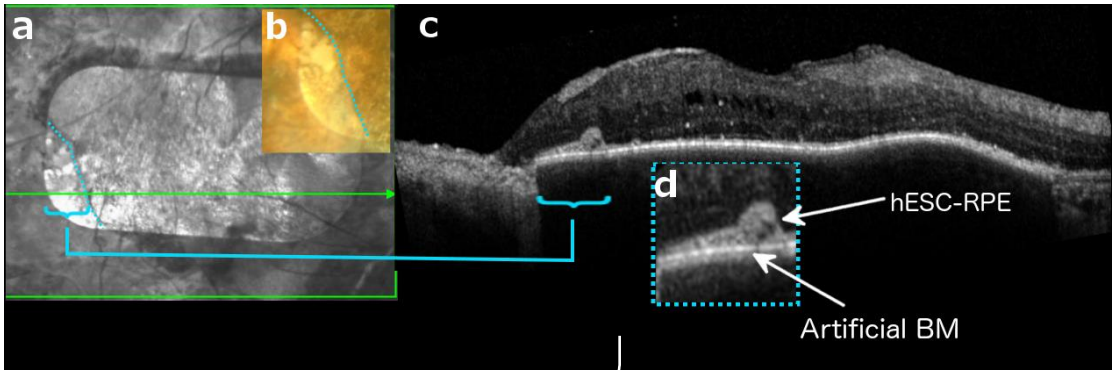

Figure 3-9: Subject 2, month 4 SD-OCT through the depigmented corner of the patch. (a) and (b): IR photo and colour detail respectively with the depigmented corner demarcated. (c): OCT b-scan of the corresponding area. (d): magnification of the b-scan through the depigmented corner showing a PED-like elevation of the hESC-RPE from the artificial membrane. The RPE line is visually separated by the membrane, but continuous with the hESC-RPE layer of the rest of the patch.

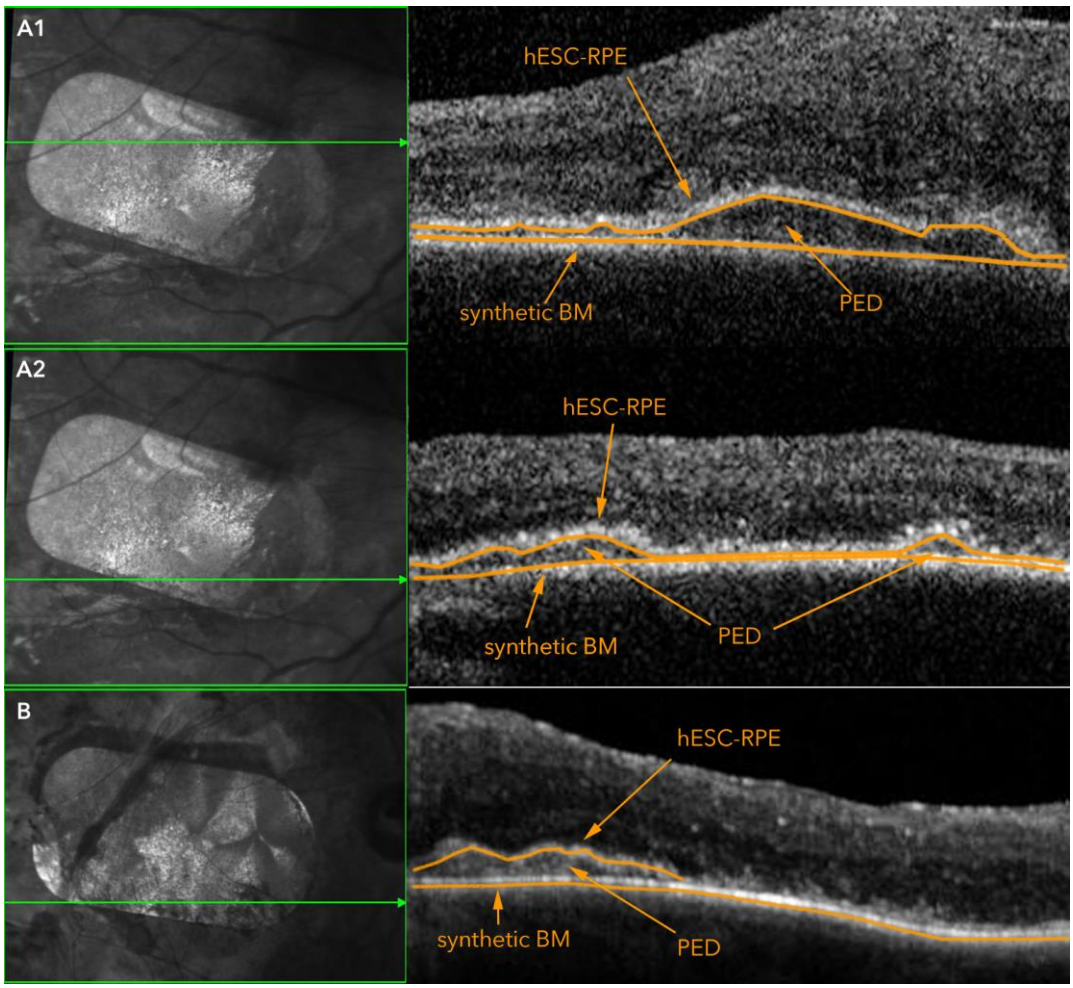

Figure 3-10: PED-like formations of the hESC-RPE. OCT scans of the hESC-RPE patch of subject 1 (A1 and A2) and subject 2 (B), on year 1 post-implantation. The inner border of the hESC-RPE layer and outer border of the synthetic BM have been outlined, in order to highlight the small PEDs in two different sections of the graft.

- A large PED was found off the patch in the 1st subject's post-operative year 1 OCT scans. It was nearly 1 disc diameter away from the patch edge and outside of the supero-temporal arcade (**Fig. 3-11**). This was considered as a possible reactivation of the background disease (Idiopathic Polypoidal Choroidal Vasculopathy) away form the patch and was monitored closely. Its course will be described in the 2nd year results in chapter 4.

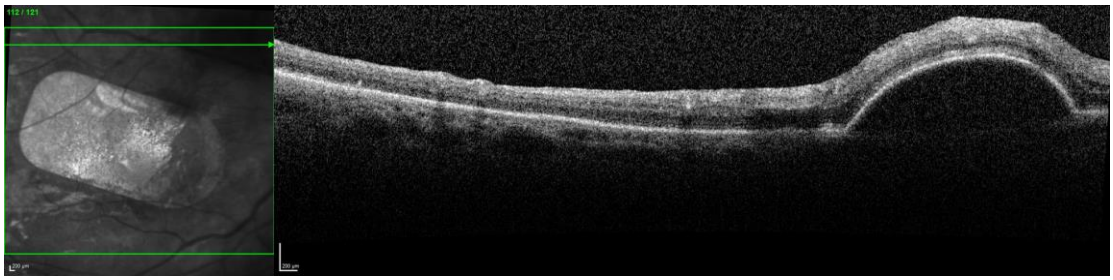

Figure 3-11: Host RPE detachment of subject 1. Year 1 SD-OCT showing a PED on a distant (superior) to the patch location.

- Some signs of inflammation and fibrotic reaction of the inner retina were found in both subjects. Retinal fibrosis and scarring occurred around the accessing retinotomy, and some epiretinal membrane (ERM) formation was found in both subjects. Additionally, in subject two, a thick fibrotic band developed over the temporal half of the patch, which progressed with time, inducing mechanical traction and thickening of the underlying retina, but without evidence of neurosensory retinal detachment or schisis, but possibly with an associated PED (**Fig. 3-12**).

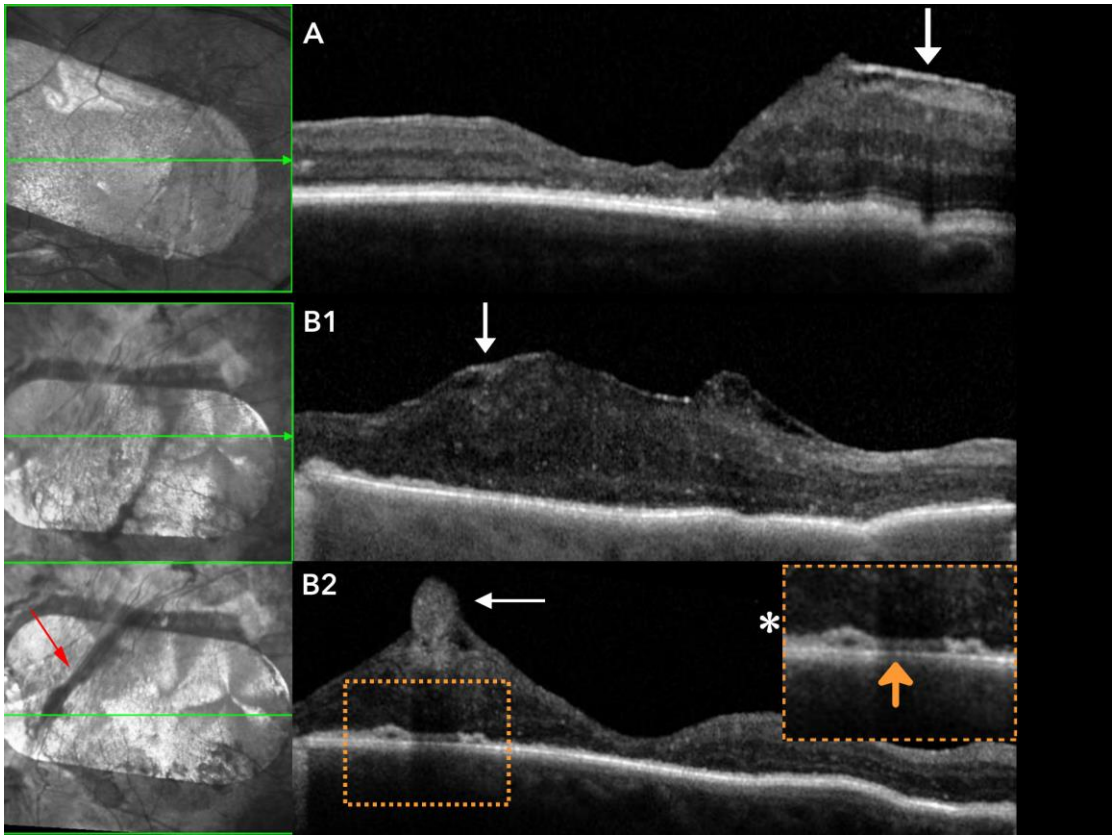

Figure 3-12: OCT scans showing ERM formation in both subjects. A: subject 1, month 6 scan showing the ERM (white arrow) over the nasal thickened retina. B1: subject 2, month 6 scan showing ERM and scarring (white arrow) of inner retina. B2: subject 2 year 1 scan showing excessive scarring over the temporal part of the patch with a fibrotic band (red arrow) "crossing" the full width of the graft and its cross-section (white arrow) in the b-scan. (*) Magnification of the outer retina layers below the fibrotic band showing a possible traction-induced PED (orange arrow). No neurosensory retinal detachment or schisis is seen in either subject.

3.3.3. Fundus Fluorescein Angiography

Fundus Fluorescein Angiography (FFA) revealed that the perfusion of the choroid under the patch was maintained in both subjects during the study period. The background fluorescence at the site of the patch, seen in the early arterial phases of the FFA, was detectable in both subjects from the early post-operative period and until 1 year of f/up. This fluorescence had the characteristic "ground glass" appearance and was considered a sign of preserved perfusion of the underlying choroid. No hypo-fluorescent gaps were noticed in this diffuse fluorescence, which was covering the signal of the large choroidal vessels throughout most of the patch's surface. In the early post-

implantation FFAs (month 1), this background fluorescence appeared less bright than the one reflected by the “host” retina away from the patch, however in the later follow-up FFAs (months 6 and 12) it appeared to have increased in intensity and seemed similar to the one of the surrounding “normal” tissues (**Fig. 3-13**).

In both subjects the edges of the patch showed reduced fluorescence. Additionally, marked background hypo-fluorescence gaps, with only the large outer choroidal vessels appearing perfused (Haller’s and Sattler’s layers) was seen temporally to the graft and matched the retinal locus, which was used for access to the subretinal space (through the surgical retinotomy)(**Fig. 3-13**, blue arrows). We assume that this represents the trauma of the overlying host retina, RPE and choriocapillaris, caused by the surgical manipulations during the clearance of sub-macular blood and insertion of the hESC-RPE patch. Conversely, early and late hyper-fluorescence was emitted by areas surrounding and adjacent to the patch, which represented window defects from retinal atrophy caused by the surgical trauma on top of the already existing atrophy – due to AMD (**Fig. 3-13**, green arrows).

In subject 1 a markedly hypo-fluorescent area was detected on the nasal 1/3 of the patch’s surface, which later reduced to approximately 1/4 of it, by the end of the follow-up period (**Fig. 3-13A**, asterisk). This area corresponds to the area of “double” RPE and the hypo-fluorescence probably represents “masking” of the background fluorescence from the patch on top of the host RPE. Similarly, in subject 2 the inferior nasal corner of the patch was found hypo-fluorescing after month six of follow-up (**Fig. 3-13B**, asterisk). This corresponds to an area of hyperpigmentation (area (i) in 3.1.1) and its reduced reflectance possibly represents “masking” from the excessive pigment over the background reflectance.

Another finding in the first subject’s FFAs was a round area of hyper-fluorescence with well-defined borders and increasing intensity at the later phases. This was observed on the superior-temporal arcade, approximately 1 disc diameter away from the patch and it appeared initially on post-operative month 6 and became more prominent by month 12 (**Fig. 3-13A** and **X**, red arrow). It represented the superior extramacular PED, also described in the OCT scans.

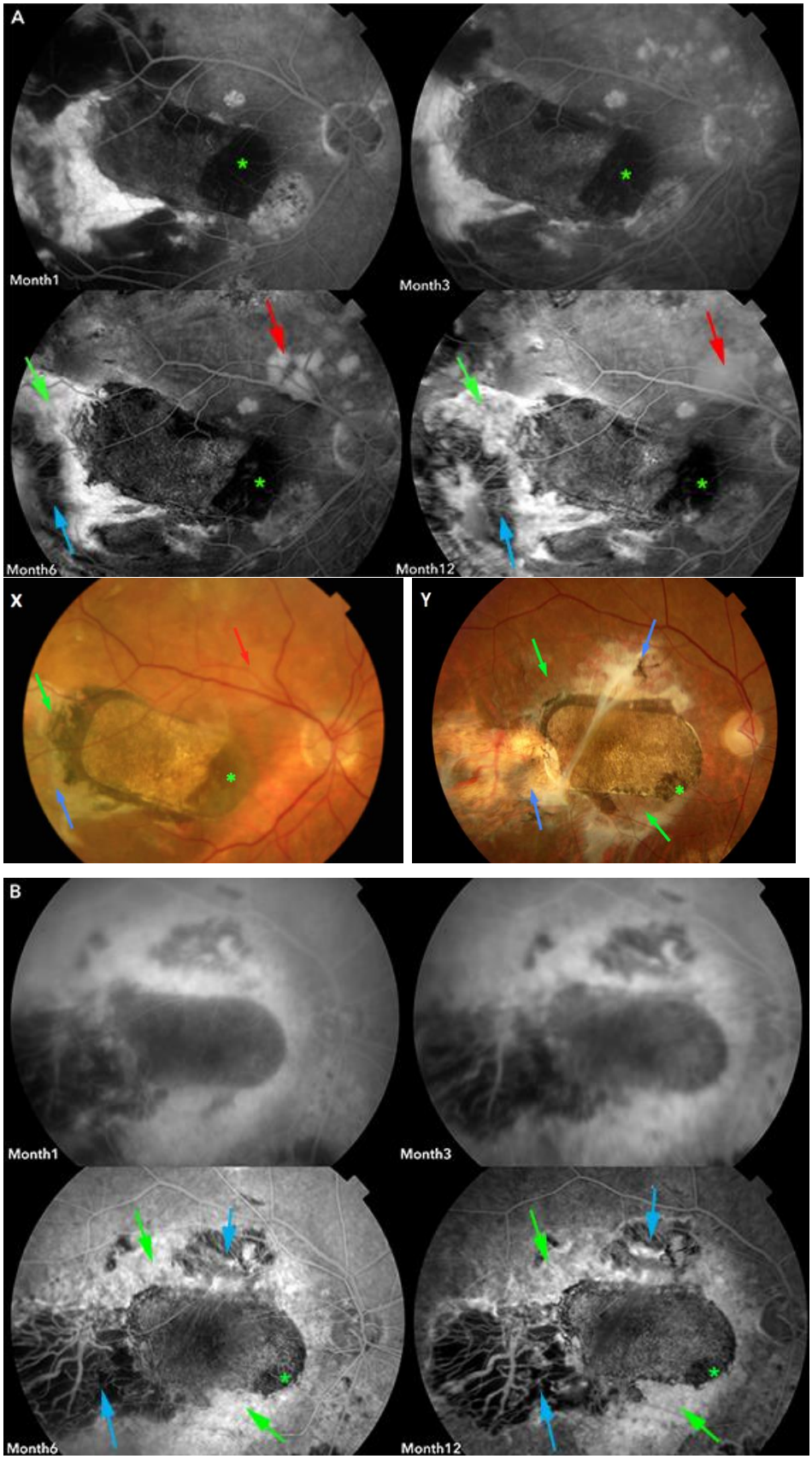

Figure 3-13: Series of early-phase FFA images during year 1 for both subjects (A and B respectively), with a corresponding CF photo (X and Y respectively) (Described in the main text).

3.3.4. Fundus Autofluorescence (FAF)

FAF images of subject 1 form the immediate post-operative period (week 1) show a low reflectance in all the area of the graft and the surrounding retina with some granular autofluorescence on the temporal half of the graft as well as on the fundus temporally to the patch, which is the area from where the patch was inserted subretinally (**Fig. 3-14**, green arrow). This grainy fluorescence decreases with time and seems to become more even by month 3. In later images we can detect a mild increase in the overall fluorescence of the temporal half of the graft, however without ever reaching the reflectance level of the surrounding "unaffected" retina. In a closer look there are also areas on the patch that initially showed no AF and started fluorescing by month 3 (**Fig. 3-14**, red arrows). In addition, we noticed that the AF of the nasal edge of the patch seems closer to that of the normal retina (**Fig. 3-14**, blue arrow). This finding supports our observation that the nasal part of the graft was inadvertently inserted underneath the host RPE, in a way that its AF source is not the implanted hESC-RPE but the host, "aged" RPE. This area reduced in size, as the host RPE retracted nasally (**Fig. 3-14**, blue dotted line) and by month 3 it started hyper-fluorescing (**Fig. 3-14**, yellow arrow), possibly indicative of host-RPE cell death. Finally, there is an area closer to the geometric centre of the patch, which shows no AF signal whatsoever and remains stable throughout the study period, possibly resembling the part of the graft that was traumatised from the surgical manipulations (**Fig. 3-14**, red arrow) and was never re-covered by RPE, however, it seems to decrease in size (**Fig. 3-14**, white asterisk).

For subject 2 we were not able to obtain useful FAF images during the first post-operative weeks, due to poor clarity of the refractive media of his operated eye (hazy cornea and silicone oil in situ). The first FAF pictures of reasonable quality were taken at three months after the implantation. In those we can detect three distinguished levels of fluorescence: the one of the "normal" retina outside the affected area, which has the strongest AF signal (**Fig. 3-15**, green arrow), the middle-intensity area that surround the graft (**Fig. 3-15**, blue arrow), and the darkest area that corresponds to the implanted hESC-RPE (**Fig. 3-15**, red arrow). By examining the follow-up images we can see that these three levels of reflectance intensity are maintained during the

study period, however the AF signal of the graft itself seems to increase and becomes more apparent at post-operative month 12. Conversely, there is a small spot close to the geometric centre of the patch that does not seem to follow this course of increasing AF and remains hypo-reflective on month 12 (Figure 3-15, yellow arrow).

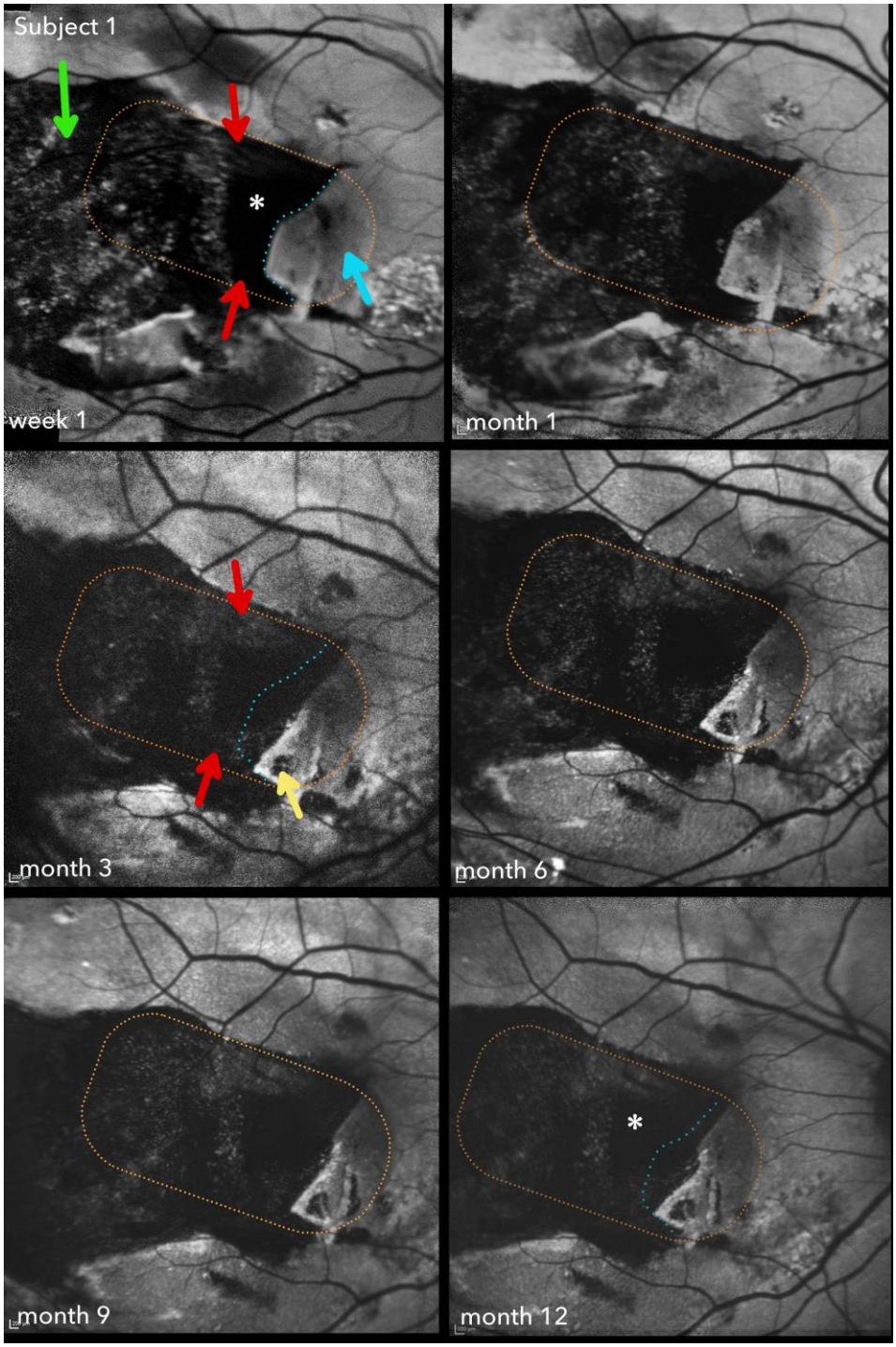

Figure 3-14: Series of FAF images from subject 1 during year 1. The hESC-RPE patch is highlighted with dotted line (Described in the main text).

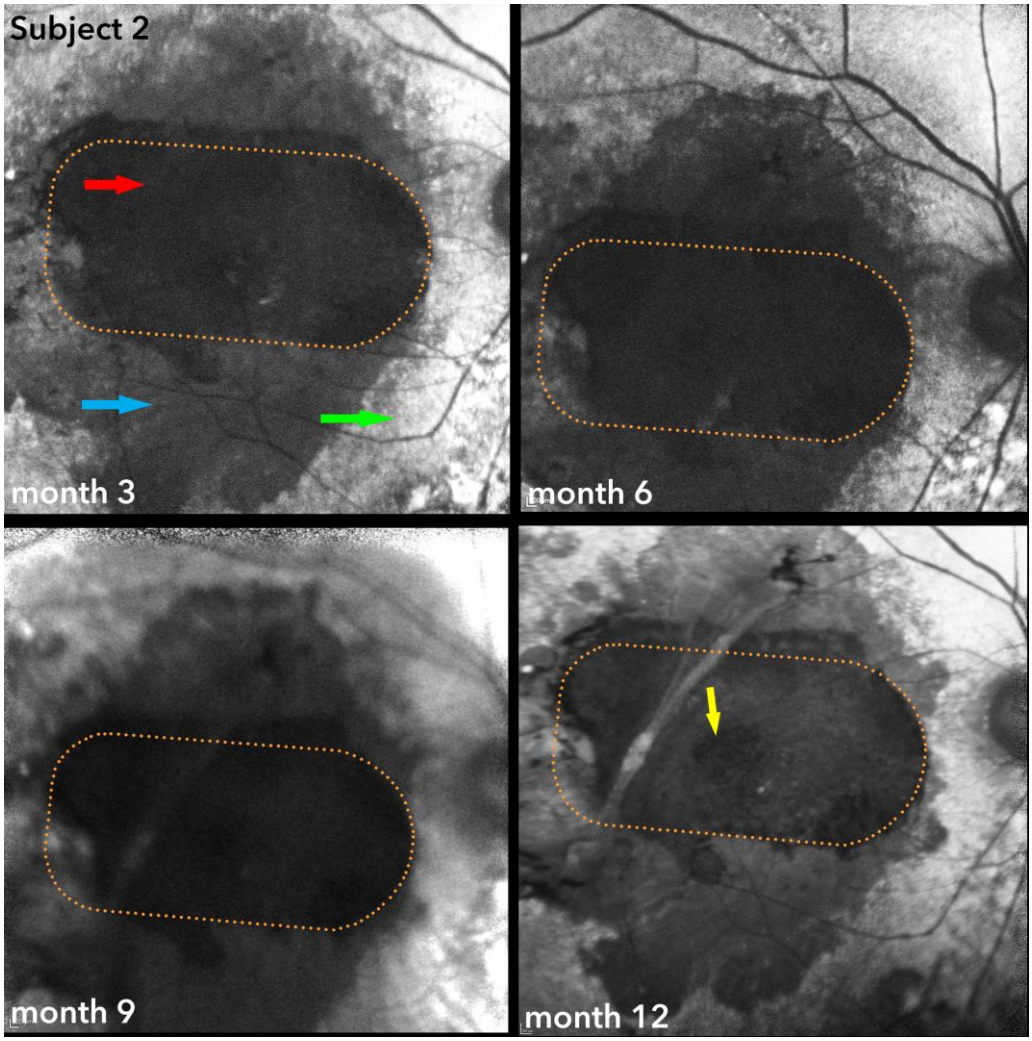

Figure 3-15: Series of FAF images from subject 2 during year 1. The hESC-RPE patch is highlighted with dotted line (described in the main text).

3.3.5. Adaptive Optics Retinal Imaging

Adaptive Optics (AO) photos of the subjects' retina were obtained by the Rtx1 Imagine Eyes AO camera, in an effort to image cone photoreceptors in the transplanted area.

Qualitative observation of the AO images from both subjects showed presence of speckled signals with similar shape, size, contrast and inter-structural distance with the cone photoreceptors of a normal retina (**Fig. 3-16**). More specifically, cone survival was demonstrated during the whole follow-up period in both subjects, over the areas corresponding to the patch. These areas also showed corresponding sensitivity in functional assessments, such as fixation and Microperimetry, as I will show in the next chapter.

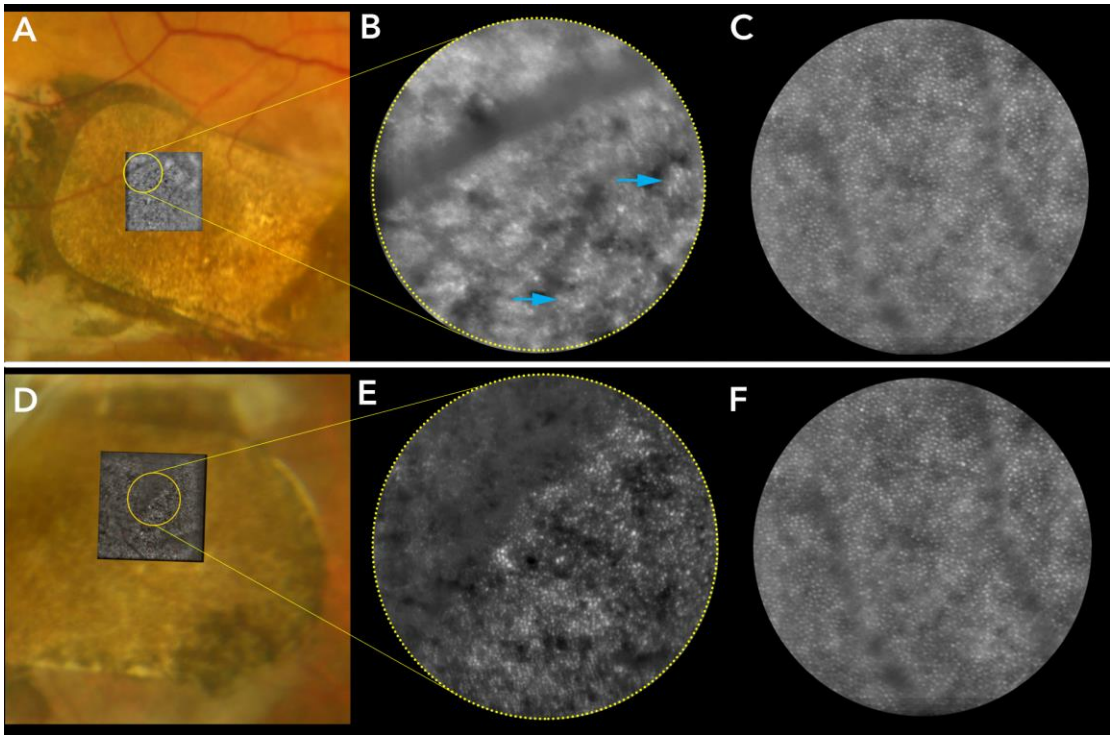

Figure 3-16: Year 1 AO images. A & D: CF photos of subjects 1 and 2 respectively, showing graft areas captured with AO (squares). B & E: further magnification of the AO images (yellow circles), showing cone-like structures in both subjects, appearing scattered in subject 1 (b) and more uniform in subject 2 (e). C & F: AO "samples" from a normal retina of equal magnification and distance from fovea for comparison purposes. The size of the "sampled" circle represents the size of the Microperimetry stimuli, projected on the subjects' retinas.

Discussion

In this chapter I reported the safety and anatomical stability following the sub-macular transplantation of a patch comprised of a hESC-RPE monolayer on a vitronectin coated artificial BM, for acute neovascular AMD. Two subjects suffering from submacular haemorrhage and scarring received the implant within 6 weeks from their acute vision loss and were monitored using multimodal imaging. Both received a course of systemic prednisolone during their peri-operative period and local depot immunosuppression thereafter.

In terms of safety, I reported 3 SAEs, two related to the surgical procedures (subject one's conjunctival dehiscence and subject two's PVR-

related retinal detachment) and one related to the concomitant medication (subject two's disturbance of diabetes control). The rest AEs were less severe and some were related to the study procedures, while others were considered as not relevant. No adverse reactions directly related to the investigational patch were noticed. No signs of uncontrolled proliferation or tumorigenicity were detected.

In terms of patch location, no significant migration was noticed along the retinal plane or the anteroposterior axis in either of the subjects. Overall, the recorded linear changes on the macular surface did not exceed 0.45 mm and were mostly in the scale of 0.15 mm from visit to visit. The rotational changes were even less significant. That being said, all measurements where done using 2-dimensional geometry, thus considering that all landmarks were at the same plane. In reality, the macular surface is a part of a sphere and thus all measurements were susceptible to errors due to positioning and centring of the photographs, as well as due to the "deformation" of the plane away from the centre of the pictures. With these limitations being consistent during all exams, I believe that the scale of the measured "movement" of the patch was insignificant, compared to the margin of error of the used method.

The hESC-RPE survived for at least one year, as demonstrated by the presence of a well-defined, pigmented patch, visible during fundoscopy and evident on CF photos. The visible patch corresponded to a distinctive and undisrupted hyper-reflective signal in the OCT scans. Specifically, this signal comprised a double-layer band consisting of an outer brighter line, representing the synthetic BM and an inner line, representing the hESC-derived RPE. It resembled accurately the light micrograph cross-section of the patch, taken in the lab during its assembly, and it remained stable and covering the whole grafted area at least for one year. The thickness of this double layer was found between 30 and 35 μm, which is very close to the thickness of the RPE-Bruch's membrane complex of normal subjects, when measured in OCT scans around the fovea (Ko et al., 2017). The patch also showed a "shadowing" effect of the underlying choroid, similar but more profound than the normal RPE, and with a steep cut-off of the OCT

reflectance at the patch's edges. FFA revealed a good choroidal background perfusion of the sheet, showing the characteristic "ground glass" fluorescence of the choriocapillaris. The absence of hypofluorescing gaps, through which the large choroidal vessels would be visible, provides a good indication that there was no significant loss of the choriocapillaris (Johnson et al., 2013). The preservation of good choroidal perfusion also indicates that there was a successful integration of the graft to the host tissues (MacLaren et al., 2007). Furthermore, OCT scans showed features of normal retinal architecture and visible segments of the outer nuclear layer and ELM/ellipsoid complex.

Additional structural assessments, such as FAF and AO retinal imaging, supported further the correlation between the hESC-RPE survival and the improvement in vision. Acknowledging that the FAF signal is affected by numerous factors that are impossible to standardize in every exam (refractive media clarity, presence of silicon oil etc.), I used the same exposure settings when obtaining the images and I analysed them attempting internal comparisons within an image, showing different intensity of AF in different parts of the patch and comparing them to the surrounding "normal" retina. The patch remained hypo-fluorescent comparing to the host RPE, but showed areas of homogenous signal, corresponding to areas of good light sensitivity. Furthermore, there were areas of the patch that had zero fluorescence in the immediate post-implantation period and started emitting AF signal later on (Figure 3-14). This AF of the patches, was maintained for one year in both subjects, suggesting that phagocytosis of photoreceptors' outer segments by the implanted cells may have commenced during the follow-up (Holz, Bellman, Staudt, Schütt, & Völcker, 2001), (Holz, Schmitz-Valckenberg, Spaide, & Bird, 2007), (Holz, 2007), (Sparrow & Duncker, 2014). Additionally, in subject 1 I detected areas of the host RPE showing abnormally high AF signal after month 3, possibly indicative of host cell death (Yung, Klufas, & Sarraf, 2016), while the adjacent transplanted hESC-RPE maintained stable fluorescence. A more detailed study on the patch's AF is attempted in chapter 6 of this thesis.

The AF signal of the hESC-RPE constitutes an indirect indication of photoreceptors' survival and function. A more direct indication was documented in the AO retinal images. The limitations of the FAF images, in

terms of media clarity and exposure conditions, also apply to the AO imaging techniques. However, I managed to capture numerous, on-the-patch clusters with cone PR characteristics that resembled the ones of a normal subject (Muthiah et al., 2014) and remained prominent for at least one year.

How these areas of good structural recovery corresponded with the function of the transplanted area will be discussed in the next chapter, where I will complete the presentation of the first year outcomes, by reporting the functional results of the investigational patch, and analyzing the correlation between structure and function in the treated macular area. The *discussion* on the first year outcomes will be completed thereafter.

Chapter 4

First year outcomes – Function

Introduction

In the previous chapter I demonstrated the safety of our investigational hESC-RPE-BM patch transplantation, and I presented the anatomical outcomes during the first year of the follow-up. In this chapter, I will report the functional results for the same period, focusing further on how these correlated with the structural support that our patch provided in both subjects.

Results

4.1. Fixation

Examination with the Nidek-MP1 device demonstrated that both subjects maintained fixation onto the patch-supported retinal area (**Fig. 4-1**). Stability of fixation was classified as “unstable”, “relatively unstable” or “stable” according to the percentage of fixation points within 2° and 4° of the gravitational centre of all testing loci. More specifically, for subject 1 the fixation stability ranged between 72% and 93%, when tested within 2° from the centre of the target and between 98% and 100%, when tested within 4° from the centre of the target. On follow-up year one it was marked as “stable” by the Nidek software with 83% of examined fixation points falling into the 2° area and 100% into the 4°. For subject 2 the fixation stability ranged between 46% and 98% within 2° and between 92% and 100% within 4° from the centre of the target. On follow-up year one it was also marked as “stable” with 98% of fixation point within the central 2° and 100% within the 4° area.

For the first subject, the fixation appeared to shift about 2° superiorly to initial post-implantation location, after one year of follow-up, however remained “on the patch”. For the second subject the fixation was also found consistently “on the patch”, however demonstrated a fluctuation of stability and retinal location.

In order to examine the topographic relation of the subjects' fixation with the centre of their fovea, I have used the algorithm described by Sunness et al.(Sunness, Bressler, Tian, Alexander, & Applegate, 1999) according to which the foveal centre is normally located at two disc diameters temporal to the disc and one third of a disc diameter inferiorly to the centre of the disc. By comparing the retinal area of fixation with the calculated foveal centre, we can see that in both subjects the preferred fixation has been shifted out of the central fovea after one year. More specifically, in subject 1 the fixation on 1 year post-op was found at approximately three degrees (3°) superiorly to the foveal centre, while in subject 2 approximately 5 degrees (5°) temporal to the centre of their fovea (**Fig. 4-2**).

It is worth mentioning here that the subjects' ability to fixate was also clinically examined on the slit-lamp during the fundoscopy, by using the 0.2 mm aperture of the lamp to project an approximately 0.3 mm bright light stimulus on their retina. With this method we found that both subjects were preferably fixating using a retinal spot located in an area closer to the geometric centre of the patch, as well as to their fovea. This fixation to bright stimulus was kept stable throughout the study period, even when the fixation tested by Nidek MP-1 had shifted to a more distant to the patch's centre area (as for subject 1 after 6 months of follow-up).

Figure 4-1: Fixation on the Nidek-MP1 device during year 1 (A for subject 1 and B for subject 2). Each square represents a test in the noted time point as a red free fundus image in the background with the fixation target (red cross) and the points of the subject's recorded fixation (light blue dots) projected on it. The rectangle in the bottom right part of each test shows the span of fixation (homocentric circles on the left) and the relative stability of it (graph on the right). Each of the blue dots represents the retinal area subtending the centre of the target at a certain time, therefore the cloud of dots statistically identifies the retinal area involved in fixating a target (within 2° in the small circle – within 4° in the larger circle). Both subjects preserved their preferred fixation within the edges of the grafted area.

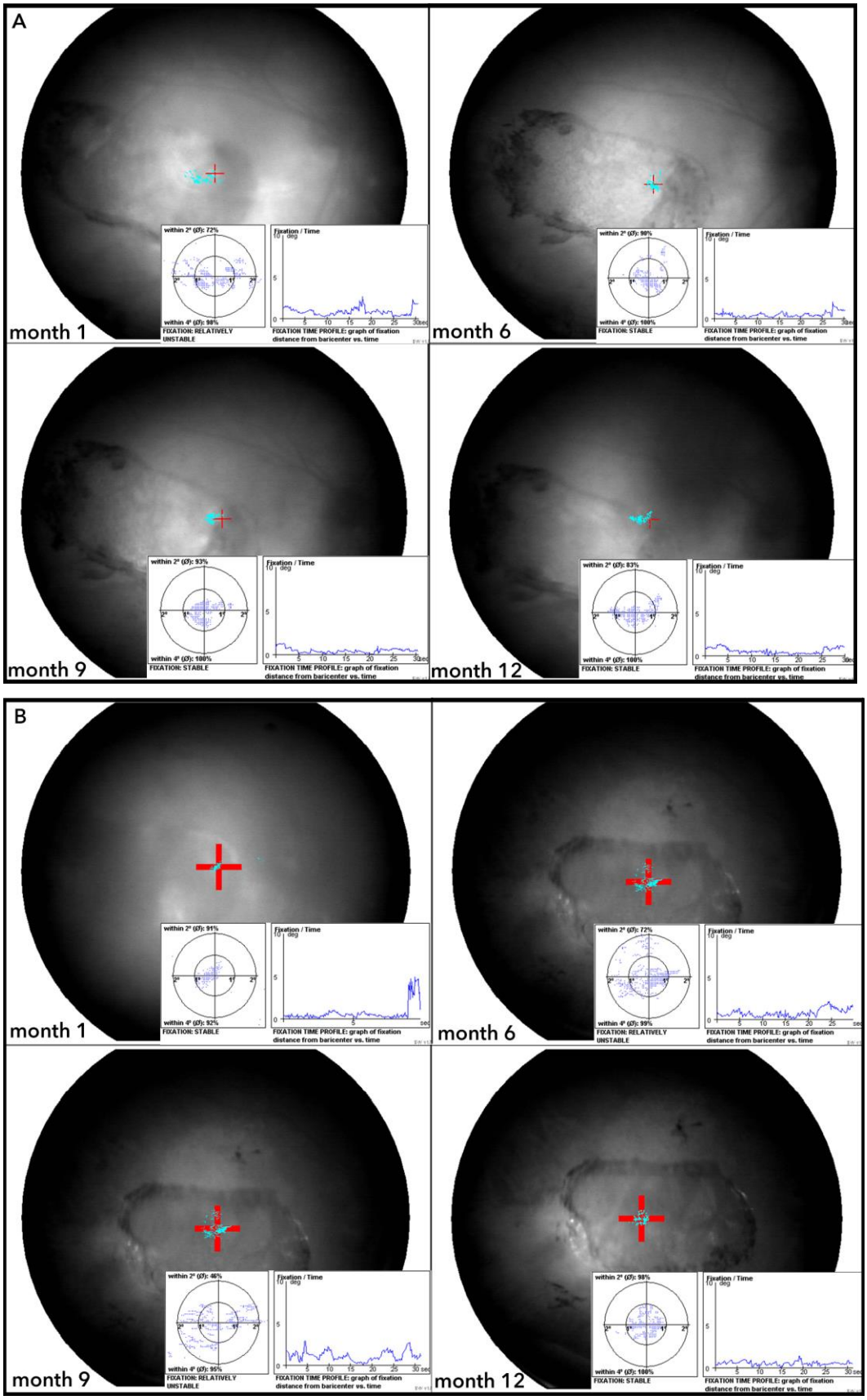
A
month 1
month 6
month 9
month 12
B
month 1
month 6
month 9
month 12

(Figure 4-1)

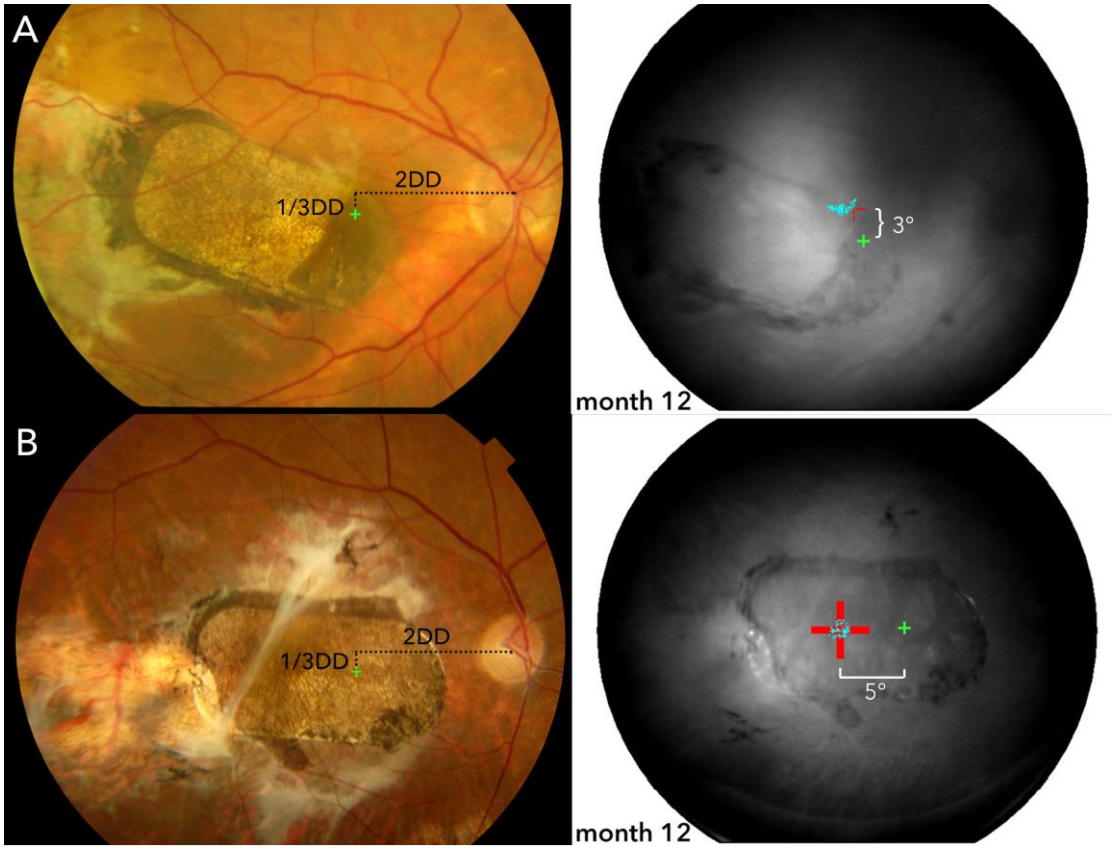

Figure 4-2: Fixation "shift" after 12 months ("A" for subject 1, "B" for subject 2). The CF photo on the left shows the estimated location of the fovea as per Suness et al. method. The red free photo on the right shows the distance of the new fixation location from the fovea.

4.2. Best Corrected Visual Acuity (Early Treatment Diabetic Retinopathy Study).

Before the screening assessment, both subjects had experienced severe acute vision loss in the study eye. For the first subject the pre-operative BCVA fluctuated between 5 and 10 ETDRS letters, dropped to 0 letters on post-operative day 1 and subsequently improved to reach 33 ETDRS letters on month 6 and 39 letters on year 1. Similarly, for the second subject the baseline BCVA was between 2 and 8 ETDRS letters, dropped to 0 immediately after the operation and then increased to reach 30 letters on month 6, which was subsequently maintained - 29 letter on year 1 of follow-up. As expected, a mild, transient decrease in ETDRS score was observed in both subjects after the ROSO surgery. This resolved over a short period and the improving trend of VA was restored in both subjects (**Fig. 4-3**). It is worth

mentioning here that for the second subject we observed a slower rate of improvement that we attributed firstly to the higher severity of the baseline disease and, secondly, to the retaining of the silicone oil for a longer period, due to the retinal detachment. The RD itself was asymptomatic and did not involve the macula and thus is unlikely to have had an impact on the VA.

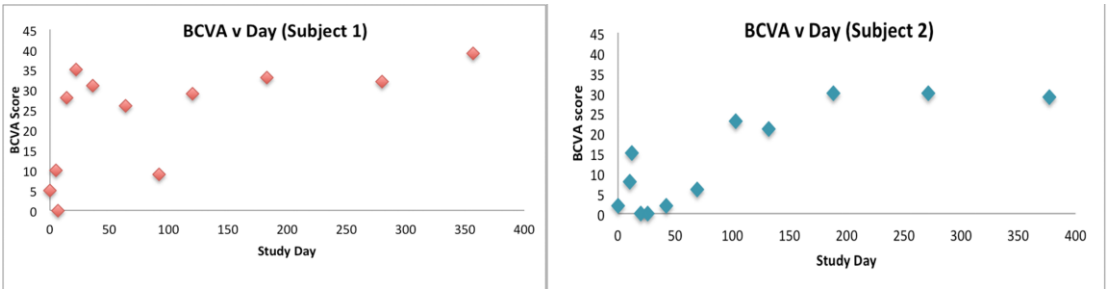

Figure 4-3: BCVA in the study eye in year 1. Graphs showing the change of BCVA in the operated eye of subject 1 (left) and 2 (right).

Table 4-1: BCVA scores of the study eye of both subjects during year 1

	Subject 1 BCVA (ETDRS letters)	Subject 2 BCVA (ETDRS letters)
Baseline	5-10	2-8
Day 1 (post-op)	0	15
Week 1	28	0
Week 2	35	0
Week 4	31	2
Week 8	26	6
Week 12	9	23
Week 16	29	21
Week 24	33	30
Week 36	32	30
Week 52	39	29

4.3. Pelli-Robson Contrast Sensitivity (CS).

Both the study subject demonstrated improvement of their contrast sensitivity in the operated eye. The CS log score for subject 1 increased from the pre-operative 0.45, to 1.35 (18 letter gain in PR chart) on month six, which was maintained after one year of follow-up. Subject 2 entered the study with a CS log score of 0, improved to 0.75 after 6 months and reached 1.05 on follow-up year one (24 letter gain in PR chart).

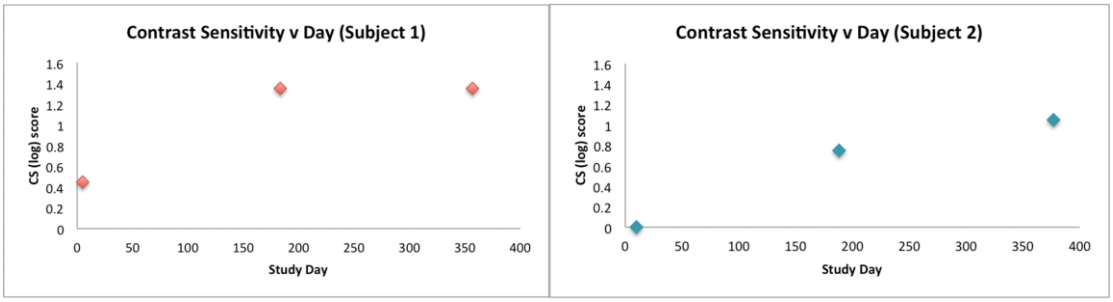

Figure 4-4: CS in the study eye in year 1. Graphs showing the change of CS in the operated eye of subject 1 (left) and 2 (right).

Table 4-2: CS scores of the study eye of both subjects during year 1

Pelli-Robson CS	Subject 1 CS (log score)	Subject 2 CS (log score)
Baseline	0.45	0
Week 24	1.35	0.75
Week 52	1.35	1.05

4.4. Maximum Reading Speed (RSmax) – Minnesota RS Test (MNREAD)

Both subjects showed an improvement in their ability to read with their operated eye, during the follow-up period. Subject 1 increased her maximum reading speed (RSmax) from 0-5 words per minute (wpm) in the screening assessments to 51.2 wpm after six months and 84.2 wpm at post-operative year 1. Subject 2 demonstrated a more modest progress starting from 0 wpm during screening, reaching 26.5 wpm after six months and 48.7 wpm after one year.

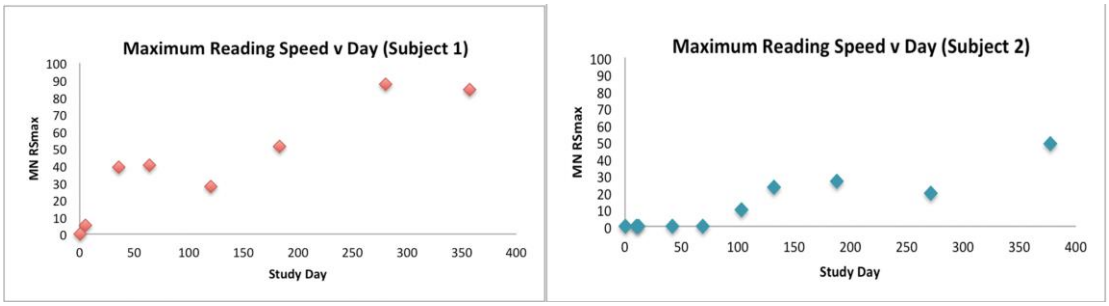

Figure 4-5: Reading speed in the study eye in year 1. Graphs showing the change of RSmax in the operated eye of subject 1 (left) and 2 (right).

Table 4-3: RSmax scores of the study eye of both subjects during year 1

MNREAD test	Subject 1 RSmax (wpm)	Subject 2 RSmax (wpm)
Baseline	0-5	0
Week 4	39	0
Week 8	40.1	0
Week 16	27.7	23
Week 24	51.2	26.5
Week 36	87.5	19.5
Week 52	84.2	48.7

4.5. Microperimetry

Microperimetry (MP) measures the differential light sensitivity (the minimum luminance of a white spot stimulus, which superimposed on a white background of uniform luminance is necessary for the stimulus perception). In our study, fundus-controlled Microperimetry (MP) was performed using customised stimuli grids and testing protocols set in the Nidek MP-1 microperimeter. Special effort was applied to adjust the examining grid in order to be projected onto the grafted area. A mean retinal sensitivity (average threshold - in dB) of the corresponding (on-the-patch) retina was calculated for each test, by dividing the sum of the sensitivities of the test loci that were projected within the boundaries of the patch with the number of these test points.

Both subjects demonstrated significant increase in light sensitivity in multiple loci of the retina over the patch during the follow-up period. Subject's 1 patch's mean sensitivity was found to improve from 0.15 dB at 1 month post-operatively to 12.57 dB at 12 months. Subject 2 showed a smaller improvement, from 0 dB at 1 month to 2.57 dB at month 12.

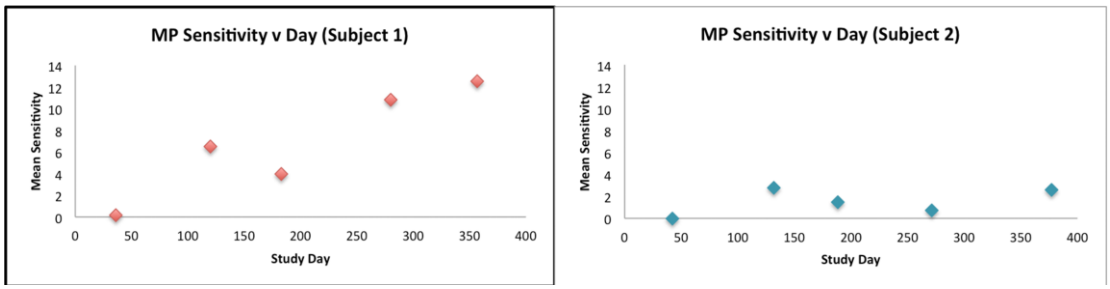

Figure 4-6: Mean MP sensitivity in the study eye in year 1. Graphs showing the change of the mean light sensitivity of the treated macular area in the operated eye of subject 1 (left) and 2 (right).

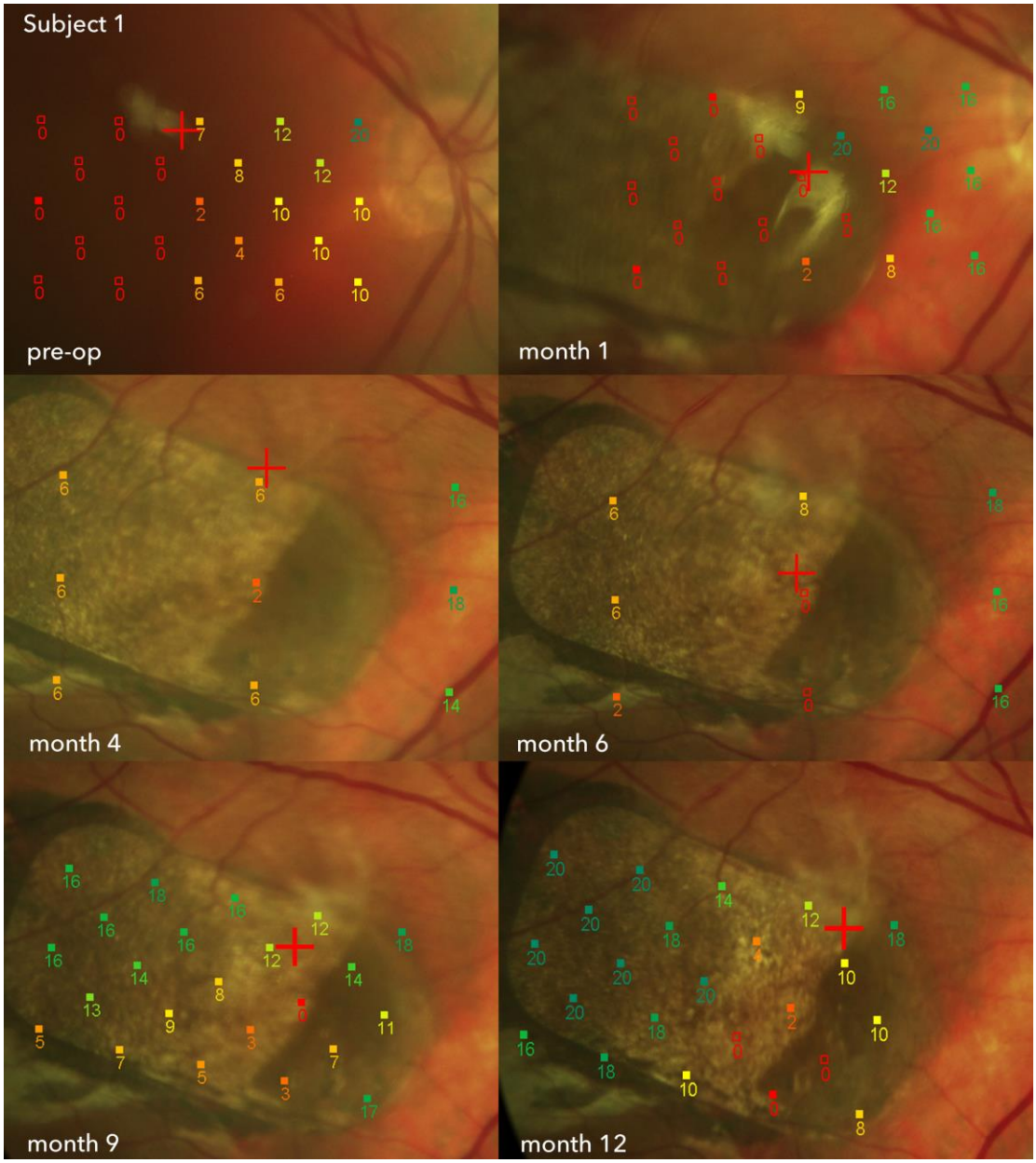

Figure 4-7: MP of subject 1 during year 1 (study eye). The numeric grid reflects the light sensitivity (in dB) of each of the examined retinal loci (corresponding coloured square “dots”).

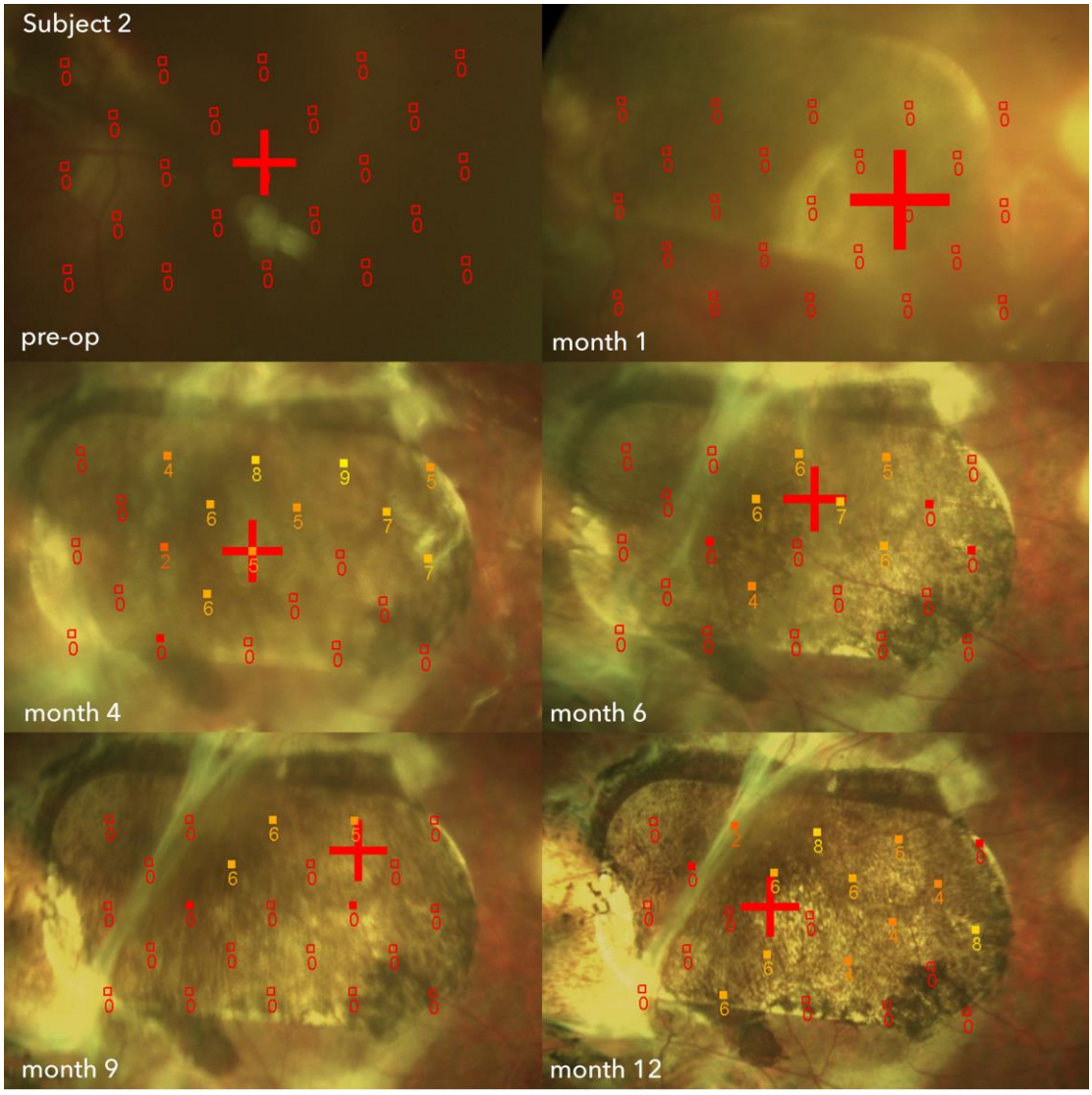

Figure 4-8: MP of subject 2 during year 1 (study eye). The numeric grid reflects the light sensitivity (in dB) of each of the examined retinal loci (corresponding coloured square "dots").

4.6. Structure – Function correlation

4.6.1. In areas of different pigmentation

In a previous section of this chapter, we observed and noted discreet areas of different levels of pigmentation at one-year post-transplantation – three (i-iii) for subject 1 and four (i-iv) for subject 2. When examining the MP pictures, we can see a correspondence between the changes in the pigmentation of the patch with time and the level of light sensitivity at multiple points.

In subject1, area (i), which represented the area of "doubled" RPE, it showed points of low sensitivity that decreased further with time. Area (iii), the area

with the denser and more stable pigmentation, started having sensitive points from month 4 and kept increasing until month 12, when it reached its maximum and close to normal sensitivity. On the contrary, in area (ii) whose pigmentation decreased with time, the MP sensitivity also demonstrated a significant decrease during the follow-up period (**Fig. 4-9A**).

Similarly, for subject 2 we have detected four discreet areas of variable pigment density: Area (iv) had the hESC-RPE compromised from the time of surgery and showed no sensitivity throughout the study. Area (i) was the most heavily pigmented area at month 12 and also showed 0 sensitivity of the examined points. Area (iii) - the most stable in terms of pigmentation - started giving some positive MP responses by month 4 (4-8 dB), which remained stable until month 12 (6-8 dB). Finally, area (ii) whose pigmentation decreased slightly with time, also showed sensitive points (5-9 dB) on month 4 and subsequently decreased (4-6 dB) until month 12 (**Fig. 4-9B**).

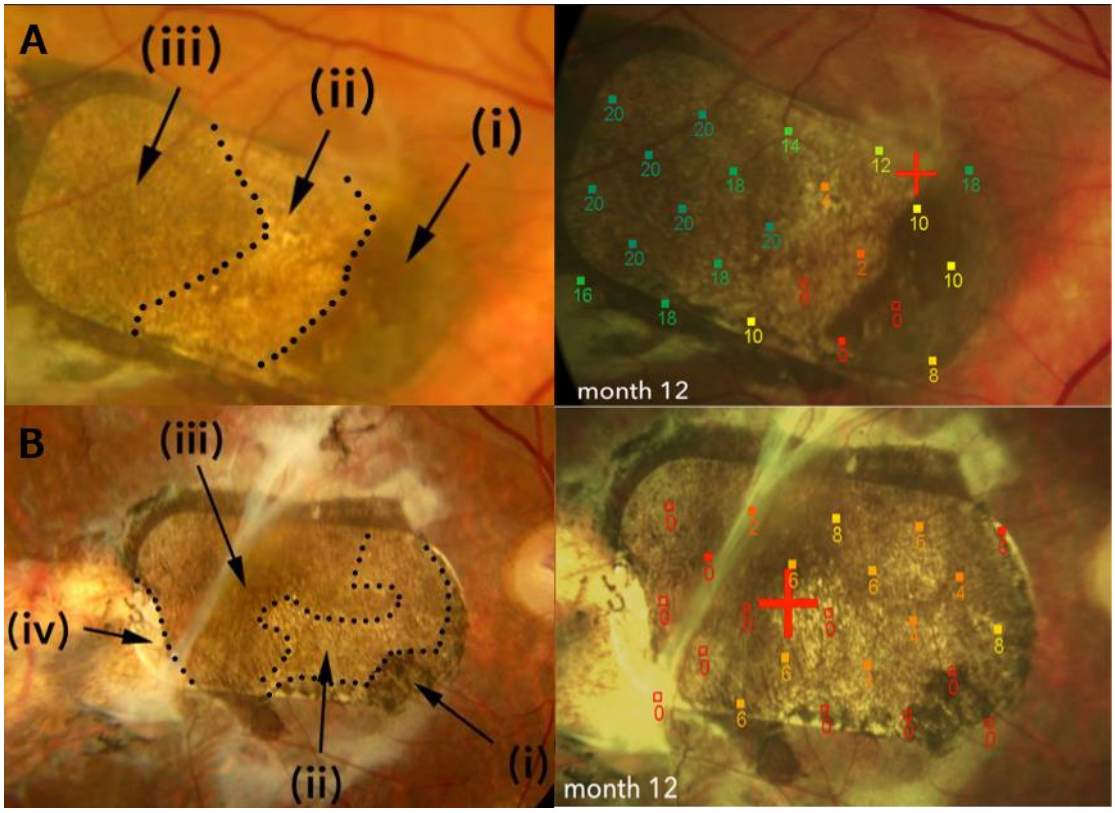

Figure 4-9: Correspondence between pigmentation and light sensitivity. CF photos and MP exams at year one, demonstrating the light sensitivity areal patterns matching the patterns of pigmentation on different areas of the grafted retina (subject 1 (A) and 2 (B)).

4.6.2. In specific light-sensitive loci

To consolidate our results, we analysed where possible the imaging characteristics of all the year 1 structural assessments, specifically focusing in areas of good light sensitivity in the MP exams. These areas were found to have good choroidal perfusion in the FFA, preserved signal of the photoreceptors' segments in the SD-OCT scans, active autofluorescence, and finally good density of cone photoreceptors-like structures in the AO images (**Fig. 4-10 and 4-11**).

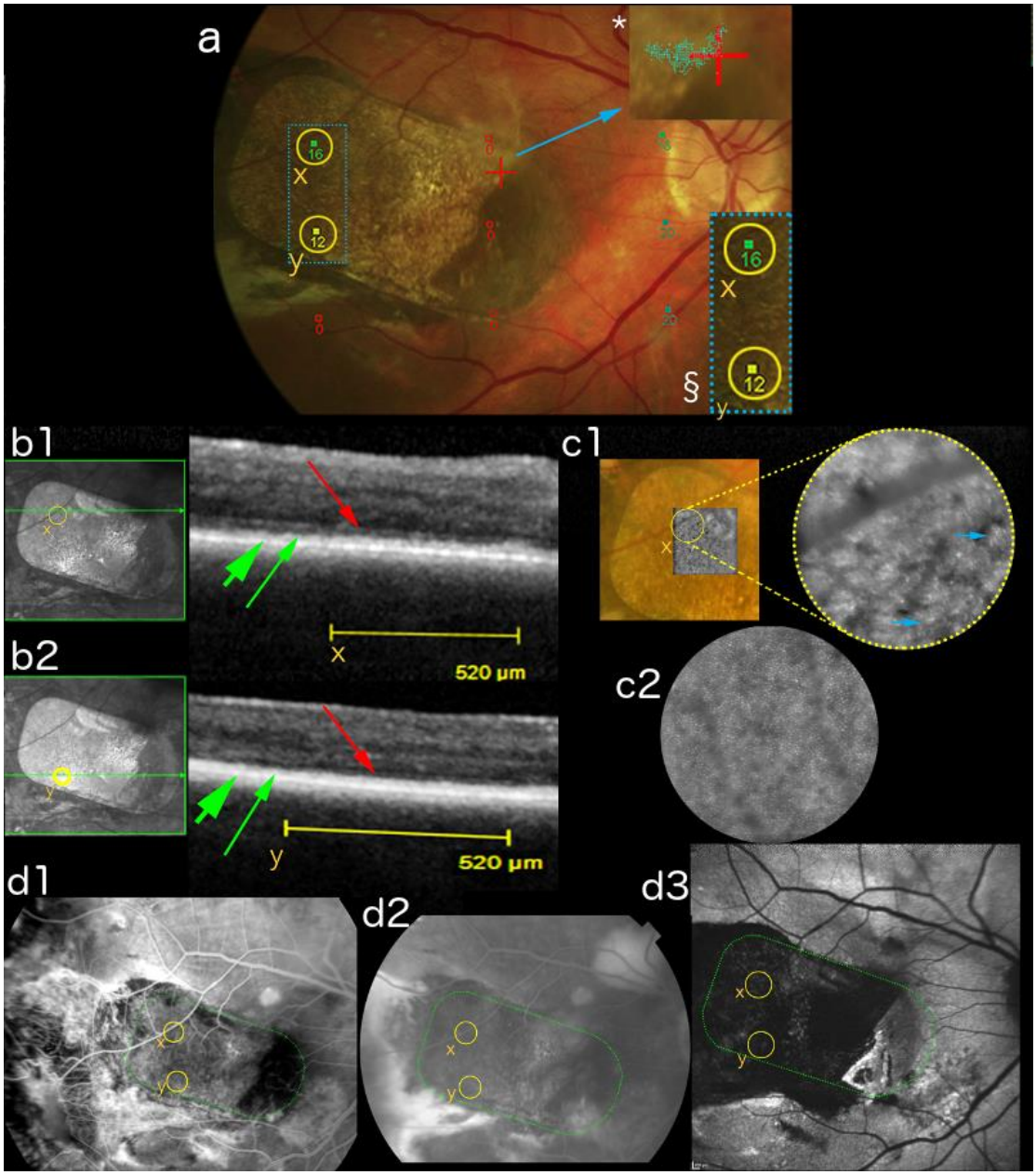

(Figure 4-10)

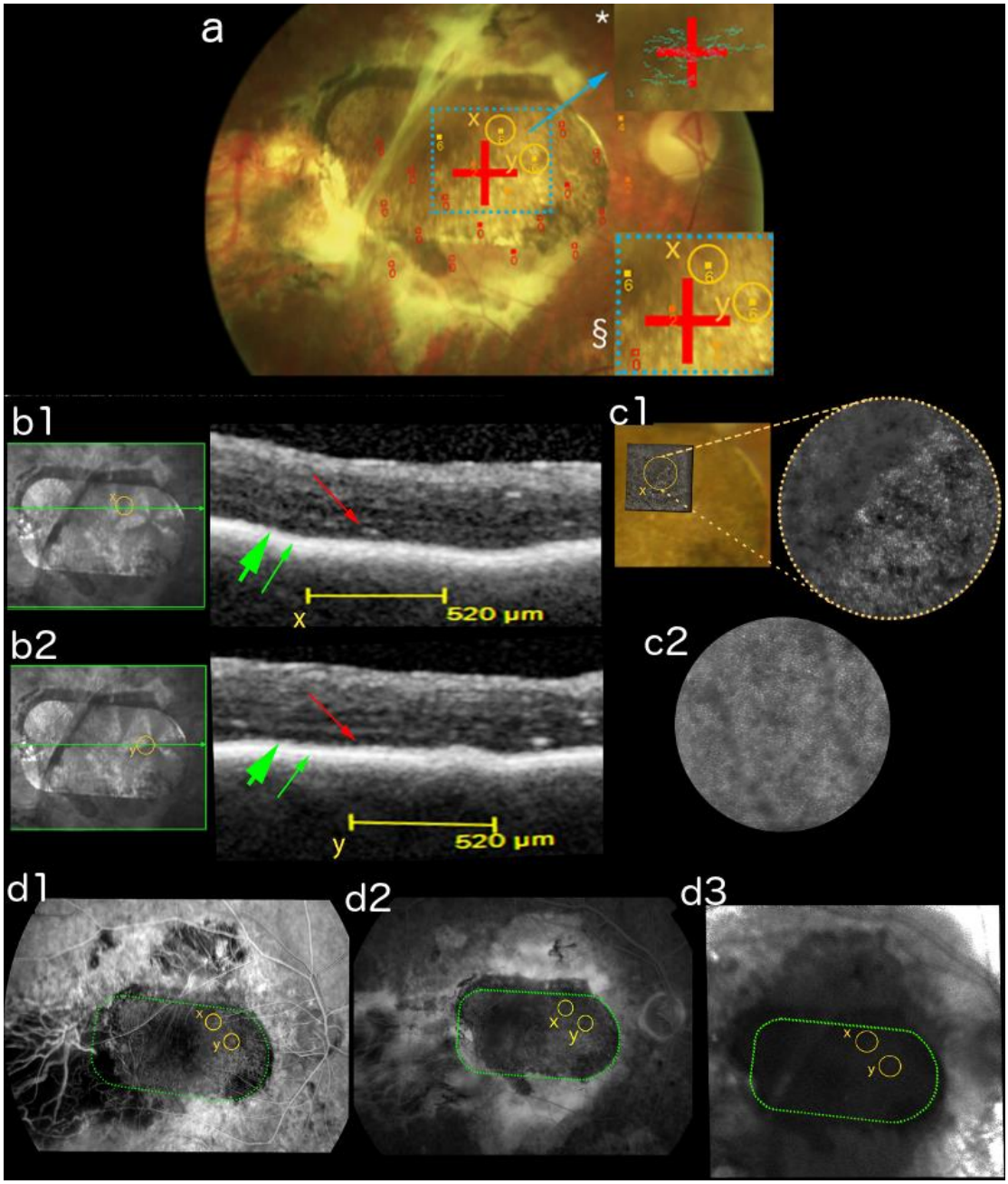

(Figure 4-11)

Figure 4-10 and 4-11: Structure-function correlation in two specific areas of the patch in subject 1 and subject 2 respectively. (a): Colour fundus photograph of microperimetry exam showing the patch covered with pigmented cells throughout and MP results with two areas of demonstrated sensitivity labeled x and y. The circles represent the extent of the visual stimulus demonstrating that it falls completely within the transplanted area. Inset (§) shows a magnified detail of the patch area with the levels of sensitivity shown by microperimetry in decibels. Inset (*) shows a close up of the fixation with the Nidek microperimeter fixation outcome superimposed. (b1) and (b2) show Spectral domain OCT sections through x and y respectively. The area on the section corresponding to x and y is indicated with a bar the length of which corresponds to the diameter of the MP stimulus

projection. The long red arrow in (b1) and (b2) indicates the ellipsoid layer. The thin and bold green arrows in (b1) and (b2) indicate the synthetic membrane and the hESC-RPE respectively. (c): Images from the Rtx1 AO fundus camera. (c1): Inset-color fundus photo with superimposed area of AO imaging. The dotted yellow circle corresponds to the area of positive micro-perimetry sensitivity marked x throughout this figure. (c1) magnified image of the area indicated by the dotted yellow line in (c1) showing bright dots corresponding to cone photoreceptors based on their size, inter-photoreceptor distance and organization (blue arrows). (c2): AO image taken from a normal subject at the same point of the retina as in (c1) for comparison. (d1): Early phase Fundus fluorescein angiogram (FFA) showing early choriodal perfusion and 'ground-glass appearance in the area of the patch and specifically the two points of demonstrated sensitivity x and y. (d2): Late phase FFA confirming continued choroidal perfusion and no leakage under the patch. (d3): SLO autofluorescence over the patch including in areas x and y showing dim but visible autofluorescence.

Discussion

This chapter presents evidence of improved retinal function following hESC-RPE – artificial BM patch transplantation, as an experimental treatment for acute neovascular AMD. Two subjects received the implant and both demonstrated a combination of good safety and structural support of the treated area (as seen in Chapter 3) with significant improvement in the visual function in the study eye, during the 1st follow-up year. Local immunosuppression – by a fluocinolone intravitreal implant – was used for the longer term, while oral prednisolone was used in the peri-operative period.

Although AMD is a bilateral, relatively symmetric disease, (Gangnon et al., 2015) it is less likely to be symmetrical in SMH as the event is so catastrophic and variable. However, it is worth considering the fellow (non-treated) eye of each subject as a form of coarse internal control. Subject 1 had a previous ocular history of subretinal haemorrhage due to wet AMD in her non-study (left) eye too. After a series of anti-VEGF injections and a vitrectomy for vitreous haemorrhage, her non-study eye VA stabilised at approximately 2/60 (Snellen VA). At the beginning of the trial her ETDRS BCVA score in the left eye was 38 letters, while during the follow-up it was

showing a mild fluctuation and by the end of the 1st year it was 38 letters, thus equivalent to the operated eye (39 ETDRS letters). Its CS(log) score showed a slight improvement from 0.75 at baseline to 1.2 after 1 year. Similarly, the RSmax increased from baseline 37.1 wpm to 80.83 wpm at 1 year. Since the severity of the disease and the visual acuity in the left eye showed no significant change during the follow-up period, we believe that the observed improvement in CS and reading speed may be attributed to a “learning effect” over these assessments. We acknowledge that this hypothesis could also apply to the treated eye, however, the latter started from a far lower VA and its increase in CS and RSmax were larger.

Subject 2 had active wet AMD disease in his non-study (left) eye, for which he was already under standard monthly intravitreal anti-VEGF treatment when he entered the trial. This eye showed a stable visual acuity, which started at 74 ETDRS letters and, on year one, was found to be 73 letters. However, this preservation of VA was achieved by a continuous monthly intravitreal anti-VEGF regimen, which until the end of the study period had failed to suppress the disease activity and the eye had persistent pigment epithelial detachment and neurosensory retina detachment, due to leakage by a neovascular membrane. Conversely, the operated eye showed no signs of CNV activity after the initial clearance of sub-retinal blood and the implantation of the hESC-RPE patch. Moreover, in terms of CS, the left eye showed deterioration from 1.95 log score at baseline to 1.5 after one year. Similarly, its reading speed decreased from 205.3 wpm to 187.5 wpm in the same period, while the treated eye demonstrated improvement in both.

Another necessary consideration is how our suggested treatment compares with the natural history of acute wet AMD complicated with submacular haemorrhage (SMH). It has been well documented that subretinal accumulation of blood can cause severe and permanent damage to the photoreceptors and the outer nuclear layer. This destructive result has been attributed to a combination of mechanisms that include *mechanical* factors, such as retraction of the clot meshwork and physical blockage of nutrient diffusion, as well as cell *toxicity* factors from the blood components and their degradation products, such as iron and haemosidirin. Permanent tissue

damage has been shown in animal models to occur within 24 hours (Glatt & Machemer, 1982) and without treatment the natural course of AMD with haemorrhage is very poor(Avery, Fekrat, Hawkins, & Bressler, 1996; Glatt & Machemer, 1982; Scupola, 1995). Various case series have indicated this guarded prognosis reporting a mean long-term VA ranging between 20/1600 and 20/200 in different series, and an overall trend towards worsening with time (Bennett, Folk, Blodi, & Klugman, 1990),(Scupola, 1995),(Avery et al., 1996),(Stanescu-Segall et al., 2016). In the Submacular Surgery Trial Report 13 (Bressler et al., 2004), the single available randomized controlled study that compared surgical removal of CNV/SMH versus observation, only 11% of the observation cohort eyes (15 of 140) had a BCVA better than 20/200 after 24 months of follow-up, while the corresponding baseline percentage was 38%. From the 140 monitored eyes 60% lost 2 or more lines (10 ETDRS letters) and 20% lost 6 or more lines (30 ETDRS letters) within 24 months, resulting in 40% of patients (56 eyes) having a BCVA of worse than 20/800 by the end of the 2 years period.
In our two subjects, the study eye VA did not show any downwards trend during the first year. On the contrary, both showed continuous improvement, until year 1 for subject 1 and month 6 for subject 2, and their VA was preserved thereafter at 20/125 and 20/250 respectively.

As it would be expected for a severe disease with a poor prognosis, numerous therapeutic approaches have been attempted. However, review of the relevant literature shows that acute haemorrhagic AMD has no definite treatment proven to be consistently superior to others. Within the obvious limitations, I will discuss and compare the results of our experimental stem cell treatment with the alternatives that have previously been reported.

Until the emergence of the anti-VEGF therapies, the available treatment options for neovascular AMD were laser photocoagulation, verteporfin photo-dynamic therapy (PDT) and macular surgery, including macular translocation. At present, repeated intravitreal injection of anti-VEGF agents is the treatment of first choice for the vast majority of wet AMD cases, as it has been proven superior to the other options(Khanna et al., 2019). Only a small percentage of patients, and mainly those with severe submacular

haemorrhage due to bleeding from CNV or choroidal polyps (or less commonly after failure of anti-VEGF treatment) are now considered unlikely to benefit from long-term anti-VEGF treatment. The spectrum of treatment approaches for this group extends from relatively *minimal* invasive treatments, such as displacement of SMH with expansile gas alone, to complex macular translocation surgery or autologous RPE transplantation. As well as the range of surgical options, various adjuvants to the surgery have been used such as intravitreal or subretinal injection of tissue plasminogen activator (TPA), or intravitreal anti-VEGF (as monotherapy or adjunct therapy). These techniques, as well as the more recent, experimental stem cell-based approaches have been outlined in detail in the Introduction / literature review of this thesis (Chapter 1) and their results have been summarized in the tables below.

Table 4-4: Reported VA changes in minimal interventions for AMD+SMH

Approach	aVEGF monotherapy	Gas monotherapy	aVEGF / Gas	TPA / Gas	aVEGF/Gas/ TPA
Mean VA change	+ <10	+15	+30	+23	+15

Table 4-5: Reported VA changes in major surgical approaches for AMD+SMH

Approach	PPV / SMH removal	PPV / TPA / Gas	PPV / TPA / aVEGF/ Gas	PPV / aVEGF +TPA / Gas	Macular transloca tion	Auto- /Homologous RPE transplantation
Mean VA change	+22	0	+40	+14	+5	+ <5

Table 4-6: Reported VA changes in SC approaches for AMD

Approach	(ACT) Ocata Therapeutics	CHA Biotech	RIKEN	CPCB
VA change	+14 (median)	+ 1-9	0	-4 – +17

It is important to note here that any positive outcomes of the interventions listed above have to be weighted against the appreciable risk of complications, such as retinal detachment, PVR, macular hole, RPE rip, vitreous haemorrhage and recurrent SMH. Larger level 1 trials with more standardized approaches are still needed in order to make conclusions on the safety and efficacy of such methods.

Compared to the cell suspension approach, it is possible that the delivery of the therapeutic cells in a pre-formatted monolayer is beneficial for their polarization in an apical-basal manner and for the development and preservation of the inter-cellular tight junctions (Georgiadis, da Cruz, & Coffey, 2017). Pre-clinical studies using RPE cells suspensions have shown the potential of monolayer orientation of the cells, however, they also showed the presence of irregular distribution and formation of multiple layers, which can result in increased risk of graft failure and even damage of adjacent photoreceptors (Binder, 2011; Crafoord et al., 1999). The promising results of our approach could be partially justified by overcoming these disadvantages using the cell-patch method and partially to our decision to try our cell therapy in cases of acute wet AMD, where the permanent death of photoreceptors has not yet been fully established.

It is also well documented that the target tissue initially affected by the AMD is the BM-RPE complex while the photoreceptors are affected later on the course of the disease. For a RPE replacement therapy to achieve vision restoration there should be viable photoreceptors to rescue. Studies on macular translocation and autologous RPE transplantation have shown that early intervention, before severe photoreceptor loss and retinal atrophy are established, is critical for the reversal of vision loss(da Cruz et al., 2007; Uppal et al., 2007). Furthermore, previous cell suspension trials have highlighted the critical role of a healthy Bruch's membrane for the successful integration of the transplanted cells and their long-term survival(Gullapalli et al., 2005; Tezel et al., 1999; Tsukahara et al., 2002). Compared to our cases, the modest functional outcome of the first reported iPSC-RPE sheet case (Mandai et al., 2017) could be attributed primarily to the long-standing (four years) severe vision loss pre-operatively and secondarily to the absence of a

scaffold-like structure to replace the compromised host BM. In our study both subjects were operated within 6 weeks from the acute VA loss, therefore ahead of an extensive photoreceptors' death. In addition, we used an artificial polymeric biocompatible membrane to secure the intra-operative manipulation of the graft and support its structural and functional integrity in the long term, and thus compensate for the damage of the host's BM caused by the submacular haemorrhage and the primary AMD disease process.

Even though the BCVA is by default considered as a universal index of visual resolution, it represents only a narrow aspect of visual function, limited to the ability to read specific sharp-edged characters in the highest possible signal-to-background contrast and from a fixed distance. In the real world, the identification of objects and images, as well as the ability to read, require more complex visual processes that cannot be examined by any single visual function test. Hence, understanding the impact of vision loss in retinal disease, as well as assessing the benefits of a potential treatment requires a broader and multi-functional examination of the quality of vision.

Contrast Sensitivity (CS) tests have been proven to provide additional information and in many cases to reflect visual function and dysfunction with higher sensitivity than visual acuity (Fletcher & Schuchard, 2006; Marmor, 1986; Sekuler, Admas, Biederman, & Carr, 1986; Solomon et al., 2019)
In our study, both subjects demonstrated a significant improvement in the CS scores of their operated eye. More specifically, subjects 1 and 2 showed an 18-letter and 24-letter gain, respectively, in the Pelli-Robson chart, by the end of year one. It has been suggested that the CS changes can have a more significant impact on the patients' quality of vision than the ones of VA alone (Patel, Chen, da Cruz, Rubin, & Tufail, 2011), (Roh, Selivanova, Shin, Miller, & Jackson, 2018). Although the quantitative correlation between VA and CS changes is not fully defined, it has been reported that a 6-letter change in CS can affect the quality of vision as much as a 15-letter change in VA (Monés & Rubin, 2004). In this sense our subjects have demonstrated a more significant improvement in their CS than the actual VA, which we believe represents an additional support of success in restoring function following our experimental treatment. This should also reflect in their reading ability. Especially for subjects with low vision it seems that the correlation of the CS function with

the ability to read may be stronger than the one of VA (Leat & Woodhouse, 1993).

The process of reading is comprised of multiple visual factors that can be affected by the disease and potentially improved by its treatment. Testing the ability to read with one eye, examines a combination of functional factors, such as visual acuity reserve, contrast reserve, field of view and size and density of any central scotoma (in cases of maculopathy)(Whittaker & Lovie-Kitchin, 1993). That said, a post-therapy improvement in the reading ability should reflect a corresponding improvement individually in some - if not all - of these factors.
In our trial, both the subjects showed increase of the reading speed (RSmax) in their treated eye, which we believe reflects an overall improvement in their macular function. Moreover, this gain in reading ability was superior to the one reported from patients of the SST trial (Bressler et al., 2004).

The final assessments that manifest the functionality of our graft are fixation and microperimetry. It has been well documented that fixation is broadly compromised in patients with neovascular AMD, with a large number of them using a retinal area of more than 5° within which their fixation fluctuates(Pedersen, Sjølie, Vestergaard, Andréasson, & Møller, 2016). It has also been reported that a stable fixation is usually associated with better functional (in terms of visual acuity) and anatomical (in terms of outer retina architecture in OCT scans) outcomes of anti-VEGF treatment(Mathew, Pearce, & Sivaprasad, 2012; Sivaprasad, Pearce, & Chong, 2011). Our patients not only retained fixation stability after one year, having 100% of the tested points within the 4° area of the given target, but also demonstrated this area to be completely over the patch-supported macula. However, they both had a “relocation” of their centre of fixation to a locus adjacent to their “calculated” pre-implantation foveal centre. More specifically, subject one’s and two’s fixation centers were shifted nearly 3° and 5° respectively, from their baseline foveal centre. This “eccentric” fixation is a well-documented early implication of exudative AMD with subfoveal CNV, nevertheless is commonly associated with compromised fixation stability, which our two

subjects did not show. In a study of 179 eyes with nAMD by Fujii *et al.* 103 eyes (67%) had unstable or relatively unstable fixation (18% and 39% respectively), while 75% had central fixation within 2° of the fovea(Fujii, de Juan, Humayun, & Sunness, 2003). Our two subjects maintained a stable fixation after one year, even though its centre was re-located. My hypothesis is that this might represent a result of the foveal damage induced by the initial sub-macular haemorrhage and/or the intra-operative manipulations, which forced a repositioning of the subject's preferred fixation to a healthier macular area. The fact that this healthier area was found entirely on the patch, and especially on a pigmented and sensitive (as seen in MP) position, supports the presumed structural and functional integrity of the grafted retina, compared with the adjacent degenerated areas.

Apart from the automated test, the fixation was also examined in the slit-lamp, with a brighter stimulus than the one of the NIDEK perimeter. In this test both subjects demonstrated a stable fixation, more centrally on the patch and closer to their fovea. A stable fixation with this technique has been described as a good indication of residual foveal function in a patients selection algorithm for macular translocation (Uppal et al., 2007). Our subjects maintained this "foveal" bright light fixation even when their NIDEK fixation had shifted. This provides another indication of rescued photoreceptor function over the patch.

The concept of Microperimetry for examination of retinal sensitivity was initially introduced in the early 1980s and its application in age-related retinal degeneration was recently reviewed by Midena *et al*.(Midena & Pilotto, 2017). It is considered as particularly suitable for assessing macular degenerative diseases and their therapeutic approaches, including autologous RPE-choroid transplantation(Nicola K Cassels, John M Wild, Tom H Margrain, Victor Chong, & Jennifer H Acton, 2017),(Chen et al., 2010; 2008; MacLaren et al., 2007) and macular translocation for neovascular AMD (Chieh, Stinnett, & Toth, 2008).

As MP measures the light sensitivity of specifically selected macular loci, it can provide more thorough information about changes in visual function in patients with AMD than the simple evaluation of visual acuity or contrast sensitivity. Fujii *et al.* have suggested a sequence of visual loss for patients

with exudative AMD(Fujii et al., 2003). After analysing the Microperimetry exams of 179 eyes, they concluded that the dysfunction of vision usually starts with reduced retinal light sensitivity, which is followed by visual acuity deterioration and finally deficiency of fixation stability and fixation eccentricity. This course of functional loss is aligned with corresponding structural damage caused by the disease, which is characterised by the gradually increasing RPE deficiency and photoreceptor loss. Conversely, MP studies of macular translocation and autologous RPE-choroid transplantation have shown improvement of retinal sensitivity over the grafted areas and this has been attributed to a healthier structural background for the surviving photoreceptors(Chen et al., 2008; Chieh et al., 2008; MacLaren et al., 2007). In our study both subjects demonstrated a combination of improved retinal sensitivity and fixation stability maintained to one year of follow-up. Furthermore, the topographic pattern of the patch's MP sensitivity matched consistently the topographic pattern of its pigmentation density, which supports the hypothesis of viable, pigmented hESC-RPE cells structurally and metabolically supporting the overlying photoreceptors for at least one year.

The major limitation of all of the observations in the last two chapers (3 and 4) is the small number of patients that are described. Furthermore, the lack of any histological studies makes it impossible to draw definite and direct conclusion about the fate of the implanted hESC-derived RPE cells. However, to my knowledge, this discussion and the associated article, incorporates the broadest combination of positive functional assessments that have been demonstrated so far, as well as solid indications that these encouraging outcomes originated from the retinal area that received the investigatory implant. In addition to a larger number of subjects, a longer follow-up is also necessary in order to establish both the safety and efficacy of our proposed therapy. However, we believe that the combination of preserved retinal anatomy with improved visual function in both our subjects after one year can only be attributed to the rescue of photoreceptors due to an efficient support by the healthy "zero-year-old" stem cell-derived RPE-BM implant.

Chapter 5

Second year outcomes

Introduction

In the previous chapters I discussed the structural and functional results of the hESC-RPE-BM patch one year after its transplantation into the submacular space of two subjects with advanced wet AMD and severe vision loss. Both subjects demonstrated sufficient safety – both ocular and systemic, good structural integrity of the patch and the related tissues, and significant functional recovery with all visual tests improving during the first year of follow-up. I also demonstrated a strong correlation between the anatomical support of the retina-RPE-BM complex, provided by the transplant, and the rescue of photoreceptors that lead to improved vision. In this chapter, I will present the longer-term outcomes of the studied therapy, in terms of its safety, its structural and functional results and the presumed fate of the implanted hESC-RPE cells, two years post-operatively.

Results

5.1. Safety outcomes

In general, the investigational hESC-RPE patch was well tolerated by both subjects for the whole follow-up period. There were no signs of acute or severe rejection, or of uncontrolled proliferation or tumorigenicity within the two years. No systemic adverse reactions were found related to the patch. Both subjects were only under local immunosuppression during the second year, by an intravitreal fluocinolone implant. Specifically, subject one had a *RETISERT* implant (Bausch+Lomb), injected in month 3, with assumed steroid release duration of approximately 30 months. Subject two had an *ILUVIEN* implant (Alimera Sciences Limited), injected in month 3, with assumed duration of action of approximately 36 months. No elevation of the intra-ocular pressure (IOP) or other local adverse effect was noted as a response to the topical or the intravitreal steroids, in either subject.

5.1.1. SAEs

During the first year we reported 3 serious adverse events, none of which was related to the investigational transplant (Chapter 3.2). During the second follow-up year we reported one single SAE, which was a transient ischemic attack (TIA) in subject 2 at post-op month 23. It was not related to his involvement in our study but likely to his long-standing arterial hypertension, diabetes and atherosclerosis. He was hospitalized for one day and recovered without sequelae.

5.1.2. AEs

Less severe events included:

Subject 1

- *Charles Bonnet* syndrome, which started around month 18 and was attributed to the bilaterally compromised vision
- Conjunctival irritation in the study eye, due to a recurring erosion of the conjunctiva over the site of the Retisert implant insertion (**Fig. 5-1**). It was causing a transient protrusion of the scleral suture (used to stabilize the intravitreal steroid implant) and it was healing spontaneously until it would erode again. Due to its transient nature, no definite treatment was decided and only symptomatic relief with eye lubricants was required.
- Re-activation of the background disease – wet AMD, in the study eye (**Fig. 5-2**). This was first suspected in year one FFA and OCT scans, when an extramacular PED was noticed, outside the superior-temporal arcade. Two months later, on month 14, it was associated with subretinal fluid (SRF) and an anti-VEGF injection (Aflibercept) was given. It responded fully to the treatment and both the PED and the SRF were completely absorbed two weeks after the first injection. This result was maintained with a “treat-and-extend” regimen that required another 5 injections during the second year, despite the absence of any signs of recurrence. For the whole period, the lesion remained restricted in a distal to the hESC-RPE location, constituting no threat for the integrity of the patch and related retina.

Subject 2

- Skin purpura attributed to the post-TIA anti-coagulant treatment and thus unrelated to the study transplant or procedures.

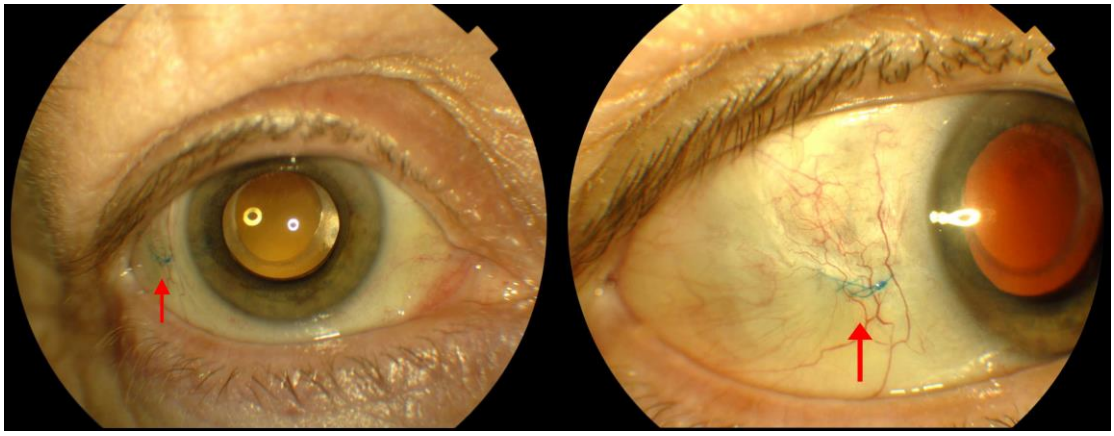

Figure 5-1: Adverse event of the surgical procedure in subject 1.
Protruding scleral suture in subject one's study eye, at year 2. The 8-0 Prolene suture (red arrow) was used to suspend the Retisert implant form the sclera into the vitreous cavity. No significant conjunctival erosion or inflammation is noticed.

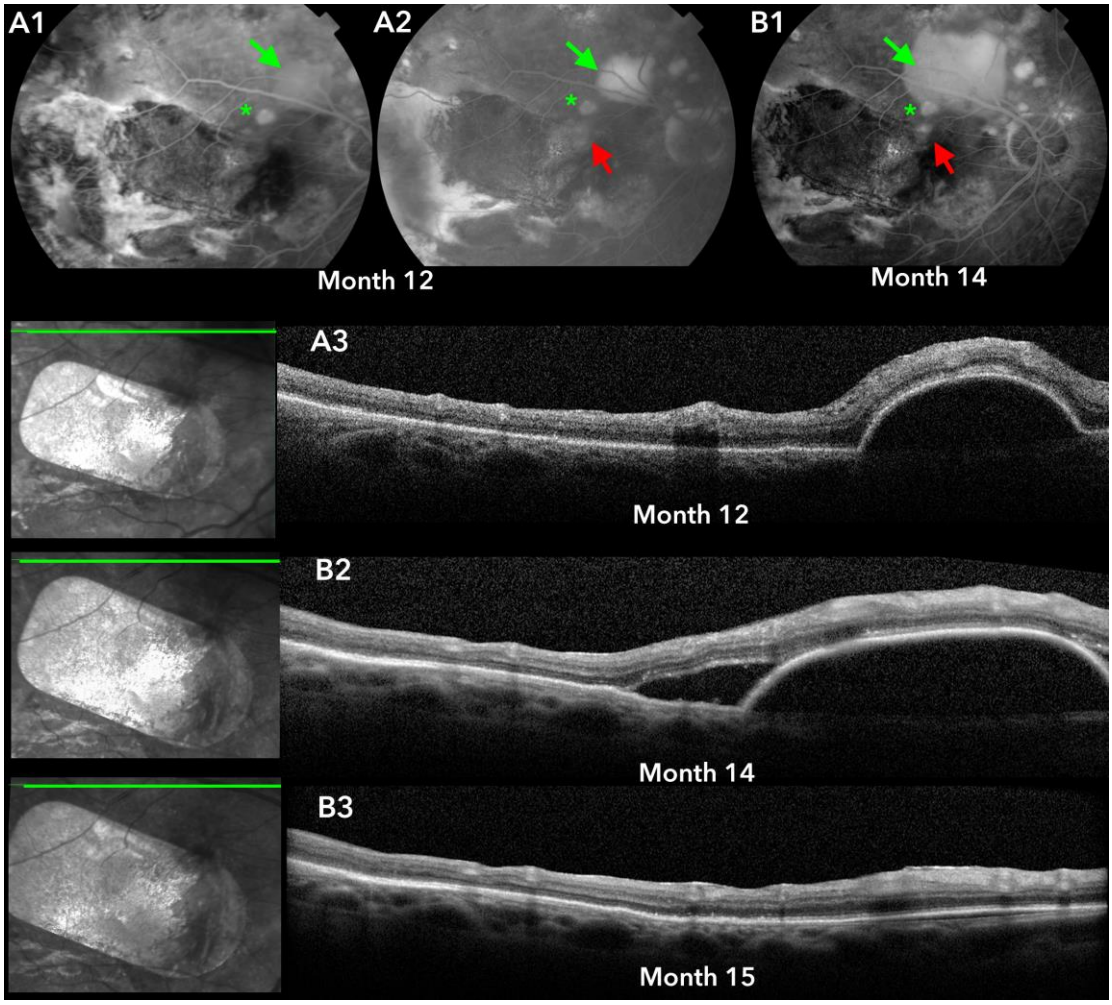

Figure 5-2: Recurrence and subsequent resolution of the baseline disease in subject 1. (A1, A2) Fundus fluorescein angiogram at post-op year 1, early and mid- phases respectively. Background choroidal perfusion is shown covering the bulk of the treated area. A PED is visible as a hyper-fluorescing spot (green arrow), adjacent to the superior-temporal arcade and separated from the hESC-RPE patch by not affected retina. The smaller hyper-fluorescing dot (*) represents a window defect due to atrophy. The ill-defined hyperfluorescence at the superior edge of the patch (red arrow) represents “staining” of a fibrotic lesion. (A3) SD-OCT scan through the affected area (green line in the near infrared photograph at the left) at year 1, confirming the presence of a PED in a distal to the patch location. (B1) FFA – late phase – two months later demonstrating enlargement of the PED, while the window defect (*) and the staining (§) have remained stable. (B2) SD-OCT through the affected area confirming the presence of PED which now is associated with sub-retinal fluid. (B3) SD-OCT scan through the same area 2 weeks after an intra-vitreal anti-VEGF injection showing complete resolution of both the PED and the SRF.

5.2. Structural outcomes

After the initial operations, both subjects had fully re-attached maculas and the transplanted patch was positioned under the fovea. As mentioned in chapter 3, subject 2 subsequently sustained a peripheral retinal detachment before the oil was removed and had surgery to treat this. In both cases the silicone oil was removed successfully, and the retinas remained attached and the patch in its sub-foveal position throughout the 2 years of follow-up. Monitoring with Slit lamp biomicroscopy and documented by colour fundus (CF) photography shows that the patch retained its shape, size, sub-retinal position and location in the macular area over the two years follow-up period (**Fig. 5-3, 5-4**).

5.2.1. CF photography – visual assessments

The position of the patch was examined using the same method as for year one (described in 2.4.2). CF photos from year 1, month 18 and year 2 were assessed. The results are demonstrated on table 5-1. For the antero-posterior direction, the patch was considered to be stable in the subretinal space and in the OCT scans was found to be flat, with no malformation during the 2nd year.

No significant migration of the patch was noticed in either subject. The measured changes in the controlled distances were in the scale of 0.05 mm for the linear ones and 0.2° for the rotational ones. These “changes” are very unlikely to represent an actual systematic movement of the patch, and are believed to fall into the error margins of the used method, as these have been described in the previous chapters.

Table 5-1: Measurements of the patch's position and orientation during year 2, for both subjects.

	od-gc (mm)	**bf1–gc** (mm)	**bf2–gc** (mm)	**od-gc^d1** (degrees)
Subject 1				
Y1	5.79	3.45	3.45	55.2°
M18	5.73 (-0.06)	3.45 (0.00)	3.45 (0.00)	55.3° (+0.1)
Y2	5.76 (+0.03)	3.45 (0.00)	3.48 (+0.03)	55.6° (+0.3)
Subject 2				
Y1	4.62	4.65	3.03	39.5°
M18	4.62 (0.00)	4.62 (-0.03)	3.06 (+0.03)	39.3° (-0.2)
Y2	4.59 (-0.03)	4.62 (0.00)	2.97 (-0.09)	39.5° (0.0)

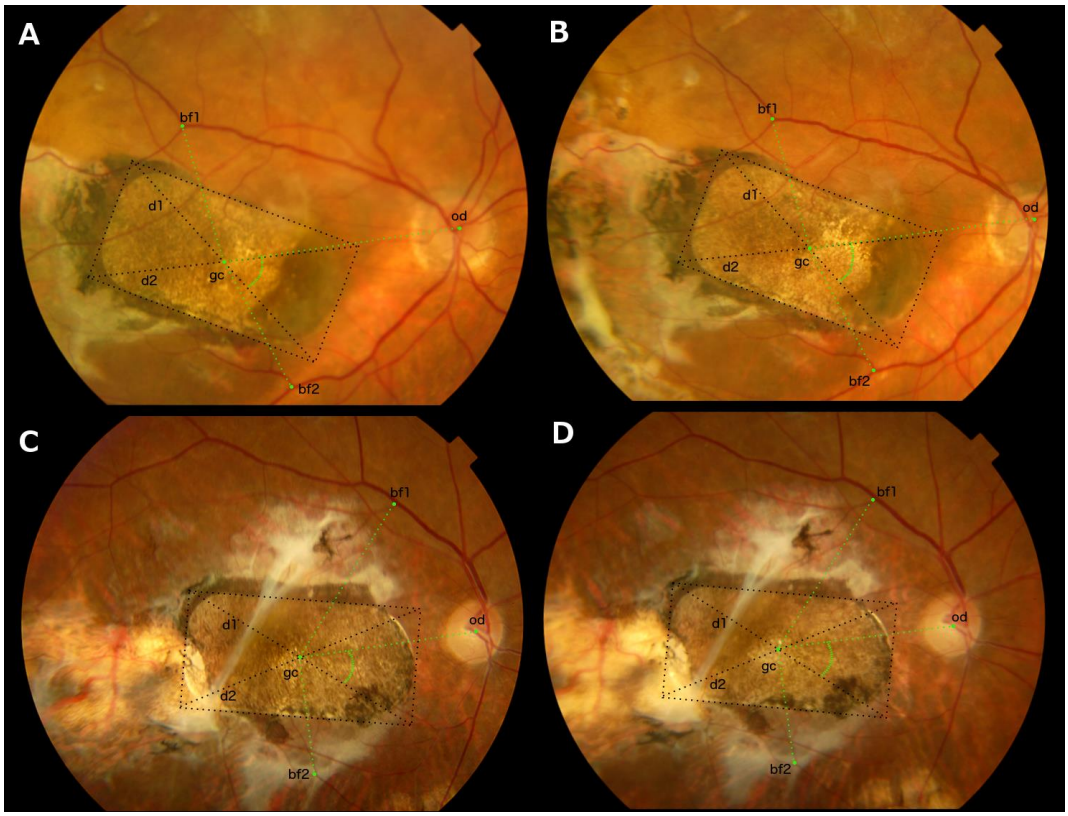

Figure 5-3: Assessment of the patch's location for the study period. Year 1 and 2 CF photos from subject 1 (A&B) and 2 (C&D), respectively. Measured distances and angles are shown with green dotted lines. (od) centre of the optic disc, (gc) geometric centre of the patch, (bf1) superior bifurcation, (bf2) inferior bifurcation, (d1)&(d2) diagonals of the patch.

The pigmentation, which remained relatively uniform for both subjects over the first year, manifested regional changes during year two. The previously described areas of different pigment density (chapter 3.2.1) were maintained, though with some small alterations.

Specifically, in subject 1, again three areas of distinct pigment density were observed at year 2 as had been described in year 1 (**Fig. 5-4, A2-3**):

(i) The darker nasal segment that initially covered the 1/3 of the patch's surface, but later reduced in size, and stabilized at approximately 1/4 of the patch by month 18.

(ii) The middle part of the patch, which had lost some of its pigmentation by year one and continued to decolorise during the second year, and

(iii) a part with even saturation at the temporal ½ of the graft, which remained stable and densely pigmented up to the two years follow-up.

Similarly in subject two's patch, we observed the same four distinct areas of pigmentation as in year 1 (**Fig. 5-4, B2-3**):

(i) The densely pigmented part, covering the inferior nasal corner of the patch. Its pigmentation initially appeared homogenous with the rest of the patch, but it soon it increased markedly, and finally reached its darkest hue during year 2.

(ii) The less pigmented middle nasal part of the patch including its geometrical centre, whose pigmentation decreased further during the second year.

(iii) The intermediately saturated hue of the superior and temporal part, which remained stable throughout the whole two years, and

(iv) The small fully decolorised area located at the inferior-temporal end of the patch (bottom left corner), which was noticed from the immediate post-implantation period and its shape, size and colour did not change throughout the two years.

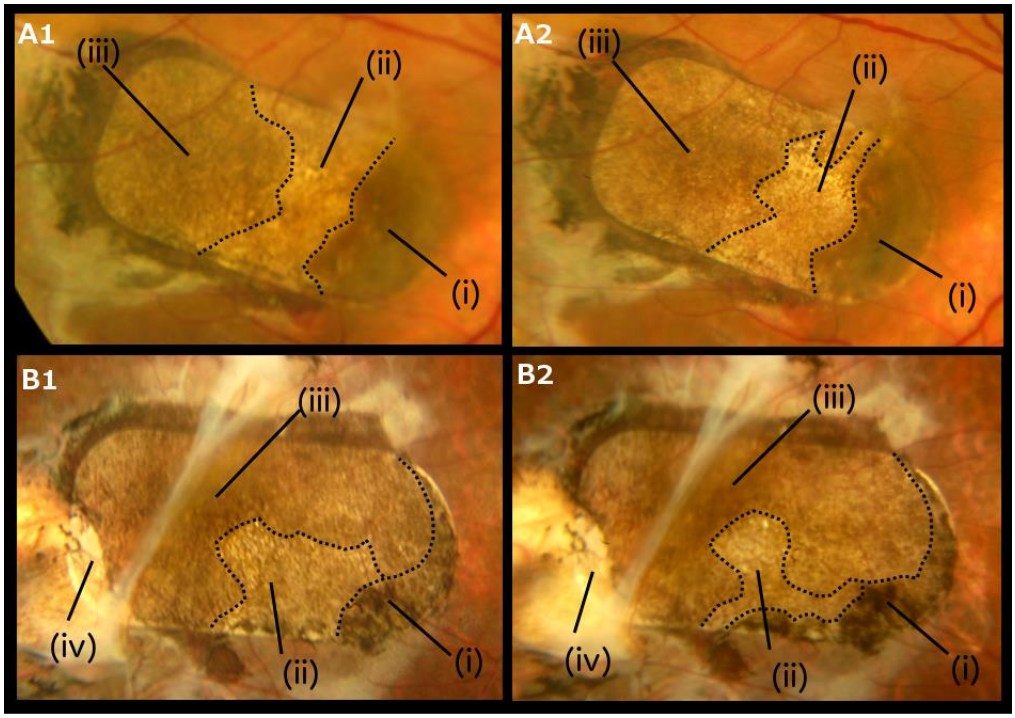

Figure 5-4: Pigmentation of the patch in year 2. Changes in the pigment density of the patch with time in both subjects. Year 1 (A1, B1) and year 2 (A2, B2) CF photos of subjects one and two, respectively. The annotated areas (i)-(iii) separated by black dotted line in (A1, A2) represent the patch's three segments of distinctive pigment density mentioned in the main text, for subject 1. Similarly, the annotated areas (i)-(iv) in (B1, B2) represent the four segments of the patch with distinctive pigmentation mentioned in the main text, for subject 2.

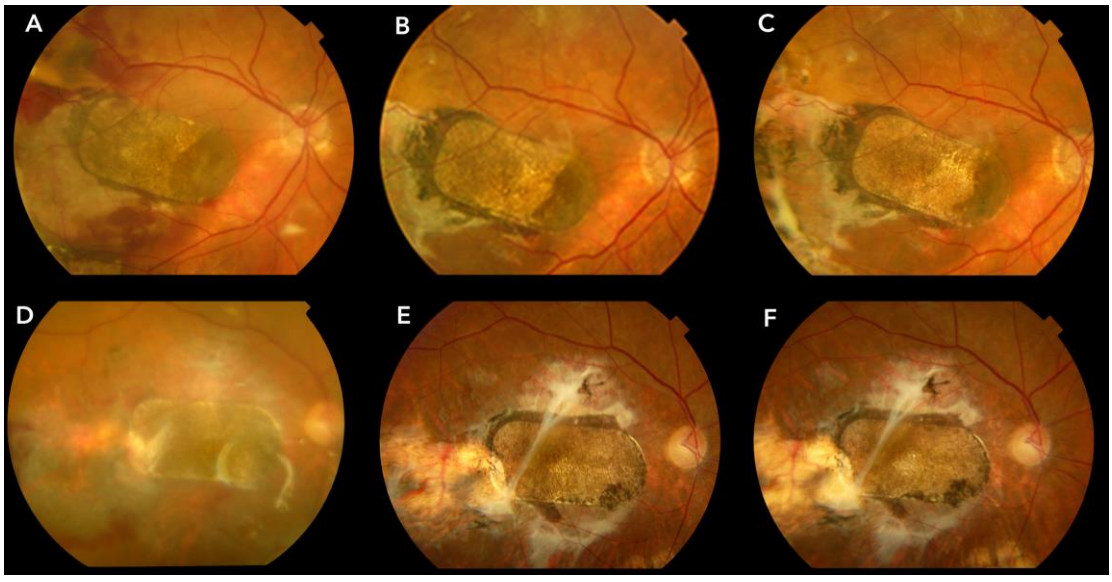

Figure 5-5: Extension of the pigmentation outside the patch's edges. Colour fundus photographs at month one (A and D), year one (B and E) and year two (C and F) of subjects 1 and 2 respectively. No noticeable change of the pigment expansion occurred during the second year.

As I showed in chapter 3, both cases had a centrifugal expansion of the patch's pigmentation outside its margins, which had stopped by the end of month 3 (chapter 3.2.1). During the second year this extension remained stable, showing no further growth (**Fig. 5-5**). A further analysis and documentation of the nature of this phenomenon will be made in chapter 6.

5.2.2. SD-OCT - Retinal ultrastructure

In the previous chapter, I analysed the OCT features of the hESC-RPE-BM patch during the 1st year. The imaging of the patch remained relatively stable during the 2nd year. In this part, I will mostly focus on the OCT characteristics of the neurosensory retina over the patch, showing the changes of its ultrastracture over the two years of the study period.

As mentioned in the previous chapter, from the early post-operative period, the SD-OCT scans revealed a continuous, hyper-reflective, double band in the outer retina, representing the two layers of the implant – the hESC-RPE monolayer and the polyester membrane. This finding appeared in both subjects' scans, covering almost the whole grafted area and was retained for the two years of follow up (**Fig. 5-6E** and **5-8E**).

In subject one's early scans, I detected a residual fold of native RPE on top of the nasal side of the patch, which corresponds to the area of darker pigmentation seen in the CF photos. This area showed some contraction with time and after the first year its outer retinal layers appeared disorganized and, by year two, the distinction of any RPE band in this location was not possible (Figure 5-6 A to D). In subject 2 a small part of the outer band appears "stripped-off" in the infero-temporal corner of the patch. It shows similar reflectance and continuity to the rest of the hESC-RPE and resembles a thickened and partially detached part of it. The area is visible on the CF photos, and was noted from the very first, early post-op exams (**Fig. 3-9**). The appearance on CF photos and OCT has remained unchanged for the two years. The rest of the hESC-RPE band on OCT remained typical and continuous during the two years (**Fig. 5-8E**).

In terms of the neurosensory retina (NSR), in case 1 SD-OCT scans showed preservation of its multilayer structure over the large proportion of the grafted area for two years. Specifically, distinct nerve fiber, plexiform and nuclear layer segmentation was visible (Figure 5-6E). In case 2 the layers were less distinct and the margins appeared “merged” in most of the cross-sections from month 6 onwards (Figure 5-8). In both subjects there was a visible outer retina hyper-reflective line between the ONL and the hESC-RPE, considered as consistent with the rescued ELM-ellipsoid zone complex, and identifiable until the end of the study period. Both subjects also had a decrease in the NSR thickness seen from the early OCT exams. More specifically, subject one had a marked retinal thinning on the temporal margins of the “double RPE” area, noted from post-operative month one, which gradually worsened to become an almost full-thickness hole during the second month, which closed spontaneously one month later (**Fig. 5-6 & 5-8**). Apart from this focal tissue loss, the overall thickness of the NSR over the patch was lower than normal, while the retina over the “double RPE” area was found abnormally increased (**Fig. 5-6**). Similarly, the second subject’s OCT scans showed a locally decreased thickness close to the center of the patch, which reached an almost full thickness defect at 4 months that subsequently improved and stabilized until the end of the 2nd year follow-up. For both subjects the area where the most marked retinal thinning was noticed corresponded to the area of their “anatomical” (pre-operatively) fovea. This was also the area of observed reduced pigmentation of the patch (**Fig. 5-4**, area “ii” for both subjects). The retina over the nasal part of the patch had normal thickness at year two, while the temporal part appeared thickened due to a marked epiretinal fibrosis (**Fig. 5-8**). Both subjects showed some cystic degeneration with time, which for subject 1 was limited over the nasal “double RPE” area, while for subject 2 was more general over the area of the patch (**Fig. 5-6, 5-8**).

Both subjects developed some epiretinal fibrosis, which for the first was detected over the nasal part as a thin ERM, and for the second was more broadly spread and formed a dense strand over the temporal part of the SC sheet (**Fig. 5-6, 5-8**). Both subjects also developed some retinal and subretinal scarring, which for subject 1 was more prominent temporally to the

grafted area (corresponding to the surgical pathway of the patch insertion) (Figure 5-7), while for subject 2 was more significant and extended superiorly, temporally and inferiorly to the patch (Figure 5-9). This scarring was established by year one and remained stable during the second year.

5.2.3. Fundus autofluorescence (FAF)

Subject 1

Fundus autofluorescence (FAF) images initially showed some granular autofluorescence spread over the grafted area and adjacent temporal fundus. The nasal part of the patch (where the native RPE overlapped the implanted one) showed an AF signal close to the intensity of the native fundus. Temporally to this “double-RPE” area there was no AF signal at the patch, corresponding to an area of tissue loss in OCT. Subsequently, the FAF surface and strength decreased but the reflectance became more homogenous by month 3, particularly over the temporal half of the patch. The area outside the patch lost its intense AF by month 6, while the hESC-RPE maintained a low but stable autofluorescence with no significant changes during the second year (**Fig. 5-10**).

Subject 2

There was no early detection of FAF. The first signal was captured at month 3. The patch was hypo-fluorescent (relative to normal RPE fluorescence) with a low but homogenous signal. This increased with time and on year 1 images we can detect distinctive AF intensities: an evenly hypo-fluorescing patch with an almost “quiet” centre, corresponding to the area of severe central thinning on OCT (**Fig. 5-10, B4**); an area of intermediate brightness surrounding the patch, and the higher reflectance of the native RPE. This distribution was maintained until the end of the second year (**Fig. 5-10, B5**).

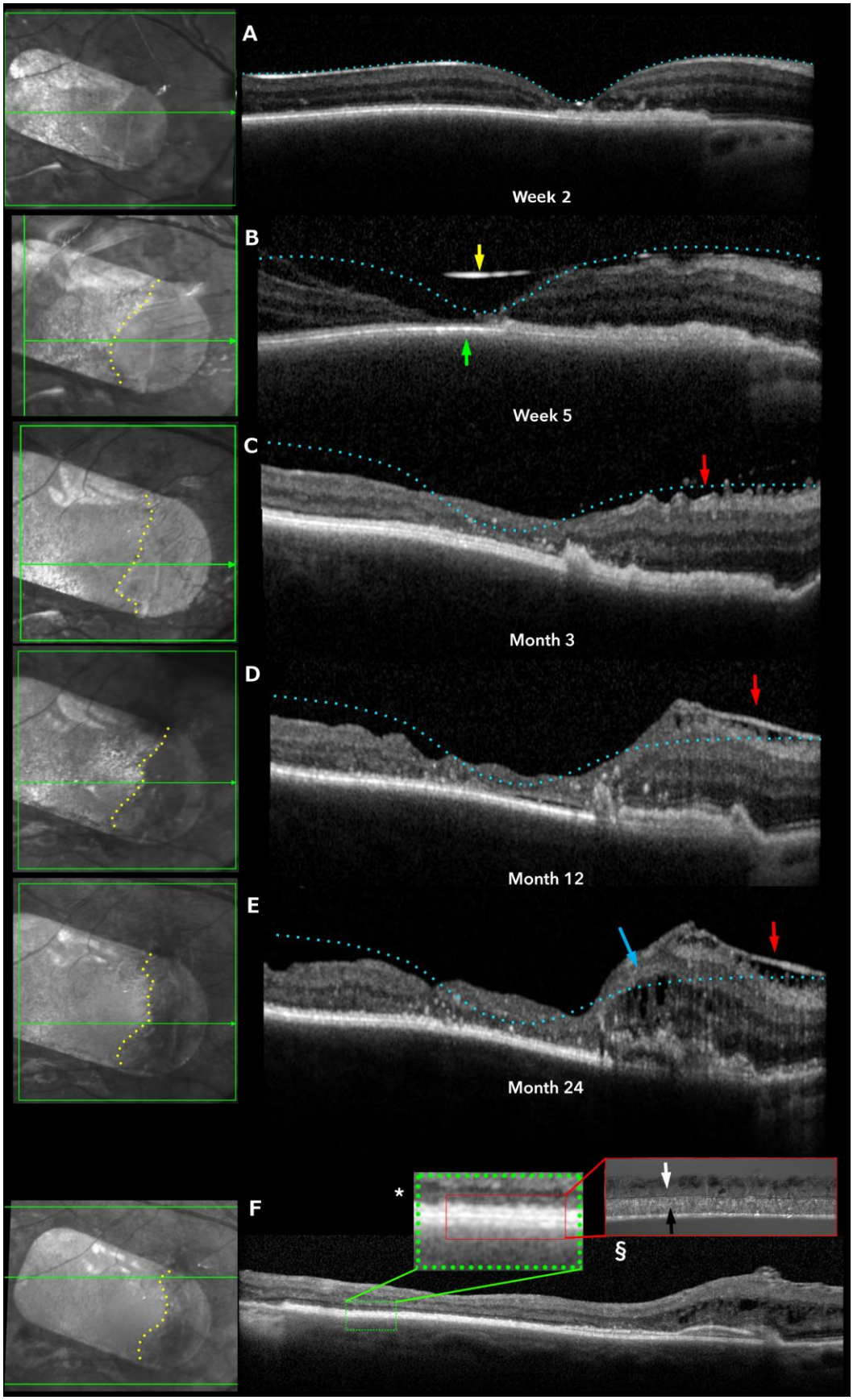

Figure 5-6: SD-OCT series of subject 1 during the study period. Near infrared photos at the left part indicate the plane of the b-scan at the right. Scans from the same retinal location (B-E) have been exported using the

follow-up option of the Heyex software (Heidelberg-Spectralis). (A) SD-OCT from post-op. week 2, before significant structural changes occurred, thus showing normal retinal thickness (blue dotted line for contour). (B) scan from week 5 showing severe retinal thinning to an almost full thickness defect (green arrow). The hyper-reflective line inner to retinal contour (yellow arrow) represents the silicone oil interface. (C) SD-OCT from post-op month 3 showing retinal reformation and closure of the defect. An ERM is appearing over the nasal part (red arrow). (D and E) SD-OCT scans from post-op. year 1 and 2 respectively, showing stabilization of the retinal thickness over the bulk of the patch, with some thickening later cystic changes in the nasal part of the treated retina (blue arrow in E). (F) SD-OCT scan through the whole patch from post-op. year 2. Good retinal segmentation and preservation of the double-layered structure of the patch seen in the higher magnification square (*). Correlation of the in vivo cross-section of the patch (*) with the in-vitro Electron Micrograph cross section (§), taken from an equivalent patch after manufacturing. The hESC-derived cells (white arrow) are visible immobilized and polarized on the synthetic BM (black arrow). The yellow dotted line in the near infrared photos indicate the contraction of the “double-RPE” segment during the study period.

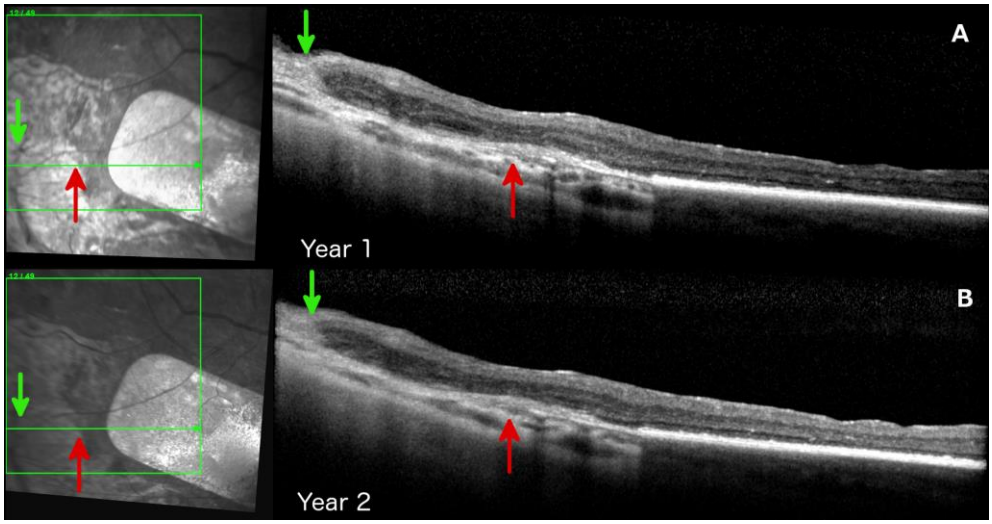

Figure 5-7: Subretinal scarring in subject 1. Year one (A) and two (B) NIR images (left) and OCT scans (right) including the area of the patch’s surgical insertion. The red arrows indicate the area of subretinal scarring which is hyper-reflective in the OCT. The green arrows indicate the retinal scarring from the area of the surgical pathway to insert the patch.

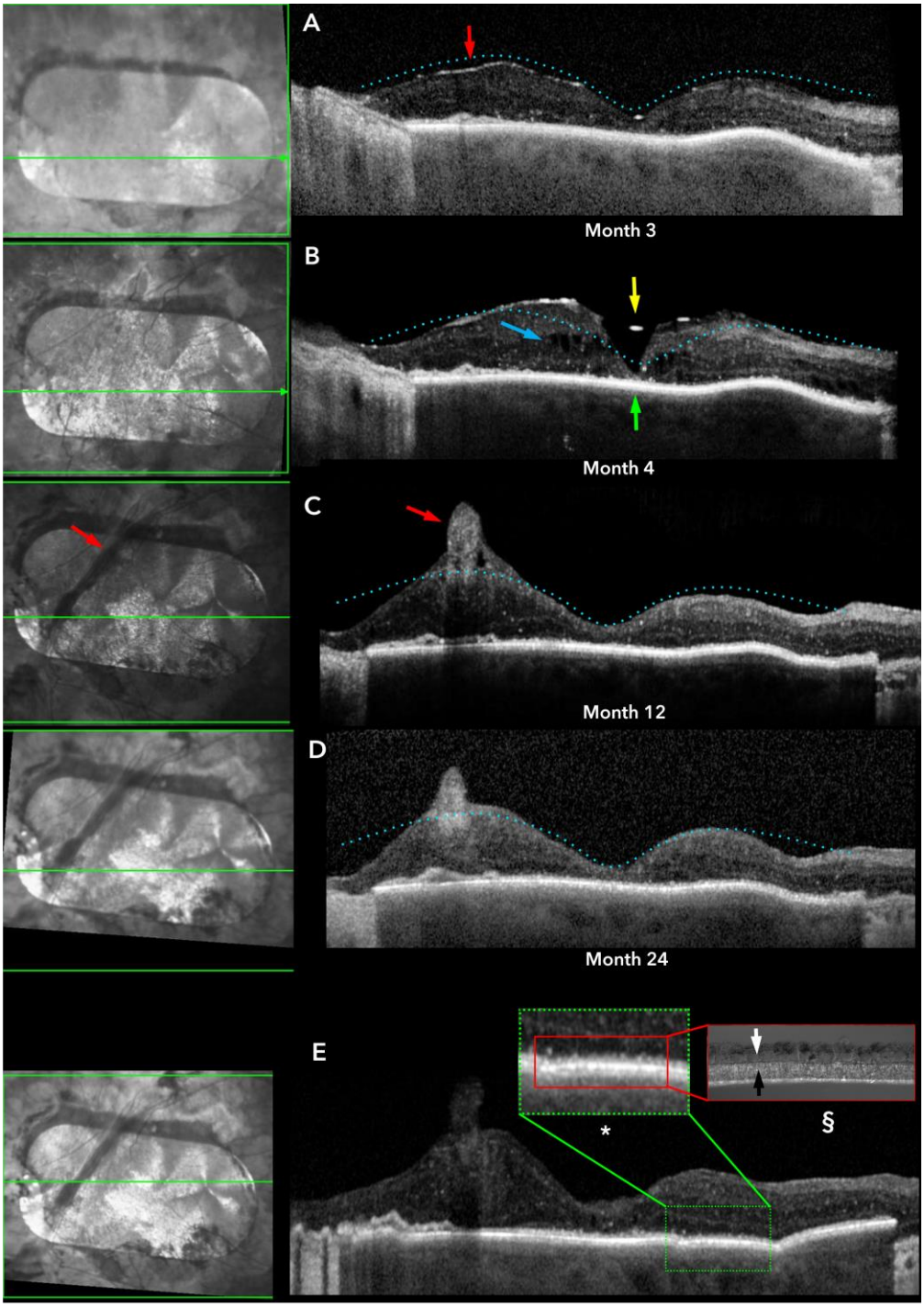

Figure 5-8: SD-OCT series of subject 2 during the study period. Near infrared photos at the left part indicate the plane of the b-scan at the right. Scans from the same retinal location (A-D) have been exported using the follow-up option of the Heyex software (Heidelberg-Spectralis). (A) SD-OCT from post-op. month 3 showing preservation of the foveal contour (blue dotted line) with a mild ERM (red arrow). (B) SD-OCT from post-op month 4 showing severe retinal thinning to an almost full thickness defect (green arrow) and cystic changes (blue arrow). The hyper-reflective line inner to retinal contour (yellow arrow) represents the silicone oil interface. (C) SD-OCT from post-op month 12 showing retinal reformation and closure of the defect. A fibrotic strand is appearing over the temporal part (red arrow) without significant retinal traction. (C and D) SD-OCT scans from post-op. year 1 and 2

respectively, showing stabilization of the retinal thickness over the bulk of the patch, reformation of the cystic changes and preservation of the foveal contour and of the segmentation in the nasal part of the treated retina. (E) SD-OCT scan through the patch from post-op. year 2. Preservation of the double-layered structure of the patch seen in the higher magnification square (*). Correlation of the in vivo cross-section of the patch (*) with the in-vitro Electron Micrograph cross section (§), taken from an equivalent patch after manufacturing. The hESC-derived cells (white arrow) are visible immobilized and polarized on the synthetic BM (black arrow).

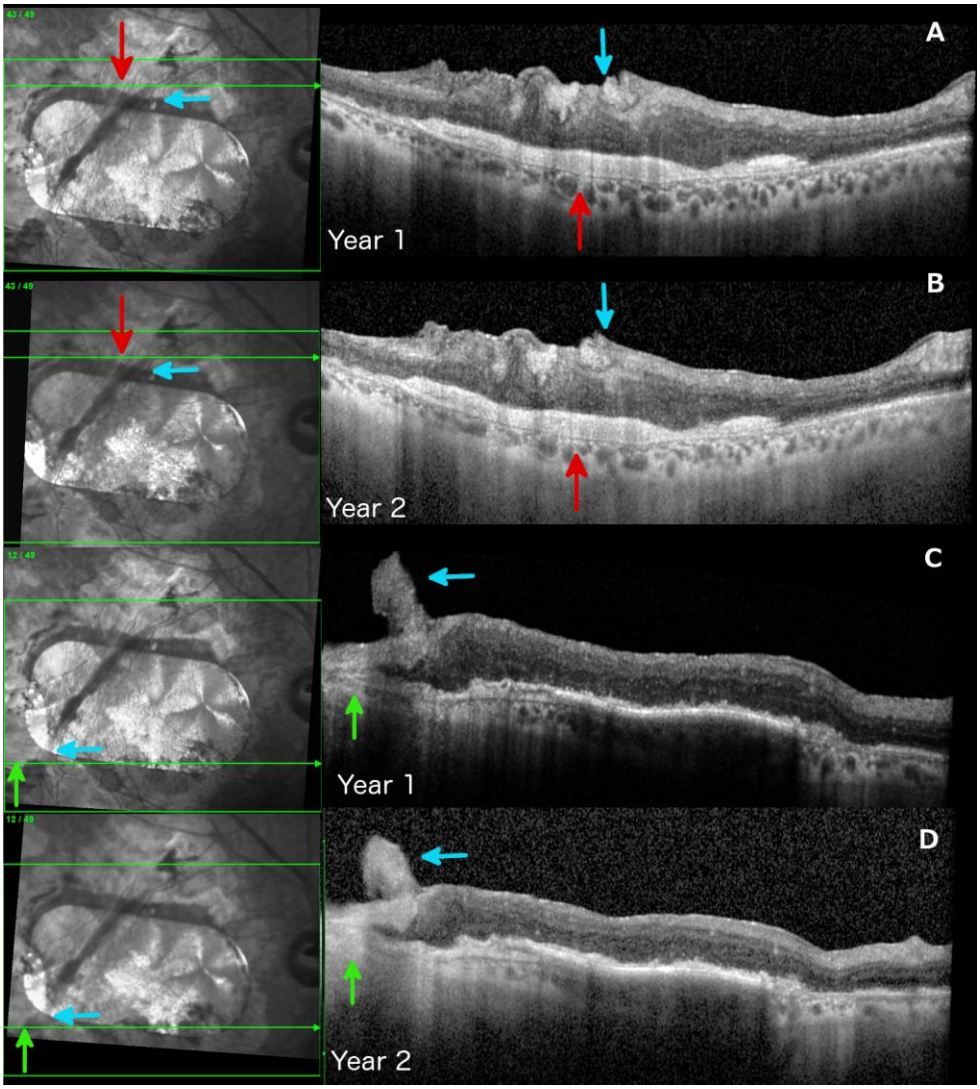

Figure 5-9: Subretinal scarring in subject 2: Year one (A&C) and year two (B&D) NIR (left) and OCT scans (right) from the areas of the scarring. The red arrows indicate the subretinal scarring which is hyper-reflective in the OCTs and is marked anteriorly and temporally to the patch. The green arrows indicate the retinal scarring in the area of the surgical incision for the insertion of the patch. The blue arrows indicate the thick epiretinal fibrous band that developed by the end of year one and remain stable during the second year.

5.2.4. Adaptive optics – imaging of photoreceptors

As in year one, AO retinal imaging continued to show photoreceptor-like structures during the 2nd year in both subjects. On months 12, 18 and 24, in both cases, AO demonstrated the presence of multiple cone photoreceptor signals. Importantly, cones were also documented for both subjects specifically in areas corresponding to the retinal loci over the patch that had positive responses in the Microperimetry tests (**Fig. 5-10**).

5.2.5. Background disease recurrence

As mentioned in 5.1, in the subject one's 1-year follow-up scans, we detected a pigment epithelium detachment (PED) superiorly to the supero-temporal arcade. It was associated with SRF two months later, which did not reach the patch but remained 1 disc-diameter away from its edge (**Fig. 5-2**). Subject 2 did not manifest any features of recurrence, particularly no subretinal fluid, hemorrhage, PED nor exudate.

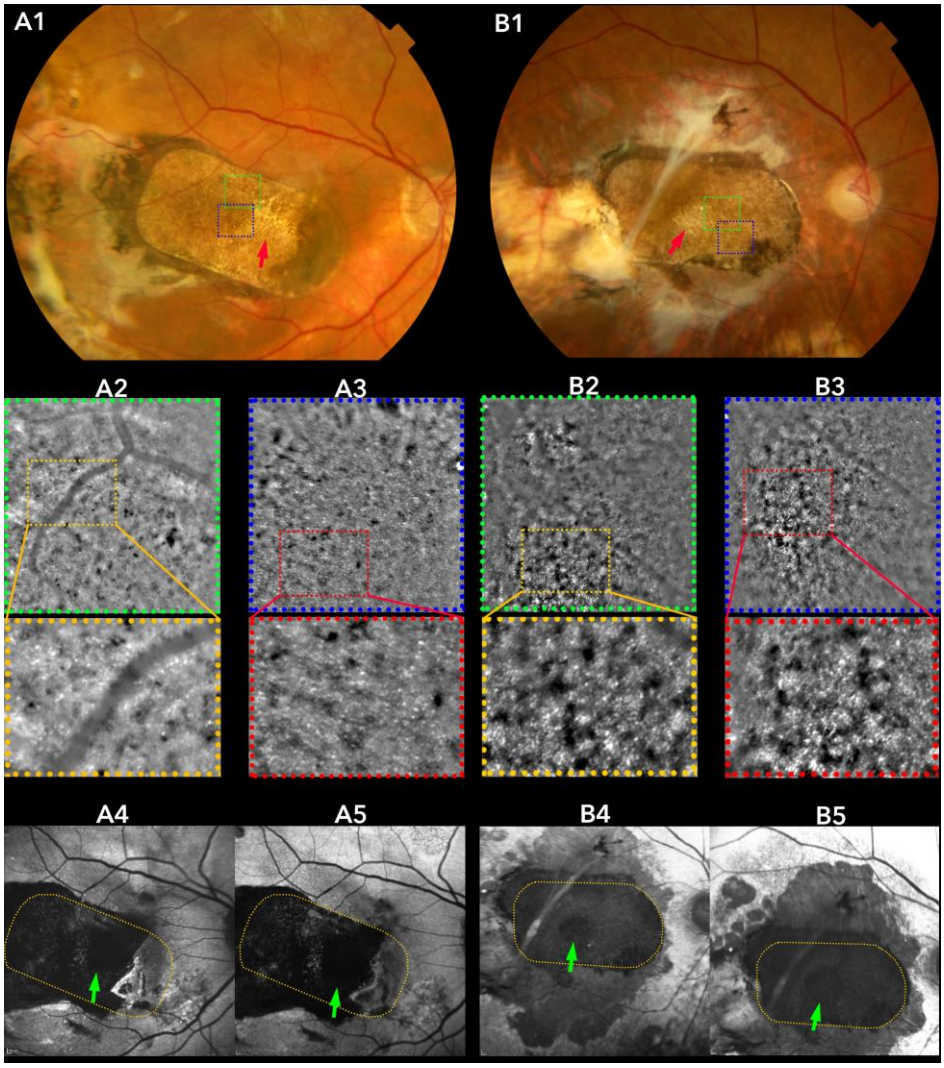

Figure 5-10: Structure-function correlation at cellular level for both subjects. (A1, B1) color fundus photographs at post-operative year 2 for subject 1 and 2 respectively. The hESC-RPE patch appears stable and pigmented throughout the bulk of its surface. Dotted green and blue squares in A1 and B1 represent areas of even pigmentation that were captured with the adaptive optics RTX1 camera. (A2 - B3) AO images from the retinal loci highlighted in A1 and B1, at 2 years post-op (A2, A3 for subject 1, B2, B3 for subject 2). Higher magnification (yellow and red dotted squares) reveals the presence of multiple clusters with cone-photoreceptor characteristics. (A4 – B5) Fundus auto-fluorescence (FAF) photographs from post-op year 1 (A4 and B4) and post-op. year 2 (A5 and B5) from subjects 1 and 2 respectively. The position of the patch is delineated with a yellow dotted line. A4 and A5 show preserved FAF reflectance at the temporal half of subject one's patch (location that also appears evenly pigmented in A1), and a "quiet" area (green arrows) corresponding to an area of decreased pigment density in A1 (red arrow). B4 shows for subject 2 a good FAF signal at year 1, with a "quiet" center (green arrow), corresponding to a de-pigmented area seen in B1 (red arrow). B5 shows preservation with some decrease of the FAF at year 2, together with an enlargement of the less fluorescing center (green arrow).

5.3. Function outcomes

As previously reported, both subjects had a significant improvement in the visual function tests of the study-eye during the first post-operative year, and this was documented. During the second year, subject 1 showed some general decline in her functional performance but remained significantly improved comparing to baseline. The improvement that was seen in subject 2 was maintained until the end of the second year.

5.3.1. Best Corrected Visual Acuity

ETDRS best corrected visual acuity (BCVA) improved post-operatively in both cases and remained significantly better than baseline until year two. Subject 1 started with 10 ETDRS letters and reached 33 on month 6, 39 on year 1 preserved until month 18 and subsequently declined to 26 letters on year 2 test (**Fig. 5-11, A1**). The second subject's baseline BCVA was 8 ETDRS letters and reached 30 on month 6, 29 on year one, 27 on month 18 and 23 letters on the 2-year follow up (**Fig. 5-11, C1**).

5.3.2. Reading Speed

Both subjects showed an improvement in their ability to read with their operated eye, as measured with Minnesota Reading Speed test. Subject 1 increased her maximum reading speed (RSmax) from 5 words per minute (wpm) in the screening assessment to 51.2 wpm after six months, 84.2 wpm on year 1 and 65.9 wpm on year 2. Subject 2 started from 0 wpm at baseline, reaching 26.5 wpm after six months, 48.7 wpm after one year and 41.1 wpm at year 2 (**Fig. 5-11, A2,C2**).

5.3.3. Contrast Sensitivity

Pelli-Robson contrast sensitivity (CS) improved in both subjects. The CS log score for subject 1 increased from the pre-operative 0.45 to 1.35 on month 6, which was maintained until year one and declined to 1.05 on year 2. Subject 2 started with 0 CS log score on baseline and improved to 0.75, 1.05 and 0.9 on month 6, 12 and 24 respectively (**Fig. 5-11, A3,C3**).

5.3.4. Fixation

Examination of fixation with the Nidek-MP1 device demonstrated that during the first year both subjects maintained fixation over the RPE graft. More specifically, for subject 1 the fixation stability ranged between 72% and 93% for fixation within 2° from the centre of the target and between 98% and 100% for fixation within 4° from the centre of the target. On follow-up year one it was marked as “stable” by the Nidek software with 83% of examined fixation points falling into the 2° area and 100% into the 4° (**Fig. 5-11, B1-B3**). For subject 2 the fixation stability ranged between 46% and 98% within 2° from the centre of the target and between 92% and 100% within 4° from the centre of the target. On follow-up year one it was also marked as “stable” with 98% of fixation point within the central 2° and 100% within the 4° area (**Fig. 5-9, D1-D3**).

During the second year, the first subject’s fixation stability started to deteriorate and on month 18 was marked “unstable” with 17% of points within 2° and 70% within 4° and was shifted towards the superior nasal corner of the patch with many points falling outside the grafted area. On year 2 it was found “relatively unstable” with 28% within 2° and 76% within 4°, and most of the points falling on the patch, albeit close to its edges (**Fig. 5-11, B4**). Subject 2 kept a consistently stable fixation during the second year with 81% in 2° and 100% in 4° on month 18, and 99% in 2° and 100% in 4° on year 2. His fixation also remained constantly over the geometrical centre of the graft (**Fig. 5-11, D4**).

5.3.5. Microperimetry

Both subjects demonstrated sensitivity of the retina over the hESC-RPE graft by Microperimetry (MP) assessments, from post-operative month 4 and until the end of the second year. For the first subject the maximum result was reached at the year 1 exam, when the temporal half of the patch demonstrated multiple loci of normal sensitivity (18 and 20 dB), while the nasal half gave subnormal but still positive responses (**Fig. 5-12, A2**). During the second year, the sensitivity deteriorated and at the year 2 exam only the temporal half remained sensitive, but at a significantly lower level (**Fig. 5-12, A3**). The average dB sensitivity of retinal loci over the patch went from 0 at

baseline to 12.57 dB on year 1 and dropped to 8.95 dB on month 18 and to 8.83 dB by year 2 (**Fig. 5-13**).

The second subject initially had modest MP results, with smaller number of responsive loci with subnormal sensitivity, but improved significantly until year 1 and was retained with a trend to improve further until year 2 (**Fig. 5-12, B2-3**). The average “on-the-patch” retinal sensitivity was 0 at baseline and increased to 2.57 dB on year 1, 2.56 dB on month 18 and 3.26 dB on year 2 (**Fig. 5-13**).

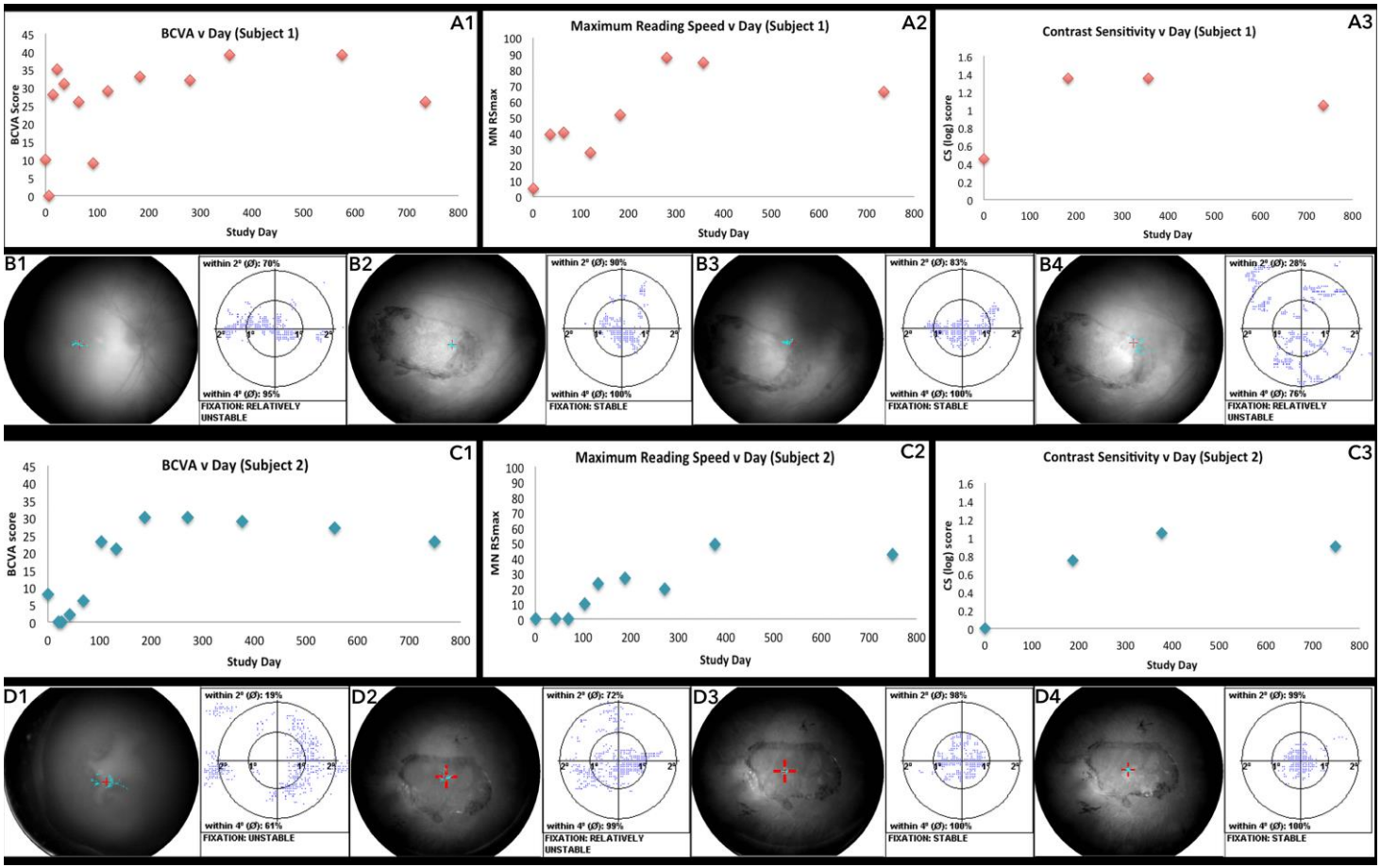

Figure 5-11: Visual function of both subjects during the study period (study eye). (A1, C1) change in best corrected visual acuity (ETDRS letters), (A2, C2) change in maximum reading speed (RSmax – words per minute), as measured with Minnesota Reading Test, (A3, C3) change in Pelli-Robson contrast sensitivity (log score) of subjects 1 and 2, respectively. (B1-B4, D1-D4) Fixation examination using the Nidek MP-1 microperimeter for subjects 1 and 2. In the standard fixation representation (red-free fundus photo – left) each of the blue dots represents the retinal area subtending the center of the target at a certain time. In the graph to the right of each photo, the cloud of dots statistically identifies the retinal area (within 2° and 4° of the fixating center) involved in fixating the target: (B1, D1) at baseline, (B2, D2) at 6 months, (B3, D3) at 12 months, (B4, D4) at 2 years, for subjects 1 and 2 respectively. The fixation is characterized accordingly as “Unstable”, “Relatively Unstable”, or “Stable” by the Nidek MP-1 software.

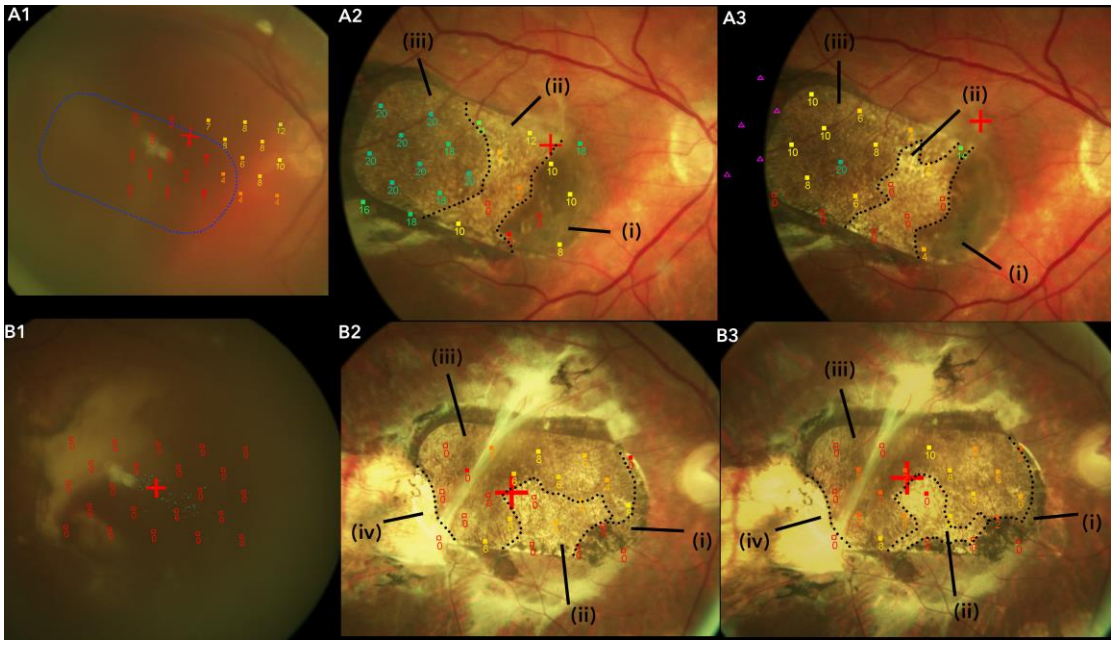

Figure 5-12: Pigmentation to Microperimetry correlation. Changes in the pigment density of the patch with time and correlation with the (MP) sensitivity of the overlying retina, for both subjects. (A1, B1) baseline, (A2, B2) year 1 and (A3, B3) year 2 MP exams registered on corresponding retinal photos, of subjects 1 and two respectively. The blue dotted line in A1 represents a pre-operative approximation of the retinal area treated with the hESC-RPE patch. For subject 2 such an approximation was not possible, due to the poor quality of the pre-operative photo, combined with the distortion of the retinal structures from the excessive sub-macular haemorrhage and fibrosis. The numerical values represent the retinal sensitivity (in dB) of each of the examined loci. The annotated areas (i)-(iii) separated by black dotted line in (A2, A3) represent the patch's three segments of distinctive pigment density mentioned in the main text, for subject 1. Similarly, the annotated areas (i)-(iv) in (B2, B3) represent the four segments of the patch with distinctive pigmentation mentioned in the main text, for subject 2.

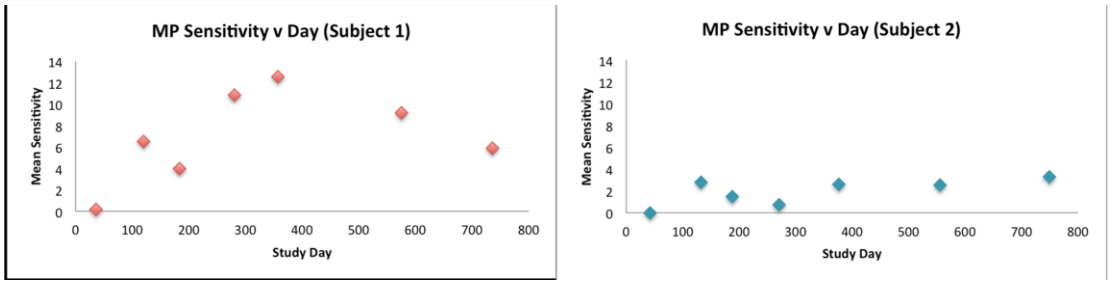

Figure 5-13: Microperimetry changes (mean) in the study period: Graphs showing the change of the mean MP sensitivity of the treated macular area in the operated eye of subject 1 (left) and 2 (right).

Discussion

After two years of follow-up, I have demonstrated that our investigational implant – comprised of a hESC-derived RPE monolayer on a vitronectin coated, synthetic polyester basement membrane – has been safe and well tolerated. Furthermore, it has provided structural support and positive functional results in the two treated individuals with severe, neovascular AMD to 2 years.

Neither of the subjects showed any signs of ectopic growth, cell uncontrolled proliferation or tumorigenicity, either locally or distant to the patch, during the two years. No major signs of acute or severe immune rejection were detected either. The AE's including SAE's that were noted in the second year, were related either to the vitreoretinal surgical operations, to the concomitant immunosuppressive treatment, or to the subjects' general health issues.

It has been documented that the critical period for uncontrolled proliferation after stem cells transplantation is the first few months, when potential teratoma formation would constitute a severe complication(Hentze et al., 2009; Klimanskaya, Chung, Becker, Lu, & Lanza, 2006; Thomson et al., 1998). Already, however, the long-term safety of subretinal injection of hESC-derived RPE cells has been well demonstrated by Schwartz et al.(Schwartz et al., 2016). After monitoring 18 patients for 4 years, they noted no signs of inflammatory rejection and no hyperproliferation or tumorigenic adverse events related to the cell suspension therapy. For the cell-sheet approach there are only 5 other cases in the literature, with follow-up range between 4 to 12 months, which also had no serious adverse events or any sign of malignant proliferation, either locally or systemically, after one year(Mandai et al., 2017),(Kashani et al., 2018). Our two hESC-RPE transplant recipients were monitored for two years and showed equivalent safety profiles.

Apart from the implanted cells, another safety concern was the biocompatibility of the synthetic basement membrane. In the two years of this study, I did not detect any signs of toxicity or rejection of the substrate material. Furthermore, the demonstrated preservation of the structure and function of the overlying retina, can be considered as a sign of preserved metabolic transport through the synthetic BM, between the retina and choroid. To my knowledge, this is the first human study of a hESC-RPE-artificial BM complex transplantation with 2-years follow-up, and the absence of any adverse reaction specifically associated with the patch also indicates the biocompatibility and safety of the polyester material in the subretinal space.

I have reported epiretinal and pre-retinal fibrosis in both subjects and a PVR retinal detachment in the second. All these are well described complications of pars plana vitrectomy and macular surgery (Falkner et al., 2006; Romano, Valldeperas, Vinciguerra, & Wong, 2011; Stanescu-Segall et al., 2016) and thus have not been associated with the investigational product, but considered to reflect the baseline disease severity and the complexity and extent of these early operations.

Similar to year one, SD-OCT imaging during the second year continued to demonstrate a continuous hyper-reflective outer retinal band, which was consistent with the signal from the implanted hESC-RPE-BM patch. The overlying retina showed some preservation of its segmentation, which was more apparent in subject 1, where all the layers where distinct. In subject 2 the segmentation appeared more disorganized, nevertheless the foveal contour was better preserved. In subject 1 I also noticed an area of structural disorganisation, with abnormal thickening and cystic degeneration, which was the retina overlying the nasal part of the patch. I have already mentioned that this was the area of “doubled” RPE (hESC-RPE and host RPE), which also showed compromised function, in terms of retinal sensitivity. This structure-function correlation over an inadvertently damaged RPE, provides indication that it is the healthy, implanted

hESC-RPE that supported the better retinal structure and function over the rest of the patch.

Both cases had a general reduction in the retinal thickness over the patch, which reached to an almost full thickness defect, but was subsequently “covered” by a process that resembled retinal “remodelling”. Interestingly, the location of this defect corresponded to the location of the subjects’ fovea, which was also the area of pigment reduction and lower AF signal in both subjects (area “ii”). A possible explanation for this defect might be the lower blood perfusion of this area, as it corresponded to the “avascular zone”. This area, by definition, has no retinal circulation and its perfusion comes from the choroidal circulation only. Thus it is more vulnerable in situations that affect its perfusion. The positive correlation between the retinal thickness in this area and the condition of its blood perfusion has been demonstrated in both healthy subjects and in cases of compromised microvasculature, such as in diabetic retinopathy (Dubis et al., 2012), (Yu et al., 2016), (Bates et al., 2018). It is possible that the disruption of the choroidal perfusion from both the severe background disease and the surgically induced tissue trauma resulted in the corresponding loss of retinal thickness. If this is the case, the observed subsequent remodelling and covering of the defect might have been a result of the patch’s integration, which allowed the choroidal circulation to perfuse the overlying retina.

The survival of the transplant and maintenance of its basic structure after two years is also the first indication of immune tolerance of the hESC-RPE-BM complex. Potential signs of acute or sub-acute rejection would have included lymphocyte infiltration, uveitis and cystoid macular oedema, none of which were observed during the follow up period. In terms of immunosuppression, apart from the peri-operative oral prednisolone (aimed at suppressing the primary inflammatory reaction to the surgery), only local steroids were used during the second year, in the form of a long-acting intraocular implants of fluocinolone acetonide. It may be that the long-term survival of the patch in both subjects can be partially attributed to the concomitant immunosuppression and partially to the

immunoprotective features of functional RPE cells(Strauss, 2005; Wenkel & Streilein, 2000). The RPE cells contribute to the preservation of the immunomodulation of the subretinal space both passively, with their inter-cellular tight junctions, and actively with expression of surface factors, such as TGF-β, PEDF and DC95, CD59, CD46 (Bikun Xian, 2015; Thumann, Dou, Wang, & Hinton, 2013). Although it is possible that this immunological privilege is compromised in macular degeneration, the survival and structural integrity of the graft after two years in both cases may constitute an indication of preserved immunomodulatory function of the hESC-RPE cells, additional to the local anti-inflammatory action of the steroid depot. I acknowledge that it is impossible to exclude a low-grade, subclinical, chronic rejection as the cause of the implant's gradual depigmentation between year 1 and year 2 of follow-up. In the case of a rejection, the hyperpigmented parts of the patch could represent accumulations of macrophages containing phagocytosed melanin from affected RPE cells, originating from the areas of decreasing pigmentation. The abundant presence of macrophages in the choroid and RPE-BM level has been well documented (Chinnery, McMenamin, & Dando, 2017), as well as their para-inflammatory role in AMD and chorioretinal pathology in general (Cherepanoff, McMenamin, Gillies, Kettle, & Sarks, 2010; McLeod et al., 2016). Activation of macrophages and their migration into areas of cell loss could be part of the reason for the change in pigmentation and function via a mechanism of gradual, late-onset rejection. In our cases the two observations – the regional depigmentation and the focal hyperpigmentation – were distant to each other, both time-wise and location-wise. The darker areas on the grafts appeared as early as post-operative week 8 and were located mainly on the outer edges, while the depigmentation seems to have started after year 1 and involved the centre of the patch. Especially for the first case, the noticeable decline in the graft's homogeneity combined with a functional deterioration of the overlying retina, may represent a slow onset form of rejection of the therapeutic cells. Such a reaction has been reported as a significant cause for late failure after RPE transplantation, and can occur from months to years after the operation (da Cruz et al., 2007). This form of rejection

is more prevalent after allogeneic RPE grafts and can also manifest with macular oedema, leakage in FFA, graft depigmentation, fibrous encapsulation and recurrence of CNV(Algvere, Berglin, Gouras, & Sheng, 1994; Algvere, Gouras, & Kopp, 1999). In our cases, apart from a local decrease of the transplant's pigment, none of these other signs of rejection were detected. In the first subject, the vascular leakage resulting in a PED and SRF after year 1 was extramacular, distal to the edge of the patch and unlikely to have been a sign of rejection.

The investigations and examinations showed preservation of pigmentation of the patch in both subjects for at least 2 years, though there was clear regional decline in the second year. The pigmentation was associated with a continuous hyper-reflective subretinal band with RPE characteristics in the OCT scans, throughout most of the transplant area for the same period. In the first ever trial of subretinal injection of hESC-RPE cell suspension, Schwartz et al. demonstrated increased pigmentation in 72% of the host eyes, some of which presented cell foci on the inner aspect of BM in OCT scans, which were considered as thickening or reconstruction of the RPE (Schwartz et al., 2012). Autofluorescence imaging of these areas showed a close to normal reflectance in some cases and no reflectance in others, while in one eye the AF signal faded with time. The follow-up period was 3 to 12 months, while systemic immunosuppression with tacrolimus and mycophenolate mofetil was used for 3 months. Improvement of visual acuity was noticed in 6 of the 9 treated eyes. However, the absence of more area-specific assessments, such as Microperimetry and cell-resolution imaging, limited the correlation between these structural and functional outcomes. Overall, they did not establish good evidence linking the development of subretinal pigmentation and the preservation or improvement of vision (Schwartz et al., 2012; 2015; 2016). Moreover, their delivery by cell suspension retains an ambiguity as to the distribution and orientation of the transplanted RPE. Lack of RPE polarization and formation of a monolayer with tight junctions, can jeopardise the long-term survival of both the implanted cells and the supported photoreceptors (Binder, 2011; Crafoord et al.,

1999). It is likely that a patch delivery method overcomes these issues of distribution and polarization (Georgiadis et al., 2017).

In a single case of iPSC-RPE sheet transplantation for neovascular AMD, Mandai et al. reported positive safety and feasibility of their method, together with imaging indicating likely survival of the graft and preservation of the external limiting membrane and outer nuclear layer of the neural retina (Mandai et al., 2017). No systemic immunosuppression was used, as the patch was considered autologus. The visual acuity was not improved and the Microperimetry based retinal sensitivity of the grafted area remained at 0 dB post-operatively, though with signs of fixation shifting closer to the fovea. Although this was essentially a safety and feasibility study, in order for there to be rescue of visual function, it has to be attempted before the established, irreversible photoreceptors loss and retinal atrophy that was likely present in their case(da Cruz et al., 2007; Uppal et al., 2007). Compared to our cases, which were operated ahead of such loss, the poor functional outcome of the iPSC-RPE sheet case could be attributed primarily to the long-standing (for four years) severe vision loss pre-operatively(Mandai et al., 2017). The use of a polyester scaffold might also have offered an advantage in our study, by facilitating a less traumatic implantation of the cells. Mandai et al. did not use a synthetic scaffold, and they counted on the extracellular matrix expressed by the implanted cell to play the role of a new BM (Kamao et al., 2014).

To my knowledge, our study is the first to use Adaptive Optics retinal imaging in stem cell derived RPE transplantation, though our observations were purely qualitative. The relatively poor quality of the images due to instability of fixation in case 1 and the lack of a universal focal plane for the on-the-patch macula in case 2 made it impossible to apply a consistent cone-photoreceptor counting process. However, the year 2 AO images from both subjects showed multiple structures with all the optical characteristics of cones (brightness, size, density and distribution) and especially at the areas of denser pigmentation and

higher MP sensitivity, consolidates the correlation between the improved function and the supported structure, even at a cellular level.

I reported that both subjects maintained their functional improvement for at least one year, but demonstrated some decline during the second year. Subject 1 lost almost 3 lines of BCVA (13 letters) and 3.74 dB of average retinal sensitivity associated with the patch, and subject 2 lost 1 BCVA line (6 letters), while his retinal sensitivity was preserved. Both subjects lost part of their reading speed improvement at year two. This functional deterioration could be correlated with signs of late structural failure, such as the regional depigmentation and neuroretinal atrophy. The former was correlated with a drop in Microperimetry sensitivity in the corresponding retinal loci, while the latter was more generalized and may justify the decrease in VA and reading ability.

Since the second year's immunomodulation was only a prolongation of the first year's steroid depot action, it is possible that this late-onset decline can be correlated to the wearing off of the steroid implant activity resulting in a subclinical slow-grade cell rejection. However, similar late gradual decline has also been reported in cases of autologous RPE transplantation and in cases of macular translocation (Aisenbrey, 2007; Chen, 2009; Chen et al., 2010). In such studies the rate of long-term preservation of at least 3 lines of VA gain seems to range between 17% and 25% and the decline has been attributed to either late complications or structural changes such as retina/RPE atrophy, cystic oedema, and CNV recurrence from the graft (Chen, 2009; Chen et al., 2010). Our two cases maintained at least 3 BCVA lines improvement (16 and 15 letters respectively) and fixation on the grafted retina until year two, despite some signs of structural deterioration. The aforementioned recurrence of CNV in subject 1 originated from an extramacular area, away from the transplant's edges. In contrast with the aged autologous RPE in transplantation and translocation cases, the "0-year-old" hESC-RPE patch seemed to have successfully suppressed the activity of the disease in the area of the patch in both cases for at least two years. Having said that, we acknowledge that the possibility of the

synthetic BM playing the role of a physical barrier against the growth of CNVM towards the retina cannot be excluded.

Within the limitations of a clinical trial that included only two subjects, our hESC-RPE sheet transplant appears safe and well tolerated in both. After two years of monitoring, we did not detect any stem cell-related serious adverse reactions, either ocular or general, and the noted complications were associated with either the surgery, or the concomitant medication. I acknowledge that the lack of histological correlation makes it impossible to draw definite conclusions on the SC-RPE survival and its competent integration with the host retina. However, I managed to demonstrate a combination of clinical signs, standard and advanced imaging results with corresponding functional improvement in each of the visual assessments, and the relative preservation of them in the long-term. To my knowledge, this is the first time that a stem cell-derived RPE transplantation approach shows the potential to restore visual function to such scale, and to preserve useful vision after two years. The delayed deterioration in our subjects raises the question of possible late rejection and highlights the importance of close long-term monitoring for such experimental techniques. The surgical procedure and instrumentation remains demanding and needs to be further optimized. The necessity for more cases to be studied is indisputable, but the encouraging initial results combine with the ongoing research and developments on the field, make the future establishment of a stem cell-based therapies for retinal degeneration seem more plausible than ever.

Chapter 6

The behaviour and fate of the hESC-RPE cells

Introduction

Currently, long term survival of stem cell-derived RPE cells transplanted into humans, has only been described for the cell suspension approach (Schwartz et al., 2016). For the cell-patch method, the reports in the literature, either for hESC (Kashani et al., 2018), or for iPSC (Mandai et al., 2017) do not exceed 1 year of follow-up. In the “Methods” section of this thesis (Chapter 2) I described the manufacturing process and the pre-implantation assessments of our investigational hESC-derived RPE-synthetic BM patch. I concluded that in its pre-transplantation status, the investigational product was structurally comparable to a normal “0 years old” RPE-BM complex. Subsequently, I demonstrated the anatomical and functional outcomes of the transplantation in two subjects with severe, neovascular AMD and acute vision loss, for up to two years post-operatively. The aim of this chapter is to describe in further detail the course of the therapeutic RPE cells, both on and off the investigational patch, in an attempt to examine the structural integrity of the patch throughout its surgical delivery, as well as the survival and behaviour of the cells during the 2 years of follow-up.

Results

6.1. Intact implantation of the patch in the submacular space.

The methods of the peri- and intra-operative handling of the patch to protect it from tissue damage, have been described in Chapter 2. The use of the purpose-designed punch-cutter and injector resulted in a gentle and undisrupted insertion in both subjects, with minimal cell loss (**Fig. 6-1**).
The patch was successfully delivered in both subjects, fully intact in subject 1 and with only a minor tissue trauma of the hESC-RPE layer at its inferior-temporal corner, caused by the surgical manipulation, in subject 2. This was observed in the immediate post-operative biomicroscopy and colour fundus

photographs and documented with OCT scan through the affected area, showing a probable detachment of the hESC-RPE from the synthetic membrane (Chapter 3, Fig. 3-9). Apart from this area, there were no signs of separation of the cells from the polyester BM.

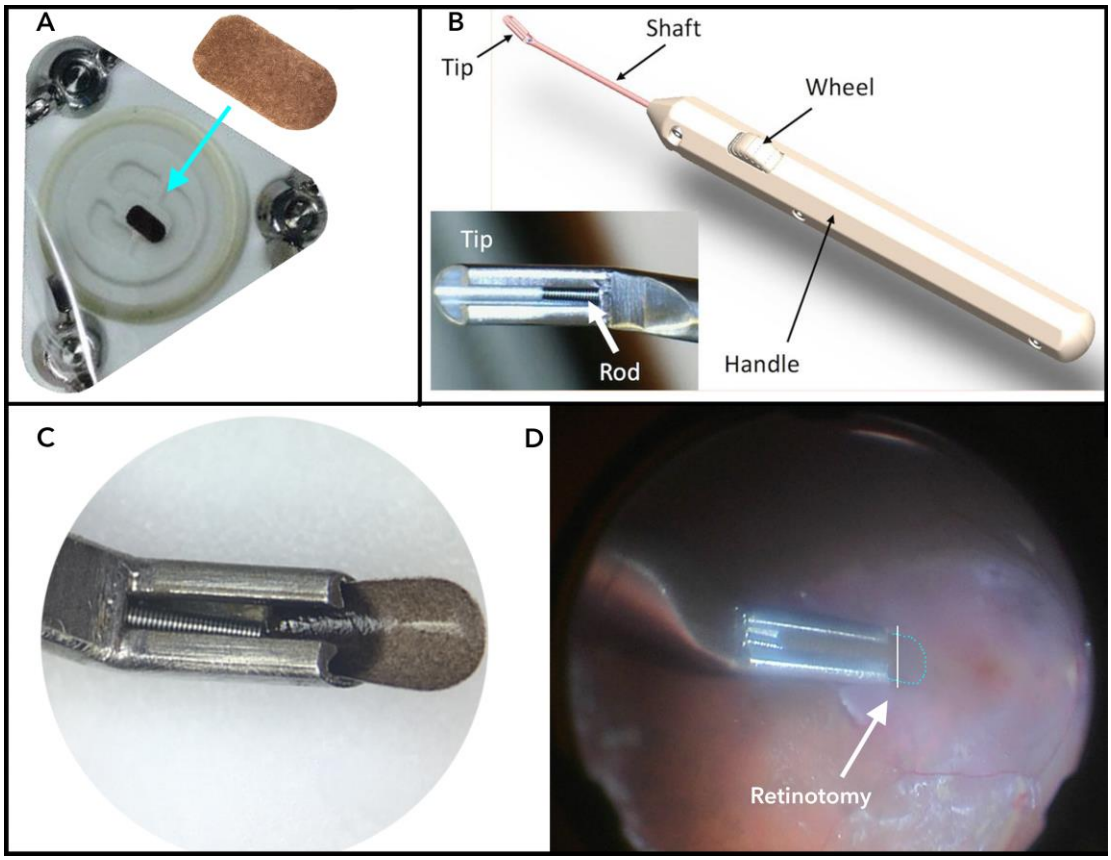

Figure 6-1: Purpose-designed equipment for the handling and the delivery of the investigational patch. (A) Custom-built container, including the hESC-RPE-BM patch, which is also shown in larger scale at the top of the picture, (B) Purpose-designed tool for the subretinal delivery of the patch, (C) Representation of the patch half-inserted into the tip of the introducer in a semi-wrapped form, (D) snapshot from the surgical video at the moment of delivery, showing the submacular insertion of the patch.

6.2. The hESC-RPE cells *on* the patch

The structural results from the multimodal imaging of the implanted hESC-RPE and the treated macular area, as well as the functional results on the subjects'

vision, have already been reported in the previous chapters (3-5). In the *Discussion* of this chapter, I will try to examine whether hESC-RPE *on* the patch demonstrated functions of a normal RPE and maintained its critical support to the overlying neurosensory retina.

6.3. The hESC-RPE cells *off* the patch.

In both subjects we noticed the development of a dense pigmentation outside the edges of the hESC-RPE patch. This started from the early post-implantation period (month 1) and showed a significant growth during the first 3 months, followed by a minimal further extension until month 6, when it appeared to stabilise. The same multimodal imaging techniques used for the patch, were used to examine this phenomenon of pigmentation extension.

6.3.1. CF Photographs

In the first subject a thin band of pigmentation can be seen outside the borders of the graft, as early as in the 2 weeks post-operative CF photos. It is mostly detected externally to the inferior and temporal edges of the patch, extending also to its superior-temporal corner. Its margins are well defined, it appears darker than the pigmentation of the graft itself and it surrounds approximately half of its perimeter. On the outside, it seems to merge visually with the whitish lesion that represents sub-retinal scarring and corresponds to the sub-retinal “pathway” through which the patch was inserted underneath the macula during the initial implantation surgery.

During the following weeks (week 4 to week 8), this pigmented band appears to extend outwards and become irregular in shape, nevertheless maintaining its orientation in terms of the graft’s perimeter. It still appears to extend from the inferior and temporal edges, covering also its supero-temporal corner. The temporal side expansion is more marked than the inferior and it seems to “encroach” underneath the subretinal scar. The extension has a centrifugal orientation and it does not seem to surround further the superior and nasal edges

of the graft. In terms of colour, the pigmentation maintains its darker hue and remains clearly distinguishable from the patch and the adjacent tissues. On week 10 we can see a clump-like pigmentary formation extending from the inferior border of the pigmentation, which is retained until the end of the study (**Fig. 6-2**). However, it is not clear from the CF photos whether this is a new finding or an older one that was revealed at this point due to thinning and increased transparency of the overlying scar-like tissues. Likewise, the temporal expansion shows some further growth that is unclear if it comprises a "revealing" phenomenon due to retraction of the covering fibrotic layer, or a true increase in size. Otherwise, the overall area and hue of the pigment extension appears considerably stable, demonstrating minimal changes from week 10 onwards and until the end of the follow-up.

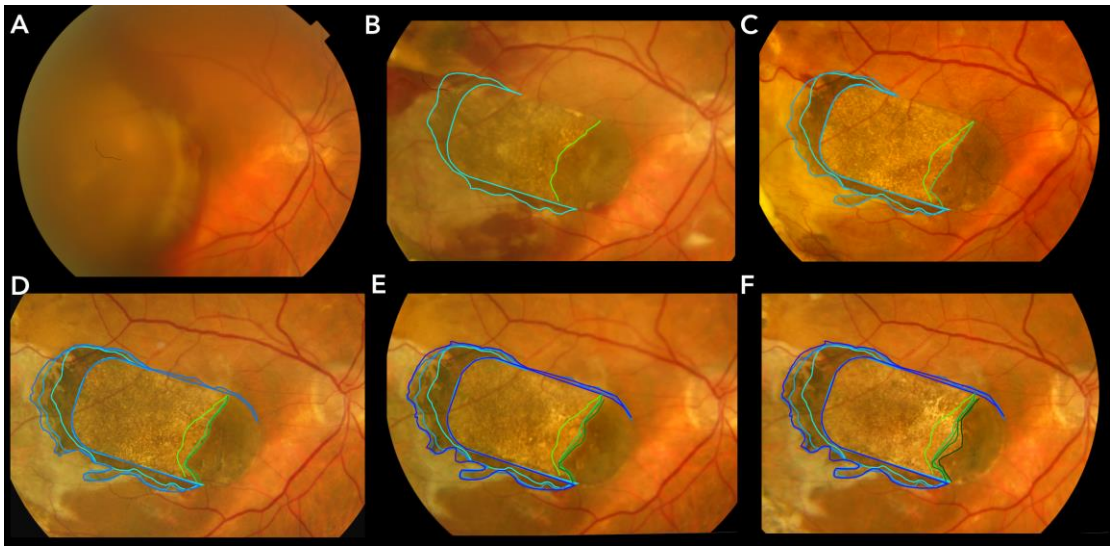

Figure 6-2: Pigment extension outside the patch for subject 1. Series of CF photos at baseline (A) and at months 1, 3, 6, 12, and 24 (B), (C), (D), (E) and (F) respectively. The blue lines demonstrate the extension of pigmentation outside the patch's edges. Different shades of blue - from lighter to darker - correspond to different time points, going from earlier to later borders of pigment extension, respectively. The green lines demonstrate the retraction of the darker (nasal) segment of the over-the-patch retina, deemed to be an area where host RPE overlade the implanted hESC-RPE (mentioned in text as "double RPE"). Different shades of green represent different time points for the borderline of this segment: lighter shades correspond to earlier times and darker shades to later times.

In the second subject the first sign of pigment expansion outside the patch can be detected in the 4th week's CF photos, as a very thin band over its superior

edge, most prominent on the supero-temporal corner. In these pictures its margins are ill defined, but this is probably because of the overall lower quality of the images due to hazy media. On week 8, this superior band is thicker and denser and now encircles the top left corner of the graft, expanding outside its temporal edge. We can also detect a new clump-shaped pigmented formation extending from the temporal half of the graft's inferior edge (**Fig. 6-3**). The margins of the pigmentation are now steeper and well defined, even through the semi-transparent epiretinal fibrosis that has formed superiorly to the patch. Similarly to subject 1, the hue of the pigmentation is darker than that of the graft's surface. By week 16 the expansion of pigment has almost reached it's final dimensions, maintaining its superior orientation (with the exception of the inferior "clump" projection) and with minimal – if any – further change until the end of the study.

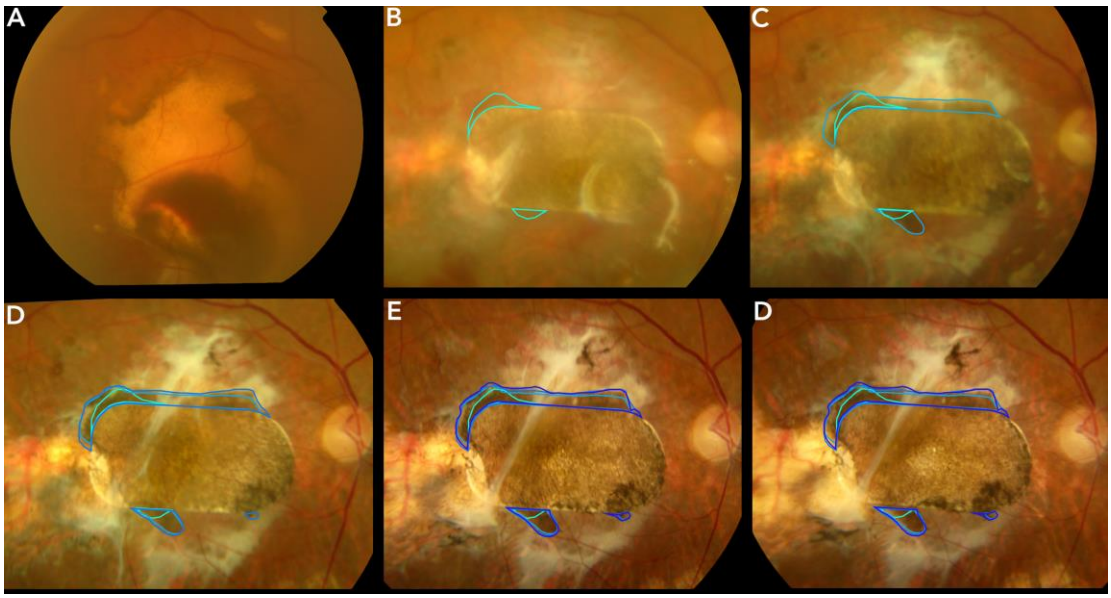

Figure 6-3: Pigment extension outside the patch for subject 2. Series of CF photos at baseline (A) and at months 1, 3, 6, 12, and 24 (B), (C), (D), (E) and (F) respectively. The blue lines demonstrate the extension of pigmentation outside the patch's edges. Different shades of blue - from lighter to darker - correspond to different time points, going from earlier to later borders of the pigment extension, respectively.

6.3.2. Fundus fluorescein angiography

As I have already described in chapter 3, in both subjects' early angiograms the main graft was slightly hypofluorescent in all the phases of the examination, but in later follow-ups it demonstrated comparable fluorescence with the host retina, maintaining the choroidal flush in the early phases, and increasing its signal in the later ones. In terms of the pigmented area out of the patch's borders, its behaviour during the FFAs did not show any significant differences from the main patch.

In the first subject's angiogram from post-operative month 1, the inferior to the patch extension of fluorescence appears granular and with the same intensity with the main area of the graft and gives the impression of "spill-out" fluorescence similar to the ground glass appearance of the capillary bed, as in the major proportion of the patch's area. The temporal extension seems slightly hyper-fluorescent in later phases, because of the "staining" effect of the overlying fibrotic tissue. In both areas, the borders of the patch are ill defined and the extension merges visually with the graft. This fluorescence pattern is maintained for one year of follow-up FFAs, with the extended "RPE" area demonstrating equivalent reflectance to the directly adjacent areas of the main hESC-RPE (**Fig. 6-4**).

Similarly, in the second subject's angiograms the retinal area corresponding to the pigment expansion can be seen by second month's (week 8) exam as an iso-fluorescent "band" over the superior borders of the patch and a clump-shaped addition inferiorly. Here the whole patch appears hypo-fluorescent when compared with the host retina, but still shows clearly perfusion of the patch's background, in a grainy pattern during the early phases, which becomes denser later. The patch's superior borders appear sharper but the inferior edge merges with the extension in a similar way with the first subject. From month 6 the patch's fluorescence appears increased and now is similar to the host retina, with some small hypo-fluorescent parts. Likewise, the extended area follows the reflectance of the main patch and now the borders have faded

giving a clearer impression of “spill-out”-like outgrowth. This behaviour is maintained until the last FFA follow-up on year 1 (**Fig. 6-5**).

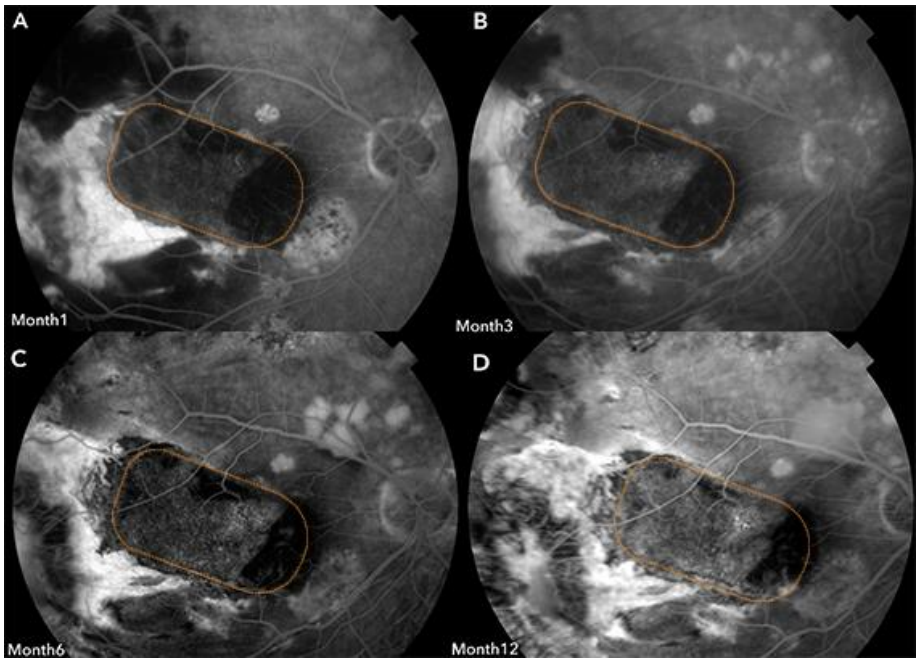

Figure 6-4 (in previous page): FFA (early venous phases) of subject 1: (A), (B), (C) and (D) for months 1, 3, 6 and 12 respectively. The patch is outlined with the dotted line. The reflectance from the area of extended pigmentation has similar intensity with the main surface of the patch, and it is easily distinct from the adjacent “staining” of the scar tissue.

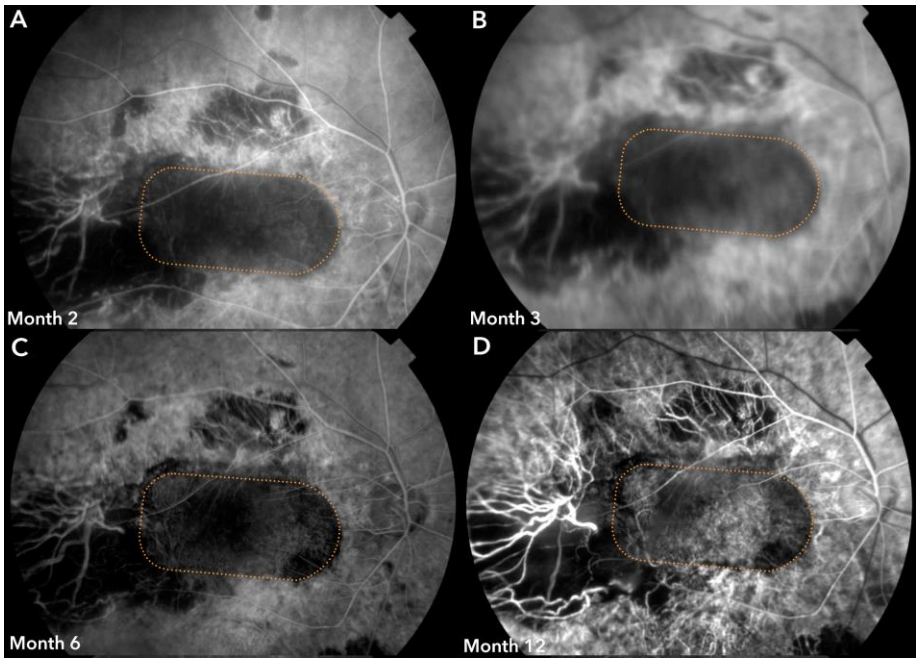

Figure 6-5: FFA (arterial phases) of subject 2: (A), (B), (C) and (D) for months 2, 3, 6 and 12 respectively. The patch is outlined with the dotted line. The

reflectance from the area of extended pigmentation has similar intensity with the main surface of the patch, and it is easily distinct from the absence of fluorescence of the adjacent atrophic tissue.

6.3.3. Fundus Autofluorescence

The limitations of AF images in terms of standardisation and inter-image comparisons have already been acknowledged in the previous chapters. Likewise, here I will describe only intra-image observations, comparing the AF signal of the investigated extension with other areas of the treated fundus.

In the first subject the extension off the patch can be visually distinguished in the week 4 AF images: the area adjacent to the supero-temporal corner shows almost no AF and thus appears darker than the adjacent on-the-patch area. However, the inferior zone demonstrates a granular fluorescence, which is very similar to the appearance of the fluorescing areas of the main hESC-RPE patch. The AF “silence” of the temporal area is maintained throughout the study, while the signal from the inferior extension decreases gradually and after month 6 we can barely detect very few scattered dots of AF, which fade completely by month 12 (**Fig. 6-6, A-C**).

For subject 2 we were not able to capture any usable AF images until post-operative week 12, due to media opacities. On week 12 we can see a weak but homogenous AF reflectance coming from both the graft and the areas of pigment extension. The borders between them cannot be distinguished. This pattern is maintained in the following exams and on month 12 there is a clearer but still low AF signal emitted from the graft’s surface, as well as from the extended areas, both the superior-superotemporal zone and the inferior clump-shaped extension (**Fig. 6-6, D-F**).

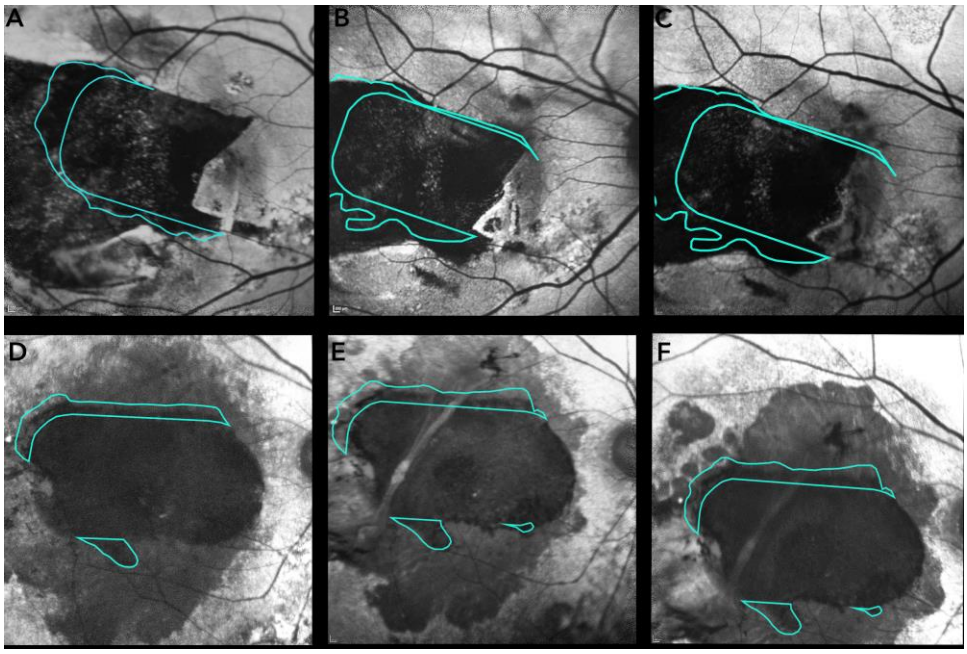

Figure 6-6: AF reflectance from the area of extended pigmentation (outlined in blue). (A), (B) and (C) from post-op months 1, 12 and 24 respectively for subject 1. (D), (E) and (F) from post-op months 3, 12 and 24 respectively for subject 2.

6.3.4. Optical coherence tomography

As already mentioned, in the first subject the earliest signs of pigment extension appeared in the second post-operative week's images. OCT b-scans through this extension inferiorly to the patch show a thin hyper-reflective outer band continuous to the hESC-RPE band of the main graft and with identical characteristics (**Fig. 6-7A**). It appears to extend on top of the host's Bruch's membrane and to stop at the same point that the edge of the extended pigmentation stops (as seen in the matched NIR picture). The brightness of this band is equivalent to the one of the implanted RPE, while the adjacent host RPE appears slightly darker in the grey scale. Both the reflectivity and the thickness of this presumed hESC-RPE band can be easily distinguished from the highest reflectivity of the artificial BM of the graft and also from the well-defined line of moderate reflectivity that represents the host BM. In addition, posteriorly to this complex, we can see the choroid having a reflectance of equivalent strength and clarity to the adjacent normal (not grafted) choroid (in contrast with the choroid of

the grafted area, which is impossible to detect due to the light being reflected by the synthetic BM).

The resemblance of this extended band with the RPE is more obvious on the week 24 OCT scan and especially in b-scans that cut through the previously described “clump-like” pigment protrusion of the inferior edge (**Fig. 6-7B**). In these images we can see a highly reflective outer band interrupted by hypo-reflective patches of “naked” BM, as the b-scan cuts alternatively through pigmented and non-pigmented areas. The hyper-reflective lines correspond to the hyper-pigmented parts and the hypo-reflective patches to the non-pigmented gaps. In order to highlight this pattern, I obtained some vertical OCT scans on month 12 visit. In these slices the bright line of the presumed RPE appears continuous as the scan passes through the pigment extension and the main graft and it is interrupted only by darker segments, as the scan passes through non-pigmented areas (**Fig. 6-7C**). With regards to the retina overlying this outer layer in question, it appears similar to the adjacent retina of both sides (the grafted and the host). Its thickness is comparably lower than normal, but this also applies to the rest of the neighboring retina and with both the nuclear and plexiform layers are detectable, nevertheless with an irregular contour due to the adjacent scarring (**Fig. 6-7, A-C**).

These tomographic characteristics of the outer pigmented band are maintained in all the follow-up OCT scans. The linear extension of the presumed hESC-RPE layer grows further in parallel with the host’s BM and remains well defined from both the host RPE, which appears darker, and the grafted RPE, which has same brightness but is distinguished by the outer hyper-reflective synthetic BM, and the almost complete shadowing of the choroid. Similar to the CF photos, the expansion of this band seems to stop after post-op week 12.

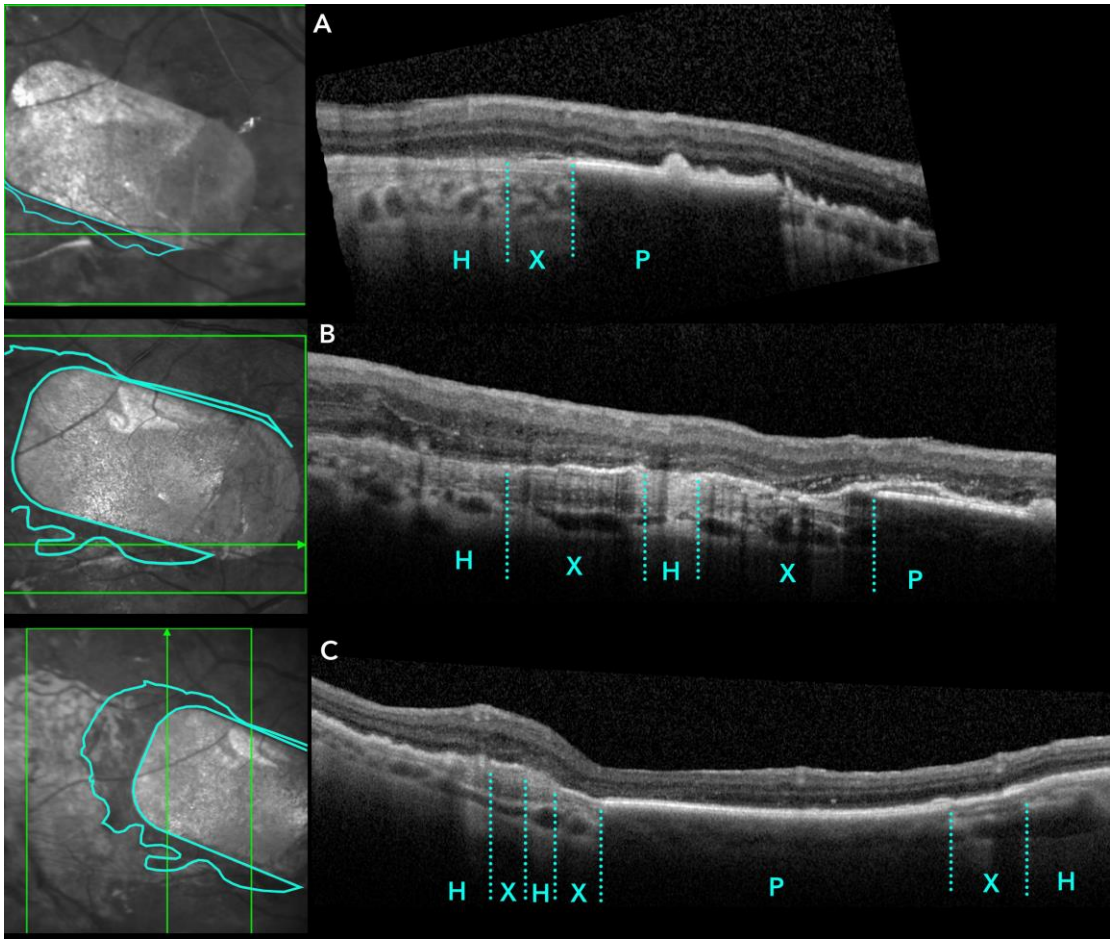

Figure 6-7: SD-OCT of the pigment extension area in subject 1. b-scans (right) and matched NIR pictures (left) of subject 1, at week 2 (A), month 6 (B) and year 1 (C). Outlined with blue in the NIR pictures is the edge of the area of pigment extension. The blue dotted lines in the b-scans indicate the corresponding margins of the areas in cross-section: P=hESC-RPE patch, X=extension of pigmentation, H=host tissue.

For the second subject, the first detectable OCT signal of the extended pigmentation area was obtained on the month 1 visit. As for subject 1, we see a hyper-reflective band continuous and of equivalent reflectivity with the hESC-RPE band of the implant, appearing to grow outwards from its top temporal corner (**Fig. 6-8A**). It is inner to the host's BM and its brightness in the grey scale seems intermediate between the markedly hyper-reflective line of the artificial BM and the adjacent hypo-reflective outer band of the host retina. In another cross-section in week 8 OCT we can also see the continuous RPE-like line outgrowing from the graft's hESC-RPE to the clump-shaped pigment extension bellow the inferior edge of the patch. The host's thinner BM line is maintained outer to this

extension, while a small “notch” seems to separate the extension from the deformed host’s RPE line (**Fig. 6-8B**). These characteristics are maintained in the subsequent follow-up OCT scans from both the superior and inferior extension of pigmentation.

In this case the distinction between the presumed RPE expansion and the outer host RPE is not always possible due to the poorer quality of the scans caused by the longer retained silicon oil. However, in the vertical OCT scans of week 52 the band in question is more clearly continuous with the grafted hESC-RPE in both the superior and inferior extensions and the transition to the adjacent host tissue is sharper and well defined (**Fig. 6-8C**). Similarly to subject 1, the overlying retina does not show any significant differences comparing to the adjacent grafted or host retina. The nuclear and plexiform layers here are more ill-defined and the retinal contour and thickness are significantly distorted due to the traction induced by the marked pre-retinal fibrosis over the temporal half of the graft. However, this deformation applies similarly to all three described retinal segments (host, grafted and outgrown from the graft).

6.3.5. Microperimetry

For both subjects, the areas of pigment extension were away from their fixation centre. That means that the visual acuity, contrast sensitivity and reading speed examinations (all related to the central vision) cannot be used to assess the function of these areas. Therefore, the only signs of visual function of the retina overlying the pigment extension could come from the corresponding light sensitivity in the MP exams. The MP stimuli grid was purpose-designed to examine the light sensitivity of the retina over the hESC-patch, however, there were various points projected outside the patch and into the area of extended pigmentation. For those points the sensitivity (in dB) was found either 0, or close to zero during the study period (**Fig. 6-9**).

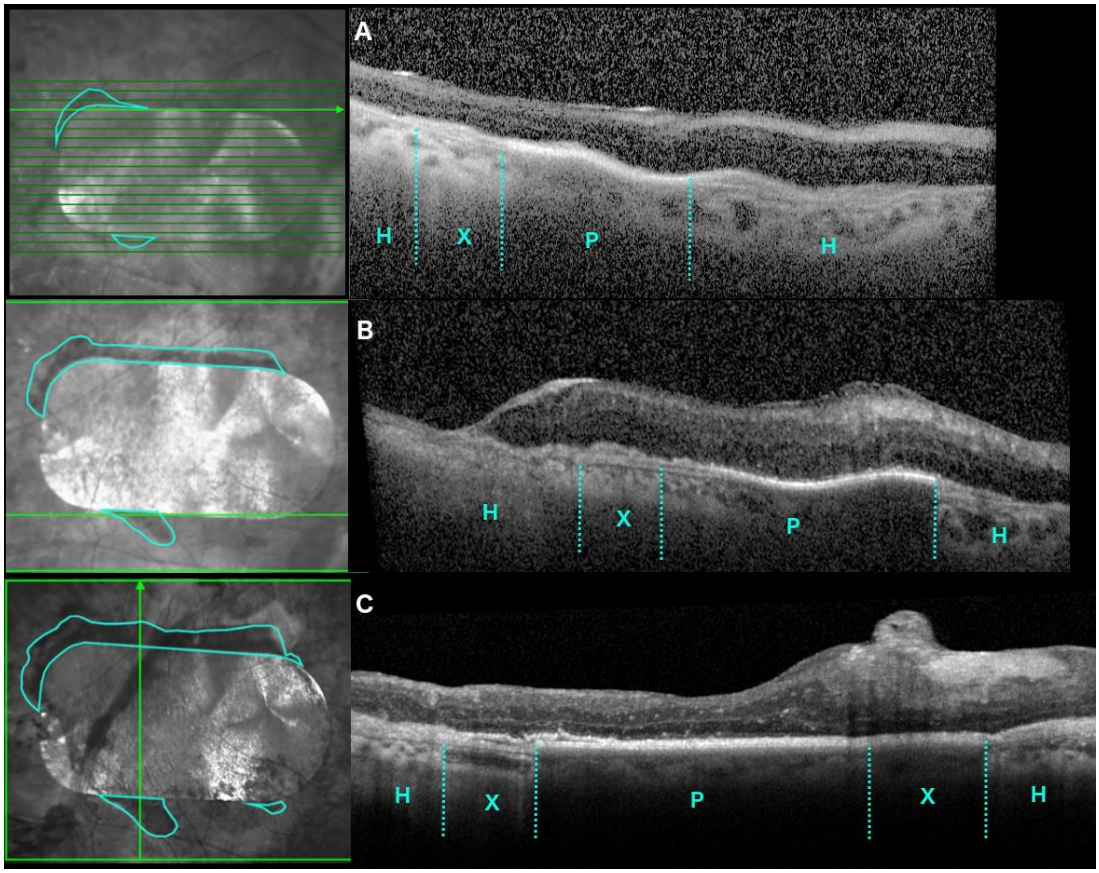

Figure 6-8: SD-OCT of the pigment extension area in subject 2. b-scans (right) and matched NIR pictures (left) of subject 2, at week 4 (A), week 8 (B) and year 1 (C). Outlined with blue in the NIR pictures is the edge of the area of pigment extension. The blue dotted lines in the b-scans indicate the corresponding margins of the areas in cross-section: P=hESC-RPE patch, X=extension of pigmentation, H=host tissue.

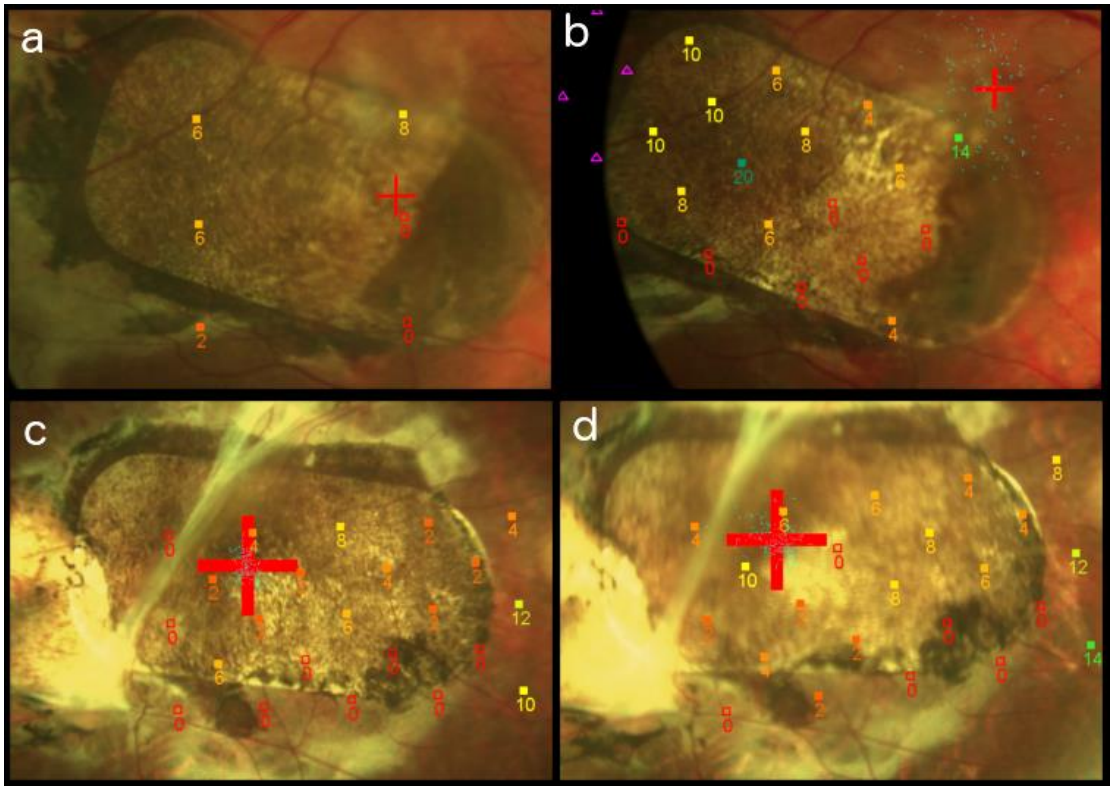

Figure 6-9: Microperimetry in the area of pigment extension. MP loci in or close to the area of pigment extension. a and b, MP exams of months 6 and 12 respectively from subject 1, showing low (2dB) or zero light sensitivity close to the area of pigment extension, adjacent to the inferior border of the patch. c and d, MP exams of months 12 and 24 respectively from subject 2, showing low (2-4dB) or zero sensitivity close to the inferior club-shaped area of pigment extension.

6.4. Discussion

I have demonstrated that the preparation and delivery of the hESC-RPE-BM complex using purpose-designed devices facilitated its atraumatic implantation in both subjects. Another protective element against the intra-operative damage of the cells was the polyester substrate (the synthetic BM), which in addition to optimising the polarisation and survival of the cells, facilitated the loading of the patch in the injector, and the subretinal delivery and “unwrapping” of the patch in

the target location at the submacular space. The early post-operative imaging supported the relatively intact structure of the patch, in both subjects.

6.4.1. Cell function as proof of survival

Since a histological assessment was not feasible in this study, the survival and function of the hESC-RPE can only be examined indirectly, by looking for signs of anatomical survival and, functionality of the implanted cells. The anatomical outcomes have already been analysed in the *Discussion* sections of the previous chapters. In Chapter 1, I have also listed the specific functions of the normal RPE and the significant role it plays for vision. Hereby, I will examine whether the implanted cells demonstrated these functions, providing adequate support to the retinal anatomy and the subject's vision.

6.4.1.1. Absorption of light:

The absorption of light has been attributed to the intracellular pigments of the RPE, with melanin being the main representative (Thumann et al., 2013). A time sequence of CF photos showed a sustained pigmentation of the patch with small regional changes, throughout the study period (Appendix 1). Additionally, proof of light absorption is provided by both the absence of light signal penetration of the graft and the absence of light reflectance and scattering through the neuro-retina, in OCT scans (Chapter 3, Figure 3-7).

6.4.1.2. Outer blood-retina barrier:

Comprising the inter-cellular tight junctions between adjacent RPE cells, it passively prevents the free transportation of fluid and metabolic elements between the retina and choroid (Katamay & Nussenblatt, 2013). In neither of the two subjects did we detect any subretinal or intraretinal fluid, drusen, or other substance aggregation. In contrast, in both we detected small PEDs as elevations of the hESC-RPE band and separation from the synthetic BM (Chapter 3, Figure 3-10). We believe that this provides some evidence of structural integrity of the graft-RPE monolayer tight junctions, since it is likely that

in order for fluid to accumulate in the potential space between the RPE and BM, the inter-cellular tight junctions need to be functioning. Hence, the presence of small PEDs on the surface of the implant suggests the maintenance of the polarisation of the cells and the basic function of the outer blood-retina barrier.

6.4.1.3. Transport of nutrients, ions and water - Retina-RPE apposition:

The high metabolic activity of the retina results in continuous water production, which is critical to be removed by functional RPE cells either by active transport or via the Aquaporin-1 channels (Thumann et al., 2013). Excess water in the retina would result in subretinal and intraretinal accumulation, macular oedema and photoreceptor loss. The absence of SRF and the preserved tight adherence between the neurosensory retina and the RPE in both subjects throughout the study period, provide possible signs of functionality for the RPE cells.

6.4.1.4. Secretion of cytokines and growth factors:

These are believed to maintain the structural and functional integrity of the choriocapillaris, as well as the antiangiogenic and neuroprotective environment of the photoreceptors (Thumann et al., 2013) and hence, maintain an avascular outer retina. None of our study subjects showed any signs of subretinal or sub-RPE neovascularisation in the transplanted area, during the 2 years, as tested by FFAs and OCT scans throughout the trial. We saw that subject 1 had a significant PED, well outside of the patch, complicated with SRF during post-implantation year 2. We believe it reflected a re-activation of the primary disease (wet AMD – IPCV) in a distant to the transplanted location. We decided to treat this re-activation with intra-vitreal anti-VEGF injection (Aflibercept) and two weeks later both the PED and the SRF were found fully resolved. This therapeutic result was preserved by a series of intra-vitreal Aflibercept injections administered on a “treat-and-extend” scheme (Chapter 5, Fig. 5-2).

6.4.1.5. Visual Cycle – supporting vision:

Phagocytosis of the photoreceptors' (PR) outer segments and recycling of the rhodopsins are the main functions by which the RPE supports PR metabolism and thus vision (Sparrow, Hicks, & Hamel, 2010). It is strongly supported that the target tissue of AMD is the RPE and that retinal degeneration and vision loss is a result of the RPE deficiency caused from the disease (Bird, 2013). Having said that, improvement and preservation of the visual function in the study subjects should provide a solid proof of the hESC-RPE functionality. In the previous chapters (3 to 5) we saw that both subjects were benefited by the cell treatment, as their visual function improved post-operatively, in all of the tested modalities. They both showed significant increase in BCVA, contrast sensitivity, reading ability and improvement in their fixation and in the overall light sensitivity of the treated retinal area. This improvement remained significant after two years, even though for the first subject there was some deterioration during the second year. More importantly, it was supported by a fairly stable anatomy of the transplant and the related tissues, showing a close structure-to-function correlation.

Another finding supporting the implant's functionality is the fundus autofluorescence (FAF) that both subjects demonstrated during the study period. It has been well documented that the AF of the RPE is attributed to the accumulation of intracellular lipofuscin, which is considered to be mainly derived from the phagocytosis and incomplete digestion of photoreceptors' outer segments during the visual cycle. The lipofuscin forms granules that accumulate within the RPE cells as a function of age, resulting in the fundus AF increasing significantly with age. (F. C. Delori, Dorey, & Staurenghi, 1995; F. C. Delori, Goger, & Dorey, 2001; Wing, Blanchard, & Weiter, 1978) Another source of autofluorescent granules is the RPE cell autophagy. This is a process of removing defective organelles and proteins, in order to maintain cellular homeostasis and it is also age-related (Boulton, 2014). The relative contribution of the two mechanisms is still to be studied; nevertheless, it is broadly believed that the first pathway plays the most significant role in RPE autofluorescence.

Boulton et al. have shown that AF granules can be observed in cultured primary human RPE cells, within 2 weeks of daily feeding with photoreceptors' outer segments and that the number of AF granules increases with time (Boulton, McKechnie, Breda, Bayly, & Marshall, 1989). In their experiment they fed their RPE cultures with purified bovine rod OS in a way that each RPE cell was exposed to approximately 200 OS daily, comparing to the approximately 40 OS in vivo daily exposure. It has also been reported that some cytoplasmic AF can be detected in RPE cells as young as those of six weeks premature foetal eyes (Wing et al., 1978). Having said that, there is no literature known to the author on the timeline of in vivo AF of human RPE, early enough to be compared to the transplanted "0-year-old" SC-derived RPE that has never before been exposed to POS.

Apart from RPE cells, lipofuscin granules together with other autofluorescent deposits can accumulate in macrophages in the outer retina and subretinal space (Sekiryu et al., 2012; Sekiryu, Oguchi, Arai, Wada, & Iida, 2011; SPAIDE, 2008). Furthermore, subretinal blood devitalised in the extracellular space can also form autofluorescent compounds (Ito, Nakano, Yamamoto, Hiramitsu, & Mizuno, 1995; Sawa, Ober, & Spaide, 2006). These alternative sources of AF could possibly justify the very early (from week 1 post-implantation) granular AF of the first subject's graft (**Fig. 6-10**), as a result of residual devitalised blood from their extracted subretinal haemorrhage, or as a result of the aggregation of macrophages during the early post-operative inflammatory reaction. However, the preservation of the background AF of the implant until the completion of the study, as well as the increase of its intensity with time in both subjects, are suggestive that the implanted hESC-RPE cells demonstrate some degree of POS phagocytosis. (Chapters 3 & 5, **Fig. 3-14, 15 & 5-10**). This is also supported by the observation that the areas of the patch with preserved AF for the long-term also showed a higher light sensitivity as this was assessed by Microperimetry (**Fig. 6-10**). Conversely, the parts of the implant showing minor or no AF, such as the mid-nasal area for subject 1 and geometric

centre and nasal edge for subject 2, also demonstrated the lowest if any sensitivity in light stimuli.

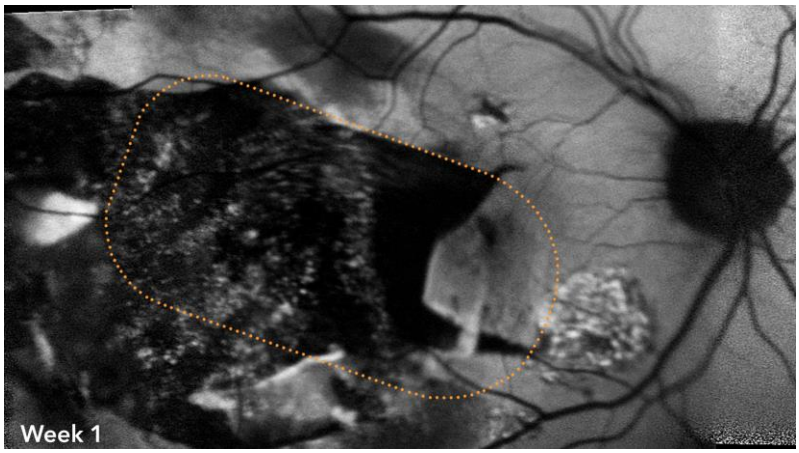

Figure 6-10: AF photograph of subject 1 on post-op week 1: Spectralis BluePeak Blue Laser Autofluorescence. The dotted line indicates the location of the hESC-RPE patch. Granular AF is detected on the temporal half of the patch, AF "silence" in the middle-nasal part and host-like AF in its nasal edge (due to the overlying host RPE).

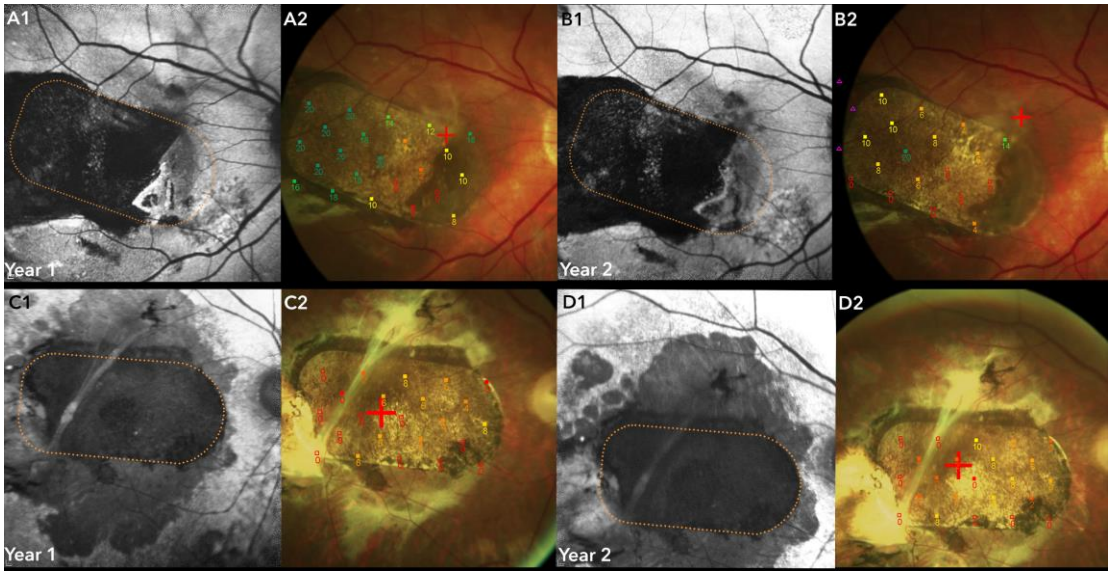

Figure 6-11: Correlation between AF and MP sensitivity: A1,2 & B1,2 FAF photos and MP exam on year one and two respectively, for subject 1. C1,2 & D1,2 same series for subject 2.

6.4.2. Immune tolerance as proof of survival.

The long-term maintenance of the immune privileged subretinal environment reflects the immunomodulation properties of the RPE, both passive and active. The former comprises of the tight inter-cellular junctions and low levels of major histocompatibility antigen expression. The latter includes expression from RPE cells of soluble and surface factors that promote immune privilege, such as TGF-β, PEDF, and CD95, CD59, CD46 (Katamay & Nussenblatt, 2013).

Our hypothesis that the hESC-RPE cells survived during the study is also supported by the absence of apparent signs of immune rejection, which may be partially attributed to the immunoprotective features of the implanted cells and partially to the concomitant immunosuppression that both subjects received (peri-operative oral prednisolone and depot local fluocinolone acetonide implant). Immune rejection is considered as a major barrier to the long-term survival of the graft (da Cruz et al., 2007) and is manifested by signs that include infiltration of inflammatory cells (mostly monocyte-like cells), disruption of the graft structure, vascular leakage, cystoid macula oedema (CMO) and depigmentation of the graft, and may even progress to its fibrous encapsulation (Algvere et al., 1994; Sheng et al., 1995). It also appears that the risk of rejection is higher in subfoveal grafts than ones implanted in an extrafoveal location (Algvere et al., 1999). Our two cases did not show any clinical or imaging signs of inflammation, apart from a regional depigmentation and some epiretinal fibrosis. Interestingly, the former occurred mainly during the second follow-up year and was noticed in the area of the pre-transplantation fovea for both subjects (**Fig. 6-12**). If this was a result of a subclinical low-grade immune reaction to the implanted cells it remains unclear; however, the fact that the depigmentation occurred at the most prone to rejection locus in both grafts, combined with a possible “wearing off” effect of the local (depot) immunosuppression and the corresponding functional drop (in case 1), support the late rejection hypothesis. Again, the need for histological assessments is necessary for definitive conclusions, especially given the pathophysiological mechanism of such a rejection is poorly understood. As for the epiretinal fibrosis, our opinion is that this is reflective of the extent of the

background disease, combined with the scarring effect of the significant surgical manipulations of the treated tissues.

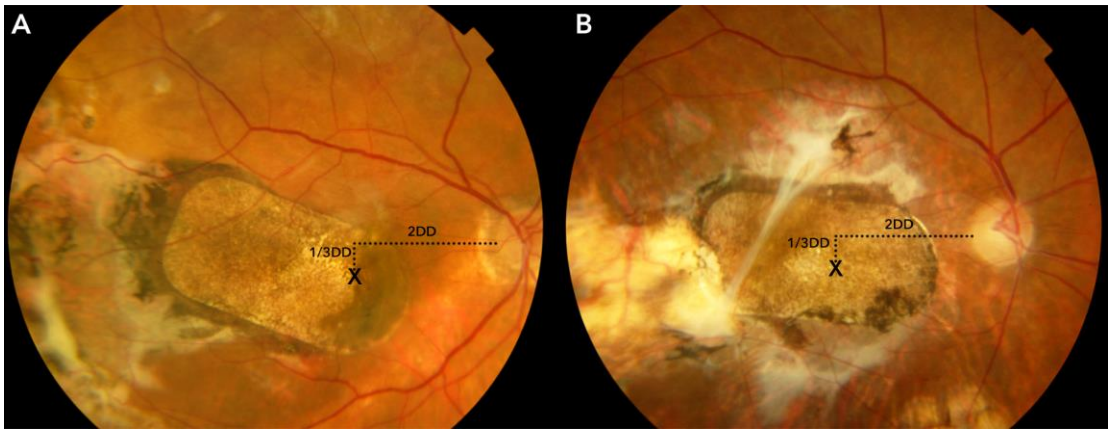

Figure 6-12: Topographic correlation of the regional depigmentation to the pre-operative fovea. Colour fundus photographs on year 2 for subject 1 (A) and 2 (B), showing the anatomical proximity of the most de-pigmented area of the patch to the estimated (according the to the Sunness et al. method (Sunness et al., 1999)) centre of the fovea.

6.4.3. Behaviour of the hESC-RPE cells

The retinal pigment epithelium is considered to be amongst the most reactive tissues in the eye. It can respond to a variety of stimuli such as trauma, inflammation, infection, as well as neoplastic and degenerative processes. This response is most commonly expressed with RPE hyperplasia, but it can also involve hypertrophy or atrophy, cell migration, or very rarely true neoplastic proliferation. (Frayer, 1966; Jampel et al., 1986)

6.4.3.1. Behaviour of the therapeutic *cells on* the patch.

In the previous chapters (3 to 5) I described the changes of the pigmentation of the patch during the 2-year post-operative monitoring. Both subjects showed areas that remained stable, as well as areas of increased and decreased pigment density with time. For case 1, the temporal half of the patch remained stable, while the nasal half showed some de-pigmentation (temporally) and some hyperpigmentation (nasally)(**Fig. 6-13A**). For the former (area (ii)), a possible

explanation could be the loss (atrophy) of hESC-RPE cells due to immune reaction/rejection, or their migration to adjacent areas on and off the patch. For the latter (area (i)), I have already described the insertion of the patch under the host RPE, which resulted in a “double RPE” area, hence the darker hue. This area kept changing until year two, showing a decrease in size, which could have been a result of an outwards “movement” of the RPE (towards the nasal edge of the graft), with or without corresponding retraction of the overlying retina (**Fig. 6-2**). Late OCT scans through this part revealed a detachment of the hESC-RPE form the underlying synthetic BM, and an abnormal thickening with cystic degeneration of the overlying retina (Chapter 5, **Fig. 5-6**). For case 2, the two edges of the patch demonstrated the two opposite edges of the pigmentation spectrum, with the inferior-temporal corner being completely “bleached” from possible surgical trauma, and the nasal corner being heavily pigmented by the end of the study (**Fig. 5-5B**, areas (iv) and (i) respectively). For the former, I have already shown the PED-like appearance of the hESC-RPE from the synthetic BM, revealed in OCT scans (Chapter 3, **Fig. 3-9**). The fact that this corner of the patch was used to hold and manipulate it during the operation leads to the hypothesis of a surgical trauma that detached the RPE layer. Furthermore, a probable damage of the vitronectin coating of the synthetic BM could explain the fact that this area remained stable and did not show any signs of tissue healing with RPE growth. For the latter, the hyperpigmentation of the nasal corner, possible explanations should include migration or proliferation of RPE cells (RPE hyperplasia), or aggregation of macrophages engulfing melanin. Similarly to subject one’s patch, the regional decrease in pigment density (area (ii)) could mean either loss or movement of the implanted cells. In none of the cases did we notice any signs of uncontrolled, neoplastic proliferation.

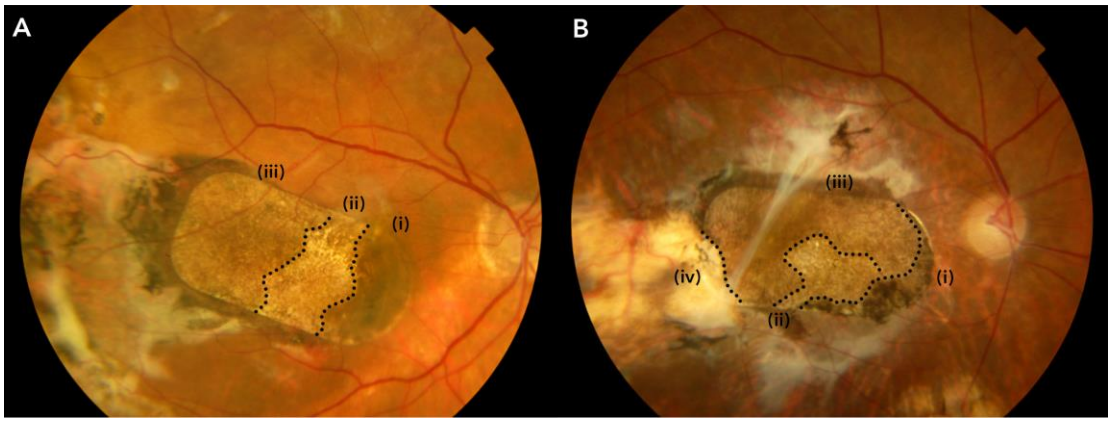

Figure 6-13: Pigmentation at year 2. CF photographs showing the areas of distinct pigment density of the patch by the end of the study period, for subject 1 (**A**) and 2 (**B**) respectively.

6.4.3.2.. Behaviour of the therapeutic cells *off* the patch

Both subjects developed a “spill-out” pigmentation outside the edges of the patch. It was ill-shaped, but well defined from the surrounding tissues and it stopped expanding 6 months post-op. This observation raises the question of the nature of this pigmentation, which however, can only be answered hypothetically, since only a histological assessment would be able to provide definite conclusions. More specifically, it is critical for both the safety and efficacy of this experimental transplantation to investigate the following questions:

- is this unidentified finding RPE?
- where does it originate from?
- Does it hold any potential for function?

Is it RPE?

The differential diagnosis of a clinical observation of dense hyperpigmentation in the fundus includes hyperplasia and/or migration of the RPE. This hyperplasia or migration is most commonly seen as a response to inflammation, tissue trauma, or a neoplastic processes. Subretinal inflammation usually results in a more dramatic RPE hyperplasia, the extent of which is depended on the intensity, the duration and the location of the inflammatory stimulus (Frayer, 1966). Especially for the macular area, inflammatory processes tend to generate more severe

hyperplasia and pigmentation than those in the retinal periphery. Mild, subacute or chronic chorioretinitis can stimulate a slow, continuous and extensive hyperplasia, which in fundoscopy can appear as a gradually enlarging pigmented lesion. Conversely, intense acute inflammation can produce a massive RPE cell proliferation, which usually appears as hypo-pigmented fundus lesions surrounded by “rings” of hyperpigmentation.

The reparative properties of the RPE, as a response to tissue damage, have been well studied both in vitro, but also in cases of surgical excision of CNV membranes (Hsu, Thomas, Ibanez, & Green, 1995; P. F. Lopez et al., 1995; Sugino, Wang, & Zarbin, 2003; Valentino et al., 1995; H. Wang, Ninomiya, Sugino, & Zarbin, 2003). Localised RPE defects generated by the surgical trauma can be resurfaced by various mechanisms, namely cell spreading, cell migration and cell proliferation. The overall process represents a “wound healing” process, with RPE cells acting as a first line defence in the reconstruction of choroidal and retinal injuries. They demonstrate in the eye functions analogous to this of fibroblasts in the rest of the body, with proliferation and fibrous metaplasia playing a significant role in re-establishing adequate chorioretinal adhesion, as well as in the formation of subretinal scars (Frayer, 1966).

In the earlier trials of subretinal injection of hESC-RPE cell suspension, Schwartz et al. also demonstrated increased pigmentation in 72% of the host eyes, which, combined with OCT signs of cell foci on the inner aspect of BM, were considered as thickening or reconstruction of the RPE (Schwartz et al., 2012). Mandai et al. also reported an extension of the pigmentation and of the RPE-like OCT signal, further from the iPSC-RPE patch’s edges, in their single published case 3 months post-operatively (Mandai et al., 2017). Conversely, Kashani et al. did not observe any significant signs of RPE cell migration in their 4 cases of hESC-RPE implants (Kashani et al., 2018). As with ours, none of these studies was supported by histological evidence and thus their assumptions on this phenomenon remains speculative.

In our two cases, there were no clinical signs of inflammation at the time of the development of the pigment extension. A subclinical low-grade reaction

resulting in changes and even loss of a number of the implanted cells and dispersion of melanin cannot be ruled out. However, this would be most likely to occur during the late follow-up period, where there was only local immunosuppression with the depot steroid implants in their reducing phase. On the contrary, the observed pigmentation developed during the early post-implantation period, when the subjects were under maximum immunosuppression with both systemic and local steroids. Likewise, we cannot exclude the possibility of aggregation of pigment-engulfing macrophages playing a part in the extended pigmentation, but this would also require inflammatory pathways overcoming the immunosuppression.

Having said that, we believe that a more plausible explanation would be the activation of the RPE as a part of a reparative process triggered by the surgical injury at the chorioretinal junction. It might be that the surgically induced trauma in the subretinal space stimulated the RPE cells and activated their proliferation and migration towards the RPE-tissue gaps, which as expected, were more prominent near the edges of the patch, and along the surgical pathway of its subretinal insertion. This hypothesis is also supported by the fact that the growth of pigmentation occurred mainly in the first post-operative months and in parallel with the chorio-retinal scarring around the surgical incision(s).

Is it of implant's or host's tissue origin?

Further to our assumption that the observed pigment extension represented an extension of the RPE via migration and hyperplasia, the question as to whether it originated from our hESC-derived implant or the outlying host RPE remains to be answered. Firsty, the centrifugal pattern of expansion, as seen in the time sequence of CF photos of both subjects, is more consistent with an implant's origin, since it starts form the edge of the patch and extends outwards with time (**Fig. 6-2, 6-3**). Conversely, a host RPE expansion would be expected to show an inwards growth pattern, starting from the edges of the surgically excised/traumatised native tissue and expanding with time towards the edges of the patch, in an effort to repair the induced "wound". I also showed that the OCT

scans through this area revealed a hyper-reflective RPE-like band, continuous with the patch's RPE and not the host's. It appeared to grow with time from the former to the latter, in a "gap-filling" (wound-healing) pattern. In addition, both the background fluorescence in the FFA and the AF reflectance of this area were more alike to the main hESC-RPE graft's than to the surrounding host retina. Finally, the ability of hESC-RPE implanted cells to expand was also shown in the initial stem cell-derived RPE cell suspension study, where the expansion was observed in areas of geographic atrophy where there was loss of the host RPE (Schwartz et al., 2016).

Does it function?

As for the on-the-patch RPE, we can only make indirect assumptions on the functionality of this RPE extension. Based on the MP results, the light sensitivity of the corresponding retina appeared to be close to zero. While this may reflect the inability of this "RPE" to support the visual cycle, it is more likely that the tissue damage of the outer retina around the patch's edges was a more significant cause of function loss. Furthermore, the extended "RPE" seems to maintain the RPE-neurosensory retina adhesion (so SRF noticed), as well as part of the NSR segmentation and architecture, as seen in the OCT scans.

6.4.3.3. Possible migration through the retina?

Apart from the RPE changes along the subretinal plane ("horizontal", on and off the therapeutic patch), we also have to consider the possibility of cell migration towards the inner retina ("vertical"), along the retinal surface and even in the vitreous cavity. It is well documented that such migration plays an important role in the pathogenesis of various retinal abnormalities, such as proliferative vitreoretinopathy (PVR) (Leschey, Hines, Singer, Hackett, & Campochiaro, 1991) and choroidal neovascularization (H. Miller, Miller, & Ryan, 1986). More specifically, transformed RPE cells are the major component in the pathophysiology of the formation of tractional fibro-cellular membranes in the

inner and outer surfaces of the retina (Wiedemann, Yandiev, Hui, & Wang, 2013).

Fundoscopy throughout the study did not reveal any visual signs of RPE cells “spill-out” in the vitreous cavity (“tobacco dust” sign), as a result of cell migration through the whole thickness of the neurosensory retina. As for intra-retinal migration, some hyper-reflective intra-retinal clusters were observed in both subjects. Such clusters have been suggested to represent anterior migration of shed RPE aggregations within the NSR, in AMD cases, especially adjacent to areas of severe RPE disruption (**Fig. 6-14, A-C**)) (Ho et al., 2011), (Curcio, Zanzottera, Ach, Balaratnasingam, & Freund, 2017). Compared to such examples, the findings in our subjects were small in size and with no light back scattering in OCT scans; however, as they were also noticed in disrupted areas of the hESC-RPE patch, such as the nasal part in subject one and the infero-temporal corner of the patch in subject 2, it is possible that they were signs of RPE cell shedding anteriorly (**Fig. 6-14, D** and **E**).

Furthermore, subject 2 developed a PVR-related retinal detachment two months post-operatively and, later, a marked, thick, fibrotic, epiretinal strand, which remained for the whole study period. The former was in the inferior periphery, away from the patch and was repaired with a retinectomy surgery, which re-apposed the retina with no recurrence or sequelae. The latter was located at the posterior pole, crossing the width of the treated area, over its inner surface, without however inducing any significant traction to the adjacent retina, and thus left untreated. Subject 1 also developed some epiretinal fibrosis, which mainly affected the nasal edge of the patch (area of “double RPE”).

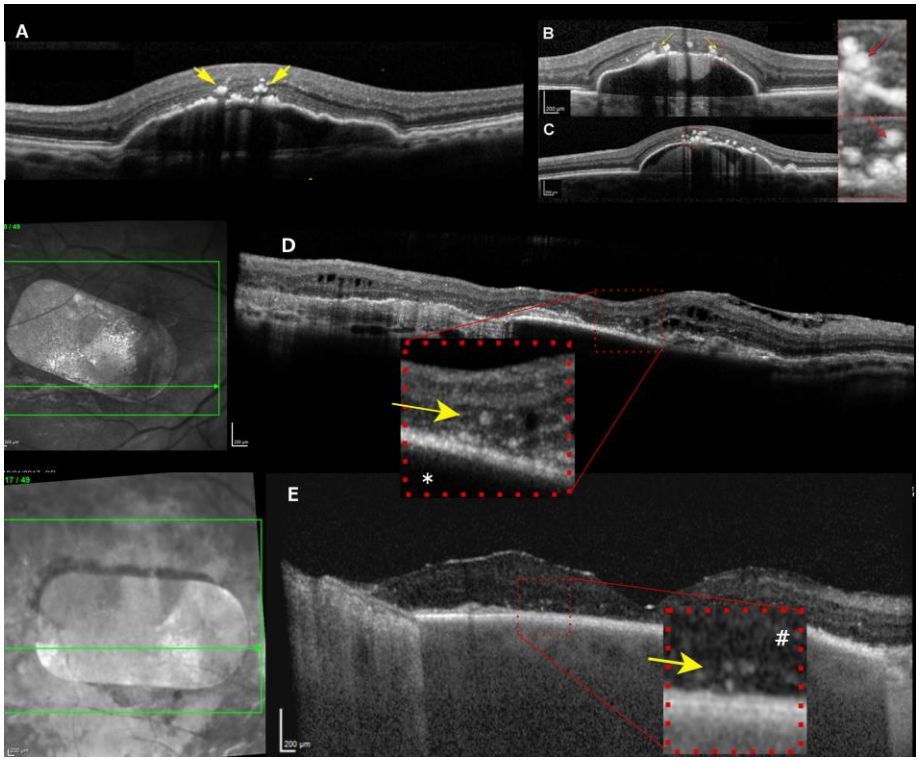

Figure 6-14: Intraretinal RPE migration. (A-C) examples of intraretinal clusters of shed RPE cells (yellow arrows) over areas of RPE disruption in cases of wet AMD as published by Ho et al (Ho et al., 2011). They are hyper-reflective with a "signal shadow" bellow them, characteristic of back scattering. (D) Similar, but less marked finding in the area of the "double RPE" of subject one (yellow arrow in magnified area (*)). (E) small, hyper-reflective clusters over the inferotemporal corner of the patch in subject 2 (yellow arrow in magnified area (#)) Both findings may represent anterior hESC-RPE migration.

Even if it is not possible to exclude an involvement of the implanted hESC-RPE cells to the pathology of these fibrous reactions, I believe that they are more related to the pre-operative severity of the disease (already established chorioretinal scarring and haemorrhage), combined with the complexity of the vitreo-retinal operations alone (Romano et al., 2011; Stanescu-Segall et al., 2016; Wiedemann et al., 2013). As the hESC-derived RPE cells seemed to have remained essentially on the patch, with only localized sub-retinal expansion and only subtle, if any, intra-/epi-retinal migration, I do not feel that these scarring phenomena are likely to be directly associated with the investigational patch.

As for the role of the hESC-RPE "vertical" migration in CNV formation, neither of the two subjects developed new CNV in the area of the patch. Subject

two showed no signs of CNV recurrence during the two years, while subject one's leaking lesion, described in chapter 5, was away from the patch and considered as a result of a PCV lesion, as this was the background condition of this subject.

6.5. Conclusion

In this chapter I investigated the long-term survival and behaviour of the implanted hESC-derived RPE, in the two study subjects. In the absence of histology, I have used indirect methods to support my hypothesis that the implanted cells survived and maintained RPE structure and function, and that the pigmented extension off the patch was due to transplanted hESC-RPE.

Starting from the intra-operative manipulation with the purpose-designed introducer to make it as less traumatic for the transplant as possible, I managed to show that the tissue maintained its form in the peri- and post-operative period. Subsequently, I showed that the implanted RPE fulfilled the role of the normal RPE in the two main aspects of its function – the anatomical barrier and physiological support. The preservation of its pigmentation and autofluorescence, the sustained light sensitivity of the supported retina and finally the absence of signs of severe rejection for up to two years. All of these factors combine to provide indirect, but nevertheless strong support for the persistence, structural integrity and the continued function of the transplanted cells on the investigational patch. These results were achieved long-term with predominantly local immunosuppression, while systemic regimens were administered only for the peri-operative periods.

Some changes in the pigment density of the patch were observed in both subjects. Areas of increased pigmentation were attributed to the surgically induced host-over-transplant "double" RPE (subject 1) or tissue trauma (subject 2), as well as to possible reactive hyperplasia of the cells, with or without the contribution of macrophages aggregation.

Finally, I assessed the behaviour of the implanted hESC-RPE cells in terms of their possible migration out of the patch. I showed a centrifugal extension of the pigment outside of the borders of the patch, resembling an outwards migration of the RPE cells. This was supported by sequential photographs and OCT scans. Regarding the functional characteristics of this extension, I did not obtained any signals of light sensitivity from these areas. Taking into consideration the morphology of these pigmentary formations and the natural role of the RPE in the “wound-healing” processes, my hypothesis is that the observed extension represented a possible migration of hESC-RPE cells, originating from the patch and moving towards the host RPE, in a reparative “gap-filing” pattern. I acknowledge that these assumptions remain hypothetical, but to my knowledge, I report the most thoroughly investigated cases of stem cell-derived RPE-patch transplantation in the literature so far.

Chapter 7

Discussion, Future directions and Conclusions

7.1. Aims of the thesis

This thesis aimed to:
(1) Examine whether subretinal transplantation of a hESC-derived RPE monolayer on a vitronectin coated synthetic BM can be feasible, safe and efficacious as a potential treatment of severe neovascular AMD,
(2) Describe the one and two-year structural and functional outcomes of this approach in the first two patients, and
(3) Investigate the role of immunosuppression in the survival of the transplant.

7.2. Summary of key findings.

Chapters 3 and 4 provided data indicating safety, efficacy and stability of the hESC-RPE patch transplant in both patients, during the first year. The survival of the transplanted hESC-RPE is demonstrated by the visible persistence of a pigmented layer over the patch corresponding to a clear RPE-BM signal on OCT scans, combined with distinct auto-fluorescence by SLO as a first indication of the RPE cellular function. Both cases maintained features of normal retinal architecture and specifically, visible areas of the photoreceptor outer segments. Most importantly, both patients demonstrated significant improvement in visual function tests, specifically fixation stability, visual acuity, contrast sensitivity, microperimetry and reading speed, which were maintained during the first year. These results were promising, given the severity of the baseline disease, whose natural course can potentially lead to central blindness.

Systemic oral prednisolone was used only peri-operatively, with local depot immunosuppression used for the second half of the first year and ongoing. No significant clinical signs of rejection were noted. In terms of safety, the most significant adverse ocular event was a PVR-related retinal detachment in subject 2, distal to and not involving the grafted area and most probably attributable to

the complex surgical procedure, rather than the transplant. No signs of uncontrolled cell proliferation or tumorigenicity were detected.

In chapter 5 the 2-year outcomes of our approach were described and analysed. Again, the hESC-RPE transplant appeared safe, with no related serious adverse events either local or systemic. The structural integrity of the graft was demonstrated by preserved pigmentation, clear RPE-BM signal in the OCT scans, preserved, although reduced (compared to year 1), autofluorescence and no major clinical signs of rejection. In both of our cases only local immunosuppression was given, with one intraocular steroid implant, over the final 18 months of the first 2 years. Retinal architecture was preserved in many areas, although others showed some atrophy and disorganisation. Visual function (VA, CS, MP and RS) remained significantly improved compared to the baseline level, although it showed some reduction when compared to year-1 results. Most importantly, I reported good structure-function correlation, with the areas of preserved pigmentation matching clearly the areas of good light sensitivity.

In chapter 6 I provided a more in-depth analysis of the behaviour and fate of the implanted hESC-RPE cells, both on and off the investigational patch. I showed that the implanted RPE fulfilled the structural and physiological role of the natural RPE in most, if not all, of its aspects. I also provided possible explanations for the observed changes on and off the graft. Finally, I reported a probable graft-to-host, centrifugal migration of the cells, as a result of a wound-healing phenomenon, which provides further strength to my hypothesis on the survival and function of the hESC-RPE transplant.

7.3. Proof of principle and rationale

Age-related macular degeneration is a potentially blinding disease, especially in the wet-neovascular form. The current consensus for its treatment is a long-term,

repeating course of intravitreal injections that can slow down the progression, but do not constitute a *therapy.*

Since the RPE has been identified as the target tissue of the disease, the idea of replacing it has been tried in several therapeutic strategies. Macular translocation and autologous RPE transplantation have provided the proof of principle, but their technical complexity and high risk of complications have prevented their broad uptake and application (Aisenbrey et al., 2007), (Uppal et al., 2007), (Chen et al., 2010), (Majji & de Juan, 2000), (Chen et al., 2009), (Peyman et al., 1991), (da Cruz et al., 2007). Nevertheless, these trials have informed subsequent research on the case selection, the therapeutic time windows and the obstacles needed to overcome, such as the transplants availability. Their promising outcomes showed the potential of RPE replacement to restore vision, as long as there are photoreceptors to rescue. This is the case in wet AMD with acute vision loss, as in our two subjects, compared to the late transplantation cases in geographic atrophy, where the photoreceptors loss is already established.

We chose embryonic stem cells to derive our RPE. Compared to iPSC, the hESC are “0-year-old” cells and can be genetically selected and controlled specifically for the target disease. Furthermore, they can provide a continuous supply of transplants, independent of the patients’ disease course (Ramsden et al., 2013). Their main disadvantage is that they produce heterologous tissues and thus there is a potential need for immunosuppression to prevent rejection. The iPSC are considered to not require immunosuppression, however they may contain mutations or epigenetic defects caused by their reprogramming (Oswald & Baranov, 2018).

7.4. Results in the light of the literature

RPE transplantation for AMD was one of the first in humans study to use hESC-derived transplants and the first ever for iPSC-derived ones. For the former, a hESC-RPE cell suspension was injected in the submacular space of atrophic AMD patients, and Tacrolimus was used for immunomodulation (Schwartz et al., 2012), (Schwartz et al., 2015), (Schwartz et al., 2016). For the latter, an iPSC-RPE cell sheet was surgically implanted in the submacular space of an eye that had previously undergone a 3-year course of anti-VEGF injections for wet AMD. No immunosuppression was given (Mandai et al., 2017). Both these first studies provided valuable data on the safety, probable integration and survival of the implanted cells, as indicated mainly by the pigmentation changes observed in the fundus. In terms of function, both showed very limited visual improvement. Most importantly, they informed subsequent research on the structural disadvantages of the cell suspension approach, the limitations of treating established atrophy, the therapeutic window for RPE replacement and the need for immunomodulation according to the cell source. More studies have followed, using different types of stem cell sources, and targeting both types of the AMD.

We chose cases of acute wet AMD for our study. Both our subjects suffered from sudden vision decline due to RPE rip and submacular haemorrhage and both received the hESC-RPE patch within 6 weeks from this decline, which is a period short enough for the photoreceptors to have survived. Compared to the aforementioned studies, the promising results we observed, with both subjects showing a significant improvement in all the vision tests, support these selection criteria. Peri-operative systemic and long-term local steroids appeared enough for the preservation of the transplant to two years.

These baseline characteristics of our subjects also raise the question of how our approach compares with other, more conventional treatments. I have already reviewed in chapter one the numerous strategies, from minimal

interventions to major surgical operations that have been described for the management of submacular haemorrhage due to neovascular AMD. The best outcomes, in terms of *final* visual acuity, seem to be achieved by the milder interventions, such as the intravitreal injection of anti-VEGF, tPA and gas, while the best outcomes in terms of vision *gain* seem to be achieved by surgical operations to remove the subretinal blood and scar, combined with injection of anti-VEGF and tPA (Stanescu-Segall et al., 2016). This difference may reflect the less severity of the cases chosen to be managed with minimal interventions compared to those which undergo surgery. Our final (year 2) visual acuities were 26 EDTRS letters (≈20/300) for subject 1 and 23 ETDRS letters (≈20/360) for subject 2. Similar and even better results have been reported to be achieved with conventional treatments. However, these strategies do not address the issue of a damaged RPE, which can be the result of both the baseline disease and the surgical intervention. The available long-term data from such reports are limited, but it is very unlikely that the vision can be preserved when the RPE is severely compromised. Our approach combined the surgical removal of the submacular haemorrhage with the implantation of a new, healthy RPE, with a relatively small extension of the surgical manipulations (for the insertion of the patch after the blood removal), compared to a “conventional” surgery. The preservation of significantly improved vision for two years in both subjects supports our strategy of RPE replacement. The observation of the possible role of this RPE in a “wound healing” process against the submacular tissue damage offers further promise.

7.5. Strengths of the Thesis

The basic strength of this study was the prospective design of the clinical trial, with inclusion/exclusion criteria that narrowed the recruitment both in terms of baseline disease severity and time passed from vision loss. This prevented from selection bias and increased the possibility of demonstrating efficacy, apart from

safety. Another major strength was the inclusion of all of the currently available structural and functional assessments. The subjects were monitored closely with a series of CF photos, FFAs, FAF, SD-OCT scans, AO retinal imaging, as well as BCVA, CS, MNRead, Microperimetry and fixation that allowed a solid comparison between the anatomical findings and the vision outcomes. All visual function tests, apart from the Microperimetry, were performed by independent research optometrist, so there was no examiner bias. The Microperimetry was operated by myself, but this is an automated exam and the patients' performance cannot be affected by the examiner. To my knowledge, there is no other relevant study that has collected such a wide variety of multimodal imaging procedures and functional tests. The co-localisation of pigmentation, perfusion, retinal architecture, microperimetry and direct photoreceptors' imaging (AO) of the transplanted area provides the most solid structure-function correlation in the literature up to present. Finally, another significant strength was the longitudinal monitoring of our subjects for at least 2 years. According to the available literature, this is the first study of a hESC-RPE patch transplantation to report results for more than one year post-operatively.

7.6. Limitations of the Thesis

The first limitation of this thesis is the low number of cases. Given the fact that the safety of our approach was the primary outcome in question, a larger series of patients would be required for an accurate assessment of the surgical and post-surgical risk. This limitation became more profound by the serious adverse event – the retinal detachment – of subject 2. Although this could have been a complication of the surgical operation alone, a larger number of subjects would be necessary to address the possible role of the hESC-RPE patch to a PVR development. The rest of the safety profile of both cases over two years is encouraging, but again, it is difficult to generalize with only two subjects tested.

Another significant limitation is the absence of histology, which makes it impossible to draw definite conclusions on the fate of the implanted hESC-RPE cells. A cellular analysis to the level of histology is – by design – not realistic in such a preliminary human trial. However our thorough structure-function correlation with the co-localization of choroidal perfusion, survival of hESC-RPE, retinal sensitivity and imaging of photoreceptors provides the maximum amount evidence of the transplant's survival and function that can possibly be obtained without histology.

The ambiguity of the possible effect of the surgery alone is another limitation we need to acknowledge. The removal of the submacular haemorrhage and neovascular tissue has been reported to offer functional improvement; however, the longevity of our results, combined with the structure-function co-localisation that we have demonstrated exceeds these reports. Moreover, to support the claim that the hESC-RPE patch has no part in our results it would require a study showing similar efficacy without the preservation of RPE after the submacular surgery. To our knowledge, there is no such demonstration in the literature.

Finally, another limitation is the absence of a control group with which our results could compare. I acknowledge that this lack makes it impossible to *prove* that the observed improvement is certainly attributed to the transplant. The severity of the baseline condition, with such catastrophic and variable events as the submacular haemorrhage and scarring in both subjects, would anyway limit the possibility to define a group with similar enough characteristics to allow a safe comparison based only on receiving or not the transplant. In addition this was an innovative and experimental approach, whose primary outcome was the safety of the transplantation, which we managed to support without the need of controls. Finally, a coarse internal comparison was attempted with the subjects' fellow eye, which also had neovascular AMD, but without the acute deterioration from a large submacular haemorrhage.

7.7. Implications for practice

Although this is a preliminary study that included only two cases, its possible future impact on the everyday practice can expand in a major scale. AMD is among the most common causes of irreversible blindness and especially in the aging population of the developed world, it is expected to affect millions of people. Previous strategies of autologous RPE transplantation were unable to expand their application to a level that could cover the demand, in terms of patient's volume. Our hESC-RPE is manufactured outside the body, comes from a single semi-immortalised cell source, without a "harvesting" step and thus it can constitute a potentially continuous flow of transplantation material. Moving away from the "harvesting" techniques also allows us to simplify the surgical procedure and reduce the risk of complications. Furthermore, we provide good indications that the integration and survival of such transplants can be supported for the long-term with only local immunosuppression. This may expand its delivery in cases where systemic immunosuppression has a high risk or is contra-indicated.

Our suggested approach, of a bioengineered transplant overcomes availability problems that limit other transplantation therapies, such as the corneal grafts. Our hESC-RPE can be produced and stored in large volumes relative to the incidence of the target disease. In addition, our surgical technique and the purpose-designed introducer, where the patch can be preloaded in a folded form that requires smaller incisions for its delivery, can resemble the most broadly used surgical paradigm in medical surgery, the intraocular lens implantation after cataract removal. I believe that the extension of this work to a phase III study will lead to a paradigm shift for the management of advanced AMD.

Another implication of this study in the current practice is that it shows that a properly regulated trial can be adequately safe for the patients, even if it belongs in an innovative and "unmapped" field such as the stem cell transplantation. This has acquired a major importance after the relatively recent

reports of devastating complications from unregulated stem cell-derived "therapies", in private clinics. The open communication of our favourable results balances the negative publicity that these sporadic cases brought to this field of research and can encourage both researchers to continue working on such approaches, and the patients to stay away from poorly regulated, commercially driven and over-promising "therapies" and to encourage them to participate in well regulated trials.

7.8. Implications for research

By the time we communicated the first year outcomes of our study the only available relevant data were from the ACT trial of a cell suspension and from the RIKEN trial of a cell sheet. Since then, numerous *in-human* studies have been registered, using hESC, iPSC, and retinal progenitor cells (RPC), against the most common retinal degenerative diseases and retinal dystrophies, which I have tabulated in Chapter 1. In terms of RPE cell derivation, most of the challenges have been identified and various research teams around the worlds have produced their own transplants and some are in the process of trialling them in humans. Our study provides a promising strategy for both the hESC-RPE transplant production and its surgical delivery. However, many questions remain to be answered with future research.

First of all, larger cohorts of patients are required to consolidate the results. The safety signals we showed are good, but they do not constitute a *proof*, until more subjects received the patch. Secondly, the question about a subclinical transplant rejection and thus about the appropriate immunomodulation is still to be answered. The role that the inflammatory cells, such as macrophages, and their migration and activation play in the observed post-transplantation phenomena (such as the pigmentation extension) is still to be studied. Future trials should be able to compare local versus systemic immunosuppression, as well as different regimens that will include steroids and

non-steroidal agents, that have gained significant ground in the management of ocular inflammations. Thirdly, we have to investigate further how these experimental treatments compare with more “conventional” approaches. At present, there is no consensus on the management of severe neovascular AMD with subretinal haemorrhages or RPE tears and all available data come from small, non-randomised case series with different baseline characteristics. Even if the catastrophic and variable course of such conditions makes it very difficult to organise randomised, controlled studies, we still need to define the success of the “conventional” approaches, in order to make safe comparisons with the experimental ones.

Following a more definite conclusion on the safety, our study and other similar ones have to proceed to phase III clinical trials to examine their efficacy and their value in the everyday clinical practice. It’s worth mentioning here that the continuous development in the ophthalmic imaging technology offers a huge assistance in improving the way we document our results. The lack of histology is a limitation well acknowledged and one that is not expected to be resolved; however, technologies like the OCT and the AO imaging keep increasing their achieved definition and are expected to approach “histological” levels in the future. This may be a way to make safer observations about the behaviour and fate of the implanted cells in future trials.

Moving forward, as RPE replacement becomes more standardised, our regenerative strategies should expand in order to include other types of macular degeneration, such as the geographic atrophy and other conditions in which the choroid and the photoreceptors have been affected or are primarily targeted. For example, a layer of “choriocapillaris-like” blood vessels that can be attached in the outer side of the hESC-RPE-BM patch, so as to enhance its blood perfusion and secure the transplant-host integration; or the derivation and delivery of photoreceptors’ precursor to replace their loss and restore vision. The latter brings up even more challenges than the RPE replacement. Stem cell-derived

3D cultures of full thickness retina patches and their experimental delivery in animal models has already been attempted, as well as derivation and implantation of RPCs, PR precursors and neuronal progenitors that are expected to differentiate into photoreceptors in the subretinal environment. However, the integration of these cells in the host's neural tissue and the required axons' regeneration and "rewiring" into the host's visual pathway are challenges that will take years of research to overcome.

Finally, our study provides valuable information on the field of biocompatible materials and suggests a surgical technique and equipment for the delivery of the hESC-RPE-BM. For the former, we suggest the use of a porous polyethylene terephthalate (PET) membrane, as a substrate for the seeding of the hESC-RPE cells. We found that this membrane provides adequate structural support without evident signs of compromised perfusion or substance exchange between the cells and the extracellular environment or the choroid circulation. Other studies are trying different substrate materials or rely on the extracellular matrix secreted by the implanted cells, to play the role of a basement membrane. The relevant data in humans are still very early and the cases are too few to draw definite guidelines, and these bioengineering questions are open for further studies.

For the surgical technique and equipment, we used the standard and broadly applicable pars-plana vitrectomy and we suggest a purpose-designed introducer that can deliver the transplant in a relatively atraumatic and also intuitive, for the average vitreo-retinal surgeon, way. Our technique appeared safe and efficient in our two cases, but still there is space for improvement and optimisation of the delivery. Current and future research on robotics engineering and on multimodal image-guided surgical applications is expected to offer significant help in optimising the delivery of such therapies. The limitation of the human skills can be overcome by robotic-assisted surgery, so as these therapies to become safer, more efficient, more reproducible, and accessible to a broader range of surgeons, for the large volumes of patients that need them.

7.9. Conclusion

The work presented in this Thesis provides evidence of feasibility, safety and efficacy of submacular transplantation of hESC-derived RPE on a synthetic basement membrane, as a potential treatment for severe neovascular AMD. It shows that it is possible to overcome the bioengineering challenges of cellular differentiation as well as the surgical challenges of delivery of the therapeutic cells in their physiologic form within the context of disease, and to achieve functional recovery maintained for at least two years. These findings support the notion that pluripotent cell-based tissue transplantation is a potentially powerful treatment strategy for currently untreatable neuro-degenerative diseases, as well as for other conditions, which manifest with irreversible cell loss.

Additionally, this work indicates that local immunosuppression may be adequate for the long-term survival and function of the transplanted cells, in cases of closed-system target organs, such as the eye. This challenges the general belief that systemic immunosuppression is necessary to minimize the risk of rejection and maintain the results for a prolonged period. In the future, detailed information about cell survival and behaviour, and the role of immune modulation will become more critical in progressing the field. The two patients will remain under regular follow-up for at least 5 years, in order to support further the long-term safety, especially in terms of tumorigenicity. More patients are also to be recruited in this phase and potentially continue with a phase III trial in the near future.

My thesis represents a step forward on the route to cell replacement therapy, becoming a reality as a strategy in regenerative medicine. The two years of my study may represent a small advancement, however, this project is a part of a larger, decades-long scientific effort to discover alternative tissue sources and transplant delivery strategies to treat AMD. The body of work that my thesis forms part of, is one of the first worldwide to demonstrate visual recovery following a stem cell derived transplantation therapy for a retinal

degeneration. I strongly believe that our results will be useful to a broad spectrum of the scientific community and across many subspecialties of medicine. Therefore, I feel that being a part of this effort, I have had the invaluable opportunity to be a part of an important period in the history of regenerative medicine.

Bibliography

Aisenbrey, S. (2007). Long-term follow-up of macular translocation with 360 degrees retinotomy for exudative age-related macular degeneration. - PubMed - NCBI. *Archives of Ophthalmology (Chicago, Ill. : 1960)*, *125*(10), 1367–1372. http://doi.org/10.1001/archopht.125.10.1367

Aisenbrey, S., Bartz-Schmidt, K. U., Walter, P., Hilgers, R.-D., Ayertey, H., Szurman, P., & Thumann, G. (2007). Long-term Follow-up of Macular Translocation With 360° Retinotomy for Exudative Age-Related Macular Degeneration. *Archives of Ophthalmology (Chicago, Ill. : 1960)*, *125*(10), 1397–1372.

Algvere, P. V., Berglin, L., Gouras, P., & Sheng, Y. (1994). Transplantation of fetal retinal pigment epithelium in age-related macular degeneration with subfoveal neovascularization. *Graefe's Archive for Clinical and Experimental Ophthalmology = Albrecht Von Graefes Archiv Für Klinische Und Experimentelle Ophthalmologie*, *232*(12), 707–716.

Algvere, P. V., Gouras, P., & Kopp, E. D. (1999). Long-term outcome of RPE allografts in non-immunosuppressed patients with AMD. *European Journal of Ophthalmology*, *9*(3), 217–230.

Arias L, & J, M. (2010). Transconjunctival sutureless vitrectomy with tissue plasminogen activator, gas and intravitreal bevacizumab in the management of predominantly hemorrhagic age-related macular degeneration. *Clinical Ophthalmology*, *4*, 67–62.

Arnhold, S., Klein, H., Semkova, I., Addicks, K., & Schraermeyer, U. (2004). Neurally Selected Embryonic Stem Cells Induce Tumor Formation after Long-Term Survival following Engraftment into the Subretinal Space. *Investigative Ophthalmology & Visual Science*, *45*(12), 4251. http://doi.org/10.1167/iovs.03-1108

Avery, R. L., Fekrat, S., Hawkins, B. S., & Bressler, N. M. (1996). Natural History Of Subfoveal Subretinal Hemorrhage In Age-Related Macular Degeneration. *Retina*, *16*(3), 183–189.

Bates, N. M., Tian, J., Smiddy, W. E., Lee, W.-H., Somfai, G. M., Feuer, W. J., et al. (2018). Relationship between the morphology of the foveal avascular zone, retinal structure, and macular circulation in patients with diabetes mellitus. *Scientific Reports*, 1–12. http://doi.org/10.1038/s41598-018-23604-y

Bennett, S. R., Folk, J. C., Blodi, C. F., & Klugman, M. (1990). Factors prognostic of visual outcome in patients with subretinal hemorrhage. *American Journal of Ophthalmology*, *109*(1), 33–37.

Bikun Xian, B. H. (2015). The immune response of stem cells in subretinal transplantation. *Stem Cell Research & Therapy*, *6*(1), 134. http://doi.org/10.1186/s13287-015-0167-1

Binder, S. (2011). Scaffolds for retinal pigment epithelium (RPE) replacement therapy. *The British Journal of Ophthalmology*, *95*(4), 441–442. http://doi.org/10.1136/bjo.2009.171926

Binder, S., Krebs, I., Hilgers, R.-D., Abri, A., Stolba, U., Assadoulina, A., et al. (2004). Outcome of Transplantation of Autologous Retinal Pigment

Epithelium in Age-Related Macular Degeneration: A Prospective Trial. *Investigative Ophthalmology & Visual Science*, *45*(11), 4151–4160. http://doi.org/10.1167/iovs.04-0118

Binder, S., Stolba, U., Krebs, I., Kellner, L., Jahn, C., Feichtinger, H., et al. (2002). Transplantation of autologous retinal pigment epithelium in eyes with foveal neovascularization resulting from age-related macular degeneration: a pilot study. *American Journal of Ophthalmology*, *133*(2), 215–225. http://doi.org/10.1016/S0002-9394(01)01373-3

Bird, A. C. (2013). Chapter 64 - Pathogenetic Mechanisms in Age-Related Macular Degeneration. *Retina* (Fifth Edition, pp. 1145–1149). Elsevier Inc. http://doi.org/10.1016/B978-1-4557-0737-9.00064-3

Bloom, S. M., & Singal, I. P. (2011). The outer Bruch membrane layer: a previously undescribed spectral-domain optical coherence tomography finding. *Retina (Philadelphia, Pa.)*, *31*(2), 316–323. http://doi.org/10.1097/IAE.0b013e3181ed8c9a

Boulton, M. E. (2014). Studying melanin and lipofuscin in RPE cell culture models. *Experimental Eye Research*, *126*, 61–67. http://doi.org/10.1016/j.exer.2014.01.016

Boulton, M., McKechnie, N. M., Breda, J., Bayly, M., & Marshall, J. (1989). The formation of autofluorescent granules in cultured human RPE. *Investigative Ophthalmology & Visual Science*, *30*(1), 82–89.

Bressler, N. M., Bressler, S. B., Childs, A. L., Haller, J. A., Hawkins, B. S., Lewis, H., et al. (2004). Surgery for hemorrhagic choroidal neovascular lesions of age-related macular degeneration: ophthalmic findings: SST report no. 13. - PubMed - NCBI. *Ophthalmology*, *111*(11), 1993–2006.e1. http://doi.org/10.1016/j.ophtha.2004.07.023

Bressler, N. M., Bressler, S. B., Hawkins, B. S., Marsh, M. J., Sternberg, P., Thomas, M. A., Submacular Surgery Trials Pilot Study Investigators. (2000). Submacular surgery trials randomized pilot trial of laser photocoagulation versus surgery for recurrent choroidal neovascularization secondary to age-related macular degeneration: I. Ophthalmic outcomes submacular surgery trials pilot study report number 1. *American Journal of Ophthalmology*, *130*(4), 387–407.

Cahill, M. T., Stinnett, S. S., Banks, A. D., Freedman, S. F., & Toth, C. A. (2005). Quality of life after macular translocation with 360 degrees peripheral retinectomy for age-related macular degeneration. *Ophthalmology*, *112*(1), 144–151. http://doi.org/10.1016/j.ophtha.2004.06.035

Cakir, M., Cekiç, O., & Yilmaz, O. F. (2010). Pneumatic displacement of acute submacular hemorrhage with and without the use of tissue plasminogen activator. *European Journal of Ophthalmology*, *20*(3), 565–571.

Campochiaro, P. A., Jerdon, J. A., & Glaser, B. M. (1986). The extracellular matrix of human retinal pigment epithelial cells in vivo and its synthesis in vitro. *Investigative Ophthalmology & Visual Science*, *27*(11), 1615–1621.

Carr, A.-J. F., Smart, M. J. K., Ramsden, C. M., Powner, M. B., da Cruz, L., & Coffey, P. J. (2013). Development of human embryonic stem cell therapies for age-related macular degeneration. *Trends in Neurosciences*, *36*(7), 385–

395. http://doi.org/10.1016/j.tins.2013.03.006
Carr, A.-J., Vugler, A. A., Hikita, S. T., Lawrence, J. M., Gias, C., Chen, L. L., et al. (2009a). Protective Effects of Human iPS-Derived Retinal Pigment Epithelium Cell Transplantation in the Retinal Dystrophic Rat. *PLoS ONE*, *4*(12), e8152. http://doi.org/10.1371/journal.pone.0008152
Carr, A.-J., Vugler, A., Lawrence, J., Li Chen, L., Ahmado, A., Chen, F. K., et al. (2009b). Molecular characterization and functional analysis of phagocytosis by human embryonic stem cell-derived RPE cells using a novel human retinal assay.
Chang, M. A., Do, D. V., Bressler, S. B., Cassard, S. D., Gower, E. W., & Bressler, N. M. (2010). Prospective one-year study of ranibizumab for predominantly hemorrhagic choroidal neovascular lesions in age-related macular degeneration. *Retina*, *30*(8), 1171–1176. http://doi.org/10.1097/IAE.0b013e3181dd6d8a
Chawla, S., Misra, V., & Khemchandani, M. (2009). Pneumatic displacement and intravitreal bevacizumab: A new approach for management of submacular hemorrhage in choroidal neovascular membrane. *Indian Journal of Ophthalmology*, *57*(2), 155. http://doi.org/10.4103/0301-4738.45511
Chen, F. K., Uppal, G. S., MacLaren R. E., Coffey, P. J., Rubin, G. S., Tufail A., Aylward G. W., da Cruz, L. (2009). Long-term visual and microperimetry outcomes following autologous retinal pigment epithelium choroid graft for neovascular age-related macular degeneration. *Clinical & Experimental Ophthalmology, (37)3, 275-85*.
Chen, F. K., Patel, P. J., Uppal, G. S., Rubin, G. S., Coffey, P. J., Aylward, G. W., & da Cruz, L. (2009). A Comparison of Macular Translocation with Patch Graft in Neovascular Age-Related Macular Degeneration. *Investigative Ophthalmology & Visual Science*, *50*(4), 1848–1855. http://doi.org/10.1167/iovs.08-2845
Chen, F. K., Patel, P. J., Uppal, G. S., Tufail, A., Coffey, P. J., & da Cruz, L. (2010). Long-term outcomes following full macular translocation surgery in neovascular age-related macular degeneration. *British Journal of Ophthalmology*, *94*(10), 1337–1343. http://doi.org/10.1136/bjo.2009.172593
Chen, F. K., Uppal, G. S., Rubin, G. S., Webster, A. R., Coffey, P. J., & da Cruz, L. (2008). Evidence of Retinal Function Using Microperimetry following Autologous Retinal Pigment Epithelium-Choroid Graft in Macular Dystrophy. *Investigative Ophthalmology & Visual Science*, *49*(7), 3143–8. http://doi.org/10.1167/iovs.07-1648
Cherepanoff, S., McMenamin, P., Gillies, M. C., Kettle, E., & Sarks, S. H. (2010). Bruch's membrane and choroidal macrophages in early and advanced age-related macular degeneration. *British Journal of Ophthalmology*, *94*(7), 918–925. http://doi.org/10.1136/bjo.2009.165563
Chieh, J. J., Stinnett, S. S., & Toth, C. A. (2008). Central and Pericentral Retinal Sensitivity After Macular Translocation Surgery. *Retina*, *28*(10), 1522–1529. http://doi.org/10.1097/IAE.0b013e318186c634
Chinnery, H. R., McMenamin, P. G., & Dando, S. J. (2017). Macrophage physiology in the eye. *Pflügers Archiv - European Journal of Physiology*,

469(3-4), 1–15. http://doi.org/10.1007/s00424-017-1947-5

Crafoord, S., Algvere, P. V., Seregard, S., & Kopp, E. D. (1999). Long-term outcome of RPE allografts to the subretinal space of rabbits. *Acta Ophthalmologica Scandinavica*, *77*(3), 247–254. http://doi.org/10.1034/j.1600-0420.1999.770301.x

Curcio, C. A., Zanzottera, E. C., Ach, T., Balaratnasingam, C., & Freund, K. B. (2017). Activated Retinal Pigment Epithelium, an Optical Coherence Tomography Biomarker for Progression in Age-Related Macular Degeneration. *Investigative Ophthalmology & Visual Science*, *58*(6), 1–16. http://doi.org/10.1167/iovs.17-21872

D'Cruz, P. M., Yasumura, D., Weir, J., Matthes, M. T., Abderrahim, H., LaVail, M. M., & Vollrath, D. (2000). Mutation of the receptor tyrosine kinase gene Mertk in the retinal dystrophic RCS rat. *Human Molecular Genetics*, *9*(4), 645–651.

da Cruz, L., Chen, F. K., Ahmado, A., Greenwood, J., & Coffey, P. (2007). RPE transplantation and its role in retinal disease. *Progress in Retinal and Eye Research*, *26*(6), 598–635. http://doi.org/10.1016/j.preteyeres.2007.07.001

da Cruz, L., Fynes, K., Georgiadis, O., Kerby, J., Luo, Y. H., Ahmado, A., et al. (2018). Phase 1 clinical study of an embryonic stem cell–derived retinal pigment epithelium patch in age-related macular degeneration. *Nature Biotechnology*, *15*, 283. http://doi.org/10.1038/nbt.4114

Daley, G. Q. (2017). Polar Extremes in the Clinical Use of Stem Cells. - PubMed - NCBI. *The New England Journal of Medicine*, *376*(11), 1075–1077. http://doi.org/10.1056/NEJMe1701379

de Jong, P. T. V. M. (2006). Age-related macular degeneration. *The New England Journal of Medicine*, *355*(14), 1474–1485. http://doi.org/10.1056/NEJMra062326

Delori, F. C., Dorey, C. K., & Staurenghi, G. (1995). In vivo fluorescence of the ocular fundus exhibits retinal pigment epithelium lipofuscin characteristics. *… & Visual Science*.

Delori, F. C., Goger, D. G., & Dorey, C. K. (2001). Age-related accumulation and spatial distribution of lipofuscin in RPE of normal subjects. *Investigative Ophthalmology & Visual Science*, *42*(8), 1855–1866.

Diniz, B., Thomas, P., Thomas, B., Ribeiro, R., Hu, Y., Brant, R., et al. (2013). Subretinal Implantation of Retinal Pigment Epithelial Cells Derived From Human Embryonic Stem Cells: Improved Survival When Implanted as a MonolayerSubretinal Implantation of RPE Cells From hESC. *Investigative Ophthalmology & Visual Science*, *54*(7), 5087–5096. http://doi.org/10.1167/iovs.12-11239

Dubis, A. M., Hansen, B. R., Cooper, R. F., Beringer, J., Dubra, A., & Carroll, J. (2012). Relationship between the Foveal Avascular Zone and Foveal Pit Morphology. *Investigative Ophthalmology & Visual Science*, *53*(3), 1628–9. http://doi.org/10.1167/iovs.11-8488

Falkner, C. I., Leitich, H., Frommlet, F., Bauer, P., & Binder, S. (2006). The end of submacular surgery for age-related macular degeneration? A meta-analysis. *Graefe's Archive for Clinical and Experimental Ophthalmology = Albrecht Von Graefes Archiv Für Klinische Und Experimentelle*

Ophthalmologie, *245*(4), 490–501. http://doi.org/10.1007/s00417-005-0184-3
Fletcher, D. C., & Schuchard, R. A. (2006). Visual Function in Patients With Choroidal Neovascularization Resulting From Age-Related Macular Degeneration: The Importance of Looking Beyond Visual Acuity. *Optometry and Vision Science : Official Publication of the American Academy of Optometry*, *83*(3), 178–189. http://doi.org/10.1097/01.opx.0000204510.08026.7f
Frayer, W. C. (1966). Reactivity of the retinal pigment epithelium: an experimental and histopathologic study. *Transactions of the American Ophtalmological Society*, *64*, 586–643.
Fujii, G. Y., de Juan, E., Humayun, M. S., & Sunness, J. S. (2003). Characteristics of visual loss by scanning laser ophthalmoscope microperimetry in eyes with subfoveal choroidal neovascularization secondary to age-related macular …. *American Journal of …*. http://doi.org/10.1016/S0002-9394(03)00663-9
Fujikawa, M., Sawada, O., Miyake, T., Kakinoki, M., Sawada, T., Kawamura, H., et al. (2013). Comparison of pneumatic displacement for submacular hemorrhages with gas alone and gas plus tissue plasminogen activator. *Retina*, *33*(9), 1908–1914. http://doi.org/10.1097/IAE.0b013e318287d99d
Gangnon, R. E., Lee, K. E., Klein, B. E. K., Iyengar, S. K., Sivakumaran, T. A., & Klein, R. (2015). Severity of Age-Related Macular Degeneration in 1 Eye and the Incidence and Progression of Age-Related Macular Degeneration in the Fellow Eye. *JAMA Ophthalmology*, *133*(2), 125–14. http://doi.org/10.1001/jamaophthalmol.2014.4252
Georgiadis, O., da Cruz, L., & Coffey, P. (2017). Stem Cell-Derived RPE Transplantation: The Feasibility and Advantages of Delivery as Monolayers. In *Cellular Therapies for Retinal Disease* (Vol. 85, pp. 19–31). Cham: Springer, Cham. http://doi.org/10.1007/978-3-319-49479-1_2
Glatt, H., & Machemer, R. (1982). Experimental subretinal hemorrhage in rabbits. *American Journal of Ophthalmology*, *94*(6), 762–773.
Gopalakrishan, M., Giridhar, A., Bhat, S., Saikumar, S. J., Elias, A., & N, S. (2007). Pneumatic displacement of submacular hemorrhage: safety, efficacy, and patient selection. *Retina*, *27*(3), 329–334. http://doi.org/10.1097/01.iae.0000231544.43093.40
Gullapalli, V. K., Sugino, I. K., Van Patten, Y., Shah, S., & Zarbin, M. A. (2005). Impaired RPE survival on aged submacular human Bruch's membrane. *Experimental Eye Research*, *80*(2), 235–248. http://doi.org/10.1016/j.exer.2004.09.006
Guthoff, R., Guthoff, T., Meigen, T., & Goebel, W. (2011). Intravitreous injection of bevacizumab, tissue plasminogen activator, and gas in the treatment of submacular hemorrhage in age-related macular dege... - PubMed - NCBI. *Retina*, *31*(1), 36–40. http://doi.org/10.1097/IAE.0b013e3181e37884
Handwerger, B. A., Blodi, B. A., Chandra, S. R., Olsen, T. W., & Stevens, T. S. (2001). Treatment of submacular hemorrhage with low-dose intravitreal tissue plasminogen activator injection and pneumatic displacement. *Archives of Ophthalmology (Chicago, Ill. : 1960)*, *119*(1), 28–32.

Hashemi, H., Khabazkhoob, M., Jafarzadehpur, E., Emamian, M. H., Shariati, M., & Fotouhi, A. (2012). Contrast Sensitivity Evaluation in a Population-Based Study in Shahroud, Iran. *Ophthalmology*, *119*(3), 541–546. http://doi.org/10.1016/j.ophtha.2011.08.030

Hassan, A. S., Johnson, M. W., Schneiderman, T. E., Regillo, C. D., Tornambe, P. E., Poliner, L. S., et al. (1999). Management of submacular hemorrhage with intravitreous tissue plasminogen activator injection and pneumatic displacement. - PubMed - NCBI. *Ophthalmology*, *106*(10), 1900–1907. http://doi.org/10.1016/S0161-6420(99)90399-8

Haupert, C. L., McCuen, B. W., Jaffe, G. J., Steuer, E. R., Cox, T. A., Toth, C. A., et al. (2001). Pars plana vitrectomy, subretinal injection of tissue plasminogen activator, and fluid-gas exchange for displacement of thick submacular hemorrhage in age-related macular degeneration. *American Journal of Ophthalmology*, *131*(2), 208–215.

Hentze, H., Soong, P. L., Wang, S. T., Phillips, B. W., Putti, T. C., & Dunn, N. R. (2009). Teratoma formation by human embryonic stem cells: Evaluation of essential parameters for future safety studies. *Stem Cell Research*, *2*(3), 198–210. http://doi.org/10.1016/j.scr.2009.02.002

Hesse, L., Schroeder, B., Heller, G., & Kroll, P. (2000). Quantitative effect of intravitreally injected tissue plasminogen activator and gas on subretinal hemorrhage. *Retina*, *20*(5), 500–505. http://doi.org/10.1097/00006982-200005000-00011

Ho, J., Witkin, A. J., Liu, J., Chen, Y., Fujimoto, J. G., Schuman, J. S., & Duker, J. S. (2011). Documentation of Intraretinal Retinal Pigment Epithelium Migration via High-Speed Ultrahigh-Resolution Optical Coherence Tomography. *Ophthalmology*, *118*(4), 687–693. http://doi.org/10.1016/j.ophtha.2010.08.010

Hoffman, L. M., & Carpenter, M. K. (2005). Characterization and culture of human embryonic stem cells. *Nature Biotechnology*, *23*(6), 699–708. http://doi.org/10.1038/nbt1102

Holz, F. G., Bellman, C., Staudt, S., Schütt, F., & Völcker, H. E. (2001). Fundus autofluorescence and development of geographic atrophy in age-related macular degeneration. *Investigative Ophthalmology & Visual Science*, *42*(5), 1051–1056.

Holz, F. G., Schmitz-Valckenberg, S., Spaide, R. F., & Bird, A. C. (2007). Atlas of Fundus Autofluorescence Imaging. Springer Science & Business Media.

Hsu, J. K., Thomas, M. A., Ibanez, H., & Green, W. R. (1995). Clinicopathologic studies of an eye after submacular membranectomy for choroidal neovascularization. *Retina*, *15*(1), 43–52.

Hynes, S. R., & Lavik, E. B. (2010). A tissue-engineered approach towards retinal repair: Scaffolds for cell transplantation to the subretinal space. *Graefe's Archive for Clinical and Experimental Ophthalmology = Albrecht Von Graefes Archiv Für Klinische Und Experimentelle Ophthalmologie*, *248*(6), 763–778. http://doi.org/10.1007/s00417-009-1263-7

Iacono, P., Parodi, M. B., Introini, U., La Spina, C., Varano, M., & Bandello, F. (2014). Intravitreal ranibizumab for choroidal neovascularization with large

submacular hemorrhage in age-related macular degeneration. - PubMed - NCBI. *Retina*, *34*(2), 281–287. http://doi.org/10.1097/IAE.0b013e3182979e33
International Stem Cell Initiative, Adewumi, O., Aflatoonian, B., Ahrlund-Richter, L., Amit, M., Andrews, P. W., et al. (2007). Characterization of human embryonic stem cell lines by the International Stem Cell Initiative. *Nature Biotechnology*, *25*(7), 803–816. http://doi.org/10.1038/nbt1318
Ito, T., Nakano, M., Yamamoto, Y., Hiramitsu, T., & Mizuno, Y. (1995). Hemoglobin-induced lipid peroxidation in the retina: a possible mechanism for macular degeneration. - PubMed - NCBI. *Archives of Biochemistry and Biophysics*, *316*(2), 864–872.
Jager, R. D., Mieler, W. F., & Miller, J. W. (2008). Age-related macular degeneration. - PubMed - NCBI. *The New England Journal of Medicine*, *358*(24), 2606–2617.
Jampel, H. D., Schachat, A. P., Conway, B., Shaver, R. P., Coston, T. O., Isernhagen, R., & Green, W. R. (1986). Retinal Pigment Epithelial Hyperplasia Assuming Tumor-like Proportions. *Retina*, *6*(2), 105–112.
Johnson, R. N., Fu, A. D., McDonald, H. R., Jumper, J. M., Ai, E., Cunningham, E. T., Jr., & Lujan, B. J. (2013). Chapter 1 - Fluorescein Angiography: Basic Principles and Interpretation. *Retina* (Fifth Edition, pp. 2–50.e1). Elsevier Inc. http://doi.org/10.1016/B978-1-4557-0737-9.00001-1
Kamao, H., Mandai, M., Okamoto, S., Sakai, N., Suga, A., Sugita, S., et al. (2014). Characterization of human induced pluripotent stem cell-derived retinal pigment epithelium cell sheets aiming for clinical application. - PubMed - NCBI. *Stem Cell Reports*, *2*(2), 205–218. http://doi.org/10.1016/j.stemcr.2013.12.007
Karampelas, M., Sim, D. A., Keane, P. A., Papastefanou, V. P., Sadda, S. R., Tufail, A., & Dowler, J. (2013). Evaluation of retinal pigment epithelium-Bruch's membrane complex thickness in dry age-related macular degeneration using optical coherence tomography. *The British Journal of Ophthalmology*, *97*(10), 1256–1261. http://doi.org/10.1136/bjophthalmol-2013-303219
Kashani, A. H., Lebkowski, J. S., Rahhal, F. M., Avery, R. L., Salehi-Had, H., Dang, W., et al. (2018). A bioengineered retinal pigment epithelial monolayer for advanced, dry age-related macular degeneration. *Science Translational Medicine*, *10*(435), eaao4097. http://doi.org/10.1126/scitranslmed.aao4097
Katamay, R., & Nussenblatt, R. B. (2013). Chapter 27 - Blood–Retinal Barrier, Immune Privilege, and Autoimmunity. *Retina* (Fifth Edition, pp. 579–589). Elsevier Inc. http://doi.org/10.1016/B978-1-4557-0737-9.00027-8
Kawasaki, H., Suemori, H., Mizuseki, K., Watanabe, K., Urano, F., Ichinose, H., et al. (2002). Generation of dopaminergic neurons and pigmented epithelia from primate ES cells by stromal cell-derived inducing activity. *Proceedings of the National Academy of Sciences*, *99*(3), 1580–1585. http://doi.org/10.1073/pnas.032662199
Keilhauer, C. N., & Delori, F. O. C. (2006). Near-infrared autofluorescence imaging of the fundus: visualization of ocular melanin. - PubMed - NCBI. *Investigative Ophthalmology & Visual Science*, *47*(8), 3556–3564.

http://doi.org/10.1167/iovs.06-0122
Kevany, B. M., & Palczewski, K. (2010). Phagocytosis of Retinal Rod and Cone Photoreceptors. *Physiology*, *25*(1), 8–15. http://doi.org/10.1152/physiol.00038.2009
Khanna, S., Komati, R., Eichenbaum, D. A., Hariprasad, I., Ciulla, T. A., & Hariprasad, S. M. (2019). Current and upcoming anti-VEGF therapies and dosing strategies for the treatment of neovascular AMD: a comparative review. *BMJ Open Ophthalmology*, *4*(1), e000398–8. http://doi.org/10.1136/bmjophth-2019-000398
Kitahashi, M., Sakurai, M., Yokouchi, H., Kubota-Taniai, M., Mitamura, Y., Yamamoto, S., & Baba, T. (2014). Pneumatic displacement with intravitreal bevacizumab for massive submacular hemorrhage due to polypoidal choroidal vasculopathy. *Clinical Ophthalmology*, 485. http://doi.org/10.2147/OPTH.S55413
Klimanskaya, I., Chung, Y., Becker, S., Lu, S.-J., & Lanza, R. (2006). Human embryonic stem cell lines derived from single blastomeres. *Nature*, *444*(7118), 481–485. http://doi.org/10.1038/nature05142
Klimanskaya, I., Hipp, J., Rezai, K. A., West, M., Atala, A., & Lanza, R. (2004). Derivation and Comparative Assessment of Retinal Pigment Epithelium from Human Embryonic Stem Cells Using Transcriptomics. *Cloning and Stem Cells*, *6*(3), 217–245. http://doi.org/10.1089/clo.2004.6.217
Ko F, Foster PJ, Strouthidis NG, Shweikh Y, Yang Q, Reisman CA, Muthy ZA, Chakravarthy U, Lotery AJ, Keane PA, Tufail A, Grossi CM, Patel PJ (2017). UK Biobank Eye & Vision Consortium. Associations with Retinal Pigment Epithelium Thickness Measures in a Large Cohort: Results from the UK Biobank. Ophthalmology. 2017 Jan;124(1):105-117. doi: 10.1016/j.ophtha.2016.07.033. Epub 2016 Oct 6. PMID: 27720551.
Kuriyan, A. E., Albini, T. A., & Flynn, H. W., Jr. (2017a). EDITORIAL The Growing "'Stem Cell Clinic'" Problem. *American Journal of Ophthalmology*, *177*, xix–xx. http://doi.org/10.1016/j.ajo.2017.03.030
Kuriyan, A. E., Albini, T. A., Townsend, J. H., Rodriguez, M., Pandya, H. K., Leonard, R. E., II, et al. (2017b). Vision Loss after Intravitreal Injection of Autologous "Stem Cells" for AMD. *The New England Journal of Medicine*, *376*(11), 1047–1053. http://doi.org/10.1056/NEJMoa1609583
Leat, S. J., & Woodhouse, J. M. (1993). Reading performance with low vision aids: relationship with contrast sensitivity. *Ophthalmic and Physiological Optics*, *13*(1), 9–16. http://doi.org/10.1111/j.1475-1313.1993.tb00420.x
Leschey, K. H., Hines, J., Singer, J. H., Hackett, S. F., & Campochiaro, P. A. (1991). Inhibition of growth factor effects in retinal pigment epithelial cells. *Investigative Ophthalmology & Visual Science*, *32*(6), 1770–1778.
Lewis, H., & s, V. M. (1997). Tissue plasminogen activator-assisted surgical excision of subfoveal choroidal neovascularization in age-related macular degeneration: a randomized... - PubMed - NCBI. *Ophthalmology*, *104*(11), 1847–1851.
Li, L. X., & Turner, J. E. (1988). Inherited retinal dystrophy in the RCS rat: prevention of photoreceptor degeneration by pigment epithelial cell

transplantation. *Experimental Eye Research*, *47*(6), 911–917.
Lina, G., Xuemin, Q., Qinmei, W., & Lijun, S. (2015). Vision-related quality of life, metamorphopsia, and stereopsis after successful surgery for rhegmatogenous retinal detachment. *Eye*, *30*(1), 40–45. http://doi.org/10.1038/eye.2015.171
Liu, Y., Xu, H. W., Wang, L., Li, S. Y., Zhao, C. J., Hao, J., et al. (2018). Human embryonic stem cell-derived retinal pigment epithelium transplants as a potential treatment for wet age-related macular degeneration. *Cell Discovery*, *4*(1), 483. http://doi.org/10.1038/s41421-018-0053-y
Lopez, P. F., Yan, Q., Kohen, L., Rao, N. A., Spee, C., Black, J., & Oganesian, A. (1995). Retinal pigment epithelial wound healing in vivo. *Archives of Ophthalmology (Chicago, Ill. : 1960)*, *113*(11), 1437–1446.
Lopez, R., Gouras, P., Kjeldbye, H., Sullivan, B., Reppucci, V., Brittis, M., et al. (1989). Transplanted retinal pigment epithelium modifies the retinal degeneration in the RCS rat. *Investigative Ophthalmology & Visual Science*, *30*(3), 586–588.
Lu, B., Malcuit, C., Wang, S., Girman, S., Francis, P., Lemieux, L., et al. (2009). Long-term safety and function of RPE from human embryonic stem cells in preclinical models of macular degeneration. - PubMed - NCBI. *Stem Cells*, *27*(9), 2126–2135. http://doi.org/10.1002/stem.149
Lund, R. D., Adamson, P., Sauvé, Y., Keegan, D. J., Girman, S. V., Wang, S., et al. (2001). Subretinal transplantation of genetically modified human cell lines attenuates loss of visual function in dystrophic rats. *Proceedings of the National Academy of Sciences*, *98*(17), 9942–9947. http://doi.org/10.1073/pnas.171266298
Lund, R. D., Wang, S., Klimanskaya, I., Holmes, T., Ramos-Kelsey, R., Lu, B., et al. (2006). Human embryonic stem cell-derived cells rescue visual function in dystrophic RCS rats. *Cloning and Stem Cells*, *8*(3), 189–199. http://doi.org/10.1089/clo.2006.8.189
Lüke, C. (2001). Electrophysiological changes after 360° retinotomy and macular translocation for subfoveal choroidal neovascularisation in age related macular degeneration. *British Journal of Ophthalmology*, *85*(8), 928–932. http://doi.org/10.1136/bjo.85.8.928
Machemer, R., & Steinhorst, U. H. (1993). Retinal separation, retinotomy, and macular relocation II. A surgical approach for age-related macular degeneration? *Graefe's Archive for Clinical and Experimental Ophthalmology = Albrecht Von Graefes Archiv Für Klinische Und Experimentelle Ophthalmologie*, *231*(11), 635–641. http://doi.org/10.1007/BF00921957
MacLaren, R. E., Uppal, G. S., Balaggan, K. S., Tufail, A., Munro, P. M. G., Milliken, A. B., et al. (2007). Autologous Transplantation of the Retinal Pigment Epithelium and Choroid in the Treatment of Neovascular Age-Related Macular Degeneration. *Ophthalmology*, *114*(3), 561–570.e2. http://doi.org/10.1016/j.ophtha.2006.06.049
Majji, A. B., & de Juan, E. (2000). Retinal pigment epithelial autotransplantation: morphological changes in retina and choroid. *Graefe's Archive for Clinical and Experimental Ophthalmology = Albrecht Von Graefes Archiv Für*

Klinische Und Experimentelle Ophthalmologie, *238*(9), 779–791. http://doi.org/10.1007/s004170000132

Mandai, M., Watanabe, A., Kurimoto, Y., Hirami, Y., Morinaga, C., Daimon, T., et al. (2017). Autologous Induced Stem-Cell–Derived Retinal Cells for Macular Degeneration. *The New England Journal of Medicine*, *376*(11), 1038–1046. http://doi.org/10.1056/NEJMoa1608368

Marmor, M. F. (1986). Contrast sensitivity versus visual acuity in retinal disease. *British Journal of Ophthalmology*, 553–559.

Mathew, R., Pearce, E., & Sivaprasad, S. (2012). Determinants of Fixation in Eyes With Neovascular Age-Related Macular Degeneration Treated With Intravitreal Ranibizumab. *American Journal of Ophthalmology*, *153*(3), 490–496.e1. http://doi.org/10.1016/j.ajo.2011.08.034

McLeod, D. S., Bhutto, I., Edwards, M. M., Silver, R. E., Seddon, J. M., & Lutty, G. A. (2016). Distribution and Quantification of Choroidal Macrophages in Human Eyes With Age-Related Macular Degeneration. *Investigative Ophthalmology & Visual Science*, *57*(14), 5843–13. http://doi.org/10.1167/iovs.16-20049

Meyer, C. H., Scholl, H. P., Eter, N., Helb, H.-M., & Holz, F. G. (2008). Combined treatment of acute subretinal haemorrhages with intravitreal recombined tissue plasminogen activator, expansile gas and bevacizumab: a ret... - PubMed - NCBI. *Acta Ophthalmologica*, *86*(5), 490–494. http://doi.org/10.1111/j.1600-0420.2007.01125.x

Midena, E., & Pilotto, E. (2017). Microperimetry in age: related macular degeneration. *Eye*, *31*(7), 985–994. http://doi.org/10.1038/eye.2017.34

Miller, H., Miller, B., & Ryan, S. J. (1986). The role of retinal pigment epithelium in the involution of subretinal neovascularization. *Investigative Ophthalmology & Visual Science*, *27*(11), 1644–1652.

Monés, J., & Rubin, G. S. (2004). Contrast sensitivity as an outcome measure in patients with subfoveal choroidal neovascularisation due to age-related macular degeneration. *Eye*, *19*(11), 1142–1150. http://doi.org/10.1038/sj.eye.6701717

Muthiah, M. N., Gias, C., Chen, F. K., Zhong, J., McClelland, Z., Sallo, F. B., et al. (2014). Cone photoreceptor definition on adaptive optics retinal imaging. *The British Journal of Ophthalmology*, *98*(8), 1073–1079. http://doi.org/10.1136/bjophthalmol-2013-304615

Nicola K Cassels, B., John M Wild, P. D., Tom H Margrain, P., Victor Chong, M. F., & Jennifer H Acton, P. (2017). The use of microperimetry in assessing visual function in age-related macular degeneration. *Survey of Ophthalmology*, *63*(1), 1–40. http://doi.org/10.1016/j.survophthal.2017.05.007

Nirwan, R. S., Albini, T. A., Sridhar, J., Flynn, H. W., & Kuriyan, A. E. (2019). Assessing “cell therapy” clinics offering treatments of ocular conditions using direct-to-consumer marketing websites in the United States. *Ophthalmology*, *0*(0). http://doi.org/10.1016/j.ophtha.2019.03.019

Nourinia, R., Bonyadi, M. H. J., & Ahmadieh, H. (2010). Intravitreal Expansile Gas and Bevacizumab Injection for Submacular Hemorrhage Due to Neovascular Age-related Macular Degeneration. *Journal of Ophthalmic &*

Vision Research, *5*(3), 168–174.
Olivier, S., Chow D. R., Packo, K. H., Mathew W. McC., Awh C. C. (2004). Subretinal recombinant tissue plasminogen activator injection and pneumatic displacement of thick submacular hemorrhage in Age-Related macular degeneration. *Ophthalmology*, *111*(6), 1201–1208. http://doi.org/10.1016/j.ophtha.2003.10.020
Oswald, J., & Baranov, P. (2018). Regenerative medicine in the retina: from stem cells to cell replacement therapy. *Therapeutic Advances in Ophthalmology*, *10*(2079), 251584141877443–21. http://doi.org/10.1177/2515841418774433
Papavasileiou, E., Steel, D. H. W., Liazos, E., McHugh, D., & Jackson, T. L. (2013). Intravitreal tissue plasminogen activator, perfluoropropane (C3F8), and ranibizumab or photodynamic therapy for submacular hemorrhage secondary to ... - PubMed - NCBI. *Retina*, *33*(4), 846–853. http://doi.org/10.1097/IAE.0b013e318271f278
Patel, P. J., Chen, F. K., da Cruz, L., Rubin, G. S., & Tufail, A. (2011). Contrast Sensitivity Outcomes in the ABC Trial: A Randomized Trial of Bevacizumab for Neovascular Age-Related Macular Degeneration. *Investigative Ophthalmology & Visual Science*, *52*(6), 3089–5. http://doi.org/10.1167/iovs.10-6208
Pedersen, K. B., Sjølie, A. K., Vestergaard, A. H., Andréasson, S., & Møller, F. (2016). Fixation stability and implication for multifocal electroretinography in patients with neovascular age-related macular degeneration after anti-VEGF treatment. *Graefe's Archive for Clinical and Experimental Ophthalmology = Albrecht Von Graefes Archiv Für Klinische Und Experimentelle Ophthalmologie*, *254*(10), 1897–1908. http://doi.org/10.1007/s00417-016-3323-0
Pennington, B. O., & Clegg, D. O. (2016). Pluripotent Stem Cell-Based Therapies in Combination with Substrate for the Treatment of Age-Related Macular Degeneration. *Journal of Ocular Pharmacology and Therapeutics*, jop.2015.0153–11. http://doi.org/10.1089/jop.2015.0153
Peyman, G. A., Blinder, K. J., Paris, C. L., Alturki, W., Nelson, N. C., & Desai, U. (1991). A Technique for Retinal Pigment Epithelium Transplantation for Age-Related Macular Degeneration Secondary to Extensive Subfoveal Scarring. *Ophthalmic Surgery, Lasers and Imaging Retina*, *22*(2), 102–108. http://doi.org/10.3928/1542-8877-19910201-12
Piccolino, F. C., Borgia, L., Zinicola, E., Iester, M., & Torrielli, S. (1996). Pre-injection fluorescence in indocyanine green angiography. *Ophthalmology*, *103*(11), 1837–1845.
Ramsden, C. M., Powner, M. B., Carr, A. J. F., Smart, M. J. K., da Cruz, L., & Coffey, P. J. (2013). Stem cells in retinal regeneration: past, present and future. *Development*, *140*(12), 2576–2585. http://doi.org/10.1242/dev.092270
Rein, D. B. (2009). Forecasting age-related macular degeneration through the year 2050: the potential impact of new treatments. - PubMed - NCBI. *Archives of Ophthalmology (Chicago, Ill. : 1960)*, *127*(4), 533–540.
Roh, M., Selivanova, A., Shin, H. J., Miller, J. W., & Jackson, M. L. (2018). Visual acuity and contrast sensitivity are two important factors affecting vision-

related quality of life in advanced age-related macular degeneration. *PLoS ONE*, *13*(5), e0196481–12. http://doi.org/10.1371/journal.pone.0196481
Romano, M. R., Valldeperas, X., Vinciguerra, P., & Wong, D. (2011). Sub-macular surgery: is still an option for age-related macular degeneration? *Current Drug Targets*, *12*(2), 190–198.
Sacu, S., Stifter, E., Vécsei-Marlovits, P. V., Michels, S., Schütze, C., Prünte, C., & Schmidt-Erfurth, U. (2008). Management of extensive subfoveal haemorrhage secondary to neovascular age-related macular degeneration. *Eye*, *23*(6), 1404–1410. http://doi.org/10.1038/eye.2008.267
Sandhu, S. S., Manvikar, S., & Steel, D. H. W. (2010). Displacement of submacular hemorrhage associated with age-related macular degeneration using vitrectomy and submacular tPA injection followed by intravitreal ranibizumab. *Clinical Ophthalmology*, *4*, 637–642.
Sawa, M., Ober, M. D., & Spaide, R. F. (2006). Autofluorescence and retinal pigment epithelial atrophy after subretinal hemorrhage. *Retina*, *26*(1), 119–120.
Schraermeyer, U., Thumann, G., Luther, T., Kociok, N., Armhold, S., Kruttwig, K., et al. (2001). Subretinally transplanted embryonic stem cells rescue photoreceptor cells from degeneration in the RCS rats. *Cell Transplantation*, *10*(8), 673–680.
Schwartz, S. D., Hubschman, J.-P., Heilwell, G., Franco-Cardenas, V., Pan, C. K., Ostrick, R. M., et al. (2012). Embryonic stem cell trials for macular degeneration: a preliminary report. *The Lancet*, *379*(9817), 713–720. http://doi.org/10.1016/S0140-6736(12)60028-2
Schwartz, S. D., Regillo, C. D., Lam, B. L., Eliott, D., Rosenfeld, P. J., Gregori, N. Z., et al. (2015). Human embryonic stem cell-derived retinal pigment epithelium in patients with age-related macular degeneration and Stargardt's macular dystrophy: follow-up of two open-label phase 1/2 studies. *The Lancet*, *385*(9967), 509–516. http://doi.org/10.1016/S0140-6736(14)61376-3
Schwartz, S. D., Tan, G., Hosseini, H., & Nagiel, A. (2016). Subretinal Transplantation of Embryonic Stem Cell–Derived Retinal Pigment Epithelium for the Treatment of Macular Degeneration: An Assessment at 4 Years. *Investigative Ophthalmology & Visual Science*, *57*(5), ORSFc1–9. http://doi.org/10.1167/iovs.15-18681
Scupola, A. (1995). Natural history of macular subretinal extensive hemorrhages in age related macular degeneration. *Vision Research*, *35*(1), S218. http://doi.org/10.1016/0042-6989(95)98836-x
Seaton, A. D., & Turner, J. E. (1992). RPE transplants stabilize retinal vasculature and prevent neovascularization in the RCS rat. *Investigative Ophthalmology & Visual Science*, *33*(1), 83–91.
Sekiryu, T., Iida, T., Sakai, E., Maruko, I., Ojima, A., & Sugano, Y. (2012). Fundus autofluorescence and optical coherence tomography findings in branch retinal vein occlusion. *Journal of Ophthalmology*, *2012*(3), 638064–8. http://doi.org/10.1155/2012/638064
Sekiryu, T., Oguchi, Y., Arai, S., Wada, I., & Iida, T. (2011). Autofluorescence of the Cells in Human Subretinal Fluid. *Investigative Ophthalmology & Visual*

Science, *52*(11), 8534–8541. http://doi.org/10.1167/iovs.11-8012
Sekuler, R., Admas, A. J., Biederman, I., & Carr, R. E. (1986). Emergent Techniques for Assessment of Visual Performance (pp. 1–14).
Sheng, Y., Gouras, P., Cao, H., Berglin, L., Kjeldbye, H., Lopez, R., & Rosskothen, H. (1995). Patch transplants of human fetal retinal pigment epithelium in rabbit and monkey retina. *Investigative Ophthalmology & Visual Science*, *36*(2), 381–390.
Shienbaum, G., Garcia Filho, C. A. A., Flynn, H. W., Jr., Nunes, R. P., Smiddy, W. E., & Rosenfeld, P. J. (2013). Management of Submacular Hemorrhage Secondary to Neovascular Age-Related Macular Degeneration With Anti–Vascular Endothelial Growth Factor Monotherapy. *American Journal of Ophthalmology*, *155*(6), 1009–1013. http://doi.org/10.1016/j.ajo.2013.01.012
Sivaprasad, S., Pearce, E., & Chong, V. (2011). Quality of fixation in eyes with neovascular age-related macular degeneration treated with ranibizumab. *Eye*, *25*(12), 1612–1616. http://doi.org/10.1038/eye.2011.223
Skottman, H., Dilber, M. S., & Hovatta, O. (2006). The derivation of clinical-grade human embryonic stem cell lines. *FEBS Letters*, *580*(12), 2875–2878. http://doi.org/10.1016/j.febslet.2006.03.083
Solomon, S. D., Lindsley, K., Vedula, S. S., Krzystolik, M. G., & Hawkins, B. S. (2019). Anti-vascular endothelial growth factor for neovascular age-related macular degeneration. *Cochrane Database of Systematic Reviews*, *53*(3), 1152–164. http://doi.org/10.1002/14651858.CD005139.pub4
Song, W. K., Park, K.-M., Kim, H.-J., Lee, J. H., Choi, J., Chong, S. Y., et al. (2015). Treatment of macular degeneration using embryonic stem cell-derived retinal pigment epithelium: preliminary results in Asian patients. *Stem Cell Reports*, *4*(5), 860–872. http://doi.org/10.1016/j.stemcr.2015.04.005
Sonoda, S., Spee, C., Barron, E., Ryan, S. J., Kannan, R., & Hinton, D. R. (2009). A protocol for the culture and differentiation of highly polarized human retinal pigment epithelial cells. - PubMed - NCBI. *Nature Protocols*, *4*(5), 662–673. http://doi.org/10.1038/nprot.2009.33
Spaide, R. (2008). Autofluorescence from the outer retina and subretinal space. *Retina*, *28*(1), 5–35. http://doi.org/10.1097/IAE.0b013e318158eca4
Spaide, R. F., & Curcio, C. A. (2011). Anatomical correlates to the bands seen in the outer retina by optical coherence tomography: literature review and model. *Retina (Philadelphia, Pa.)*, *31*(8), 1609–1619. http://doi.org/10.1097/IAE.0b013e3182247535
Sparrow, J. R., Hicks, D., & Hamel, C. P. (2010). The retinal pigment epithelium in health and disease., *10*(9), 802–823.
Sparrow, J., & Duncker, T. (2014). Fundus Autofluorescence and RPE Lipofuscin in Age-Related Macular Degeneration. *Journal of Clinical Medicine*, *3*(4), 1302–1321. http://doi.org/10.3390/jcm3041302
Stanescu-Segall, D., Balta, F., & Jackson, T. L. (2016). Submacular hemorrhage in neovascular age-related macular degeneration: A synthesis of the literature. *Survey of Ophthalmology*, *61*(1), 18–32. http://doi.org/10.1016/j.survophthal.2015.04.004
Stanga, P. E., Kychenthal, A., Fitzke, F. W., Halfyard, A. S., Chan, R., Bird, A. C.,

and Aylward, G. W. (2001b) Retinal pigment epithelium translocation and central visual function in age related macular degeneration: preliminary results. Int Ophthalmol 23, 297-307.
Strauss, O. (2005). The Retinal Pigment Epithelium in Visual Function. *Physiological Reviews*, *85*(3), 845–881. http://doi.org/10.1152/physrev.00021.2004
Strunnikova, N. V., Maminishkis, A., Barb, J. J., Wang, F., Zhi, C., Sergeev, Y., et al. (2010). Transcriptome analysis and molecular signature of human retinal pigment epithelium. - PubMed - NCBI. *Human Molecular Genetics*, *19*(12), 2468–2486. http://doi.org/10.1093/hmg/ddq129
Sugino, I. K., Wang, H., & Zarbin, M. A. (2003). Age-related macular degeneration and retinal pigment epithelium wound healing. *Molecular Neurobiology*, *28*(2), 177–194. http://doi.org/10.1385/MN:28:2:177
Sunness, J. S., Bressler, N. M., Tian, Y., Alexander, J., & Applegate, C. A. (1999). Measuring geographic atrophy in advanced age-related macular degeneration. *Investigative Ophthalmology & Visual Science*, *40*(8), 1761–1769.
Taylor-Weiner, H., & Graff Zivin, J. (2015). Medicine's Wild West — Unlicensed Stem-Cell Clinics in the United States. *The New England Journal of Medicine*, *373*(11), 985–987. http://doi.org/10.1056/NEJMp1504560
Tezel, T. H., Kaplan, H. J., & Del Priore, L. V. (1999). Fate of human retinal pigment epithelial cells seeded onto layers of human Bruch's membrane. *Investigative Ophthalmology & Visual Science*, *40*(2), 467–476.
Thomas, B. B., Zhu, D., Zhang, L., Thomas, P. B., Hu, Y., Nazari, H., et al. (2016). Survival and Functionality of hESC-Derived Retinal Pigment Epithelium Cells Cultured as a Monolayer on Polymer Substrates Transplanted in RCS RatsRetinal Pigment Epithelium Transplantation. *Investigative Ophthalmology & Visual Science*, *57*(6), 2877–2887. http://doi.org/10.1167/iovs.16-19238
Thomson, J. A., Itskovitz-Eldor, J., Shapiro, S. S., Waknitz, M. A., Swiergiel, J. J., Marshall, V. S., & Jones, J. M. (1998). Embryonic Stem Cell Lines Derived from Human Blastocysts, *282*(5391), 1145–1147. http://doi.org/10.1126/science.282.5391.1145
Thumann, G., Dou, G., Wang, Y., & Hinton, D. R. (2013). Chapter 16 - Cell Biology of the Retinal Pigment Epithelium. *Retina* (Fifth Edition, pp. 401–414). Elsevier Inc. http://doi.org/10.1016/B978-1-4557-0737-9.00016-3
Treumer, F., Klatt, C., Roider, J., & Hillenkamp, J. (2009). Subretinal coapplication of recombinant tissue plasminogen activator and bevacizumab for neovascular age-related macular degeneration with submacular haemorrhage. *British Journal of Ophthalmology*, *94*(1), 48–53. http://doi.org/10.1136/bjo.2009.164707
Treumer, F., Roider, J., & Hillenkamp, J. (2012). Long-term outcome of subretinal coapplication of rtPA and bevacizumab followed by repeated intravitreal anti-VEGF injections for neovascular AMD wi... - PubMed - NCBI. *British Journal of Ophthalmology*, *96*(5), 708–713. http://doi.org/10.1136/bjophthalmol-2011-300655

Tsukahara, I., Ninomiya, S., Castellarin, A., Yagi, F., Sugino, I. K., & Zarbin, M. A. (2002). Early Attachment of Uncultured Retinal Pigment Epithelium from Aged Donors onto Bruch's Membrane Explants. *Experimental Eye Research*, *74*(2), 255–266. http://doi.org/10.1006/exer.2001.1123

Turner, L. G. (2015). US clinics marketing unproven and unlicensed adipose-derived autologous stem cell interventions. - PubMed - NCBI. *Regenerative Medicine*, *10*(4), 397–402. http://doi.org/10.2217/rme.15.10

Uppal, G., Milliken, A., Lee, J., Acheson, J., Hykin, P., Tufail, A., & da Cruz, L. (2007). New algorithm for assessing patient suitability for macular translocation surgery. *Clinical & Experimental Ophthalmology*, *35*(5), 448–457. http://doi.org/10.1111/j.1442-9071.2007.01528.x

Valentino, T. L., Kaplan, H. J., Del Priore, L. V., Fang, S. R., Berger, A., & Silverman, M. S. (1995). Retinal pigment epithelial repopulation in monkeys after submacular surgery. *Archives of Ophthalmology (Chicago, Ill. : 1960)*, *113*(7), 932–938.

van Meurs, J. C., & Van Den Biesen, P. R. (2003). Autologous retinal pigment epithelium and choroid translocation in patients with exudative age-related macular degeneration: short-term follow-up. *American Journal of Ophthalmology*, *136*(4), 688–695. http://doi.org/10.1016/S0002-9394(03)00384-2

van Zeeburg, E. J. T., & van Meurs, J. C. (2013). Literature Review of Recombinant Tissue Plasminogen Activator Used for Recent-Onset Submacular Hemorrhage Displacement in Age-Related Macular Degeneration. *Ophthalmologica*, *229*(1), 1–14. http://doi.org/10.1159/000343066

van Zeeburg, E. J. T., Maaijwee, K. J. M., & van Meurs, J. C. (2018). Visual acuity of 20/32, 13.5 years after a retinal pigment epithelium and choroid graft transplantation. - PubMed - NCBI. *American Journal of Ophthalmology Case Reports*, *10*, 62–64. http://doi.org/10.1016/j.ajoc.2018.01.042

van Zeeburg, E. J. T., Maaijwee, K. J. M., Missotten, T. O. A. R., Heimann, H., & van Meurs, J. C. (2012). A Free Retinal Pigment Epithelium–Choroid Graft in Patients With Exudative Age-Related Macular Degeneration: Results up to 7 Years. *American Journal of Ophthalmology*, *153*(1), 120–127.e2. http://doi.org/10.1016/j.ajo.2011.06.007

Vugler, A., Carr, A.-J., Lawrence, J., Chen, L. L., Burrell, K., Wright, A., et al. (2008). Elucidating the phenomenon of HESC-derived RPE: anatomy of cell genesis, expansion and retinal transplantation. - PubMed - NCBI. *Experimental Neurology*, *214*(2), 347–361. http://doi.org/10.1016/j.expneurol.2008.09.007

Wang, H., Ninomiya, Y., Sugino, I. K., & Zarbin, M. A. (2003). Retinal pigment epithelium wound healing in human Bruch's membrane explants. *Investigative Ophthalmology & Visual Science*, *44*(5), 2199–2210.

Wang, S., Lu, B., & Lund, R. D. (2005). Morphological changes in the Royal College of Surgeons rat retina during photoreceptor degeneration and after cell-based therapy. *The Journal of Comparative Neurology*, *491*(4), 400–417. http://doi.org/10.1002/cne.20695

Wenkel, H., & Streilein, J. W. (2000). Evidence that retinal pigment epithelium functions as an immune-privileged tissue. *Investigative Ophthalmology & Visual Science*, *41*(11), 3467–3473.

Whittaker, S. G., & Lovie-Kitchin, J. (1993). Visual Requirements for Reading. *Optometry and Vision Science : Official Publication of the American Academy of Optometry*, *70*(1), 54–65.

Wiecek, E., Lashkari, K., Dakin, S. C., & Bex, P. (2015). A Statistical Analysis of Metamorphopsia in 7106 Amsler Grids. *Ophthalmology*, *122*(2), 431–433. http://doi.org/10.1016/j.ophtha.2014.09.006

Wiedemann, P., Yandiev, Y., Hui, Y.-N., & Wang, Y. (2013). Chapter 97 - Pathogenesis of Proliferative Vitreoretinopathy. *Retina* (Fifth Edition, pp. 1640–1646). Elsevier Inc. http://doi.org/10.1016/B978-1-4557-0737-9.00097-7

Wing, G. L., Blanchard, G. C., & Weiter, J. J. (1978). The topography and age relationship of lipofuscin concentration in the retinal pigment epithelium. *Investigative Ophthalmology & Visual Science*, *17*(7), 601–607.

Yannuzzi, N. A., & Freund, K. B. (2019). Brolucizumab: evidence to date in the treatment of neovascular age-related macular degeneration . *Clinical Ophthalmology*, *Volume 13*, 1323–1329. http://doi.org/10.2147/OPTH.S184706

Yu, J., Gu, R., Zong, Y., Xu, H., Wang, X., Sun, X., et al. (2016). Relationship Between Retinal Perfusion and Retinal Thickness in Healthy Subjects: An Optical Coherence Tomography Angiography Study. *Investigative Ophthalmology & Visual Science*, *57*(9), OCT204–7. http://doi.org/10.1167/iovs.15-18630

Yung, M., Klufas, M. A., & Sarraf, D. (2016). Clinical applications of fundus autofluorescence in retinal disease. *International Journal of Retina and Vitreous*, 1–25. http://doi.org/10.1186/s40942-016-0035-x

Zhu, D., Deng, X., Spee, C., Sonoda, S., Hsieh, C.-L., Barron, E., et al. (2011). Polarized Secretion of PEDF from Human Embryonic Stem Cell–Derived RPE Promotes Retinal Progenitor Cell Survival. *Investigative Ophthalmology & Visual Science*, *52*(3), 1573–1585. http://doi.org/10.1167/iovs.10-6413

Appendix 1. Series of CF photographs throughout the study period

Subject 1

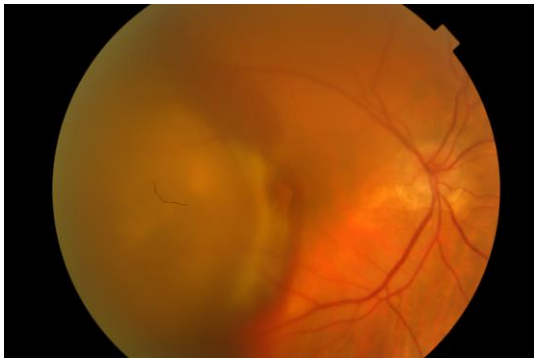

a. Subject 1, baseline

b. Subject 1, week 2

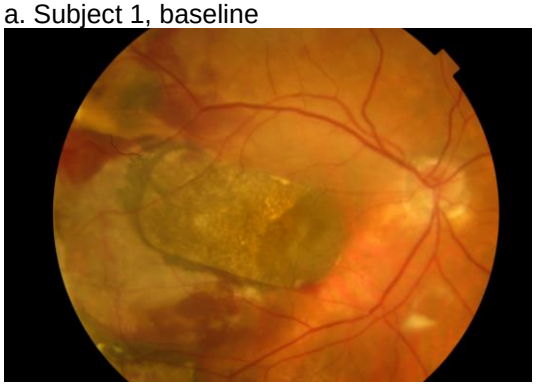

c. Subject 1, week 4

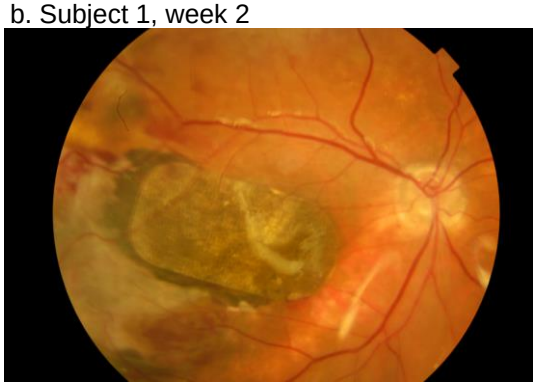

d. Subject 1, week 8

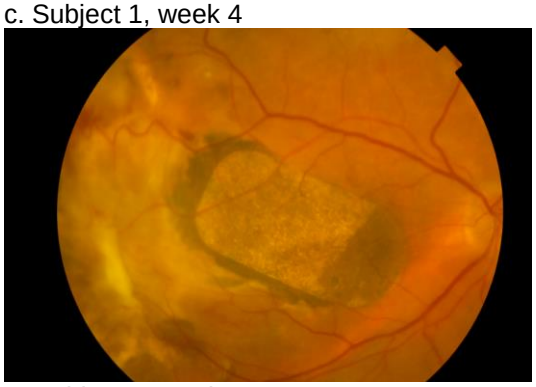

e. Subject 1, week 10

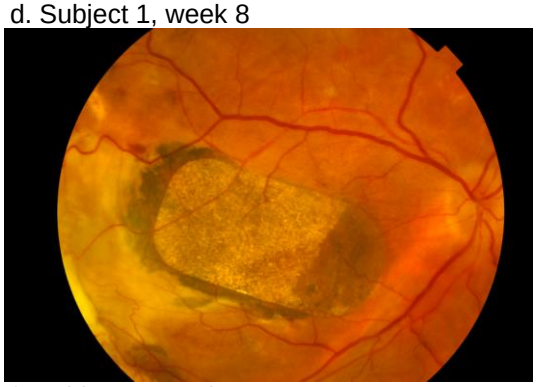

f. Subject 1, week 12

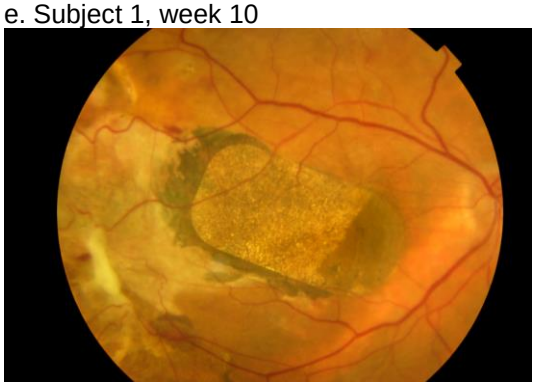

g. Subject 1, week 16

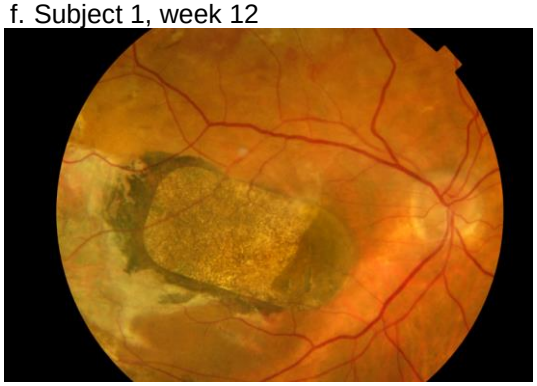

h. Subject 1, week 24

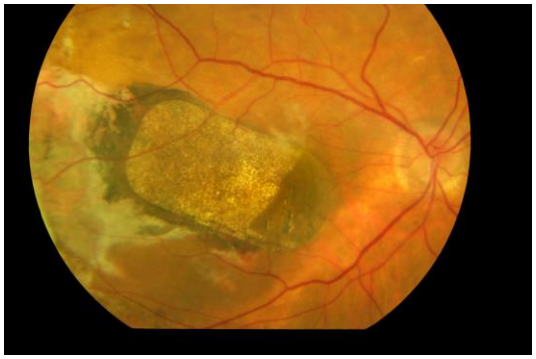

i. Subject 1, week 36

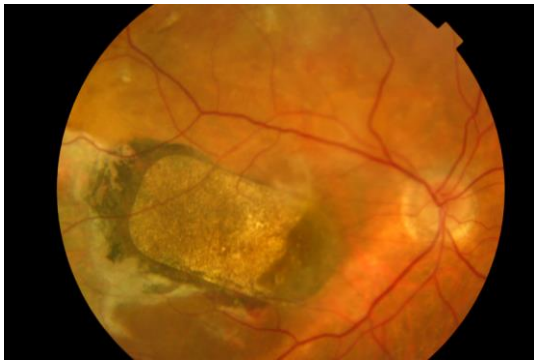

j. Subject 1, year 1

k. Subject 1, month 18

l. Subject 1, year 2

Subject 2

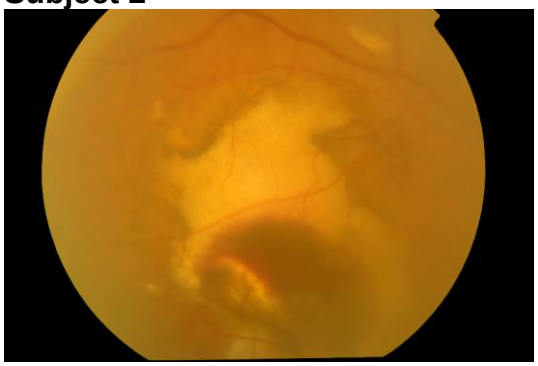

a. Subject 2, baseline

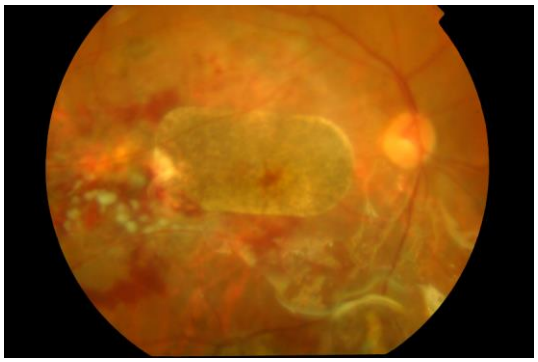

b. Subject 2, week 2

c. Subject 2, week 4

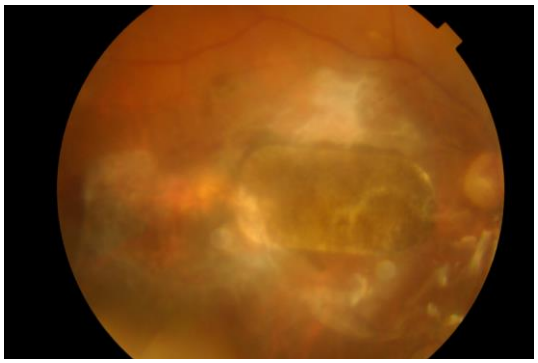

d. Subject 2, week 8

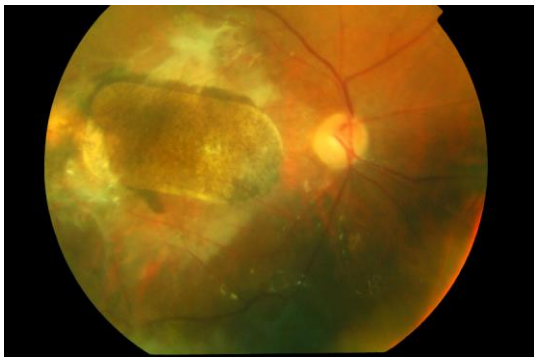

e. Subject 2, week 10

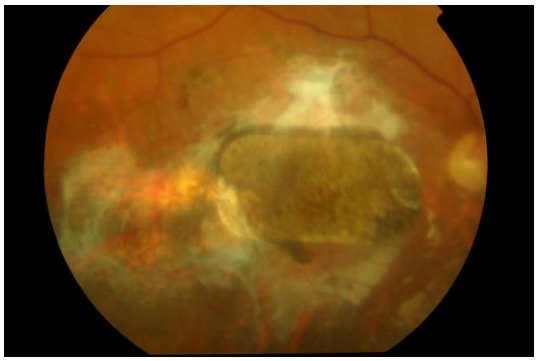

f. Subject 2, week 12

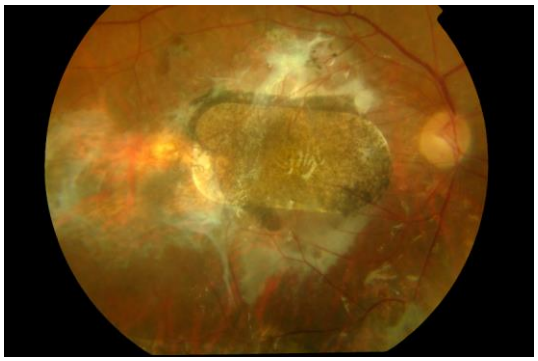

g. Subject 2, week 16

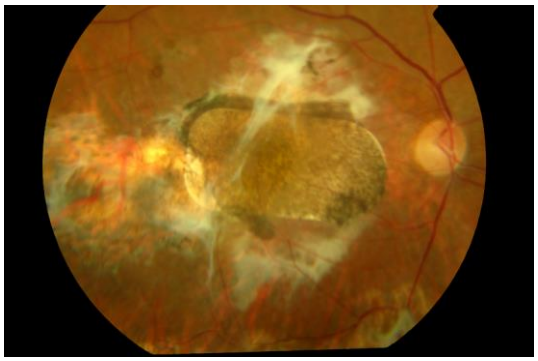

h. Subject 2, week 24

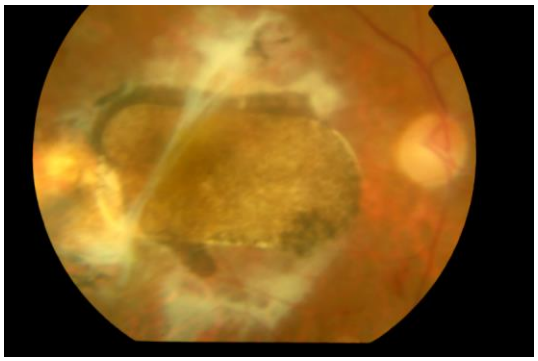

i. Subject 2, week 36

j. Subject 2, year 1

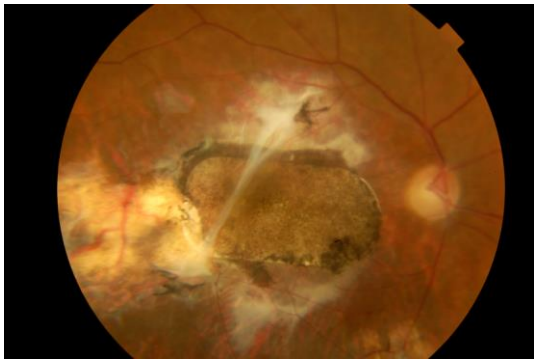

k. Subject 2, month 18

l. Subject 2, year 2

Appendix 2. Synopsis of the Clinical Pharmacology Protocol, related to this thesis (Clinicaltrials.gov: NCT01691261)**.**

CLINICAL PHARMACOLOGY PROTOCOL

PHASE 1, OPEN-LABEL, SAFETY AND FEASIBILITY STUDY OF IMPLANTATION OF PF-05206388 (HUMAN EMBRYONIC STEM CELL DERIVED RETINAL PIGMENT EPITHELIUM (RPE) LIVING TISSUE EQUIVALENT) IN SUBJECTS WITH ACUTE WET AGE RELATED MACULAR DEGENERATION AND RECENT RAPID VISION DECLINE

Compound:	PF-05206388
Compound Name:	N/A
US IND Number:	N/A
European Clinical Trial Database (EudraCT) Number:	2011-005493-37
Protocol Number:	B4711001
Phase:	1

The name, title, address and telephone number(s) of the sponsor's medical expert for the trial is documented in the study contact list located in the team SharePoint site.

SUMMARY

Pfizer Worldwide Research & Development in collaboration with University College London are developing an advanced therapy medicinal product derived from a human embryonic stem cell (hESC) line known as the SHEF-1.3. The proposed product (PF-05206388) comprises SHEF-1.3 cells differentiated to form Retinal Pigment Epithelium (RPE) cells immobilised to a vitronectin coated polyester membrane. PF-05206388 will replace RPE in the eyes of subjects with acute, declining untreatable or treatment failing wet age-related macular degeneration (AMD).

Indication

The target population of PF-05206388 in this exploratory study is subjects with wet AMD with significant recent decline in vision related to an RPE tear or submacular haemorrhage or in whom treatment with anti VEGF therapeutic agents (eg, Lucentis) is failing.

It is anticipated that RPE replacement may eventually be indicated in many atrophic and neovascular macular diseases, including inherited, inflammatory and age-related wet and dry degenerations.

Background and Rationale

Age related macular degeneration remains and will continue to be the major cause of visual disability in the developed world[1,2] despite the recent advances in anti-VEGF associated treatment of the wet form.[3,4] The dry or atrophic form of the disease remains poorly treated and in many cases of combined wet and dry degeneration, the treatment with anti-VEGF agents merely delays the onset of severe central vision loss from dry degeneration.

The visual outcome with treatment in wet AMD and the prognosis for vision in dry AMD and combined disease is often dependent on the health of the retinal pigmented epithelium (RPE).[5] The function of the RPE is critical to photoreceptor function and is thought to play a major role in the modulation of neovascular and atrophic disease of the macula.[6,7] Loss of RPE is thought to be central to the progression of all macula atrophic diseases of which dry AMD is the commonest.[8]

Evidence that RPE replacement can play a role in restoring and stabilizing vision in macular disease, both wet and dry, has come from various clinical studies on RPE replacement[9,10,11] and macular translocation[12,13,14] as well as a better understanding of these diseases. Although the best of these surgical interventions are able to restore sight to near normal levels and for extended periods,[13,14] the interventions themselves are complex and high risk, relative to the patient group that need them. Furthermore, the RPE transplanted in the existing procedures is from the patients themselves and hence likely to be old and, in some cases, potentially diseased.

The advent of stem cell technology has allowed RPE to be derived independently of direct harvesting from a donor.[15,16,17] This has created the potential for a limitless supply of transplantable cells and these are young and disease free. The complexity of the procedures

required to transplant them is significantly reduced, as there is no associated harvesting step, and the risk to the patient is commensurately reduced.[9,10,11]

The treatment paradigm of RPE replacement is also significantly different to current modalities such as anti-VEGF treatment. The latter acts by controlling a complication of the disease whereas RPE replacement aims to restore a normative architecture and thereby restore normal function. The restoration of a normal and healthy structure populated with young cells then also acts as a powerful suppressor of the disease process.[17]

In this Phase 1 trial of RPE replacement, the aim will be to evaluate the safety and feasibility/efficacy of treating subjects with wet AMD in whom there is rapidly progressing vision loss associated with RPE tears, sub-macular haemorrhage or failing anti-VEGF treatment. The recent history of vision loss will indicate that the neural retina is functioning and therefore has the potential to improve vision. Improvement of vision will be easier to document and will manifest over a shorter period of time than the outcome in atrophic disease where the endpoint would be reduction in future vision loss.

The overall goal of the development plan is to demonstrate whether surgical replacement of PF-05206388 (retinal pigment epithelium cells derived from human embryonic stem cells immobilised on a membrane) can provide a safe and effective therapy for patients suffering from degenerative retinal maculopathies. The membrane is lozenge shaped (approximately 6 mm x 3 mm) and will contain a confluent layer of RPE cells (approximately 100,000 RPE cells), at a dose of 17 mm^2.

The principle of autologous RPE replacement/translocation for patients with retinal degeneration has previously been established[9,10,11,12,13,14] but these procedures are associated with significant drawbacks due to the requirement for complicated surgeries and the age and health of the patient's transplanted RPE. Surgical replacement of allogenic hES cell derived RPE immobilised on a membrane offers the potential for a safer and more effective treatment. The improvement in safety is expected to result from the less complicated surgery and the improvement in efficacy from the use of younger and non-diseased RPE.

Objectives

The objectives of this study are to evaluate the safety, technical feasibility and efficacy of PF-05206388 in subjects with wet AMD.

Primary objectives

1. Safety of cells and membrane:

    a. Local or systemic immunological reactions or other forms of systemic toxicity.

    b. Neoplastic change or proliferation of transplanted cells.

    c. Recurrent major retinal or ocular complications (eg, retinal detachment, endophthalmitis, corneal opacification, ocular pain).

d. Migration of the membrane (PF-05206388).

2. Visual improvement/stability.

Secondary objectives

1. Anatomical and functional survival of the transplanted RPE cells over time.

2. Safety and anatomic success of surgery and delivery technique:

   a. Completion of surgery with successful sub-retinal placement of PF-05206388 (all steps of surgical protocol completed).

   b. Successful function and safety of the delivery tool - placement of undamaged PF-05206388 below the macula in the subretinal space.

   c. Successful reattachment of the retina.

   d. Absence of severe or limiting intraocular, intraoperative complications specific to the surgical technique.

3. Improvement in reading speed over time.

Endpoints

In this exploratory study, the objectives of the study will be evaluated via a variety of clinical investigations, specifically:

Primary endpoints

- Incidence and severity of adverse events.
- Change from baseline in Early Treatment Diabetic Retinopathy (ETDRS) best corrected visual acuity (BCVA) - Proportion of subjects with an improvement of 15 letters or more at Week 24.

Secondary endpoints

- Change from baseline in ETDRS best corrected visual acuity (BCVA) - Proportion of subjects with an improvement of 15 letters or more at Weeks 1, 2, 4, 8, 12, 16, 36 & 52.
- Mean change of best corrected visual acuity (BCVA) from baseline by study visit.
- Mean change from baseline in contrast sensitivity by Pelli-Robson test at Weeks 24 & 52.
- Position of PF-05206388 at Day 2 and Weeks 1, 2, 4, 8, 10, 12, 16, 24, 36 and 52 by serial biomicroscopic evaluation.

- Position and presence of pigmented RPE cells by serial fundus photography at Weeks 2, 4, 8, 10, 12, 16, 24, 36 and 52.
- Change in liver and renal function by blood tests and liver ultrasound at Weeks 24 and 52.
- Change in leakage or perfusion in normal fundal vasculature and presence of abnormal vasculature at Weeks 4, 8, 12, 24 and 52 by fundus fluorescein angiography.
- Change in central 30 degree of visual function at Weeks 4, 8, 12, 24 and 52 by Humphrey Field test.
- Change in thickness of RPE layer at Weeks 4, 8, 16, 24, 36 and 52 by B-mode orbital ultrasound.

Exploratory endpoints

- Position and presence of pigmented RPE cells Scanning Laser Ophthalmoscopy (SLO) autofluorescence at Weeks 4, 8, 12, 16, 24, 36 and 52.
- Placement of PF-05206388 by serial spectral domain Optical Coherence Tomography (OCT) scan at Weeks 4, 8, 12, 16, 24, 36 and 52.
- Evidence of diffuse retinal and RPE toxicity at Weeks 12 and 52 by full field ERG and EOG.
- Photoreceptor survival (indirect indication of RPE survival) at Weeks 16, 24, 36 and 52 by Adaptive Optics.
- Functional survival of retinal photoreceptors at Weeks 4, 16, 24, 36 and 52 by Nidek microperimetry over PF-05206388.
- Change in reading speed at Weeks 4, 8, 16, 24, 36 and 52 by Minnesota (MN) Read test.
- Detection of alloreactive antibodies (blood) at Weeks 2, 4, 8 12, 24 and 52.

Study Design and Treatments

This study is a single site, open-label study being conducted in ten male or post-menopausal female subjects with wet AMD, with either:

- Sudden vision loss associated with RPE tears or sub-macular haemorrhage; and/or
- Evidence of rapidly declining vision despite anti-VEGF treatment for wet AMD.

The study intervention comprises surgery which involves insertion of a single membrane of immobilised RPE cells (PF-05206388) into one eye (study eye) with follow-up to 52 weeks in this study.

Surgery will take place such that there is less than 6 weeks between the start of vision loss and surgery for subjects with RPE tear or sub macular haemorrhage and less than 20 weeks between the start of vision loss and surgery for subjects with anti VEGF-failing wet AMD.

Subjects will attend the hospital on an out-patient basis for up to three days during the screening interval (Day -21 to Day 0). Eligible subjects will attend the hospital on an out-patient basis the day before surgery (Day 0) for pre-surgery assessments. PF-05206388 insertion occurs the following day (Day 1). Subjects will be discharged from the hospital the day after surgery (Day 2) once the study eye is deemed to be stable and the scheduled tests for this day have been completed.

There is a second operative procedure performed at the Week 10 visit (Visit 9) whereby the silicone oil, which was inserted at the time of PF-05206388 insertion, is removed from the eye. Subjects with significant cataracts noted at screening may also be permitted to have the cataracts removed at the time of this second surgical procedure via standard of care carried out at Moorfields Eye Hospital in accordance with clinical need at investigators' discretion.

Subjects will receive an immunosuppressive and antibiotic regimen in association with both surgical procedures (Day 1 and Week 10) defined by the investigator and reflecting the standard of care consistent with this type of eye surgery. For the first procedure, subjects will receive up to 1 mg/kg oral prednisolone (up to 60 mg maximum) daily commenced 2-4 days pre-operatively and continued for at least 2 weeks followed by a tailing off over at least 1 further week. Subjects will also receive single doses of sub-tenon triamcinolone acetonide 40 mg and sub conjunctival cefuroxime (250 mg in 1 mL) post replacement. For the second procedure, subjects will receive up to 1 mg/kg oral prednisolone (up to 60 mg maximum) daily commenced 7 days pre-operatively and continued for a at least 2 weeks followed by a tailing off over at least 1 further week. Subjects will also receive an intravitreal implant of fluocinolone acetonide of either 0.19 or 0.59 mg as an anti-inflammatory agent and sub conjunctival cefuroxime (250 mg in 1 mL) post surgery.

The first surgical procedure will be carried out on Day 1, subjects are discharged from hospital on Day 2 and attend for post-surgical evaluations at Week 1, Week 2, Week 4, Week 8, Week 12, Week 16, Week 24, Week 36 and Week 52. Subjects who discontinue prior to the Week 12 Visit due to reasons unrelated to the study may be replaced to ensure 10 subjects reach at least this stage of evaluation. Each subject will be in the study for about 52 weeks from first surgery to follow up, with the screening period taking place prior to first surgery. Subjects will be invited to participate in the long-term (up to 14 years) follow up study on completion of this study.

Statistical Method

Detailed methodology for summary and statistical analyses of the data collected in this study will be documented in a Statistical Analysis Plan, which will be dated and maintained by the sponsor. This document may modify the plans outlined in the core protocol elements; however, any major modifications of the primary efficacy endpoint definition and/or its analysis will also be reflected in a protocol amendment.

Sample Size Determination

The sample size of 10 subjects has been determined based on feasibility and providing sufficient data to evaluate safety and tolerability. Assessment of efficacy is also being made and the following decision criteria will be applied to the primary efficacy endpoint, the proportion of subjects with at least a 15 letter improvement in ETDRS best corrected visual acuity (BCVA) at 24 weeks. Subjects who discontinue prior to the Week 12 Visit due to reasons unrelated to the study may be replaced to ensure 10 subjects reach at least this stage of evaluation.

The decision criteria are:

C1: At least 20% of treated subjects have an improvement of 15 letters or more in the ETDRS BCVA at 24 weeks.

C2: At least 40% of treated subjects have an improvement of 15 letters or more in the ETDRS BCVA at 24 weeks.

The Operating Characteristics for these decision criteria are displayed in the figure below.

Operating Characteristics

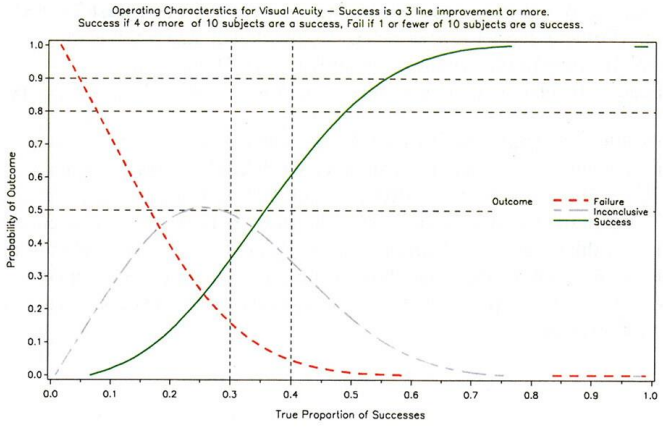

If the true success rate is 0.36 or better, we are more likely than not to meet C2. If the true success rate is 0.16 or worse, we are more likely than not to fail C1.

Efficacy Analysis

Analysis of Primary Endpoint

The primary endpoint is whether or not a subject has a 15 letter or more improvement in reading ability for the ETDRS best corrected visual acuity test at 24 weeks.

The proportion of subjects with a 15-letter improvement in reading ability at 24 weeks will be presented.

In addition, the posterior probability that the response proportion for PF-05206388 is greater than a range of values (0, 0.1, 0.2, 0.3, 0.4, 0.5) will be presented, to aid interpretation of the results. The posterior probabilities will be calculated using a Beta(1,1) distribution for the prior. This prior gives a uniform (constant) probability for any proportion in the range 0 to 1. A two-sided 90% credible interval for the response proportion for PF-05206388 will also be calculated.

Analysis of Secondary and Exploratory Endpoints

Categorical endpoints will be summarized by calculating the proportion of subjects in each category. For binary categorical endpoints a 90% credible interval may also be calculated assuming an uninformative Beta(1,1) prior. Where appropriate, proportions will be plotted against time post surgery.

When the necessary distributional assumptions are adequately satisfied continuous endpoints will be analysed by calculating a mean and 90% confidence interval. If the distributional assumptions are not adequately satisfied then an alternative non-parametric method will be used. Where appropriate, the summary statistics will be plotted against time post surgery.

Safety Analysis

Adverse events, ECGs, blood pressure, pulse rate, and safety laboratory data will be reviewed and summarized on an ongoing basis during the study to evaluate the safety of subjects. Any clinical laboratory, ECG, BP, and PR abnormalities of potential clinical concern will be described. Safety data will be listed and summarized in accordance with the current sponsor reporting algorithms.

Medical history and physical exam information collected during the course of the study will not be captured for inclusion into the study database, unless otherwise noted. However any untoward findings identified on physical exams conducted after the initial surgery will be captured as an adverse event, if those findings meet the definition of an adverse event. Data collected at screening that is used for inclusion/exclusion criteria, such as laboratory data, ECGs and vital signs will be considered source data, and will not be captured for inclusion

into the study database, unless otherwise noted. Demographic data collected at screening will be included in the study database.

Electrocardiogram (ECG) Analysis

Changes from baseline for the ECG parameters QT interval, heart rate, QTc interval, PR interval and QRS interval will be summarized by treatment and time.

The number (%) of subjects with maximum post dose QTc values and maximum increases from baseline in the following categories will be tabulated by treatment:

Safety QTc

	Borderline (msec)	Prolonged (msec)
Absolute Value	≥450-<480	≥480
Absolute Change	30-<60	≥60

In addition, the number of subjects with corrected and uncorrected QT values ≥500 msec will be summarized.

Data Monitoring Committee

This study will use an External Data Monitoring Committee (E-DMC).

The DMC will be responsible for ongoing monitoring of the safety of subjects in the study according to the Charter (See Section 3.2). The recommendations made by the DMC to alter the conduct of the study will be forwarded to Pfizer for final decision. Pfizer will forward such decisions, which may include summaries of aggregate analyses of endpoint events and of safety data which are not endpoints, to regulatory authorities, as appropriate. In this instance, such disease-related efficacy endpoints are not reported individually as SAEs.

SCHEDULE OF ACTIVITIES

The Schedule of Activities table provides an overview of the protocol visits and procedures. Refer to Study Procedures (Section 6) and Assessments (Section 7) for detailed information on each procedure and assessment required for compliance with the protocol.

	Screening	Pre-surgery assessment	Surgery (PF-05206388 insertion)	Discharge	Post surgery follow up				Surgery (removal of oil)	Post surgery follow-up				
	Day -21[a]	Day 0	Day 1	Day 2	Week 1 (±2 d)	Week 2 (±2 d)	Week 4 (±7 d)	Week 8 (±7 d)	Week 10 (±7 d)	Week 12 (±2 d)	Week 16 (±7 d)	Week 24 (±14 d)	Week 36 (±14 d)	Week 52 (±14 d)
Activity	Visit 1	Visit 2	Visit 3	Visit 4	Visit 5	Visit 6	Visit 7	Visit 8	Visit 9	Visit 10	Visit 11	Visit 12	Visit 13	Visit 14
Informed consent	X													
General medical history	X	X							X					
Admission to Moorfields Eye Hospital			X											
Drug, alcohol & tobacco history	X													
Physical examination[c]	X	X		X					X					X
Blood chemistry	X	X		X	X		X	X		X	X	X		X
Haematology	X	X		X	X		X	X		X	X	X		X
Urine safety tests	X	X								X				X
Detection of alloreactive antibodies (blood)		X				X	X	X		X		X		X
HIV, Hep B, Hep C testing	X													
Urine drug screen	X	X												
Liver ultrasound	X											X		X
Chest X-Ray	X													
ECG	X	X		X					X			X		X
Vital signs (BP & PR)	X	X	X	X	X	X	X	X	X	X	X	X	X	X
Randomisation		X												
Retained Pharmacogenomic blood sample		X												

	Screening	Pre-surgery assessment	Surgery (PF-05206388 insertion)	Discharge	Post surgery follow up				Surgery (removal of oil)	Post surgery follow-up				
	Day -21[a]	Day 0	Day 1	Day 2	Week 1 (±2 d)	Week 2 (±2 d)	Week 4 (±7 d)	Week 8 (±7 d)	Week 10 (±7 d)	Week 12 (±2 d)	Week 16 (±7 d)	Week 24 (±14 d)	Week 36 (±14 d)	Week 52 (±14 d)
Activity	Visit 1	Visit 2	Visit 3	Visit 4	Visit 5	Visit 6	Visit 7	Visit 8	Visit 9	Visit 10	Visit 11	Visit 12	Visit 13	Visit 14
Baseline reference safety blood sample		X												
Transplantation procedure			X											
Immunosuppression treatment	X[d]	X[d]	X[d]	X[d]	X[d]	X[d]		X[d]	X[d]	X[d]				
Removal of oil procedure									X					
Concomitant Medications	X----------													----X
Adverse events		X----------												----X
Biomicroscopic evaluation[e]	X	X		X	X	X	X	X	X[f]	X	X	X	X	X
Corneal pachymetry	X													
Ocular oncologist review[g]						X	X	X		X	X	X	X	X
Fundus photography	X[h]					X	X	X	X[f]	X	X	X	X	X
Spectral Domain OCT Scan	X[h]						X[b]	X[b]		X	X[b]	X[b]	X[b]	X
SLO autofluorescence	X[h]						X[b]	X[b]		X	X[b]	X[b]	X[b]	X
Fundus fluorescein angiography[j]	X[h]						X	X		X		X		X
Humphrey Field Test	X						X[b]	X[b]		X		X[b]		X
Full field ERG and EOG	X									X				X
ETDRS/logmar Best Corrected visual acuity (BCVA) - distant and near	X	X		X	X	X	X	X		X	X	X	X	X
Contrast sensitivity		X										X		X
Nidek Microperimetry	X	X[i]					X[b]				X[b]	X[b]	X[b]	X
MN Read test	X	X					X[b]	X[b]			X[b]	X[b]	X[b]	X
B-mode orbital	X	X					X	X			X	X	X	X

	Screening	Pre-surgery assessment	Surgery (PF-05206388 insertion)	Discharge	Post surgery follow up				Surgery (removal of oil)	Post surgery follow-up				
	Day -21[a]	Day 0	Day 1	Day 2	Week 1 (±2 d)	Week 2 (±2 d)	Week 4 (±7 d)	Week 8 (±7 d)	Week 10 (±7 d)	Week 12 (±2 d)	Week 16 (±7 d)	Week 24 (±14 d)	Week 36 (±14 d)	Week 52 (±14 d)
Activity	Visit 1	Visit 2	Visit 3	Visit 4	Visit 5	Visit 6	Visit 7	Visit 8	Visit 9	Visit 10	Visit 11	Visit 12	Visit 13	Visit 14
ultrasound														
Adaptive optics camera	X										X[b]	X[b]	X[b]	X
Discharge from Moorfields Eye Hospital				X										

a. Subjects attend for screening over a 3-day period from Day -14.
b. At the discretion of the investigator.
c. Screening exam may be performed on Day 0, pre-surgery. Abbreviated examination on Day 0, Day 2 & Week 10; Full exam at Week 52.
d. Refer to Section 3.1 of protocol for further detail on immunosuppressant and anti-inflammatory treatment. May continue for longer than shown on SoA depending on PI discretion.
e. Includes Goldman tonometry for IOP at all visits.
f. Before and after surgery (Week 10).
g. Ocular oncologist review will include repeat biomicroscopic evaluation and review of images from the ultrasound, fundus photography and fundus angiography.
h. Subjects who have had this test conducted within 14 days of the screening period will not require this test to be performed at screening.
i. Pre-operative (Day 1) fixation only.
j. ICG Angiogram also at screening only

Appendix 3. Synopsis of the follow-up Clinical Trial Protocol related to this thesis (Clinicaltrials.gov: NCT03102138).

LONG TERM, OPEN-LABEL, SAFETY FOLLOW UP STUDY FOLLOWING TRANSPLANTATION OF PF-05206388 (HUMAN EMBRYONIC STEM CELL DERIVED RETINAL PIGMENT EPITHELIUM (RPE)) IN SUBJECTS WITH ACUTE WET AGE RELATED MACULAR DEGENERATION AND RECENT RAPID VISION DECLINE

Compound:	PF-05206388
Compound Name:	N/A
United States (US) Investigational New Drug (IND) Number:	N/A
European Clinical Trial Database (EudraCT) Number:	Not yet known
Protocol Number:	B4711005
Phase:	1

PROTOCOL SUMMARY

Background and Rationale

Subjects who have completed 1 year follow up in B4711001 are invited to take part in this protocol. B4711001 involves administration of a PF-05206388 (consisting of Retinal Pigment Epithelial (RPE) cells on a polyester membrane) to subjects with Age Related Macular Degeneration (AMD). These RPE cells are derived from human embryonic stem cells, and because of the novelty of this approach it is considered prudent to follow these subjects for an extended period.

Objectives and Endpoints

Primary Objective

To assess the long term safety of PF-05206388.

Secondary Objective

To assess the long term efficacy of PF-05206388.

Endpoints

The primary endpoint is the incidence of serious adverse events (SAEs) and ocular adverse events (AEs).

Secondary endpoints are:

Change from baseline (pre-implantation) in ETDRS (Early Treatment of Diabetic Retinopathy Study) best corrected visual acuity (BCVA) - Proportion of subjects with an improvement of 15 letters or more at all timepoints.

Mean ETDRS BCVA and change from baseline (pre-implantation) at all timepoints.

Study Design

Study B4711001 will follow subjects for 12 months. B4711005 will follow subjects for a further 4 years with regular visits to assess safety. During each visit both eyes will be examined by biomicroscopy. Images will be taken of the study eye by fundus photography and Optical coherence tomography (OCT). Subjects will be referred to an ocular oncologist or other specialist if there is any evidence of tumour formation or other significant safety concern during the study. After 4 years subjects will be given a letter addressed to them and their General Practitioners (GPs) instructing them to immediately contact the Principal Investigator to arrange a visit if there are any serious safety concerns that may be related PF-05206388.

Statistical Methods

The numbers and proportions of subjects with Serious Adverse Events and ocular Adverse Events will be listed and summarized in accordance with Pfizer Data Standards (PDS).

SCHEDULE OF ACTIVITIES

The schedule of activities table provides an overview of the protocol visits and procedures. Refer to the study procedures (Section 6) and assessments (Section 7) sections of the protocol for detailed information on each procedure and assessment required for compliance with the protocol.

The investigator may schedule visits (unplanned visits) in addition to those listed on the schedule of activities, in order to conduct evaluations or assessments required to protect the well-being of the subject.

Visit Identifier	Day 1[a]	6 Mo[b]	12 Mo[b]	18 Mo[b]	24 Mo[b]	3 Years[c]	4 Years[c]
Visit number	**1**	**2**	**3**	**4**	**5**	**6**	**7**
Sign informed consent	X[d]						
Demography and significant medical history	X						
Brief physical exam		X	X	X	X	X	X
Eye exam by biomicroscopy		X	X	X	X	X	X
ETDRS best corrected visual acuity		X	X	X	X	X	X
Fundus photography[e]		X	X	X	X	X	X
Optical coherence tomography[e]		X	X	X	X	X	X
Provide letter for subject and general practitioner							X
History of Serious Adverse Events and Ocular Adverse Events		X	X	X	X	X	X

Abbreviations: Mo=Months, ETDRS= Early Treatment of Diabetic Retinopathy Study, RPE=Retinal Pigment Epithelium

a. All visit timings are given post the subject's final visit of study B4711001 (Week 52) which is also Day 1 of this study.
b. Plus or minus 6 weeks
c. Plus or minus 8 weeks.
d. May be signed any time prior to entering study.
e. May be discontinued if no RPE cells remain on the implant and eye exam demonstrates there are no safety concerns, at the discretion of the investigator